IJHSR International Journal of High School Research

October 2022 | Volume 4 | Issue 5
ijhighschoolresearch.org
ISSN (Print) 2642-1046
ISSN (Online) 2642-1054

Marine Biology Research at Bahamas

Unique and exclusive partnership with the Gerace Research Center (GRC) in San Salvador, Bahamas to offer marine biology research opportunities for high school teachers and students.

- Terra has exclusive rights to offer the program to high school teachers and students around world.
- All trips entail extensive snorkeling in Bahamian reefs as well as other scientific and cultural activities.
- Terra will schedule the program with GRC and book the flights from US to the GRC site.
- Fees include travel within the US to Island, lodging, meals, and hotels for transfers, and courses.
- For more information, please visit terraed.org/bahamas.html

Terra is a N.Y. based 501.c.3 non-profit organization
dedicated for improving K-16 education

Table of Contents

October 2022| Volume 4| Issue 5

Editorial Board

International Journal of High School Research

IJHSR
ijhighschoolresearch.org
RESEARCH ARTICLE

Three-Dimensional Hierarchical Porous Electrode Structure for Improved Performance in Battery Applications

Alan Wang
Westlake High School, 4100 Westbank Dr, Austin, TX 78746, Austin, TX, 78746, USA; alanwang285@gmail.com

ABSTRACT: The demand for lithium-ion batteries is rapidly increasing due to urgent needs for effective renewable energy storage. Particularly, attention has shifted towards thick electrodes, as they optimize the amount of active material in multi-battery systems, increasing the energy densities of these systems; however, thick electrodes lose capacity and stability at high output rates due to their low porosity. Current research aims to solve this by utilizing nanotechnology to create porous structures in cathode materials that greatly increase ion transport rates. Cathode materials are primarily studied since they reach 20% of anode capabilities, limiting overall performance. Previous studies have created porous channels and nanopore structures within cathode materials, but these approaches fail to resolve the inert problems of thick electrodes. This project presents a uniform three-dimensional porous network in $LiCoO_2$, a commercialized Lithium-ion battery cathode, using the polymer poly(methyl methacrylate) (PMMA) in both micrometer and nanometer scales as a template. After mixing $LiCoO_2$ with PMMA, the mixture is heated at high temperatures to burn out PMMA and sinter the templated $LiCoO_2$ powder into a monolithic electrode. The micrometer-sized pores enhance ion conductivity by shortening ion diffusion pathways, and the nanometer-sized pores improve stability by evenly distributing the battery electrolyte. Compared with commercial standards, these electrodes had up 200% greater specific capacities and 51.1% better capacity retention at high output rates, results that can be applied to numerous battery applications. This study furthers 3D nanostructure understanding and opens discussion about dual-scale porosity.

KEYWORDS: Materials Science; Nanomaterials; Energy Storage; Thick Electrodes; Porosity.

Introduction

Battery-powered devices and systems are becoming increasingly prevalent in the 21st century, as they are clean forms of energy. One of the most promising types of batteries are lithium-ion (Li-ion) batteries due to their higher energy and power densities (energy density: total amount of energy stored divided by the mass of battery; power density: rate at which electricity can be charged/discharged divided by the mass of battery), longer cycle life, and greater efficiency compared to other rechargeable battery types such as lead acid, nickel cadmium, sodium sulfur, and sodium nickel chloride.[1] Some of the popular applications for Li-ion batteries include electric vehicles, mobile devices, and robotic systems.[2] Li-ion batteries are also applicable in conjunction with energy-harvesting systems such as solar, wind and hydroelectric forms of energy.[3] While Li-ion batteries have become substantially better recently with greater energy densities, better cycling stability, faster charge/discharge rates, and lower costs, their electrochemical performance is still not sufficient to store enough energy from renewable sources to completely replace fossil fuels. Currently, cathode materials are the limiting factor in Li-ion battery cells for energy density. Anode materials such as graphene and magnetite (Fe_3O_4) can reach specific capacities of 400-1000 mAh g-1, while cathode materials such as $LiCoO_2$ and $LiFePO_4$ can only reach specific capacities of 140-170 mAh g-1.[4,5] Thus, to create Li-ion electrodes with greater energy densities and faster rate capabilities, areal mass of cathodes must be improved to meet anode capabilities.

With the introduction of nanotechnology in the past few decades, efforts to improve Li-ion battery performance are now focused on modifying the morphology (dimensions, weight, volume, porosity, structure) of existing materials. There are several methods to improve electrode energy density in Li-ion batteries, such as templating composite structures, doping cathode structures with other metals, carbon coating electrode material, and modifying electrolyte composition.[6,7] However, current efforts are mainly directed towards modifying electrode structure on a nanoscale to increase electrode porosity, especially in thick electrodes as they provide greater energy density in battery applications due to a greater ratio of active to inactive material.[8,9] Before this study, several other studies have created porous, thick cathodes using various methods such as utilizing wood's microscopic structure as a template, implementing magnetic alignment, and using laser processing to produce aligned porous channels within the cathode.[10-12] When cathode particles are oriented in channels, porosity is controlled, which increases the energy density, cycling stability, electronic conductivity in electrodes. Nevertheless, the overall density of the electrode remains relatively similar to an unmodified electrode since the pore channels are merely embedded into the electrode as better pathways for ion diffusion, but electrode areas without grooves still have the same properties as an unmodified thick electrode. Hence, while electrodes with porous channels may initially have high specific capacities and rate performance, they rapidly lose capacity at higher output rates. Additionally, metal oxides with mesoporous structures have also resulted in greater electrochemical properties such as greater energy and power densities due to a uniform and continuous pore network that permits efficient transport of electrons and ions while

DOI: 10.36838/v4i5.1

allowing fluids to pass through the internal structure.[13,14] Thus, when an electrolyte is applied to the mesoporous cathode structure, the interconnected pores cause a uniform distribution of the electrolyte, which decreases short circuit possibilities and produces more stable electrodes. While both processes modify thick electrode structure by controlling porosity, spherical polymer templating in a hierarchical format has not been utilized to create a uniformly porous electrode in combination with macropores. Moreover, several papers have adopted a hierarchical porosity strategy to improve electrode performance.[15-17] Bae *et al.* also studied $LiCoO_2$, however they implemented dual-scale pore channels into their electrode. Kwon *et al.* synthesized 3D pores by reacting GeO_2 with Zn to form pores within the Ge anode material. Vu *et al.* implemented a Carbon composite within a $LiFePO_4$ electrode to create a dual-scale porosity with nanopores. However, this study is different from these previous works as they have not introduced hierarchical porosity in both a micrometer and nanometer scale using polymer templating.

Through nanotechnology, electrode morphology and porosity can be modified at the nanoscale to increase battery performance. In this project, the porosity in $LiCoO_2$ (LCO) electrodes is controlled by creating a hierarchical pore network in a monolithic (monolith: single piece of material) thick-electrode (>300 µm thickness) using the spherical polymer poly(methyl methacrylate) (PMMA) in both a nano-size (~300 nm in diameter) and a micrometer size (30-80 µm in diameter) as templates. Both pore sizes increase ion transport rates and the surface area of the electrode. However, with the combination of the nano-sized pores and micro-sized pores, an interconnected porous network allows uniform electrolyte diffusion throughout the electrode. It is hypothesized that constructing ultra-thick free-standing monolith electrodes with a three-dimensional (3D) hierarchically interconnected pore network in Li-ion batteries will improve ion transport kinetics along the diffusion direction. Consequently, commercial LCO composite electrodes will have higher material utilization with an increased energy density while maintaining high power density, leading to more effective usage of renewable energy. Figure 1 captures the potential applications of a 3D hierarchically porous, thick LCO cathode (3D LCO) through a schematic illustration of the synthesis principle and outcome as well as the assembly process for experimentation battery cells. The experimentation battery cells used in this project were half coin cells (C-2032; Half Coin Cell: Li-ion battery assembled with only cathode material and lithium metal as anode to restrict results to cathode capabilities), and each cell contains a positive case, current collector, 3D LCO cathode monolith, liquid battery electrolyte, Li-metal, metal spacer, metal spring, and negative case. The liquid battery electrolyte is depicted on both sides of the separator since even though it is applied on top of the separator, the electrolyte imbues throughout the separator material, which coats both the cathode and the Li-metal.

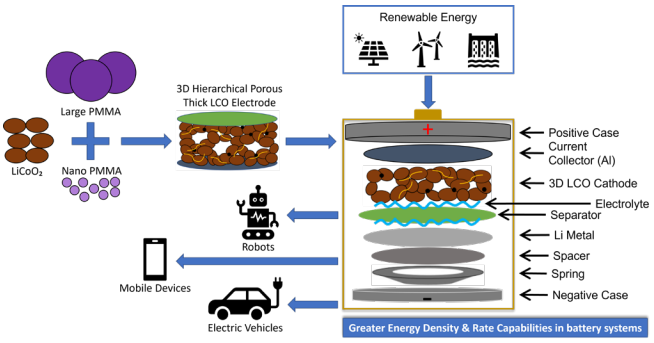

Figure 1: Schematic illustration of various applications of 3D hierarchical porous, thick LCO electrode with C-2032 coin cell assembly.

Methods

This section summarizes the procedures required to synthesize and test Li-ion battery cells using 3D LCO as a cathode in a Li-ion half-cell. Figure 2 depicts a flow chart of the experimental procedures with the utilized research equipment and the specified products at each step of the experimental process.

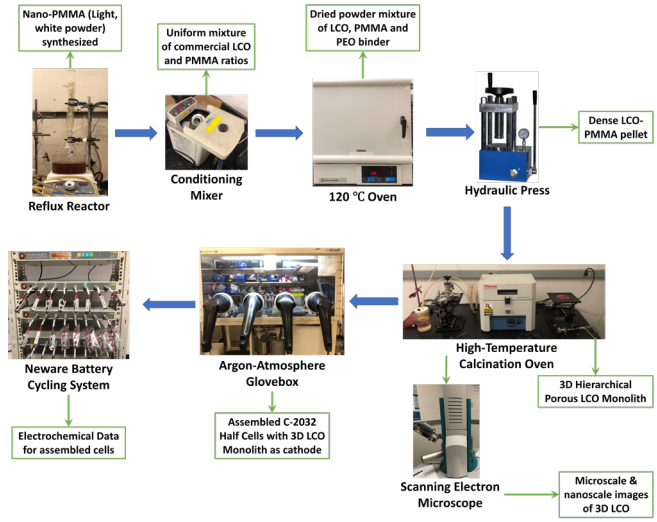

Figure 2: Schematic flow chart of experimental procedures required to synthesize, assemble, and test half Li-ion cells with 3D LCO monoliths as the cathode material (blue arrows: experimental steps; green arrows/boxes: attained products at specified steps).

Nanometer-sized PMMA Synthesis:

Nanometer-sized PMMA (nano PMMA) was synthesized via emulsion polymerization of the monomer methyl methacrylate (MMA), according to Peng *et al.*[18] First, 0.002 g sodium dodecyl sulfate was dissolved in 50 mL deionized water as a surfactant (surfactant: chemical agent that decreases solvent surface tension to permit effective reaction between different substances). Next, 7 g methyl methacrylate monomer and 0.056 g potassium peroxodisulfate, the initiator (initiator: chemical agent that initiates the polymerization process), were dissolved into the solution with continuous magnetic stirring. After, the solution underwent a reflux system reaction bubbled with nitrogen gas for 20 minutes to ensure that all oxygen gas was removed. Then, the reflux system was stirred for 2.5 hours at 70 °C to ensure reaction completion. After, the remaining solution was centrifuged and inserted into a 120 °C oven to dry so all solvents were evaporated.

3D Hierarchical Porous $LiCoO_2$ Monolith Synthesis:

Various PMMA ratios were tested to find the best performing measurements, but all monolith samples had 250 mg of $LiCoO_2$ active commercial powder (Sigma Aldrich), 50 mg PMMA (large and/or small), and 0.025 mL 10% weight polyethylene oxide (PEO)-lithium bistriflimide (TFSI) in acetonitrile solution (PEO solution serves as polymer binder between $LiCoO_2$ and PMMA). The PMMA ratios tested were 25 mg small PMMA with 25 mg large PMMA (25s/25L), 40 mg small PMMA with 10 mg large PMMA (40s/10L), and 50 mg small PMMA (50s). $LiCoO_2$ and respective PMMA amounts were first mixed using a conditioning mixer (Thinky Mixer AR-100) for 30 minutes to create a uniform mixture of $LiCoO_2$ and PMMA. Then, the LCO:PMMA mixture was ground together with the PEO-TFSI solution in a mortar and pestle for about 2 minutes until the mixture was powdered. After, 100 mg samples were weighed out and diced on a glass board to ensure material particle size uniformity, then dried for about 5 minutes in a 120 °C oven so the PEO-TFSI solvent was evaporated. Then, each sample was inserted into a hydraulic press for 1 minute at a pressure of 10 tons to create 3D hierarchically porous LCO (3D LCO) pellets. Afterward, each pellet was placed on a bed of commercial $LiCoO_2$ and calcined from 20 °C to 400 °C at a 2 °C /min ramping rate, then held at 400 °C for 2 hours, then heated 400 °C to 850 °C at a rate of 1 °C/min, then held at 850 °C for 2 hours, then cooled to room temperature naturally. The 3D LCO pellets were then placed on a bed of commercial LCO so that surface pore sites on the pellet would also be covered by LCO. The calcination oven was first set to a temperature of 400 °C to burn out the PMMA templates and PEO binder and was then set to 850 °C to sinter the electrode to form a single solid monolith material from the initial powder sample.

Electrode Assembly:

Once 3D LCO monolith has successfully been calcinated, the final step was electrode assembly. First, 10% conductive carbon (Super P) in N-methylpyrrolidone (NMP) solution was drop-casted onto the monolith until the monolith was sufficiently coated so that the monolith's surface and pores would both be covered by conductive carbon. Next, the monoliths were inserted into a vacuum oven at 120 °C overnight to evaporate the NMP solvent. After the monoliths were dry, 2032 half coin battery cells were assembled with the current collector, the monolith as the electrode, a separator, about 0.1 mL 1.0 M $LiPF_6$ (dissolved in 50/50 mixture of Ethylene Carbonate and Diethyl Carbonate) electrolyte solution Li-metal plate, a metal spacer, and a metal spring and tested on a Neware cycling machine system.

Results and Discussion

This section presents the results gathered for the 25s/25L, 40s/10L, and 50s samples after synthesis. Micrometer and nanometer scale images were taken by a Scanning Electron Microscope (SEM, Vega3 Tescan & Quanta FEG) and electrochemical data was tracked by a Neware battery testing system (Neware BT4000) for half coin cells containing 3D LCO.

Morphology Analysis :

In Figure 3, a schematic illustration for the electrode design of the 3D LCO electrode is shown. Figures 3a and 3b represent current thick electrodes, and Figures 3c, 3d, 3e, and 3f represent the newly synthesized 3D porous LCO electrode.

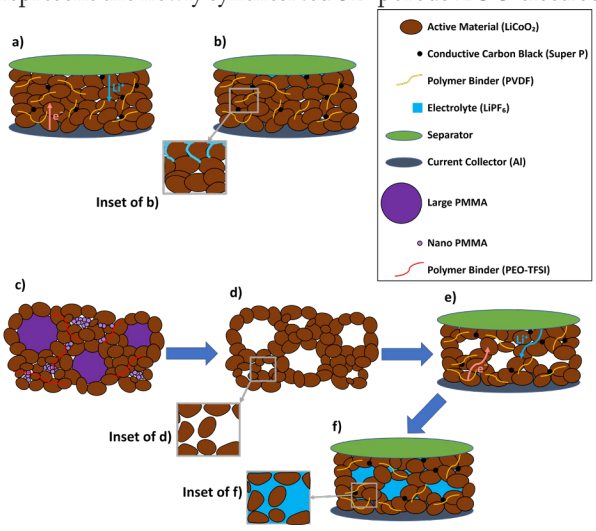

Figure 3: a: Thick LCO commercial electrode (Control); b: Control electrode with electrolyte; inset of b: Nanoscale depiction of electrolyte diffusion in control electrode; c: LCO mixed with large and nano PMMA before sintering; d: 3D porous LCO electrode after sintering; inset of d: Nanoscale depiction of 3D LCO electrode after sintering; e: 3D LCO electrode with conductive carbon and polymer binder; f: 3D LCO electrode with electrolyte; inset of f: Nanoscale depiction of electrolyte diffusion in 3D LCO.

As seen in Figures 3a and 3b, current thick electrodes cause Li ions to have much longer ion transport rates due to their lack of porosity and higher density. This causes thick electrodes to have worse rate performance than thin electrodes. In inset of Figure 3b, electrolyte diffusion is shown at the nanoscale. Due to the lack of porosity, the electrolyte remains near the top of the application spot, causing an uneven electrolyte distribution, which leads to significantly worse ion transport kinetics. Figure 3c depicts the initial mixing between LCO, large PMMA, nano PMMA, and the PEO-TFSI polymer binder. After sintering the electrode at high temperatures, Figure 3d shows the monolith product. Figure 3d's inset displays the electrode on a nanoscale and how mesopores formed by nano PMMA aggregates are present. Figure 3e displays the Li ion and electron pathways in the 3D LCO electrode, which have faster rates due to the increased porosity. Figure 3f shows electrolyte diffusion in the 3D LCO electrode, and the inset of Figure 3f illustrates how by adding nano PMMA into the electrode, the electrolyte can evenly spread throughout the electrode, allowing for greater ion transport kinetics.

To verify the existence of both large and small pores, SEM was used to observe the morphology, uniformity, and material size. In Figure 4, SEM images of large PMMA and nano-PMMA are shown respectively in 4a and 4b. Figures 4c, 4d, and 4e are images of the 25S/25L, 40S/10L, and 50S 3D LCO samples respectively at a 50 μm scale. In Figures 4f, 4g, and 4h, images of 25S/25L, 40S/10L, and 50S LCO samples

DOI: 10.36838/v4i5.1

are shown respectively at a 200 µm scale. The large PMMA in Figure 4a is shown to have a diameter of 30-80 µm, while nano PMMA particles have a diameter of ~300 nm. However, Figure 4b portrays how nano PMMA particles tend to aggregate, which causes the micropores found in Figures 4e and 4h. Figures 4c and 4d have clear evidence of larger micropores, whereas Figure 4e solely contains smaller micropores formed from nano PMMA. As seen in Figures 4f, 4g, and 4h, the samples had uniform LCO distribution throughout the material. Additionally, as the amount of nano PMMA added to each sample increased, the density of the material decreased due to a greater presence of micropores, shown in comparison between Figures 4f and 4h.

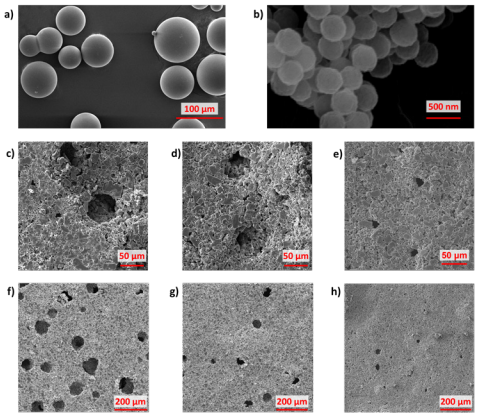

Figure 4: a: Large PMMA at 100 µm scale; b: Nano PMMA at 500 nm scale; c: 25S/25L LCO at 50 µm scale; d: 40S/10L LCO at 50 µm scale; e: 50S LCO at 50 µm scale f: 25S/25L LCO at 200 µm scale; g: 40S/10L LCO at 200 µm scale; h: 50S LCO at 200 µm scale

To determine the pore size distribution, histograms tracking pore diameter percentages for the 25S/25L, 40S/10L, and 50S samples (Figures 5a, 5b, and 5c respectively) at the 200 µm scale were created. Each histogram was created using an average of eight photos taken at various sites of the electrode, and pore diameter was found using ImageJ line drawing. In the 25S/25L and 40S/10L samples, most pores were in the projected 30-80 µm range, but there were some pores in the 80-90 µm range. These outliers are likely due to two large PMMA particles aggregating together, like the PMMA particles in the upper left corner of Figure 4a. In the 50S sample, aggregated nano PMMA particles mainly formed pores of 10-20 µm in diameter but some larger aggregates formed pores of 20-40 µm in diameter.

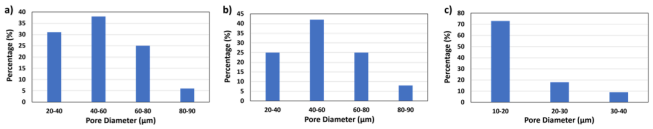

Figure 5: a: 25S/25L averaged pore histogram at 200 µm scale; 40S/10L averaged pore histogram at 200 µm scale; 50S averaged pore histogram at 200 µm scale

Electrochemical Data:

Specific Capacity (mAh g^{-1}) vs. Voltage (V), C-Rate vs. Specific Capacity (mAh g^{-1}), and C-Rate vs. Capacity Retention (%) plots for the 25S/25L, 40S/10L, and 50S LCO samples are shown in Figures 6a, 6b, and 6c respectively. These plots also include data from a standard thick electrode (~270 µm thick) to compare results with commercial capabilities. All values used for Figure 6 correspond with the discharge performance of the four cell types. From the plots in Figure 6a, all four cells reached a mid-voltage of ~3.9V at a rate of 0.1C. Additionally, all four cells had stable discharge output at a 0.1C rate as specific capacity increased, which is shown by the relatively flat middle section of the plots. However, at a 1C rate, as voltage declined, disparities between maximum specific capacities became evident. While the commercial electrode fell to a maximum capacity of 20 mAh g-1, the 25S/25L and 50S electrodes reached capacities of ~40 mAh g-1, and the 40S/10L electrode even reached a capacity of ~60 mAh g-1. As shown in Figure 6b, a large gap in specific capacity between the commercial electrode and the three 3D LCO samples forms at 0.3C that persists until 1C, revealing a significant difference in stability at higher output rates. In addition, although both the 3D LCO samples and commercial electrode decreased in capacity, the decrease rate for the commercial electrode was far greater than the rate for the 3D LCO electrodes, particularly between 0.2C to 0.5C. From Figure 6c, the capacity retention in the 25S/25L, 40S/10L, and 50S samples performed at similar efficiencies from 0.1C-1C, while the commercial electrode fell rapidly from 0.2C-0.5C. At 0.5C, the highest difference in capacity retention, at 51.1%, was between the 40S/10L and commercial electrode.

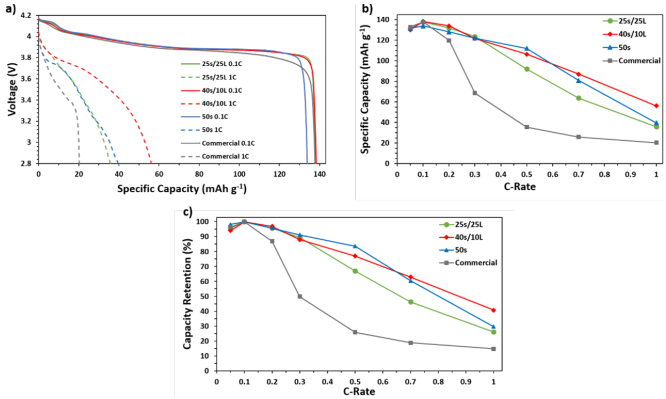

Figure 6: a: Specific Capacity (mAh g−1) vs. Voltage (V) plots of 3D LCO and commercial electrodes at 0.1C and 1C; b: Cycle Number vs. Specific Capacity (mAh g−1) plots of 3D LCO and commercial electrodes; c: Cycle Number vs. Capacity Retention (%) of 3D LCO and commercial electrodes

■ Conclusions & Future Work

In this study, $LiCoO_2$ thick electrodes with three-dimensional hierarchical pores were fabricated through polymer templating using poly(methyl methacrylate) in both micrometer and nanometer sizes. By creating an LCO electrode with a uniform pore distribution of both nanometer and micrometer pores, both electrode energy density and electrode stability are improved at all C-Rates.

The three tested samples all outperformed industry standards in energy densities and cell stability. The best performing sample, the 40S/10L ratio, had up to 200% greater specific capacities and 51.1% greater capacity retention than commercial standards. These results could potentially add 200 miles/charge to a Tesla Model S and 3 hours of battery life to an iPhone.

DOI: 10.36838/v4i4.1

conductive carbon to be more uniformly integrated in the material.

Additional future studies could include testing this synthesis approach with different cathode and anode materials, determining why trends in pore size distribution form, tracking Coulombic efficiency for these samples, and optimizing the nano and micro PMMA ratio.

Acknowledgements

The author greatly appreciates the support of this research from the Walker Department of Mechanical Engineering at the University of Texas at Austin, and particularly acknowledges Professor Guihua Yu and Dr. Xiao Zhang for their extensive help in scanning electron microscopy imaging, coin cell assembly, and research guidance.

References

1. Guney, M. S., & Tepe, Y. (2017). Classification and assessment of Energy Storage Systems. Renewable and Sustainable Energy Re views, 75, 1187–1197. https://doi.org/10.1016/j.rser.2016.11.102.. https://pubmed.ncbi.nlm.nih.gov/31467682/
2. Yang, Y., Okonkwo, E. G., Huang, G., Xu, S., Sun, W., & He, Y. (2021). On the sustainability of lithium ion battery industry – a review and perspective. Energy Storage Materials, 36, 186–212. https://doi.org/10.1016/j.ensm.2020.12.019.
3. Diouf, B., & Pode, R. (2015). Potential of lithium-ion batteries in renewable energy. Renewable Energy, 76, 375–380. https://doi.org/10.1016/j.renene.2014.11.058.
4. Goriparti, S., Miele, E., De Angelis, F., Di Fabrizio, E., Proietti Zaccaria, R., & Capiglia, C. (2014). Review on recent progress of nanostructured anode materials for Li-ion batteries. Journal of Power Sources, 257, 421–443. https://doi.org/10.1016/j.jpowsour.2013.11.103.
5. Fergus, J. W. (2010). Recent developments in cathode materials for lithium ion batteries. Journal of Power Sources, 195(4), 939–954. https://doi.org/10.1016/j.jpowsour.2009.08.089.
6. Zhang, X., Hui, Z., King, S., Wang, L., Ju, Z., Wu, J., Takeuchi, K. J., Marschilok, A. C., West, A. C., Takeuchi, E. S., & Yu, G. (2021). Tunable porous electrode architectures for enhanced Li-ion storage kinetics in thick electrodes. Nano Letters, 21(13), 5896–5904. https://doi.org/10.1021/acs.nanolett.1c02142.
7. Jyoti, J., Singh, B. P., & Tripathi, S. K. (2021). Recent advancements in development of different cathode materials for rechargeable lith ium ion batteries. Journal of Energy Storage, 43, 103112. https://doi.org/10.1016/j.est.2021.103112.
8. Singh, M., Kaiser, J., & Hahn, H. (2015). Thick electrodes for high energy lithium ion batteries. Journal of The Electrochemical Soci ety, 162(7). https://doi.org/10.1149/2.0401507jes.
9. Wu, J., Zhang, X., Ju, Z., Wang, L., Hui, Z., Mayilvahanan, K., Takeuchi, K. J., Marschilok, A. C., West, A. C., Takeuchi, E. S., & Yu, G. (2021). From fundamental understanding to engineering design of high-performance thick electrodes for scalable energy-storage systems. Advanced Materials, 33(26), 2101275. https://doi.org/10.1002/adma.202101275.
10. Lu, L.-L., Lu, Y.-Y., Xiao, Z.-J., Zhang, T.-W., Zhou, F., Ma, T., Ni, Y., Yao, H.-B., Yu, S.-H., & Cui, Y. (2018). Wood-in spired high-performance ultrathick bulk battery electrodes. Ad vanced Materials, 30(20), 1706745. https://doi.org/10.1002/adma.201706745.
11. Sander, J. S., Erb, R. M., Li, L., Gurijala, A., & Chiang, Y.-M. (2016). High-performance battery electrodes via magnetic templating. Nature Energy, 1(8). https://doi.org/10.1038/nener gy.2016.99.
12. Park, J., Jeon, C., Kim, W., Bong, S.-J., Jeong, S., & Kim, H.-J. (2021). Challenges, laser processing and electrochemi cal characteristics on application of ultra-thick electrode for high-energy lithium-ion battery. Journal of Power Sources, 482, 228948. https://doi.org/10.1016/j.jpowsour.2020.228948.
13. Peng, L., Fang, Z., Zhu, Y., Yan, C., & Yu, G. (2017). Holey 2d nanomaterials for electrochemical energy storage. Advanced Energy Materials, 8(9), 1702179. https://doi.org/10.1002/aenm.201702179.
14. Celik, E., Ma, Y., Brezesinski, T., & Elm, M. T. (2021). Ordered mesoporous metal oxides for electrochemical applications: Cor relation between structure, electrical properties and device per formance. Physical Chemistry Chemical Physics, 23(18), 10706–10735. https://doi.org/10.1039/d1cp00834j.
15. Bae, C.-J., Erdonmez, C. K., Halloran, J. W., & Chiang, Y.-M. (2012). Design of battery electrodes with dual-scale porosity to minimize tortuosity and maximize performance. Advanced Materials, 25(9), 1254–1258. https://doi.org/10.1002/adma.201204055.
16. Kwon, D., Ryu, J., Shin, M., Song, G., Hong, D., Kim, K. S., & Park, S. (2018). Synthesis of dual porous structured germanium an odes with exceptional lithium-ion storage performance. Journal of Power Sources, 374, 217–224. https://doi.org/10.1016/j.jpowsour.2017.11.044.
17. Vu, A., & Stein, A. (2011). Multiconstituent synthesis of LiFePO4/C composites with hierarchical porosity as cathode ma terials for lithium ion batteries. Chemistry of Materials, 23(13), 3237–3245. https://doi.org/10.1021/cm201197j.
18. Peng, J., Zhang, T., Zhang, H., Zhang, Z., Li, Z., Lei, G. (2012). Synthesis and electrochemical performance of three-dimen sionally ordered macroporous licoo2. Journal of Solid State Elec trochemistry, 16(9), 3079–3085. https://doi.org/10.1007/s10008-012-1752-1.

Author

Alan Wang is a junior at Westlake High School in Austin, Texas. He is interested in studying energy systems and the intersection between materials science and electrical engineering in the future.

DOI: 10.36838/v4i5.1

IJHSR
ijhighschoolresearch.org
■ RESEARCH ARTICLE

Development of Highly Efficient Cellular Uptake Cell-Penetrating Peptide for Novel Cancer Treatment

Hongji Kim
Yongsan International School of Seoul, 285 Itaewon-ro, Yongsan-gu, Seoul, 04347, South Korea; bonettekim.8680@gmail.com

ABSTRACT: Cell-penetrating peptides (CPPs) are short peptides, which can carry various types of molecules into cells. Therefore, CPPs have been predominantly used in preclinical and basic cancer research for more than 30 years. However, low cellular uptake of CPPs caused severe side effects for breast cancer treatment. CPPs are rich in positively charged amino acids such as arginine and lysine and can translocate over membranes and gain access to the cell interior. Therefore, we hypothesized that the addition of positive charge peptides on cell-penetrating peptides would enhance the cellular uptake of CPPs. In this study, we constructed three types of CPPs: BR2 (+7 charge), R9 (+9 charge), BR2-R9 (+16 charge). To localize the CPPs inside the cancer cells, we added Fluorescein isothiocyanate (FITC), which is a bright green fluorophore, on the C-terminal of each peptide. BR2-R9 showed much higher cellular uptake compared to BR2 and R9 on both human breast cancer cell lines (MCF-7 and MDA-MB-231). This result indicates that BR2-R9, which contains the most positive amino acids, can be applied for efficient drug delivery in cancer treatment. This study successfully develops a novel CPP for enhancing the cellular uptake in cancer cells and provides new insights into clinical applications of cancer treatment.

KEYWORDS: Biology; Cancer Biology; Cell-penetrating peptide; Cancer Treatment.

■ Introduction

Breast cancer occurs everywhere around the world, among women who are in the stages of puberty or later. In 2022, 2.3 million women were diagnosed with breast cancer, with about 680,000 deaths worldwide. However, near the end of 2022, 7.8 million women with breast cancer were still alive. This made breast cancer the most "prevalent" cancer globally because of its 90% 5-year survival rate.[1]

In breast cancer chemotherapy, drugs are used to target and destroy breast cancer cells. The drugs are usually injected into a vein or are also taken as pills. Chemotherapy is often used with several other treatments like surgery, radiotherapy, or hormone therapy. It helps increase the chances of a cure, reduce the risk of cancer recurrence, or lessen cancer symptoms. Importantly, if breast cancer has spread to other body parts, chemotherapy can be used as the primary treatment. However, it carries a risk of side effects such as hair loss, easy bruising, infection, and many more.[2]

In radiotherapy, high-energy X-rays, protons, or other particles are used to kill cancer cells, as cancer cells are more prone to the effects of radiation therapy than normal cells. The radiation for breast cancer may be delivered through external and internal radiation. It is an effective way to decrease breast cancer recurrence and ease the symptoms caused by cancer. Many patients also use radiotherapy if breast cancers are too big to remove through surgery or have inflammatory breast cancer. However, there may be side effects like fatigue, skin irritation, or breast swelling.[3]

Hormone therapy is used to block hormones from attaching to the receptors of cancer cells or even to reduce the body's production of hormones. This method is often used after surgery to decrease the risk of cancer recurrence. It may also be used to shrink a tumor before going into surgery. Hormone therapy is mainly used for hormone receptor-positive breast cancers, also called ER-positive or PR-positive by doctors. However, there can also be significant side effects such as nausea, vaginal irritation, muscle pain, etc. Apart from therapy, medications like tamoxifen or toremifene block hormones from attaching to cancer cells.[4]

Cell-penetrating peptides consist of peptides (short chains of amino acids) that allow entering endocytic pathways to transport the molecules across the cell membrane. Many of them are known to mediate intracellular delivery of nucleic acids, proteins, or nanoparticles.[5] The peptide sequences have a positive charge and are rich in lysine or arginine. Their physicochemical properties also classify CPPs into categories like cationic, amphipathic, and hydrophobic classes. Many approaches have been developed to enhance the permeability of therapeutic proteins by attaching them to a CPP.[6] The peptide-based delivery can increase the consumption of drugs in tumor cells and increase the effectiveness of certain treatments of either small molecule drugs or oligonucleotide-based therapeutics. Additionally, as CPP can transport cargoes into the cell, CPP-based delivery is a promising strategy for cancer drug delivery. CPP can be helpful to both chemotherapeutics and modern gene-based drugs for delivering them into tumor cells.[7]

In this study we hypothesized that the addition of positive charge peptides on cell-penetrating peptides would enhance the cellular uptake of CPPs. We constructed three types of CPPs: BR2 (+7 charge), R9 (+9 charge), BR2-R9 (+16 charge) and tested their efficacy.

■ Methods

Cell culture and maintenance:

Human breast cancer cell line MCF7 and MDA-MB-231 were purchased from Korea Cell Line Bank. RPMI 1640

DOI: 10.36838/v4i5.2

(Gibco) with 10% fetal bovine serum and 1% penicillin and streptomycin was used to culture cancer cell lines. The cells were maintained in a 37 ˚C CO_2 cell incubator.

CPP stock solution preparation:

The weight of the CPP powder was measured to prepare the stock solution for each CPP (BR2, R9, and BR2-R9). The stock concentration of 1 mM of each CPP was prepared. 1.2 mg of BR2 powder was measured, and 535.7 mL DMSO was added. 1.7 mg of R9 powder was measured, and 882.7 mL DMSO was added. 0.8 mg of BR2-R9 powder was measured, and 204.1 mL DMSO was added.

CPP delivery optimization test:

Two glass slides were prepared to test the CPP delivery efficiency. Each glass slide has eight sections. One slide was used for MCF7, and the other slide was used for MDA-MB-231. Both of the slides consisted of two no-treatment sections, and the other sections contained 5 mM and 10mM concentrations for BR2, R9, and BR2-R9 (Figure 1).

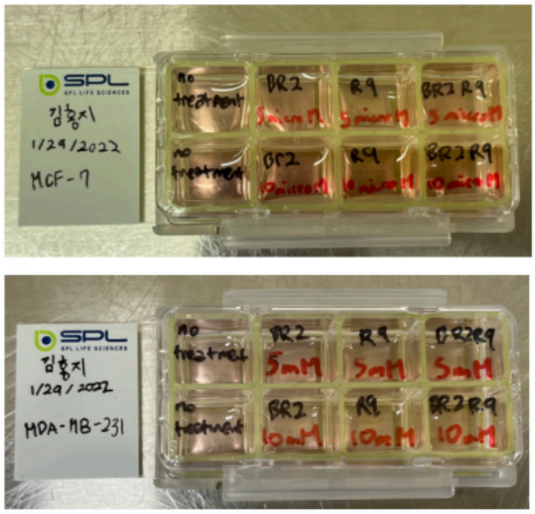

Figure 1: Cell containing slide for testing CPP delivery efficiency.

CPP delivered cell fixation and fluorescence imaging:

300 µL of methanol was added to each slide after removing all the cell media from the cell slide. The methanol was removed after 10 minutes of incubation. 15 µL of DAPI-containing mounting solution (VECTASHIELD) was added in the middle of each sample. The glass slide was covered on top of the cell containing the slide. Then, the slide was placed on the fluorescence microscope (Nikon), and the image of the cells was photographed.

Quantification of green fluorescence cells:

After the cell media was removed, we added the Trypsin-EDTA and incubated the cells for five minutes. 400µL RPMI media, cells, and the CPPs (BR2, R9, BR2R9) were added to each tube. The tubes were incubated for 10 minutes. 15 µl of the cell suspension was added into a PhotonSlide (Logos Biosystem). The LUNA-FL, a cell counting device, was used to count the green-fluorescent cells.

Results and Discussion

We used herein to design several CPP with cancer cell specificity. BR2, a motif of an anticancer peptide Buforin IIB, is a 17-amino acid peptide that was found to have cancer-specificity without toxicity to normal cells (Table 1). BR2 enters the cancer cells after targeting them with gangliosides through lipid-mediated micropinocytosis. BR2 also showed a higher membrane translocation efficiency than the other CPPs.[8]

Table 1: The CPPs used in this study and charge number.

Name	Sequence	Charge
BR2	RAGLQFPVGRLLRRLLR (17 aa)	+ 7
R9	RRRRRRRRR (9 aa)	+ 9
BR2-R9	RAGLQFPVGRLLRRLLRRLLR-RRRRRRRRR (30 aa)	+ 16

Arg[9], a synthetic homophily-arginine nonapeptide (R9), plays an essential role in cellular uptake. R9 is a cell-penetrating peptide (CPP) with a cationic guanidinium group that forms electrostatic interactions with anionic cell membrane components like phospholipids and sulfated proteoglycans.[9] The interaction can also trigger intracellular signaling and internalization in many pathways. Since R9 has a simple peptide structure with positive charges, R9 has been extensively studied with many peptide modifications for specific drug delivery.[10]

A high concentration of BR2 is needed for cancer cell delivery since BR2 shows relatively low cell delivery in cancer cells. We combined BR2 and R9 to synthesize the BR2-R9 fusion peptide to solve this problem. BR2 has a charge of +7, and R9 has a charge of +9, making BR2-R9 have a charge of +16 (Table 1). The positive charge will increase the electrostatic interaction, and this property will allow more cellular uptake in cancer cells.

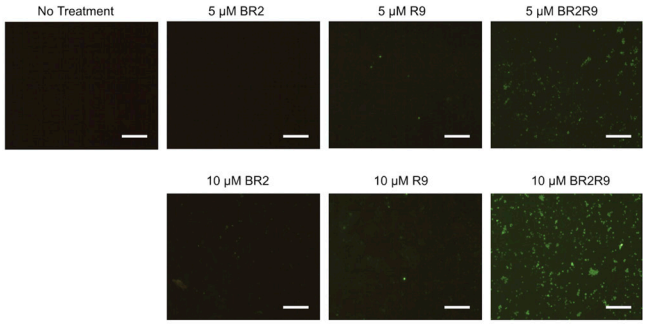

Figure 2: BR2-R9 showed the most efficient cell penetration on MCF7 breast cancer cell line. MCF7 cells were incubated with either 5 µM and 10 µM of BR2, R9, or BR2-R9 for 48 hours. The green fluorescence cells indicate the CPP uptake cells. Scale bar = 200 µm.

We aimed to analyze the cellular uptake level of BR2, R9, and BR2-R9 on MCF7 breast cancer cells. Either 5 µM and 10 µM of BR2, R9, or BR2-R9 were incubated with MCF7 cells for 48 hours. Then, we photographed the green-fluorescent positive cells using a fluorescence microscope. The green-fluorescent cells indicate the CPP cellular uptake (Figure 2). Both 5 µM and 10 µM of BR2 treatment conditions showed the lowest number of cells with green fluorescence. The treatment conditions of 5 µM and 10 µM of R9 showed

DOI: 10.36838/v4i5.2

an increased number of green-fluorescent cells compared to BR2 treatment conditions (Figure 2). This result indicates that the cellular uptake of R9 is higher than BR2. As expected, both 5 μM and 10 μM of BR2R9 treatment conditions exhibited the highest number of green-fluorescent cells than BR2 and R9 (Figure 2). We speculate that this result is due to the positive charges of BR2 and R9 fusion peptides. In conclusion, BR2R9 fusion peptides show the most efficient cellular uptake on MCF7 breast cancer cells.

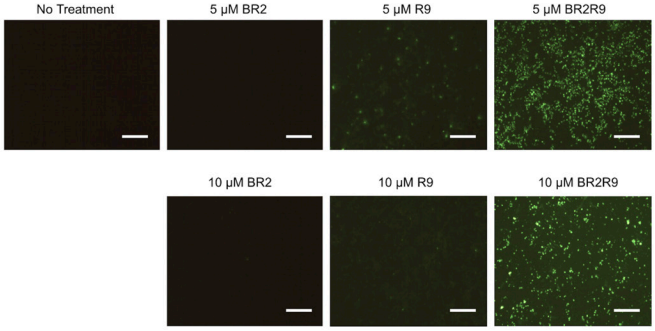

Figure 3: BR2-R9 showed the most efficient cell penetration on the MDA-MB-231 breast cancer cell line· MDA-MB-231 cells were incubated with either 5 μM and 10 μM of BR2, R9, or BR2-R9 for 48 hours. The green fluorescence cells indicate the CPP uptake cells. Scale bar = 200 μm.

Next, we analyzed the cellular uptake of CPP on different breast cancer cell lines to confirm the result in Figure 2. MDA-MB-231, which is known to have more invasive characteristics than MCF7 was used to test the cellular uptake of BR2, R9, and BR2-R9. MDA-MB-231 was incubated with 5 μM and 10 μM of BR2, R9, or BR2-R9 for 48 hours. We took photos through a fluorescence microscope to check the results of the green fluorescent positive cells. The green fluorescent cells and their CPP cellular uptake are shown (Figure 3). The 5 μM and 10 μM of BR2 treatment conditions showed the lowest number of cells with green fluorescence (Figure 3). The treatment conditions of 5 μM and 10 μM of R9 showed a greater increase in green fluorescent cells than BR2 treatment conditions (Figure 3). This result indicates that the cellular uptake of R9 is higher than BR2 in both MCF7 and MDA-MB-231. As hypothesized, both 5 μM and 10 μM of BR2-R9 treatment conditions appeared to have the highest number of green fluorescent cells than BR2 and R9 on MDA-MB-231 cells (Figure 3). Additionally, there was more cellular uptake in MDA-MB-231 than MCF7, as we can see that there are more green fluorescent cells present in MDA-MB-231 than MCF7 (Figure 3). BR2R9 fusion peptides showed the highest cellular uptake on MDA-MB-231 (Figure 3).

After the treatment of BR2, R9, and BR2-R9 on both MCF7 and MDA-MB-231, we used a cell counter device to calculate the percentage of green-fluorescent cells. We used three CPP treatment concentrations to quantify the green-fluorescent cells on MCF7 and MDA-MB-231. Each CPP was incubated with the cells for only 10 minutes. After the incubation, the cells were inserted into cell counting slides. Finally, the cell counter device quantified the percentage of green-fluorescent cells. The 0 μM CPP concentration showed no green-fluorescent cells, indicating there were no green-fluorescent cells without CPP treatment (Table 2). The 5 μM of

Table 2: · Quantification of green fluorescence cells using cell counter device.

CPP concentration	Type of CPP	Cell type	
		MCF7	MDA-MB-231
0 μM	-	0 %	0 %
5 μM	BR2	0 %	11.2 %
	R9	21.7%	4.1%
	BR2-R9	73.8%	97.6%
10 μM	BR2	0%	0 %
	R9	5.5%	4.5%
	BR2-R9	56.1%	84.1%

BR2 shows 0% green-fluorescent cells on MCF7 and 11.2% on MDA-MB-231 (Table 2). The 5 μM of R9 shows 21.7% green-fluorescent cells on MCF7 and 4.1% on MDA-MB-231 (Table 2). The 5 μM of BR2-R9 shows 73.8% green-fluorescent cells on MCF7 and 97.6% on MDA-MB-231 (Table 2). The 10 μM of BR2 shows 0% green-fluorescent cells on MCF7 and 0% on MDA-MB-231 (Table 2). The 10 μM of BR2 shows 5.5% green-fluorescent cells on MCF7 and 4.5% on MDA-MB-231 (Table 2). The 10 μM of BR2 shows 56.1% green-fluorescent cells on MCF7 and 84.1% on MDA-MB-231 (Table 2). In conclusion, BR2-R9 had the most cellular uptake in MCF7 and MDA-MB-231.

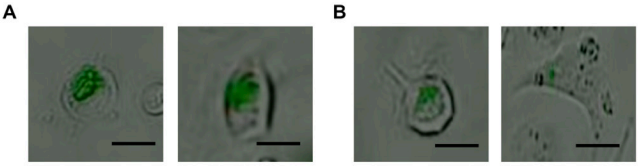

Figure 4: BR2-R9 penetrates the cell membrane and localizes inside the breast cancer cell lines. (A) Green fluorescence of BR2-R9 inside MDA-MB-231 cells. (B) Green fluorescence of BR2-R9 inside MCF7 cells. Scale bar= 10 μm.

Next, we used a 200x magnification microscope to observe BR2-R9 localization inside the breast cancer cells in higher resolution. Since BR2-R9 contains a FITC tag, which emits a green-fluorescent signal, we hypothesized that a green fluorescence signal would be detected inside the cancer cells. After we incubated MCF7 and MDA-MB-231 cells with BR2-R9 for 48 hours, the image was captured to analyze the internalization of BR2-R9. We detected that BR2-R9 was localized inside the cells as the green-fluorescent signal appears to cover about 60% of the cells. This indicates that BR2-R9 covers more than half of the cell components. We can also see that BR2-R9 CPPs were aggregated towards a certain cell membrane rather than being present in all parts of the MDA-MB-231 cells (Figure 4A). We detected that MCF7 was present inside the cells, but the green-fluorescent signal covers less than MDA-MB-231. The BR2-R9 CPPs in MCF7 were aggregated towards a certain side of the cell, similar to MDA-MB-231 (Figure 4B). In conclusion, we can see that BR2-R9 successfully penetrates the cell membrane of both MCF7 and MDA-MB-231 cells. When BR2-R9

enters the cells, they are aggregated in specific regions of the cells. Even after 48 hours of incubation, the BR2-R9 remained inside the cells. This indicates that this fusion peptide is stable in breast cancer cells for at least 48 hours.

Conclusion

The fusion peptides that we created can be used to make better drug delivery or breast cancer treatment. We can also use low concentrations of CPP, which can also lower the cost of the treatment strategies. Using low concentrations will reduce the side effects as well. The cellular cytotoxicity of CPPs can be a limitation because it was not investigated in this study. Additionally, more human cancer cells can be tested because this study only used two models. In the future, we can widen our field and experiment with other types of cancer cells and use mouse models for our study and test the CPP delivery in these different kinds of cancer cells. More investigation on how the CPP enters the cells should be studied in the future.

Acknowledgements

I would like to thank my teacher Woo Rin Lee for helping me with this project. He allowed me to work on this project in detail. Along with that, I would also like to thank my parents for supporting me.

References

1. DeSantis, C. E.; Ma, J.; Gaudet, M. M.; Newman, L. A.; Miller, K. D.; Goding Sauer, A.; Jemal, A.; Siegel, R. L. Breast Cancer Statistics, 2019. *CA Cancer J. Clin.* **2019**, 69 (6), 438–451.
2. Waks, A. G.; Winer, E. P. Breast Cancer Treatment: A Review. *JAMA* ***2019***, 321 (3), 288–300.
3. Balaji, K.; Subramanian, B.; Yadav, P.; Anu Radha, C.; Ramasubramanian, V. Radiation Therapy for Breast Cancer: Literature Review. *Med. Dosim.* **2016**, 41 (3), 253–257.
4. Abdulkareem, I. H.; Zurmi, I. B. Review of Hormonal Treatment of Breast Cancer. *Niger. J. Clin. Pract.* **2012**, 15 (1), 9–14.
5. Feni, L.; Neundorf, I. The Current Role of Cell-Penetrating Peptides in Cancer Therapy. *Adv. Exp. Med. Biol.* **2017**, 1030, 279–295.
6. Shin, M. C.; Zhang, J.; Min, K. A.; Lee, K.; Byun, Y.; David, A. E.; He, H.; Yang, V. C. Cell-Penetrating Peptides: Achievements and Challenges in Application for Cancer Treatment. *J. Biomed. Mater. Res. A* **2014**, 102 (2), 575–587.
7. Regberg, J.; Srimanee, A.; Langel, U. Applications of Cell-Penetrating Peptides for Tumor Targeting and Future Cancer Therapies. *Pharmaceuticals (Basel)* **2012**, 5 (9), 991–1007.
8. Lim, K. J.; Sung, B. H.; Shin, J. R.; Lee, Y. W.; Kim, D. J.; Yang, K. S.; Kim, S. C. A Cancer Specific Cell-Penetrating Peptide, BR2, for the Efficient Delivery of an ScFv into Cancer Cells. *PLoS ONE* **2013**, 8 (6), e66084.
9. Yamashita, H.; Kato, T.; Oba, M.; Misawa, T.; Hattori, T.; Ohoka, N.; Tanaka, M.; Naito, M.; Kurihara, M.; Demizu, Y. Development of a Cell-Penetrating Peptide That Exhibits Responsive Changes in Its Secondary Structure in the Cellular Environment. *Sci. Rep.* **2016**, 6, 33003.
10. Liu, B. R.; Huang, Y.-W.; Lee, H.-J. Mechanistic Studies of Intracellular Delivery of Proteins by Cell-Penetrating Peptides in Cyanobacteria. *BMC Microbiol.* **2013**, 13, 57.

Author

Hongji Kim is a sophomore at Yongsan International School of Seoul in South Korea. Her strong interest in the different fields of sciences led her to investigate more about biology and motivated her to spend more time researching breast cancer.

DOI: 10.36838/v4i5.2

IJHSR
ijhighschoolresearch.org
■ RESEARCH ARTICLE

Development of Dextranase for Toothpaste Supplement for Efficient Removal of Dental Biofilm

Gahyun Lee
Hong Kong International School, 1 Red Hill Rd, Tai Tam, Hong Kong, Hong Kong SAR; gclare.lee@gmail.com

ABSTRACT: The accumulation of plaque is produced by oral bacterial pathogens, *Streptococcus mutans* (*S. mutans*), which causes dental cavities. Dextranase can prevent dental caries by degrading dextran (the main component of plaque biofilm). However, dextranase is unstable in dental care products such as toothpaste. Therefore, this project aims to increase the stability and specificity of dextranase in toothpaste. We hypothesized that agarose encapsulation would increase dextranase stability and encapsulated hydroxyapatite nanoparticle (HA)-immobilized dextranase in toothpaste would increase biofilm (produced by *S. mutans)* degradation specificity. We tested the immobilization yield with a DNSA assay. The results indicated that 5 % HA was the most optimized immobilization condition. To increase the stability of the immobilized HA-dextranase by preventing dextranase degradation, agarose, a natural non-toxic polysaccharide, was used to encapsulate HA-dextranase into uniform agarose beads. To test the stability of dextranase, 1% Dextranase, 5% HA-Dextranase, and Encapsulated HA-dextranase were mixed in sodium acetate, 1 % toothpaste, and 100 % toothpaste conditions at 25 ˚C and 50 ˚C for 48 hours. The result showed that encapsulated HA-dextranase had the highest relative stability in 100% toothpaste at 50 ˚C. Biofilm formation of *S. mutans* was quantified to test the specificity of dextranase in degrading biofilm. The results showed the greatest amount of *S. mutans* degradation occurred with encapsulated HA-dextranase. Overall, immobilized HA-dextranase removed biofilm most effectively and increased the specificity of dextranase from agarose encapsulation. This research can be applied in formulating toothpaste with dextranase to increase dental plaque biofilm removal efficiency.

KEYWORDS: Molecular Biology; Biochemistry; *Streptococcus mutans*; Dextranase; Hydroxyapatite.

■ Introduction

Most toothpaste contains fluoride to help prevent dental caries.[1] However, there are limitations to fluoride in removing dental cavities. Fluoride, since it is a chemical, in large amounts can cause several health issues.[2] Excess fluoride exposure can cause skeletal fluorosis, a bone disease that impairs joint mobility, causing stiffening and fractures in bones and joints.[3] Exposure to large fluoride concentrations during childhood can result in mild dental fluorosis, where white specks appear on tooth enamel.[4] Abrasives in toothpaste is another limitation with current too. If there is a more significant number of abrasives than is safe, relative dentin abrasion (RDA) levels amount above 250 can lead to microabrasions, harming tooth enamel.

Dextranase is a substance that can be applied to toothpaste to overcome the current limitations.[5] Dextranase degrades dextrans preventing dental caries. When applying it to toothpaste, the most important problems with dextranase paste are low stability (easily degraded in toothpaste) and low specificity (randomly distributed in the mouth).[6] Therefore, in this research, dextranase is engineered to increase its stability and specificity for the efficient removal of dental biofilm. First, dextranase is encapsulated with hydrophilic agarose gel to increase stability; then, dextranase is immobilized with hydroxyapatite (HA) nanoparticles (<200nm) to enhance the specificity of degrading biofilm.

Dextranase is a hydrolase (an enzyme that uses water to break chemical bonds) that prevents tooth decay.[5] Dextranase prevents dental caries by breaking down or cleaving dextran (a complex branched glucan that is a component of plaque biofilm and occurs naturally in sucrose) and eliminating dental plaque. Due to its properties, dextranase has several industrial applications as a potential oral wash ingredient (to prevent dental caries), clearing contaminants such as dextran during cane sugar manufacturing, and synthesizing oligosaccharides.[7]

As mentioned above, dextran is a complex branched glucan, or a group of glucose polymers made by a specific bacterium, *Streptococcus mutans (S. mutans)*, and sucrose.[8] Dextran is used as plasma volume expanders and anticoagulants. Although dextran is biodegradable, it can also be cleaved by dextranase (an enzyme). In biological experiments and industry, it serves various purposes. Additionally, dextran is found naturally in sucrose, confectionery, jams, and syrups.[9]

S. mutans is a bacterium that causes the formation of dental caries and inhabits the human oral cavity.[10] It causes tooth decay when inhabiting dental plaque, a biofilm that forms on human teeth. *S. mutans* use sugars such as sucrose derived from food to build a capsule on the tooth's hard surface. Inside the formed capsule, the bacteria use more sugar to fuel metabolism and lactic acid, attacking the tooth's enamel. Moreover, *S. mutans* have specific properties that allow them to form dental caries.[11] They can colonize the tooth, which damages the tooth enamel by synthesizing sucrose and glucan, metabolizing various carbohydrates into organic acids tolerating low pH environments.

Overall, the purpose of this experiment was to engineer dextranase with two processes: 1) immobilize dextranase with hydroxyapatite nanoparticles (<200nm), 2) encapsulating the

DOI: 10.36838/v4i5.3

immobilized dextranase with hydrophilic agarose gel. Then, the stability of dextranase and specificity of degrading biofilm produced from *S. mutans* was tested. The results demonstrated increased stability and specificity of dextranase, supporting the hypothesis.

Methods

Chemicals stock solution preparation:

205.07 mg of sodium acetate (Sigma) was weighed on a weighing boat on a densimeter. The sodium acetate was added into 50 mL of water and measured and added into a 50 mL tube (BD). 80 mL of 0.5M Sodium hydroxide was measured from the previously made solution. 2.18 g of 3,5-Dinitrosalicylic acid (DNSA) (Daejung) was weighed on a densimeter. On a heating plate, at 70 ˚C, it was stirred until the DNSA powder was completely dissolved. After 30 g of Sodium potassium tartrate (Sigma) was weighed on a densimeter, it was added to the mixture. Inside the bottle, water was added up to 100 mL. 10 mL of 50 mM sodium acetate was measured into a 15 mL tube using a pipetting aid. 0.3 g of Dextran 70 (Tokyo Chemical Industry) was weighed on a weighing boat on a densimeter then added into the tube with sodium acetate. 100 mL of water was measured. 2 g of Sodium Hydroxide (Duksan) was measured using a weighing boat on a densimeter. Both 100 mL of water and 2 g of Sodium Hydroxide were added to a 250 mL glass bottle (Pyrex). To prepare 1% dextranase 1 µL of Dextranase (Sigma) and 99 µL of sodium acetate were taken with pipettes to a tube for a total of 100 µL. To prepare 1% toothpaste solution, 0.05 g of toothpaste (Perioe) was measured directly inside a 15 mL tube on a densimeter. 5 mL of 50mM sodium acetate was added into the same 15 mL tube. The solution was mixed well with a vortexer. 0.9% Sodium chloride was made with 500 mL water measured inside a beaker. 4.5 g of Sodium Chloride (Bio Basic Inc.) was weighed and added to the glass bottle. 50 mL of Paraffin liquid (Samchun) was measured and added to a glass bottle. 1.5 mL of Tween #80 (Samchun) was measured and added into a 50 mL tube (BD) to make 3 % Tween #80 in Paraffin oil. The Tween #80 liquid is an emulsifier in this solution. 2 g of agarose powder was weighed and added to the glass bottle with 50 mL of 0.9% sodium chloride to make a 4% agarose solution. The solution was microwaved so the agarose dissolved in the solution at a temperature between 80-90˚C.

Dextranase activity assay:

The DNS/DNSA method was used for the dextranase activity assay. 1 µL of the dextranase solution was put inside a 1.5 mL tube. 49 µL of sodium acetate was added to the same 1.5 mL tube to make a diluted dextranase solution. 50 µL of each (dextranase) enzyme solution and 150 µL of 3 % dextran was pipetted into 1.5 mL tubes. The contents were mixed well on a vortexer. The tubes were placed on a 60˚C heating block for 15 minutes. 200 µL of DNSA reagent was added to stop the reaction. The samples were boiled for 5 minutes on a heating plate. The samples were pipetted into 15 mL tubes containing 3 mL of distilled water added with a pipetting aid to dilute the concentration solutions and then mixed well using a pipette. In order to determine dextranase activity, the samples were pipetted into a microplate to measure the absorbance of the mixture at 540 nm using a spectrometer. The same assay was repeated for HA-dextranase Immobilization.

HA-Dextranse immobilization:

100 µL of dextranase and 9900 µL of sodium acetate were pipetted into a 15 mL tube to make 10 mL of 1 % dextranase solution. Eight 1.5 mL tubes were prepared for each Hydroxyapatite nanoparticle (HA) (Aldrich) amount. With a volume to weight ratio of 1 mL: 1 g = 100 %, the HA (g) percentage was determined. In this experiment, 0 % (0 g), 0.1 %, (0.001 g), 0.5 % (0.005 g), 1 % (0.01 g), 5 % (0.05 g), and 10 % (0.1 g) were prepared. The HA powder was measured on weighing boats inside a densimeter. The HA beads were crushed by the spoon, and powder was left on the weighing boat. The samples were incubated on a shaker for 10-12 minutes. The tubes were centrifuged at 13,800 g for 5 minutes to settle the solution from the sides of the tubes to be compacted. 1 µL of each HA-dextranase solution sample was pipetted into other tubes with 49 µL of sodium acetate. Dextranase activity assay was used to determine HA-dextranase immobilization yield by measuring the dextranase that did not bind with the HA nanobeads.

Calculation of immobilized dextranase yield:

In order to measure the activity of free dextranase and remaining dextranase activity, a DNSA assay was performed after HA-dextranase immobilization. Immobilized dextranase yield (in percent) is calculated by defining the control variable or free dextranase (C) and the supernatant variable or remaining dextranase without HA (S). Then the S value is divided by the C value and subtracted from 1. The final value is multiplied by 100 to calculate the yield in a percentage, as shown in equation (1). Immobilized dextranse yield (%) =

$$1 - \left(\frac{S}{C}\right) \times 100 \qquad (1)$$

Encapsulation of HA-dextranase:

Three buffers were prepared in agarose bead preparation for dextranase encapsulation. First, the 0.9% Sodium chloride solution was made with 500 mL of water and 4.5 g of Sodium Chloride. A 3 % Tween 80 in Paraffin oil was made with 50 mL Paraffin liquid and 1.5 Tween #80. The last buffer is a 4 % agarose solution made with 50 mL of 0.9% NaCl water and 2 g of agarose. The solution was microwaved, so the agarose dissolved in the solution at a temperature between 80-90 ˚C. The temperature of the 4 % agarose solution was measured and left until it cooled down to 65 ˚C. Immobilized HA-dextranase (5 %) was added to the 4 % agarose solution at 65˚C and then mixed well with a magnetic stirrer. The 3 % Tween 80 in Paraffin liquid solution was separated in half into 2 15 mL tubes (BD). One 15 mL tube was heated at 60-70˚C, and the other 15 mL tube was frozen at -20˚C. The heated (60-70 ˚C) paraffin liquid solution was poured into the 5 % HA-dextranase agarose solution mixture. After adding the 60-70˚C Paraffin liquid solution, the mixture was at 50˚C. With a magnetic stirrer, the solution was mixed for 10 minutes. After 10 minutes, the cold (-20 ˚C) Paraffin liquid solution was put into the mixture. When all the

DOI: 10.36838/v4i5.3

solutions were mixed well with a magnetic stirrer, the beads were observed under a microscope.

Streptococcus mutants biofilm formation and quantification:

The quantification of *Streptococcus mutans* and biofilm cells was performed in 96-well-plates. The bacteria were inoculated in LB broth. They were incubated for 24 hours at 37°C. After incubation, the supernatant from each well was removed. The biofilm remaining in each well was washed three times with sterile distilled water, followed by staining with 1% crystal violet (Biorad) solution for 15 minutes. The cells were then washed three times with sterile distilled water and air-dried for an hour. Stained biofilm cells were de-stained using 95% ethanol. After washing with sterile distilled water, 10% SDS was added to each well to lysis the biofilm-forming cells. The absorbance was measured at 600 nm.

Results and Discussion

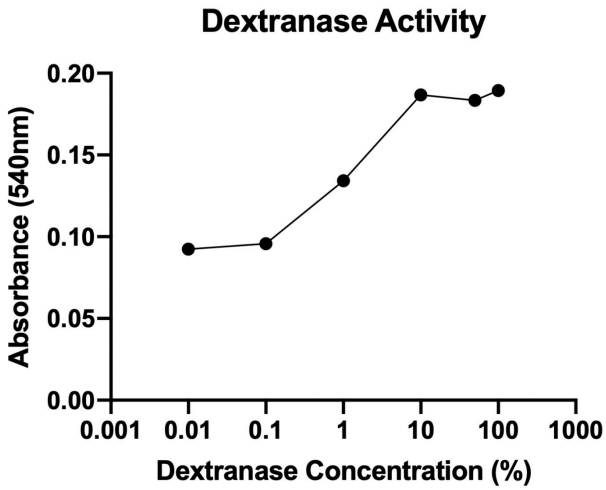

Figure 1: Effect of dextranase concentration on dextranase activity measured by DNSA assay. Line graph showing the 540 nm absorbance (n=1). Six different dextranase concentrations were prepared: 0.01, 0.1, 1, 10, 50, 100 %. For the DNSA assay, each dextranase enzyme solution was mixed with 3 % dextran. Then the samples were placed at 60°C for 15 minutes.

This experiment aims to determine a linear range of dextranase activity. The linear detection range is the region in which the amount of dextranase concentration is proportional to the absorbance (540 nm), representing dextranase activity.

The dextranase activity was measured through DNSA (3,5-dinitrosalicylic acid) assay. DNSA (3,5-dinitrosalicylic acid) assay method determined dextranase activity. The DNSA method is used in biochemistry to determine the total amount of reducing sugars. During the reaction, when the reducing sugars previously treated with DNSA are placed inside boiling water (at 100°C), the 3,5-dinitrosalicylic acid (DNSA) is reduced to 3-Amino-5-Nitrosalicylic acid (ANSA). Depending on the concentration of reducing sugar in the solution, the color of the solution turns darker, ranging from an orange to a red color. We placed the samples into a microplate inside the spectrometer to measure dextranase activity precisely using absorbance at 540 nm.

Since the optimized dextranase concentration is critical to measure the activity change of dextranase, we tested six different dextranase concentrations (in percent): 0.01, 0.1, 1, 10, 50, 100 % dextranase. At dextranase concentrations ranging from 10 to 100 %, the 540 nm absorbance is nearly constant because the dextranase activity was nearly saturated (Figure 1). Therefore, 1%, which is in the middle of the linear range of dextranase activity, was chosen to be an optimized concentration to test the change in the activity of dextranase in downstream experiments.

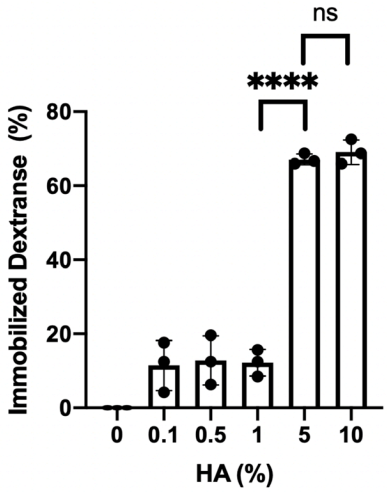

Figure 2: Effect of immobilized HA-dextranase formation yield by increasing HA concentration. Bar graph showing mean ± SD percentage of immobilized dextranase (n=3). Dextranase was immobilized by incubating dextranase with HA powder for 10 minutes· Five different HA concentrations (0 %, 0.1 %, 0.5 %, 1 %, 5 %, and 10 %) were tested. Unpaired t-test, $^{****}p < 0.0001$.

When dextranase is in the mouth, dextranase specificity decreases due to being randomly distributed throughout the mouth instead of precisely targeting dental caries and dental plaque. Hydroxyapatite nanoparticle (HA) is an inorganic, non-toxic nanomaterial used to immobilize proteins. By immobilizing dextranase with the HA bead, the dextranase will specifically sink deeper between the teeth in areas with dental plaque biofilm to degrade dextran with an increased dextranase concentration in targeted areas; therefore, dextranase specificity increases.

The purpose of determining HA-dextranase immobilization yield is to measure the most efficient yield of dextranase immobilization for a corresponding amount of HA. The optimized condition of HA-dextranase is applicable for downstream experiments, specifically in HA-dextranase encapsulation. In total, five distinct HA concentrations were tested: 0 % (0 g), 0.1 % (0.001 g), 0.5 % (0.005 g), 1 % (0.01 g), 5 % (0.05 g), and 10 % (0.1 g).

The results demonstrated that at 1 % HA, the immobilized dextranase yield is very low (~10%). However, at 5 % HA, the results showed an about 50 % increase in the immobilization yield compared to 1% HA (Figure 2). At 10 % HA, although the percentage of HA was two times the HA amount in 5 % HA, there was no significant increase in the immobilization yield. The final optimized HA-dextranase immobilization yield condition was 5 % HA.

Agarose is a natural polysaccharide obtained from red seaweed. It is edible as agarose is a natural substance without toxicity.[12] It has a high melting temperature and solidifies to a hydrogel at room temperature. Furthermore, using the

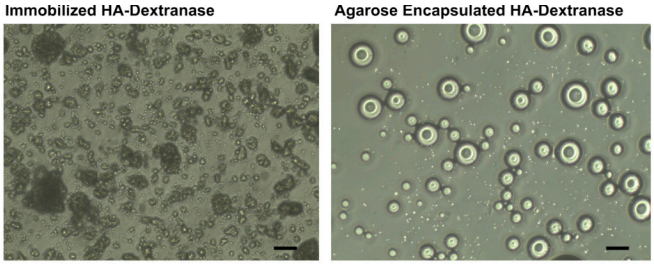

Figure 3: Different sizes of immobilized HA-Dextranase and agarose encapsulated HA-Dextranase particles were observed in the microscopic images. The difference between immobilized HA-Dextranase and agarose encapsulated HA-Dextranase is shown. Agarose encapsulated HA-Dextranase is larger with a visible coating layer. Microscopic images of naked immobilized HA-dextranase and agarose encapsulated HA-dextranase were taken. Scale bar = 200 µm.

emulsification technique, agarose encapsulation results in uniform beads.

Previous research indicated that immobilizing dextranase to an HA-dextranase complex increases the specificity of dextranase.[13] However, HA-dextranase lacks stability since dextranase is diluted throughout the entire mouth, resulting in protein degradation. Therefore, in this experiment, immobilized HA-dextranase was encapsulated by agarose beads with the emulsification technique. By encapsulating the HA-dextranase complex, we hypothesized that dextranase stability inside the toothpaste would be enhanced due to agarose encapsulation. Overall, the purpose of this experiment aimed to determine whether encapsulation of HA-dextranase was successfully conducted.

We used the same method of emulsification to prepare agarose beads for encapsulation as the previous paper described. However, in this experiment, specifically, HA-dextranase was encapsulated. From Figure 2, 5 % HA was used as the optimized condition of HA-dextranase immobilization yield. Additionally, the agarose was dissolved with a 4 % agarose solution of 50 mL NaCl and 2 g agarose.

This sample was taken from the top of the encapsulated solution to a separate tube; then, the sinking precipitate was carefully pipetted for observation under a microscope. The left image displays the HA-dextranase complex observed in a microscope in both separated and aggregated conditions (Figure 3). The small speckles on the right image are naked immobilized HA-dextranase. The encapsulated HA-dextranase is larger and circular with a visible coating layer since the agarose bead encapsulates the HA-dextranase complex (Figure 3).

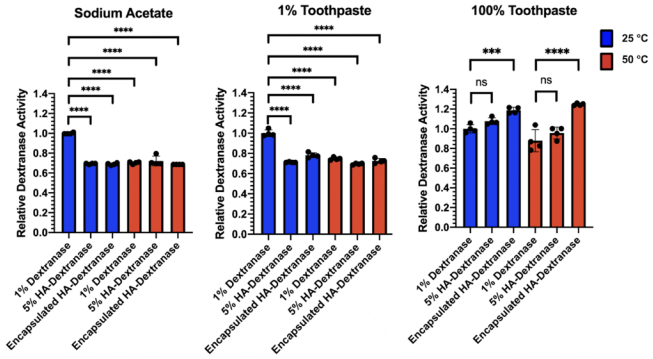

Figure 4: At both 25 °C and 50 °C, encapsulated HA-Dextranase showed the highest relative dextranase activity, indicating that agarose encapsulation provided temperature-sensitive protection. The blue bar represents 25 °C and the red bar represents 50 °C showings mean ± SD relative dextranase activity ($n=4$). Analysis of 1 % Dextranase, 5 % HA-Dextranse, and Encapsulated HA-dextranase stability in sodium acetate, 1% toothpaste, and 100% toothpaste at 25 °C and 50 °C. Two-way ANOVA and Tukey test, nsp > 0.01, ***p < 0.001, ****p < 0.0001.

Three types of dextranases (1 % Dextranase, 5 % immobilized HA-dextranase, and encapsulated immobilized dextranase) from previous experiments were tested for their stability. The stability of each dextranase type was tested under three different conditions: 100 % toothpaste, 1 % toothpaste, and sodium acetate (no toothpaste). We added both sodium acetate and toothpaste (100 % and 1 %) to each sample. To test the thermostability, each set of dextranase samples was placed at two temperature conditions: 25 ˚C and 50 ˚C, and incubated for 48 h.

Since the white translucent substances from toothpaste increased the absorbance by 540 nm, the background absorbance measurement increased. Therefore, the relative value of each condition was calculated and presented as a graph. Therefore, we used the relative value of each condition to calculate and present the data. Relative value was used to organize the data to easily compare the ratio differences of dextranase stability within each condition. We calculated the relative dextranase value by setting the average of four 1 % dextranase measurements at 25˚C as the relative value of 1.0. Every value in each condition was divided by each respective average value. The mean and standard deviation of four measurements in each condition is represented by a bar graph, while every value is also plotted as a dot (Figure 4).

In the sodium acetate condition at 25 ˚C, the stability of 5% HA-dextranase and encapsulated HA-dextranase was decreased compared to 1% dextranase. This result suggested that both HA immobilization and encapsulation were insufficient to protect dextranase from degradation in sodium acetate solution. All three samples incubated at 50 ˚C decreased the stability of all samples compared to 1% dextranase at 25 ˚C. This result showed that dextranase was not a thermostable protein (Figure 4).

In 1 % toothpaste, at both 25 ˚C and 50 ˚C, relative dextranase activity in all conditions was decreased compared to 1% dextranase at 25 ˚C. However, 1% dextranase activity at 50 ˚C was significantly decreased compared to 1% dextranase activity at 25 ˚C. This result shows that dextranase is not a thermostable protein since enzyme activity decreased in a condition with a higher temperature. 5 % HA-dextranase at 25 ˚C and 50 ˚C displayed the lowest activity compared to 1 % dextranase and encapsulated HA- dextranase in its respective temperatures (Figure 4).

At 100 % toothpaste, 1 % dextranase, immobilized HA-dextranase, and encapsulated HA-dextranase showed increased relative dextranase values. At both temperatures, immobilized HA-dextranase showed no change in dextranase activity compared to 1 % dextranase (Figure 4). However, encapsulated, immobilized HA-dextranase showed significantly higher activity than 1% dextranase at 25 ˚C and

DOI: 10.36838/v4i5.3

50 °C (Figure 4). This result demonstrates that encapsulating dextranase provides temperature-sensitive protection.

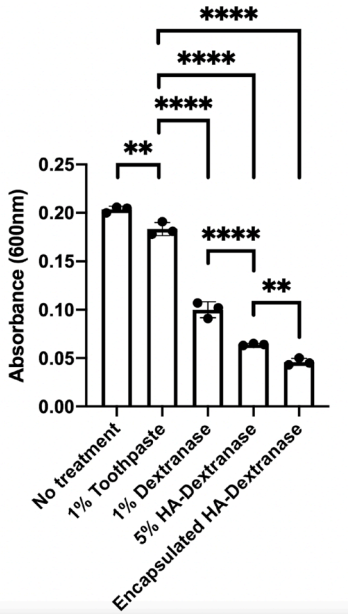

Figure 5: Encapsulated HA-Dextranase efficiently removed the biofilm produced from *S. mutans*. Bar graph showing means ± SD absorbance measurement for biofilm quantification (n=3). Quantification of biofilm produced from *S. mutants* after treatment of 1 % Dextranase, 5 % HA-Dextranse, and Encapsulated HA-dextranase in 1% toothpaste solution for 24 hours. Mean ± S.D. was plotted with statistical significance (two-way ANOVA and Tukey test): $p < 0.05$ (*) $p < 0.01$ (**).

We measured 600 nm absorbance to quantify the biofilm formation to analyze the effect of different dextranase on biofilm formation from *S. mutans* in both sodium 1% toothpaste solutions. Between the no treatment and 1 % toothpaste treated *S. mutans*, the no toothpaste showed a higher biofilm absorbance, indicating that toothpaste is effective, to an extent, in biofilm removal. However, 1 % dextranase significantly decreased the absorbance compared to no toothpaste, showing the effectiveness of dextranase in removing biofilm. Furthermore, 5 % immobilized dextranase to an HA bead to form an HA-dextranase complex showed increased efficiency of biofilm removal with an absorbance reading of 0.06. Yet, encapsulated HA-dextranase showed the most effective biofilm removal showing the lowest absorbance reading at 0.04.

■ Conclusion

We hypothesized that the stability of dextranase would increase with agarose encapsulation. This hypothesis was supported by comparing the dextranase activity determined by the DNSA assay with the increased stability of encapsulated HA-dextranase. Encapsulated HA-dextranase showed the highest relative dextranase activity in 100% toothpaste at 25 °C and 50 °C, indicating that encapsulated dextranase was most stable in 100% toothpaste. However, we only tested the stability of dextranase only after seven days of incubation with 100% toothpaste. Therefore, we should test the long-term storage of dextranase in toothpaste in the future.

A previous study indicated that dextranase specificity in removing biofilm produced by bacteria is limited in toothpaste solution.[6] Therefore, we hypothesized that the specificity of degrading biofilm produced by *S. mutans* would increase with encapsulated HA-dextranase. We quantified biofilm formation after the dextranase samples were treated in 1% toothpaste to test the specificity of three different dextranase. Figure 5 showed that encapsulated HA-dextranase had the most effective biofilm removal. However, we only tested one type of biofilm produced by *S. mutans*. Also, we only tested the effect of dextranase on biofilm removal in a 1% toothpaste condition. Therefore, further tests with various toothpaste concentrations are needed.

There are some acknowledged limitations in this study. First, some minor errors occurred while scraping HA powder from the weighing boat into the 1.5 mL tubes. This error occurred due to some HA powder sticking to the plastic weighing boat. This may cause inaccurate final concentrations of HA. Secondly, we only performed *in vitro* experiments analyzing the stability and specificity of engineered dextranase. Therefore, *in vivo* experiments such as animal experiments should be performed to verify the effect of encapsulated HA-dextranase on removing biofilm and dental cavities. Overall, this research can be applied in formulating toothpaste with dextranase to increase dental plaque biofilm removal efficiency.

■ Acknowledgements

I would like to thank Dr. Woo Rin Lee at the University of Suwon for his guidance and support throughout the research project.

■ References

1. Walsh, T.; Worthington, H. V.; Glenny, A.-M.; Marinho, V. C.; Je roncic, A. Fluoride Toothpastes of Different Concentrations for Preventing Dental Caries. *Cochrane Database Syst. Rev.* **2019**, *3*, CD007868.
2. Ullah, R.; Zafar, M. S.; Shahani, N. Potential Fluoride Toxicity from Oral Medicaments: A Review. *Iran. J. Basic Med. Sci.* **2017**, 20 (8), 841–848.
3. Roos, J.; Dumolard, A.; Bourget, S.; Grange, L.; Rousseau, A.; Gaudin, P.; Calop, J.; Juvin, R. [Osteofluorosis Caused by Excess Use of Toothpaste]. *Presse Med.* **2005**, 34 (20 Pt 1), 1518–1520.
4. Casaglia, A.; Cassini, M. A.; Condò, R.; Iaculli, F.; Cerroni, L. Dietary Fluoride Intake by Children: When to Use a Fluoride Toothpaste? *Int. J. Environ. Res. Public Health* **2021**, 18 (11).
5. Khalikova, E.; Susi, P.; Korpela, T. Microbial Dextran-Hydrolyzing Enzymes: Fundamentals and Applications. *Microbiol. Mol. Biol. Rev.* **2005**, 69 (2), 306–325.
6. Juntarachot, N.; Sirilun, S.; Kantachote, D.; Sittiprapaporn, P.; Tongpong, P.; Peerajan, S.; Chaiyasut, C. Anti-Streptococcus Mutants and Anti-Biofilm Activities of Dextranase and Its Encap sulation in Alginate Beads for Application in Toothpaste. *PeerJ* **2020**, 8, e10165.
7. Ren, W.; Cai, R.; Yan, W.; Lyu, M.; Fang, Y.; Wang, S. Purification and Characterization of a Biofilm-Degradable Dextranase from a Marine Bacterium. *Mar. Drugs* **2018**, 16 (2).
8. Gibbons, R. J.; Fitzgerald, R. J. Dextran-Induced Agglutination of Streptococcus Mutans, and Its Potential Role in the Formation of Microbial Dental Plaques. *J. Bacteriol.* **1969**, 98 (2), 341–346.
9. Tingirikari, J. M. R.; Kothari, D.; Shukla, R.; Goyal, A. Structur al and Biocompatibility Properties of Dextran from Weissella Cibaria JAG8 as Food Additive. *Int. J. Food Sci. Nutr.* **2014**, 65 (6), 686–691.
10. Nicolas, G. G.; Lavoie, M. C. [Streptococcus Mutans and Oral Streptococci in Dental Plaque]. Can. *J. Microbiol.* **2011**, 57 (1),

1–20.
11. Forssten, S. D.; Björklund, M.; Ouwehand, A. C. Streptococcus Mutans, Caries and Simulation Models. *Nutrients* **2010**, 2 (3), 290–298.
12. Zhou, Q.-Z.; Wang, L.-Y.; Ma, G.-H.; Su, Z.-G. Preparation of Uniform-Sized Agarose Beads by Microporous Membrane Emulsification Technique. *J. Colloid Interface Sci.* **2007**, 311 (1), 118–127.
13. Ding, Y.; Zhang, H.; Wang, X.; Zu, H.; Wang, C.; Dong, D.; Lyu, M.; Wang, S. Immobilization of Dextranase on Nano-Hydroxy apatite as a Recyclable Catalyst. *Materials (Basel)* **2020**, 14 (1).

Author

Gahyun Lee is currently a junior at Hong Kong International School. She is the high school varsity team tennis captain. She hopes to extend her passion for biology by pursuing a career in dentistry.

DOI: 10.36838/v4i5.3

IJHSR
ijhighschoolresearch.org
REVIEW ARTICLE

Mood Disorders Associated with Glucocorticoid Therapy: Causes, Mechanisms, and Remediation

Naisha Deorah
The Cathedral and John Connon School, Mumbai, Maharashtra, 400006, India; naisha.deorah@gmail.com

ABSTRACT:Glucocorticoids are widely used in modern medicine for the treatment of a variety of inflammatory diseases. However, the side effects of glucocorticoid treatment often include neuropsychiatric illnesses. This systematic literature review gives a brief introduction to glucocorticoids, their functions, and possible mechanisms of how they lead to psychiatric side effects. After a review of the literature, it can be concluded that patients, as well as physicians prescribing glucocorticoids, should be aware of the potential side effects of glucocorticoid therapy, the means of adverse effect prevention, and efficacious treatments of psychiatric adverse effects. The first line of treatment is dose reduction or stopping the drug. The corticosteroid-induced mania can typically be treated with antipsychotics or mood stabilizers like haloperidol, olanzapine, valproate, lamotrigine plus clonazepam. Corticosteroid-induced depression can be treated with lithium alone or lithium added to fluoxetine, venlafaxine, and low-dose fluvoxamine. Due to the lack of psychiatric assessment in large studies, generalization of data is difficult, and the risk factors and exact mechanisms behind these side effects remain unknown. Future studies should be directed towards gene mapping to help identify risk-promoting roles for certain genes, as well as genes involved in the possible signal transduction pathways to induce these neuropsychiatric side effects.

KEYWORDS: Behavioral and social sciences; Neuroscience; corticosteroid; psychosis; BDNF.

Introduction

Glucocorticoids (GCs) are immunosuppressive and anti-inflammatory steroid hormones secreted by the cortex of the adrenal glands and regulated through the hypothalamic-pituitary-adrenal axis (HPA Axis). The HPA Axis activity is increased upon physiological and emotional stress due to an increase in endogenous GCs.[1] When the HPA Axis is stimulated, corticotropin-releasing hormone (CRH) and arginine vasopressin (AVP) are released from the hypothalamic paraventricular nucleus (PVN).[1]CRH and AVP then binds their receptor CRH-R1 and V1B in the anterior pituitary, inducing the release of adrenocorticotropic hormone (ACTH) into the blood circulation. Subsequently, ACTH stimulates the adrenal gland via MC2-R (type 2 melanocortin receptor), to synthesize and secrete GC hormones into the bloodstream.[1] Figure 1 shows the workings of the HPA Axis. The HPA axis is subject to negative feedback inhibition by GCs. The genomic feedback regulation is mediated through the binding of the GCs to the glucocorticoid receptors (GRs) at the level of the PVN and the pituitary gland.[1] This represses the CR, CRH-R1, and the proopiomelanocortin (POMC) gene, which is the precursor of ACTH. The POMC gene expression is repressed by the binding of the GR to negative glucocorticoid responsive elements (nGREs)[2] and prevents it from performing its transcription functions, thus preventing more GC production. Non-genomically, GCs regulate the HPA axis via the release of endocannabinoids from CRH neurons, suppressing the subsequent release of glutamate from presynaptic excitatory synapses[3] or via GABA release at the inhibitory synapses of CRH neurons.[4] Once secreted, GCs are bound to and transported by plasma proteins.[1] Due to their lipophilic nature, GCs diffuse through the cell membrane and exert their effects.[1] Their non-polar covalent structure enables them to cross the blood-brain barrier and carry out their functions. GCs have a high affinity for brain mineralocorticoid receptors (MRs) and a low affinity for GRs.[5] GRs are expressed in virtually all organs and tissues, while MRs are located in both epithelial and nonepithelial tissues. GR functions by regulating the expression of GC-responsive genes in a positive or negative manner.[1] GCs are instrumental in the normal functioning and homeostasis of the Central Nervous System (CNS). GCs are used in the treatment of a wide variety of inflammatory conditions like allergies, back pain, dermatological, and ophthalmic conditions, gastrointestinal disorders, cancer, and lupus amongst others.[6] They influence both pro-inflammatory and anti-inflammatory cytokine secretion, thus exerting an important modulatory role on the immune system.[7] The degree of cortisol responsiveness has an important effect on susceptibility and resistance to inflammatory, autoimmune and infectious diseases.[7]

Discussion

Side effects of glucocorticoids:

Glucocorticoids, though used to suppress inflammation, are associated with numerous supraphysiological side effects including mood disorders, cognitive impairment, suicidal ideation, and anxiety.[8] GCs are secreted by the adrenal cortex. Excess endogenous glucocorticoid secretion or administration is known to cause Cushing's syndrome, with symptoms of obesity, weakness, osteoporosis, salt and water retention, and hyperglycemia.

Corticosteroid-induced reversible, anti-psychotic, cognitive deficits usually involve declarative and verbal memory, attention, and concentration.[9] These mild cognitive symptoms are

DOI: 10.36838/v4i5.4

experienced during short-term exposure to corticosteroids like dexamethasone and prednisone.[8] However, in severe cases, formal IQ may be substantially reduced and occupational performance and the ability to perform various tasks, skills, and activities may be diminished.[9] Although disturbances of mood, cognition, sleep, and behavior as well as frank delirium or even steroid-induced psychosis are possible, the most common adverse psychiatric effects of short-term corticosteroid therapy are euphoria and hypomania, occurring in temporary spells. Conversely, long-term therapy tends to induce depressive symptoms like manic behavior and psychosis. Some patients experience subtle mood disturbances, especially lability and irritability.[10] In addition to these effects, a decrease in the duration of REM sleep, and loss of brain hippocampal volume are also observed.[6] Treatment of these side effects includes adjusting the dosage or discontinuation of the corticosteroid treatment, prescribing antipsychotics, mood stabilizers such as lithium, and antidepressants.[8] Educating the patients and their families on possible side effects helps in the management of these disorders.[8]

Impact on memory, cognition, and behavior:

Corticosteroid-induced cognitive deficits without psychotic symptoms include declarative or verbal memory, and effects on concentration, recall, and analysis (steroid dementia). This is due to dysfunction in neural circuits in the hippocampus and prefrontal cortex.[11,12] Working memory is dependent on the prefrontal cortex and is involved in the tempo storage of information. This is necessary to carry out cognitive tasks like learning and reasoning.[13,14] Declarative memory, involved in the recall of verbal information, is dependent on the hippocampus.[15,16] Deficits in these functions could be the effect of prolonged GC exposure on GRs and MRs on the hippocampus due to the reduction of hippocampal volume[16] or excess glutamate accumulation in that area.[17] Declarative memory is also affected due to increased blood flow in the medial temporal lobe during GC therapy.[18] Reversible deficits in declarative memory have been reported in Cushing's disease and are greater in more severe cases.[19,20] This suggests that excess endogenous and exogenous corticosteroids produce similar cognitive impairment. Reversible cognitive deficits and mood symptoms have been observed in healthy control subjects after administration of prednisone, dexamethasone, and cortisol.[21-24] In healthy subjects, acute GC administration is associated with changes in several brain areas, decreased activity in the left hippocampus, reduced hippocampal glucose metabolism, and reduced cerebral blood flow to the posterior medial temporal lobe.[25-27] Also noted was atrophy of the right amygdala, which is an important regulator of mood and anxiety. This was correlated with the duration of prednisone treatment in a sample study.[28] Thus, excess GCs, endogenous or exogenous, have extreme ramifications on memory, cognition, and behavior.

The following excerpts from case studies have been adapted from Kenna *et.al* [8] and Judd *et.al* [6] to illustrate some of the neuropsychiatric side-effects of GC treatment and the difficulties that may be encountered in treating these.

1. Mrs. S, an 85-year-old widow, socially active woman with no prior psychiatric history, developed temporal arthritis with abrupt and permanent loss of vision in her right eye and blurred vision in her left. She developed significant depressive and psychotic symptoms that resulted in her hospitalization for apparent steroid-induced psychosis. The psychosis resolved several weeks later, and the patient was discharged but continued to become increasingly depressed. Her depressive symptoms were marked as anhedonia, apathy, and poor concentration, and she was disheveled in appearance with poor grooming and loss of function. Although her prednisone dose was lowered to 10 mg/day, she continued to decline. Four months later, after making suicidal statements and becoming assaultive toward her 24-hr caregiver, she was hospitalized again, this time for almost 2 months. She was severely depressed, hopeless, and nihilistic, with delusional guilt, visual hallucinations, poor insight, and self-neglect.

2. A married 50-year-old Caucasian woman began experiencing depression, intense fatigue, malaise, weight gain, and swelling of her lower extremities. She sought medical treatment and was found to have a pedal enema, azotaemia, and proteinuria. A renal biopsy showed acute focal and segmental glomerulosclerosis that was typical in its presentation. During the first prednisone cycle, the patient became, as she described it, "higher than a kite." She recalls being unable to sleep, lacking impulse control, and being inappropriately humorous. Her mind was flooded with unrelated thoughts, and her thinking became so disorganized that she was unable to drive. She had marked memory problems and required multiple reminders, including some pinned to her clothes, for various responsibilities and appointments. Her physician had explained that she might become "hyperactive" during prednisone treatment, but she was neither prepared for the magnitude and extent of the changes she experienced during the first cycle, nor for the depression that occurred during the first taper period and those in the other two treatment cycles.

The onset of psychiatric symptoms and their correlation with dosage:

Psychiatric side effects of corticosteroid treatment are known to have a rapid onset. A study reported a median time to onset of symptoms as early as 11.5 days.[29] Another study noted that 86% of patients developed psychiatric symptoms within a week of starting treatment.[30] Yet another study showed symptoms of corticosteroid treatment generally occurred within 2 weeks.[31] The corticosteroids dexamethasone and beta-methasone have half-lives of 36-54 hours[32] and can thus accumulate and induce psychiatric symptoms that begin after the last dose has been given.[33,34] These studies show that the psychiatric effects of GCs are immediate.

A study by the Boston Collaborative Drug Surveillance Program showed a dose-response correlation between corticosteroids. Chan *et.al* [35] showed a similar correlation in which they observed psychosis in 8% of patients receiving prednisone 90mg per day compared to 35 of patients receiving 30mg per day. Recent literature confirms the dose-response correlation of psychiatric symptoms. Olsen *et.al*[36] found a significant correlation between mood lability and prednisone

DOI: 10.36838/v4i5.4

dose in mg/kg six-week week taper from 40mg/d to zero in 32 patients with alopecia areata. In almost all of the literature on corticosteroid-induced dementia, the corticosteroid dose has been at least 60mg/d of prednisone equivalent, suggesting 60mg/d as a dose threshold in the induction of psychiatric symptoms.

Risk factors:

Researchers have found that women are more susceptible to developing depressive symptoms during initiation of oral glucocorticoid treatment, while men are more prone to developing delirium, mania, confusion, and disorientation.[6] This could be due to the sex hormone status and the influence of estrogenic and progesterone on the hypothalamic-pituitary-adrenal axis (HPA Axis).[7] The risk of delirium, depression, mania, confusion, and disorientation also increases with age.[6] Risk of suicide attempts, panic disorder, and depression increase with people with past histories of mental illness.[6] The risk of recurrence of the disorder during glucocorticoid exposure increases with the experience of a psychiatric disorder during glucocorticoid therapy.[6] Risk of psychiatric disorders in response to GC use is also dose-dependent. The presence or absence of previous psychiatric side effects does not predict responses to subsequent courses of corticosteroids i.e. a patient who has not shown any psychiatric side effects previously may still show side effects to a subsequent course of GCs. Corticosteroid-induced symptoms typically resolve with dosage reduction or discontinuation of corticosteroids.

Glucocorticoid availability at the molecular level:

Once GCs are released, there are factors responsible for the regulation of their availability to produce the required GC response. Some factors may modulate how GCs impact these adverse effects. These include corticosteroid-binding globulin (CBG), the multidrug resistance transporter (MDR), and 11β-hydroxysteroid dehydrogenase (11β -HSD), all regulated at the tissue and cell-specific level.[7] The relative concentration of these factors can dictate the availability of active GCs carry out their functions. These factors are altered under conditions of immune activation, as well as stress and antidepressant treatment.[7] 90% of circulating GCs are bound to CBG,[37] and thus the relative concentration of CBG is an important determinant of free GC. GCs exert their effects by diffusing across the cell membrane and binding to cytosolic receptors, however only unbound GCs are capable of diffusing across the membrane.[7] Previous studies have shown that stress and hypercortisolemia are associated with lower CBG concentrations,[38] while patients who responded to antidepressant amitriptyline were reported to have increased CBG levels.[39]

Modulation of MDR expression or function is also responsible for GC activity. The MDR, P-glycoprotein (Pgp), is an ATP-dependent multidrug efflux pump expressed in several tissues like the brain, liver, kidney, intestines, and adrenal glands.[7] At the blood-brain barrier, the MDR transports cortisol and the synthetic GC, dexamethasone, but not corticosterone out of the endothelial cells lining the brain.[40,41] Patients with various autoimmune diseases such as rheumatoid arthritis (RA), Crohn's disease, and lupus, exhibit high lymphocytic MDR expression and/or activity, which positively correlates with disease activity. Greater MDR expression in immune cells reduces GC availability, enhancing the synthesis and release of pro-inflammatory cytokines and increasing the inflammatory response.[7] This increased MDR expression may be secondary to treatment with high-dose GCs.[7] Altered MDR expression or function has been shown to contribute to depression.[7] Studies have demonstrated different types of antidepressants, increase GC availability in cells by inhibiting MDR function, thereby possibly reducing GC resistance.[42,43]

11β -HSD regulates GC availability by acting as a shuttle in converting GCs between their active and inactive forms. GC metabolism is mediated by 11β -HSDs. The 11β -HSDs type1 isoform acts as a reductase, converting inactive GC (cortisone) to active GC (cortisol), thus elevating cortisol levels. The type 2 isoform acts as an oxidase/dehydrogenase and inactivates GCs by converting cortisol into the inactive cortisone molecule.[44] Pro-inflammatory cytokines such as TNF- α and IL-1β have been shown to upregulate 11β -HSD 1 and downregulate 11β-HSD 2, thus favoring the formation of active GCs and controlling inflammation.[45] Enhanced expression of 11β-HSD2 or reduced expression of 11β-HSD1 has been demonstrated in autoimmune patients and could be another possible mechanism underlying GC resistance in such diseases.[7]

Too much or too little influence of GCs on mood, memory, and neuronal integrity can exert negative effects. Central 11β-HSD1 expression is high in areas that influence cognition and GC negative feedback on the HPA axis, such as the cerebellum, hippocampus, prefrontal cortex, PVN of the hypothalamus, and pituitary gland.[7]

Glucocorticoid receptor action in modulating glucocorticoid effects:

The GR belongs to the nuclear receptor superfamily of transcription factors (TFs) and is a 97 kDa protein that is expressed throughout the body.[1] They regulate gene expression by either direct interaction with specific promoter sequences called glucocorticoid response elements, or through protein-protein interactions with other transcription factors, such as NF-kB, AP-1, STAT, and NFAT.[46] There have been several polymorphisms identified in the human GR gene which may be associated with hypo or hyper function of the receptor, contributing to differential individual sensitivity to the effects of GC treatment.[7] Some polymorphisms are related to an increase or decrease in GC sensitivity and have been associated with altered susceptibility, to metabolic disorders, cardiovascular disease, autoimmune and infectious disease, neuroendocrine responses to stress, as well as altered cognition and effect.[7] Recent genetic studies have shown certain polymorphisms like Bc/1 and ER22/23EK, are associated with increased susceptibility to developing major depression, and the ER22/23EK polymorphism is associated with a faster response to antidepressants.[47,48] The polymorphism of the GR gene NR3C-1, in the promoter region, has been associated with increased susceptibility to depression.[49]

In the absence of intracellular bioactive GCs, the GR is a monomer in the cytoplasm where it resides in a multiprotein complex.[1] This chaperone complex is important for GR maturation, ligand binding, nuclear transport, and activation.[1] The composition of the chaperone complex changes during the different GR maturation/activation states.[50] Once inside the nucleus, the activated GR can go on to exert its function or it can be transported back to the cytoplasm, inhibiting the GR's transcriptional activity.[1] Nuclear export of GR is regulated by exportins and calreticulin (CRT) which bind to the GR NES, thereby disrupting the GR-DNA binding.[51,52] The balance between nuclear import and export determines the proportion of GR protein in the nucleus and has a direct influence on the strength of GR's transcriptional activities.[1] In the nucleus, the GR acts as a TF that can activate (transactivation) or inhibit (trans-repression) genes as well as modulate the function of other TFs (tethering).[1]

Sensitivity to GC action at the level of the GR can be determined by factors such as GR number, affinity, and function, including its ability to translocate to the nucleus and its interaction with other signal transduction pathways.[53,54] In addition, sensitivity to GCs depends on the expression of particular GR isoforms.[7] GRα mediates GC action, while GRβ and GR-P have been shown to mediate GRα activity and are unable to bind ligands.[7]Generally, GRβ is expressed at very low levels compared to GRα; however, its expression is increased in tissues in inflammatory diseases, and it seems to be associated with decreased sensitivity to GCs.[55] Increased GRβ expression may be related to impaired negative feedback mechanisms mediated by GRα activity and has been associated with the development and/or aggravation of symptoms in various glucocorticoid-resistant diseases, such as asthma, colitis/Crohn's, and RA.[53] Moreover, changes in expression and stability of different GR isoforms can be triggered by inflammation[56] and have also been associated with mutations or polymorphisms in the receptor.[54,57,58]

Possible mechanisms

Role of MRs and GRs in the brain-structure function analysis:

GCs penetrate the brain and bind to 2 types of receptors: GRs, expressed in cerebral neurons and glial cells, and MRs, which GCs have a higher affinity for, and are expressed in limbic brain areas like the hippocampus, which control the temperature of the body and the pituitary gland.[44] MRs have a higher affinity for endogenous corticosteroids and have been associated with cortisol-related circadian variations, while GRs have a higher affinity for dexamethasone.[7]

GRs have a lower affinity for endogenous corticosteroids, but they are activated when endogenous GC levels are high. Low cortisol levels occupy MRsd, but when GC concentrations are high, GRs are also activated since there are enough GCs to activate MRs and GRs.[44] GCs exert their effects by binding to cytosolic MRs and GRs and then translocate to the nucleus upon binding to their ligand.[59,60] The circadian cycle is a natural internal process that regulates an individual's sleep-wake cycle. The activation of both GRs and MRs occurs during the active period of the circadian cycle and in Cushing's syndrome.[7] In hippocampal cells, only 11β-HSD type 1 is expressed, which converts inactive cortisone to active cortisol.[7] Thus there is conversion to active cortisol in these areas and since the type 2 isoform is not expressed in the hippocampus and other limbic areas, there is only active cortisol circulating, leading to MR activation by GCs in these areas, and possibly explaining the changes seen in these areas during chronic exposure to GCs.[7]

GCs and neurons:

Chronic exposure to GCs inhibits regenerative sprouting of axons that follows differentiation of hippocampal neurons and reduction in the number of these neurons.[44] Brain-derived neurotrophic factor (BDNF) is involved in many functions such as neuronal growth, survival, synaptic plasticity, and memory formation and protects against stress-dependent impairment of spatial memory. Figure 2 (shown below) illustrates the cytokine-mediated repression of BDNF, and the subsequent repression of the genes involved in neuronal architecture.

It is thus important for maintaining neural architecture in brain regions such as the hippocampus and prefrontal cortex.[44] Pro-inflammatory cytokines such as IL-6, IL-1, and TNF-α play a functional role in the CNS by increasing glutamate release and decreasing the expression of glutamate transporters on relevant glial elements, releasing in decreased glutamate uptake.[61] Glutamate downregulates the expression of BDNF.[61] The cytokine mechanism provides a possible explanation for stress-related changes. Under normal physiological conditions, these cytokines give support to neurons, helping in neurogenesis and contributing to normal cognitive function.[61] However, stress-induced prolonged activation of these cytokine networks can also lead to abnormalities consistent with neuropsychiatric disorders. These include decreased neurogenesis, increased glutamatergic activation, oxidative stress, induction of apoptosis in astrocytes and oligodendrocytes, and cognitive function.[62] The pathway to these effects, especially concerning behavior, requires cytokines and inflammatory mediators to increase glutamate release and to decrease the expression of glutamate transporters on relevant glial elements, resulting in decreasing glutamate reuptake.[61] Neuroimaging techniques have provided insight into the correlation between neuroinflammation, glial dysfunction and glutamate synaptic dysfunction in depressed patients.[62] Glutamate regulates synaptic transition and plasticity by activating glutamate receptors (AMPA, NMDA, mGluR1 to mGluR8).[63] Glutamate is cleared from the extracellular space by high-affinity excitatory amino acid transporters (EAATs) which are located on neighboring glial cells.[63] Glutamate is converted to glutamine by glutamine synthetase. Glutamine is then transported back into the glutamatergic neuron, where it is hydrolyzed into glutamate by glutaminase.[63] There are no degradative enzymes in the synapse and therefore uptake by EAATs is the primary mechanism through which the action of extracellular glutamate is terminated.[63] Acute stress and GCs induce extracellular glutamate levels, possibly due to decreased ability to clear extracellular glutamate as a result of impaired glial cell uptake and metabolism, combined with

DOI: 10.36838/v4i5.4

stress-related changes in glutamate release,[63] thus raising extra-synaptic glutamate levels. Pre-synoptically, this suppresses glutamate release and post-synaptically reduces synaptic connectivity by overstimulating the NMDA receptors.[64]

Thus, GRs target glial cells by inducing glutamine synthetase activity, which converts active glutamate to inactive glutamine. This allows glutamate synthesis to reoccur in cultured astrocytes, inducing an increased release of glutamate[65-67] that induces neuronal toxicity due to the accumulation effect.[68] Abnormally high concentrations of glutamine of the receiving nerve cell can lead to effects that can cause cell damage and/or death. Animal model data suggests that N-methyl-D-aspartate (NMDA) receptor antagonists or glutamate release inhibitors (phenytoin) may block the corticosteroid effect on the hippocampus.[69] Decreased neurogenesis in the hippocampus of rats was also observed due to increased corticosterone levels induced by sleep deprivation.[70] MRS spectroscopy studies have shown characteristic reductions in glutamatergic and GABAergic neurotransmission in depressed patients.[71] The astrocyte-released glutamate acts on the extra synaptic NMDA receptors to mediate excitotoxicity, and to decrease the production of trophic factors including BDNF,[61] explaining why GRs downregulate BDNF expression, resulting in a consequent loss of spatial, verbal, and declarative memory in patients treated with exogenous GCs, and also contributing to the development of depression and anxiety.[72] Since GCs stimulate apoptosis of hippocampal neurons, chronic hypercortisolemia also leads to atrophy and cell death.[73] Cytokines, TNF-α, and IL-1 also cause astrocytes and microglia to release reactive oxygen and nitrogen species, causing an amplification of oxidative stress.[61] Thus astrocyte and microglial release of cytokines contribute to the amplification of inflammatory pathways within the brain. This leads the to loss of glial elements, oligodendrocytes, and astrocytes involved in multiple mood-relevant brain regions, including the prefrontal cortex, which is associated with the control of working memory, and the amygdala, which is associated with the body's response to stress and fear and plays a pivotal role in memory. These have emerged as fundamental morphologic abnormalities in patients with depression.[61]

In patients with Cushing's syndrome, lower brain weight, loss of brain volume, and ventricular enlargement were observed.[74-78] Hippocampal volume was also reduced in a large proportion of patients.[79-81]

HPA Axis dysfunction:

GC's are involved in glucose metabolism, inflammation, and immunity.[5] GCs have important effects on arousal, memory, and cognition as well as fetal development and aging[6] The stress-responsive PA Axis regulates GC production, and its dysfunction is implicated in the pathophysiology of anxiety, depression, and psychotic disorders related to chronic exposure to GCs.[7] Hypothalamic secretion of the corticotropin-releasing factor (CRF) stimulates the release of corticotropin (ACTH) from the anterior pituitary and the subsequent release of cortisol from the adrenal glands. The rapid effects and feedback to the hypothalamus which follow are mediated by the MRs and GRs.[6] Synthetic GCs used in treatment preferentially activate pituitary GRS, causing suppression of ACTH and preventing endogenous cortisol release.[6] Hence synthetic GCs activate GRs in the brain while depleting cortisol from MRs.[82] Prolonged application of high doses of corticosteroids can thus lead to HPA axis dysregulation. Major depressive disorder is associated with dysregulation of the HPA axis. HPA axis dysfunction, reported in patients with depression, is believed to be partly related to impaired feedback inhibition by endogenous GCs due to GC resistance[83] or due to hypersecretion of CRH.[84,85] This is due to a lack of inhibition of ACTH responses to CRH following dexamethasone pre-treatment, which points to an impaired feedback inhibition at the level of the pituitary.[7] Central 11-beta-HSD-1 expression is high in areas that influence cognition, thus possibly affecting the GC induced negative feedback mechanism of the HPA axis in areas such as the prefrontal cortex, cerebellum, hippocampus, PVN of the hypothalamus, and pituitary gland.[7] 11-beta-HSD levels have been shown to be associated with depression in certain studies, but the results are inconclusive.[86] Thus both exogenous use of high dose steroids and endogenous excess of these hormones are associated with mood disorders and depressive symptomatology, the mechanisms of which are unknown. Resolution of impaired HPA Axis function, due to administration of exogenous GCs, could cause a reduction of these disorders.

The information about infection or injury is conveyed to the brain, which sets off various mechanisms directed toward the restoration of health and homeostasis. Cytokines are chemical messengers derived from immune cells, which act as immunomodulators and neuromodulators, and mediate many of these functions. They can be classified into pro-inflammatory and anti-inflammatory cytokines. Pro-inflammatory cytokines like interleukin-1 (IL-1), interleukin 6 (IL-6), and tumor necrosis factor (TNF), augment the immune response to help remove pathogens and dispel the inflammatory challenge. Anti-inflammatory cytokines like interlukin-4-10 (IL4-10) and interleukin-13 (IL-13), dampen the immune response. The physiological and psychological effects of immune activation during infection, which are primarily mediated by the central effects of peripherally released pro-inflammatory cytokines, are collectively referred to as sickness behavior. The behavioral responses observed during infection are observed in patients after receiving their systematic administration of cytokines. Immunotherapy with IFN-α, a pro-inflammatory cytokine, has been associated with symptoms of cognitive impairment, fatigue, behavioral despair, and depression. The symptoms of sickness behaviour almost immediately disappear after terminating cytokine administration, suggesting a causal role for cytokines in mediating this condition. Alteration in the pro-inflammatory cytokine milieu can lead to behavioral changes, which are similar to those found in patients with depressive symptoms including altered sleep patterns, anhedonia, decreased activity, and cognitive dysfunction. The change of pro-inflammatory mediators is seen as a trigger of depression. There is a bidirectional relationship between the immune system and

the HPA axis in which cytokines stimulate the HPA axis, releasing

GCs which provide negative feedback control of the immune system, thus keeping a check on the inflammation.[87-89] GCs prevent the production of pro-inflammatory TH1 cytokines and increase the production of anti-inflammatory TH2 cytokines.[90] IL-6 is the primary relevant pro-inflammatory cytokine. Cytokines can stimulate the HPA Axis by acting on the brain, the pituitary, or the adrenal gland.[7] Studies have shown that pro-inflammatory cytokines can induce GC resistance by reducing GC function.[91] Reduction of GR function and affinity induced by cytokines has been found in patients with inflammatory diseases, especially those exhibiting resistance to GC treatment.[91] Reduced GR function contributes to enhanced pro-inflammatory cytokine production, associated with the development of depression.[7] There is an inverse correlation between the serum level of IL-6 and the precursor of serotonin, which is the key hormone that stabilizes our mood, feelings of happiness, and well-being.[92] Serotonin enables brain cells and other cells in the nervous system to communicate with each other and it helps with sleeping, eating, and digestion. IL-6 in depressive patients is higher.[93] Most studies on 'the cytokine theory of depression' are focused on increased levels of pro-inflammatory cytokines. The role of anti-inflammatory cytokines has been recently analyzed and a decreased IL-10 level in depressive patients has been observed[94] while confounding factors for cytokine, including certain chronic physical illnesses and medication. Hence, the elevated ratio of IL-6/IL-10 may be a contributing factor to depression.[61, 95]

Four antidepressant drugs, imipramine, venlafaxine, 1-5 hydroxytryptophan, and fluoxetine, have been found to increase the production of IL-10 (anti-inflammatory mediator).[61] Fluoxetine has been observed to lower the serum level of IFN-y (pro-inflammatory), whereas all four anti-depressants decreased the IFN-y/IL-10 ratio significantly.[61] The tricyclic anti-depressants (TCAs), selective serotonin reuptake inhibitors (SSRIs), and serotonin-norepinephrine reuptake inhibitors (SNRIs), as well as the immediate precursor of serotonin, have a common, negative, immunoregulatory effect by suppressing the IFN-y/IL-10 production ratio.96 Antidepressants promote the production of IL-10, which in turn reduces the ratio of pro and anti-inflammatory mediators.[97] IL-10 was observed to alter the balance of TH1/TH2.[98]

Current treatments:

Psychiatric disturbances resulting from corticosteroid therapy commonly resolve slowly after discontinuation of the drug or reduction of the dosage.[99] Initial treatment of corticosteroid-induced psychiatric disturbances should follow this protocol.[99] For patients receiving high-dose and long-term treatment, a taper is advised to prevent both physiologic and psychiatric corticosteroid withdrawal phenomena.[100] An inappropriate taper can result in 3 types of difficulties: (1) suppression of the hypothalamic-pituitary-adrenal axis (HPA) with the potential for secondary adrenal insufficiency, (2) recurrence of the disease for which the therapy was initiated, and (3) a corticosteroid withdrawal syndrome characterized by symptoms of adrenal insufficiency but with normal HPA function.[101] Appropriate tapering is critical and should be based on total dosage, therapy duration, and corticosteroid type. For patients who cannot tolerate corticosteroid cessation or dose reduction due to the severity of the disease, or who suddenly develop psychosis, severe agitation, aggressive behavior, or other intolerable symptom complexes, palliative pharmacotherapy is indicated, even though no definitive treatment has been identified.[99] In certain patients, pharmacotherapy may prevent corticosteroid-induced psychiatric disturbances.[69] For example, anecdotal evidence suggests that lithium may be effective for the acute treatment of corticosteroid-induced psychiatric symptoms, including mania and depression.[102,103] Lithium increases the amount of certain chemicals in the brain which stabilizes mood. Some other studies suggest that valproic acid, neuroleptics and atypical antipsychotics can be administered for treatment of these symptoms.[104-108] Valproic acid increases GABA production in the brain. GABA blocks transmission across nerves in the brain and also has an anti-anxiolytic effect.

Case studies of treatments:

The following excerpts from case studies have been adapted from Kenna *et.al*[9] and Judd *et.al*[6] in order to illustrate some of the neuropsychiatric side-effects of GC treatment and the difficulties that may be encountered in treating these.

1. Mrs. S began oral prednisone. 60 mg/day. While tapering down to 40 mg/day 1 month later, she developed significant depressive and psychotic symptoms that resulted in her hospitalization for apparent steroid-induced psychosis. The psychosis resolved several weeks later and the patient was discharged, but continued to become increasingly depressed. Although her prednisone dose was lowered to 10 mg/day, she continued to decline. Four months later, after making suicidal statements and becoming assaultive toward her 24-h caregiver, she was hospitalized again, this time for almost 2 months. In hopes of saving the remaining vision in her left eye, methotrexate was added to her prednisone 10 mg/day. She was stabilized and discharged on olanzapine 7.5 mg alternating with 10 mg q.h.s., bupropion XL 300 mg/ day, duloxetine 90 mg/day, benztropine 0.5 mg q.h.s., and, lorazepam 0.5 mg bid p.r.n. Two weeks later upon follow up, Mrs. S was neatly groomed and cheerful. She denied depressed mood, anhedonia, and suicidality. In the following months, her mood remained stable and she resumed social activities while continuing her hospital discharge medications. Olanzapine and duloxetine were gradually decreased, while bupropion, benztropine and lorazepam were discontinued after 4 months.

In the case of Mrs. S, the corticosteroids could not be discontinued and therefore the use of psychotropic treatment was required which ultimately resulted in a good prognosis.

2. The patient was started on a cycle of prednisone, beginning with 70 mg/day and tapering by 5 mg per week until the dosage was 10 mg/day because of the renal biopsy. At 10 mg/day, the proteinuria returned, and the nephrologist decided to initiate another cycle of prednisone, with the same starting dosage and tapering schedule. Once again the

DOI: 10.36838/v4i5.4

proteinuria returned when the dosage reached 10 mg/day, and the patient underwent a third cycle of prednisone, with the same result. During this time, the patient was intensely anxious, and her nephrologist prescribed alprazolam in escalating doses up to 4 mg per day, which suppressed her anxiety. After the third course of prednisone failed to ameliorate the glomerulosclerosis, the patient was started on 100 mg/day of cyclophosphamide, to continue until her urine was free of protein. She was treated with cyclophosphamide for approximately 4 months, at which time she was free of proteinuria and was asymptomatic. She was discharged from treatment and has remained asymptomatic, with continued monitoring every 3 to 6 months. Three days after starting the first prednisone cycle, the patient became, as she described it, "higher than a kite." When her depression became severe, she sought treatment on her own from a psychiatrist, who prescribed bupropion, which successfully treated the depression. Throughout the three treatment cycles, the patient's thinking remained disorganized, with memory difficulties and memory loss. These symptoms persisted for approximately 12 months, diminishing over time to the point that she was able to return to work and begin driving again. The patient continues to report experiencing memory problems, some loss of cognitive clarity, and a greater vulnerability to overreacting to stress.

This particular case study demonstrated, once again, the need for an antidepressant, in this case an SSRI, to treat the prednisone-induced depression. The patient showed deficits in cognition and memory after the first prednisone cycle itself. These symptoms however, diminished over time after discontinuation of the GCs, illustrating the possible reversibility of neuropsychiatric side-effects in some cases.

Future directions:

The literature on the treatment is limited to numerous case reports and a few small trials.[9] These provide clinical guidance, but require further studies.[9] The education of patients and their families about the risks of side-effects of GC therapy is imperative, especially since these adverse effects have a rapid onset.[9] The most common first-line treatment for GC induced neuropsychiatric symptoms is dosage reduction or discontinuation. Taper schedules, especially after long term GC treatment should be followed and patients need close monitoring for new or increased symptoms. When severe problems with mood, memory, cognition, or behaviour occur during GC treatment or withdrawal, a psychiatrist should be consulted. There are several recommendations for medication based on preliminary evidence from case studies and clinical trials. GC induced mania or mixed manic symptoms seem to respond to lithium carbonate,[9] olanzapine,[32] or phenytoin.[109] Sodium valproate appears to reverse manic-like symptoms rapidly while allowing GC treatment to continue.[110] Depressive symptoms improve with the use of selected SSRIs such as sertraline, fluoxetine, venlafaxine, and low-dosage fluvoxamine, as well as with lithium alone,[9] but not with tricyclic anti-depressants.

Speculation regarding mechanisms by which these drugs work include regulation of corticosteroid effects on dopaminergic and cholinergic systems[111,112] and modulating the decrease in serotonin release.[113] This is because corticosteroids, which regulate the activity of the raphe-hippocampal serotoninergic pathway, may affect the serotoninergic system and increase the risk for anxiety and depression.[5] A detailed, in-depth analysis of this particular pathway may prove beneficial in the future treatments of mental disorders. If the patient has underlined bipolarity, mood stimulators should be used instead of antidepressants to prevent switch into manic or mixed dysphoric states. GC induced psychosis can be prevented with atypical antipsychotics alone with lithium,[9] while GC induced delirium responds to haloperidol or atypical antipsychotics. Haloperidol can directly regulate the HPA axis and immune system through a pharmacological action via D2 receptor antagonism.[114] Memory problems induced by GCs in patients have been reduced by administration of lamotrigine[115,116] and by the NMDA receptor antagonist, memantine.[117] The beta-blocker propranolol has been found to block GC induced memory deficits in healthy subjects.[118]

Monitoring is an extremely high priority and prophylactic treatment should be considered for patients with recent history of mood or cognitive disorder. Prophylactic treatment should also be given to patients with autoimmune medical conditions like multiple sclerosis[119] and patients with other neurological disorders[120] that are characterized by mood or cognitive disturbances. These conditions may increases the risk of new onsets or exacerbations of such problems during GC withdrawal or treatment.

Since individual susceptibility to the serious mood and depressive effects of GC therapy could be due to individual variations at all levels of GC regulation, these avenues need to be further explored.[7] These include CRH signalling, GC hormone levels, factors regulating GC availability and the GR. GR polymorphisms conferring hypo or hyper sensitivity of the GR are equally important.[7] Moreover, the presence of immune activation, with excess TH1 cytokines could also contribute to HPA dysfunction and behavioural changes.[7] A closer look at these possible factors in patients requiring high dose GC administration, could reduce the risk of side-effects by effective management of these factors.

Conclusion

Corticosteroids are used in the treatment of many illnesses, but their psychiatric side-effects are of common concern to all physicians. Therefore, educating patients about these side-effects is essential. Each patient has a different level of susceptibility to neuropsychiatric effects of GC therapy, which can vary over time.[6] The risk factors include age, gender, genetic, and background factors at all levels of GC regulation, and the risk may be elevated based on an individual's past psychiatric history.[6] However, it is not possible to predict which patients will experience these adverse effects and therefore all patients should be considered at risk and monitored closely.[6] Very little data is available on the incidence and prevalence of these side-effects, and few studies have been performed.[6] The available data suggests that the psychiatric symptoms during GC therapy are dose-dependent with an early onset, and include mania, depression and psychosis.[6] Further studies on the mood and cognitive effects of GC therapy are needed.

Acknowledgements

I would like to thank the 'Lumiere Research Scholar Program' for presenting me with the opportunity to write this research paper. In addition to 'Lumiere', I would like to extend my gratitude to my mentor, Anush Swaminathan, for guiding me through the process of writing this paper and assisting me every step of the way.

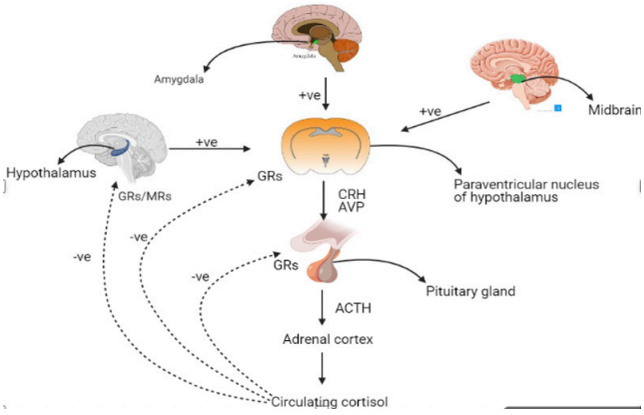

Figure 1: Shows the positive and negative interactions within the HPA Axis.

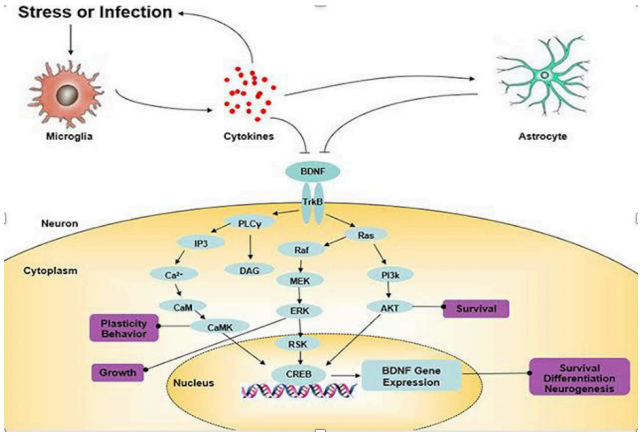

Figure 2: Shows the cytokine mediated repression of BDNF and the subsequent repression of the genes involved in neuronal architecture. The BDNF gene expression leads to survival differentiation neurogenesis. Akt, serine/threonine protein kinase; BDNF, brain-derived neurotrophic factor; CaM, calmodulin; CaMK, calcium-calmodulin-dependent protein kinase; CREB, cAMP response element-binding protein; DAG, diacylglycerol; ERK, extracellular signal-regulated kinase; IP3, inositol 1,4,5-trisphosphate; MEK, mitogen-activated extracellular signal-regulated kinase; PKC, protein kinase C; PI3K, PI-3 kinase; PLC-γ, phospholipase-Cγ; RSK, ribosomal S6 kinase; TrkB, tyrosine kinase B. (Yang *et.al*.121).

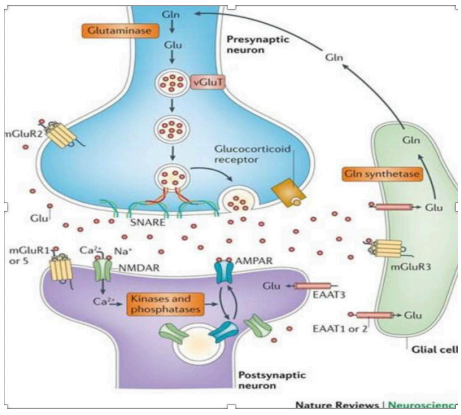

Figure 3: Neuronal glutamate (Glu) is synthesized de novo from glucose (not shown) and from glutamine (Gln) supplied by glial cells. Glutamate is then packaged into synaptic vesicles by vesicular glutamate transporters (vGluTs). SNARE complex proteins mediate the interaction and fusion of vesicles with the presynaptic membrane. After release into the extracellular space, glutamate binds to ionotropic glutamate receptors (NMDA receptors (NMDARs) and AMPA receptors (AMPARs)) and metabotropic glutamate receptors (mGluR1 to mGluR8) on the membranes of both postsynaptic and presynaptic neurons and glial cells. Upon binding, the receptors initiate various responses, including membrane depolarization, activation of intracellular messenger cascades, modulation of local protein synthesis and, eventually, gene expression (not shown). Surface expression and function of NMDARs and AMPARs is dynamically regulated by protein synthesis and degradation and receptor trafficking between the postsynaptic membrane and endosomes. The insertion and removal of postsynaptic receptors provide a mechanism for long-term modulation of synaptic strength. Glutamate is cleared from the synapse through excitatory amino acid transporters (EAATs) on neighbouring glial cells (EAAT1and EAAT2) and, to a lesser extent, on neurons (EAAT3 and EAAT4). Within the glial cell, glutamate is converted to glutamine by glutamine synthetase and the glutamine is subsequently released by System N transporters and taken up by neurons through System A sodium-coupled amino acid transporters to complete the glutamate–glutamine cycle. (Adapted from Popoli *et.al* (134)).

References

1. Timmermans S, Souffriau J, Libert C. A General Introduction to Glucocorticoid Biology. (July 2019) Vol.10 Article 1545
2. Malkoski SP, Dorin RI. Composite glucocorticoid regulation at a functionally defined negative glucocorticoid response element of the human corticotropin-releasing hormone gene. Mol Endocrinol. (1999) 13:1629–44. doi: 10.1210/mend.13.10.0351
3. Di S, Malcher-Lopes R, Halmos K, Tasker JG. Nongenomic glucocorticoid inhibition via endocannabinoid release in the hy pothalamus: a fast feedback mechanism. J Neurosci. (2003) 23:4850–7. doi: 10.1523/JNEUROSCI.23-12-04850.2003
4. Di S, Maxson MM, Franco A, Tasker JG. Glucocorticoids regulate glutamate and GABA synapse-specific retrograde transmission via divergent nongenomic signaling pathways. J Neurosci. (2009) 29:393–401. doi: 10.1523/JNEUROSCI.4546-08.2009
5. Thibaut F. Corticosteroid-induced psychiatric disorders: genetic studies are needed. European Archives of Psychiatry and Clinical Neuroscience 2019;269:623-625
6. Judd LL, Schettler PJ. Brown ES, Wolkowitz OM, Sternberg EM, Bender BG, Bulloch K, Cidlowski JA, Ronald de Kloet E, Fardet L, Joels M, Leung DYM, McEwen BS, Roozendaal B, Van Rossum EFC, Ahn J, brown DW, Plitt A, Singh G. Adverse Consequenc es of Glucocorticoid medication: psychological, Cognitive, and Behavioral Effects. Am J Psychiatry October 2014;171:10:1045-1051
7. Marques AH, Silverman MN, Sternberg EM. Glucocorticoid Dys regulations and Their Clinical Correlates: From Receptors to Ther apeutics. Ann N Y Acad Sci. 2009; 1179: 1-18.
8. Brown ES, Chandler PA. Mood and Cognitive Changes During Systemic Corticosteroid Therapy. Primary care Companion J Clin Psychiatry 3:1 February 2001; 17-21
9. Kenna HA, Poon AW, Paula de los Angeles C, Koran LM. Psy chiatric complications of treatment with corticosteroids: Review with case report. Psychiatry and Clinical Neurosciences 2011; 65: 549-560
10. Starkman MN, Schteingart DE, Schork MA. Correlation of bedside cognitive and neuropsychological tests in patients with Cushing's syndrome. Psychosomatics 1986; 27:508.
11. Wolkowitz OM, Burke H, Epel ES, Reus VI: Glucocorticoids: mood, memory, and mechanisms. Ann N Y Acad Sci 2009; 1179:19– 4
12. Weerda R, Muehlhan M, Wolf OT, Thiel CM: Effects of acute psychosocial stress on working memory related brain activity in

DOI: 10.36838/v4i5.4

men. Hum Brain Mapp 2010; 31:1418–1429
13.Oei NY, Everaerd WT, Elzinga BM, van Well S, Bermond B: Psychosocial stress impairs working memory at high loads: an as sociation with cortisol levels and memory retrieval. Stress 2006; 9:133–141
14.Zobel AW, Schulze-Rauschenbach S, von Widdern OC, Metten M, Freymann N, Grasmäder K, Pfeiffer U, Schnell S, Wagner M, Maier W: Improvement of working but not declarative memory is correlated with HPA normalization during antidepressant treat ment. J Psychiatr Res 2004; 38:377–383
15.Eichenbaum H, Otto T, Cohen NJ: The hippocampus: what does it do? Behav Neural Biol 1992; 57:2–36
16.Lupien SJ, de Leon M, de Santi S, Convit A, Tarshish C, Nair NP, Thakur M, McEwen BS, Hauger RL, Meaney MJ: Cortisol levels during human aging predict hippocampal atrophy and mem ory deficits. Nat Neurosci 1998; 1:69–73
17.Aulakh R, Singh S: Strategies for minimizing corticosteroid toxic ity: a review. Indian J Pediatr 2008; 75:1067–1073
18.de Quervain DJ, Henke K, Aerni A, Treyer V, McGaugh JL, Berthold T, Nitsch RM, Buck A, Roozendaal B, Hock C: Gluco corticoidinduced impairment of declarative memory retrieval is as sociated with reduced blood flow in the medial temporal lobe. Eur J Neurosci 2003; 17:1296–1302
19.Mauri M, Sinforiani E, Bono G et al. Memory impairment in Cushing's disease. Acta Neurol. Scand. 1993; 87: 52–55.
20.Starkman MN, Schteingart DE. Neuropsychiatric manifestations of patients with Cushing's syndrome. Relationship to cortisol and adrenocorticotropic hormone levels. Arch. Intern. Med. 1981; 141: 215–219.
21.Newcomer JW, Craft S, Hershey T, Askins K, Bardgett ME. Glucocorticoid-induced impairment in declarative memory perfor mance in adult humans. J. Neurosci. 1994; 14: 2047–2053.
22.Newcomer JW, Selke G, Melson AK, Hershey T, Craft S, Richards K, Alderson AL. Decreased memory performance in healthy hu mans induced by stress-level cortisol treatment. Arch. Gen. Psychi atry 1999; 56: 527–533.
23.Wolkowitz OM, Reus VI, Weingartner H et al. Cognitive effects of corticosteroids. Am. J. Psychiatry 1990; 147: 1297–1303.
24.Wolkowitz OM, Rubinow D, Doran AR et al. Prednisone effects on neurochemistry and behavior. Preliminary findings. Arch. Gen. Psychiatry 1990; 47: 963–968.
25.Charbonneau Y, Ravindran AV. Successful treatment of steroid-in duced panic disorder with fluvoxamine. J. Psychiatry Neurosci. 1997; 22: 346–347.
26.Finkenbine RD, Frye MD. Case of psychosis due to predni sone-clarithromycin interaction. Gen. Hosp. Psychiatry 1998; 20: 325–326.
27.Sirois F. Steroid psychosis: a review. Gen. Hosp. Psychiatry 2003; 25: 27–33.
28.Brown ES, Chamberlain W, Dhanani N, Paranjpe P, Carmody TJ, Sargeant M. An open-label trial of olanzapine for cortico steroid-induced mood symptoms. J. Affect. Disord. 2004; 83: 277–281.
29.Lewis DA, Smith RE. Steroid-induced psychiatric syndromes. A report of 14 cases and a review of the literature. J. Affect. Disord. 1983; 5: 319–332.
30.Hall RC, Popkin MK, Stickney SK, Gardner ER. Presentation of the steroid psychoses. J. Nerv. Ment. Dis. 1979; 167: 229–236.
31.Ling MH, Perry PJ, Tsuang MT. Side effects of corticosteroid therapy. Psychiatric aspects. Arch. Gen. Psychiatry 1981; 38: 471–477.
32.Clinician's Ultimate Reference. Available from URL: http://www.globalrph.com/corticocalc.htm (last accessed 19 August 2011).
33.Ferris RL, Eisele DW. Steroid psychosis after head and neck sur gery: case report and review of the literature. Otolaryngol. Head Neck Surg. 2003; 129: 591–592.
34.Galen DM, Beck M, Buchbinder D. Steroid psychosis after or thognathic surgery: a case report. J. Oral Maxillofac. Surg. 1997; 55: 294–297.
35.Chan L, French ME, Oliver DO, Morris PJ. High- and low-dose prednisolone. Transplant. Proc. 1981; 13: 336– 338.
36.Olsen EA, Carson SC, Turney EA. Systemic steroids with or without 2% topical minoxidil in the treatment of alopecia areata. Arch. Dermatol. 1992; 128: 1467– 1473.
37.Rosner W. Plasma steroid-binding proteins. Endocrinol Metab Clin North Am 1991;20:697–720. [PubMed: 1778174]
38.Tinnikov AA, et al. Serum corticosteroid-binding globulin levels in children undergoing heart surgery. Steroids 1993;58:536–539. [PubMed: 8273117]
39.Deuschle M, *et al*. Increased concentration of corticosteroid-bind ing globulin due to antidepressant treatment with amitritpyline, but not paroxetine. J Psychiatr Res 2003;37:85–87. [PubMed: 12482473]
40.Chin KV, *et al*. Regulation of mdr RNA levels in response to cyto toxic drugs in rodent cells. Cell Growth Differ 1990;1:361–365. [PubMed: 1703776]
41.Karssen AM, *et al*. Multidrug resistance P-glycoprotein hampers the access of cortisol but not of corticosterone to mouse and hu man brain. Endocrinology 2001;142:2686–2694. [PubMed: 11356720]
42.Pariante CM. The role of multi-drug resistance p-glycoprotein in glucocorticoid function: studies in animals and relevance in hu
43.Pariante CM, *et al*. Antidepressant fluoxetine enhances glucocorti coid receptor function in vitro by modulating membrane steroid transporters. Br J Pharmacol 2003;139:1111–1118. [PubMed: 12871829]
44.Lacroix A. Glucocorticoid effects on the nervous system and be haviour. UptoDate 2020
45.Chapman KE, Seckl JR. 11beta-HSD1, inflammation, metabolic disease and age-related cognitive (dys)function. Neurochem Res 2008;33:624–636. [PubMed: 17963039]
46.Revollo JR, Cidlowski JA. Mechanisms generating diversity in glucocorticoid receptor signaling. Ann N Y Acad Sci. 2009 Gluco corticoids and Mood: Clinical Manifestations, Risk Factors, and Molecular Mechanisms. In press.
47.Manenchijn L, *et al*. Clinical features associated with glucocorti coid receptor polymorphisms: an overview. Ann N Y Acad Sci. 2009 Glucocorticoids and Mood: Clinical Manifestations, Risk Factors, and Molecular Mechanisms. In Press
48.Spijker AT, Van Rossum EFC. Glucocorticoid receptor polymor phisms in major depression: focus on glucocorticoid sensitivity and neurocognitive functioning. Ann N Y Acad Sci. 2009 Glucocor ticoids and Mood: Clinical Manifestations, Risk Factors, and Mo lecular Mechanisms. In press.
49.van West D, *et al*. Glucocorticoid receptor gene-based SNP analysis in patients with recurrent major depression. Neuropsycho pharmacology 2006;31:620–627. [PubMed: 16192984]
50.Vandevyver S, Dejager L, Libert C. On the trail of the gluco corticoid receptor: into the nucleus and back. Traffic. (2011) 13:364–74. doi: 10.1111/j.1600-0854.2011.01288.x
51.Holaska JM, Black BE, Love DC, Hanover JA, Leszyk J, Paschal BM. Calreticulin is a receptor for nuclear export. J Cell Biol. (2001) 152:127– 40. doi: 10.1083/jcb.152.1.127
52.Holaska JM, Black BE, Rastinejad F, Paschal BM. Ca2+-depen dent nuclear export mediated by calreticulin. Mol Cell Biol. (2002) 22:6286– 97. doi: 10.1128/MCB.22.17.6286-6297.2002
53.Silverman MN, Sternberg EM. Neuroendocrine-immune inter

actions in rheumatoid arthritis: mechanisms of glucocorticoid resis tance. Neuroimmunology 2008;15:19–28.
54.Tait AS, Butts CL, Sternberg EM. The role of glucocorticoids and progestins in inflammatory, autoimmune, and infectious disease. J Leukoc Biol 2008;84:924–931. [PubMed: 18664528]
55.Colli LM, et al. Interindividual glucocorticoid sensitivity in young healthy subjects: the role of glucocorticoid receptor α and beta isoforms ratio. Horm Metab Res 2007;39:425–429. [PubMed: 17578759]
56.Tliba O, Cidlowski JA, Amrani Y. CD38 expression is insensitive to steroid action in cells treated with tumor necrosis factor-α and interferon-gamma by a mechanism involving the upregulation of the glucocorticoid receptor beta isoform. Mol Pharmacol 2006;69:588–596. [PubMed: 16291871]
57.Derijk RH, *et al*. A human glucocorticoid receptor gene variant that increases the stability of the glucocorticoid receptor beta-iso form mRNA is associated with rheumatoid arthritis. J Rheumatol 2001;28:2383–2388. [PubMed: 11708406]
58.Lee YM, *et al*. A mutation of the glucocorticoid receptor gene in patients with systemic lupus erythematosus. Tohoku J Exp Med 2004;203:69–76. [PubMed: 15212141]
59.Duma D, Jewell CM, Cidlowski JA. Multiple glucocorticoid receptor isoforms and mechanisms of post-translational modifica tion. J Steroid Biochem Mol Biol 2006;102:11–21. [PubMed: 17070034]
60.Joels M, *et al*. The coming out of the brain mineralocorticoid recep tor. Trends Neurosci 2008;31:1– 7. [PubMed: 18063498]
61.Chang TT, Yen YC. Cytokines and Major Psychiatric Disorders. Taiwanese Journal of Psychiatry Vol.24 No.4 2010
62.Krystal JH, Sanacora G, Duman RS. Rapid-acting glutamatergic antidepressants: the path to ketamine and beyond. Biol Psychiatry. 2013;73:1133–1141.
63.Popoli M, Yan Z, McEwen BS, Sanacora G. The stressed synapse: the impact of stress and glucocorticoids on glutamate transmission. Nature. Jan, 2012; 13:22-37.
64.Krystal JH, State MW. Psychiatric Disorders: Diagnosis to Thera py. Cell. Author manuscript;PMC March 27 2015.
65.Juurlink BH, Schousboe A, Jørgensen OS, Hertz L. Induction by hydrocortisone of glutamine synthetase in mouse primary astrocyte cultures. J Neurochem 1981; 36:136.
mans. Eur J Pharmacol 2008;583:263–271. [PubMed: 18275949]
66.Hallermayer K, Harmening C, Hamprecht B. Cellular localization and regulation of glutamine synthetase in primary cultures of brain cells from newborn mice. J Neurochem 1981; 37:43.
67.Patel AJ, Hunt A. Observations on cell growth and regulation of glutamine synthetase by dexamethasone in primary cultures of forebrain and cerebellar astrocytes. Brain Res 1985; 350:175.
68.Wolkowitz OM, Rubinow D, Doran AR, Breier A, Berrettini WH, Kling MA (1990) Prednisone effects on neurochemistry and behaviour. Preliminary findings. Arch Gen Psychiatry 47: 963-968
69.Brown ES, Sayeda N, Choic C, Tustisond N, Robertsd J, Yassad MA, Van Enkevorta E, Nakamuraa A, Ivlevaa EI, Sunderajana P, Khanb DA, Vazquez M, McEwen B, Kulikovaa A, Frola AB, Holmesa T (2019) A randomized, double-blind, placebo-controlled trial of lamotrigine for prescription corticosteroid efects on the hu man hippocampus. Eur Neuropsychopharmacol 29:376–383.
70.Mirescu C, Peters JD, Noiman L, Gould E. Sleep deprivation inhibits adult neurogenesis in the hippocampus by elevating glu cocorticoids. Proc Natl Acad Sci U S A 2006; 103:19170.Hall RC, Popkin MK, Stickney SK, Gardner ER. Presentation of the steroid psychoses. J. Nerv. Ment. Dis. 1979; 167: 229–236.
71.Sanacora G, Mason GF, Krystal JH. Impairment of GABAergic transmission in depression: new insights from neuroimaging stud ies. Crit Rev Neurobiol. 2000;14:23–45.
72.Duman RS, Monteggia LM: A neurotrophic model for stressrelat ed mood disorders. Biol Psychiatry 2006; 59:1116–1127
73.Sapolsky RM. Glucocorticoids and hippocampal atrophy in neu ropsychiatric disorders. Arch Gen Psychiatry 2000; 57:925. 24.
74.Merke DP, Giedd JN, Keil MF, et al. Children experience cognitive decline despite reversal of brain atrophy one year after resolution of Cushing syndrome. J Clin Endocrinol Metab 2005; 90:2531.
75.Momose KJ, Kjellberg RN, Kliman B. High incidence of cortical atrophy of the cerebral and cerebellar hemispheres in Cushing's disease. Radiology 1971; 99:341.
76.Trethowan WH, Cobb S. Neuropsychiatric aspects of Cushing's syndrome. AMA Arch Neurol Psychiatry 1952; 67:283.
77.Cope O, Raker JW. Cushing's disease: the surgical experience in the care of 46 cases. N Engl J Med 1955; 253:119.
78.Bourdeau I, Bard C, Noël B, et al. Loss of brain volume in endoge nous Cushing's syndrome and its reversibility after correction of hypercortisolism. J Clin Endocrinol Metab 2002; 87:1949. Boele FW, Rooney AG, Grant R, Klein M. Psychiatric symptoms in gli oma patients: from diagnosis to management. Neuropsychiatric Disease and Treatment 2015;11:1413-1420
79.Bauduin SEEC, van der Wee NJA, van der Werff SJA. Structural brain abnormalities in Cushing's syndrome. Curr Opin Endocrinol Diabetes Obes 2018; 25:285.
80.Starkman MN, Gebarski SS, Berent S, Schteingart DE. Hippo campal formation volume, memory dysfunction, and cortisol lev els in patients with Cushing's syndrome. Biol Psychiatry 1992; 32:756.
81.Burkhardt T, Lüdecke D, Spies L, et al. Hippocampal and cerebel lar atrophy in patients with Cushing's disease. Neurosurg Focus 2015; 39:E5.
82.de Kloet ER, Joëls M, Holsboer F: Stress and the brain: from ad aptation to disease. Nat Rev Neurosci 2005; 6:463–475
83.Juruena MF, Cleare AJ, Pariante CM. The hypothalamic pituitary adrenal axis, glucocorticoid receptor function and relevance to depression. Rev Bras Psiquiatr 2004; 26:189-201. [PubMed: 15645065]
84.Chrousos GP, Kino T. Glucocorticoid action networks and complex psychiatric and/or somatic disorders. Stress 2007; 10:213-219 [PubMed: 17514590]
85.Holsboer F, Ising M. Central CRH System in depression and anxiety-evidence from clinical studies with CRH1 receptor antago nists. Eur J Pharmacol 2008; 583:350-357. [PubMed: 18272149]
86.Weber B, *et al*. Increased diurnal plasma concentrations of cortisone in depressed patients. J Clin Endocrinol Metab 2000;85:1133–1136. [PubMed: 10720051]
87.Silverman MN, et al. Immune modulation of the hypothalamic-pi tuitary-adrenal (HPA) axis during viral infection. Viral Immunol 2005;18:41–78. [PubMed: 15802953]
88.Sternberg EM. Neural regulation of innate immunity: a coordi nated nonspecific host response to pathogens. Nat Rev Immunol 2006;6:318–328. [PubMed: 16557263]
89.Marques-Deak A, Cizza G, Sternberg E. Brain-immune interac tions and disease susceptibility. Mol Psychiatry 2005;10:239–250. [PubMed: 15685252]
90.Elenkov IJ. Glucocorticoids and the Th1/Th2 balance. Ann N Y Acad Sci 2004;1024:138–146. [PubMed: 15265778]
91.Pace TW, Hu F, Miller AH. Cytokine-effects on glucocorticoid receptor function: relevance to glucocorticoid resistance and the pathophysiology and treatment of major depression. Brain Behav Immun 2007;21:9–19. [PubMed: 17070667]
92.Maes M, Bosmans E, Calabrese J, *et al*.: Interleukin2 and interl eukin-6 in schizophrenia and mania: effects of neuroleptics and mood stabilizers. J Psychiatr Res 1995; 29: 141-52
93.Pike JL, Irwin MR: Dissociation of infl ammatory markers and

DOI: 10.36838/v4i5.4

natural killer cell activity in major depressive disorder. Brain Behav Immun 2006; 20: 169-74.
94.Mesquita AR, Correia-Neves M, Roque S, *et al*.: IL10 modulates depressive-like behavior. Psychiatr Res 2008; 43: 89-97.
95.Dhabhar FS, Burke HM, Epel ES, *et a*l.: Low serum IL-10 con centrations and loss of regulatory association between IL-6 and IL-10 in adults with major depression. J Psychiatr Res 2009; 43: 962-9
96.Kubera M, Maes M: Serotonin-immune interactions in major depression In: Patterson, Kordon and Christen, Editors, Neuro-im mune Interactions in Neurologic and Psychiatric Disorders. Berlin: Springer-Verlag. 2000: 79-87.
97.Kenis G, Mase M: Effects of antidepressants on the production of cytokines. Neuropsychopharmacol 2002; 5: 401-12.
98.Pestka S, Krause CD, Sarkar D, *et al*.: Interlukin-10 and related cytokines and receptors. Ann Rev Immunol 2004; 22: 24-31.
99.Warrington TP, Bostwick JM: Psychiatric Adverse Effects of Cor ticosteroids. Mayo Clin Proc. 2006;81(10):1361-1367.
100.Fricchione G, Ayyala M, Holmes VF. Steroid withdrawal psychi atric syndrome. Ann Clin Psychiatry. 1989;1:99-108.
101.Dixon RB, Christy NP. On the various forms of corticosteroid withdrawal syndrome. Am J Med. 1980;68:224-230.
102.Kemp K, Lion JR, Magram G. Lithium in the treatment of a manic patient with multiple sclerosis: a case report. Dis Nerv Syst. 1977;38:210–211.
103.Terao T, Yoshimura R, Shiratuchi T, et al. Effects of lithium on steroid-induced depression. Biol Psychiatry. 1997;41:1225–1226.
104.The Boston Collaborative Drug Surveillance Program. Acute adverse reactions to prednisone in relation to dosage. Clin Pharma col Ther. 1972;13:694–698.
105.Hall RCW, Popkin MK, Stickney RN, et al. Presentation of the steroid psychosis. J Nerv Ment Dis. 1979;167:229–236.
106.Blazer DG, Petrie WM, Wilson WP. Affective psychosis follow ing renal transplant. Dis Nerv Syst. 1976;37:663–667.
107.Silva RG, Tolstunov L. Steroid-induced psychosis: report of a case. J Oral Maxillofacial Surg. 1995;53:183–186.
108.Baloch N. Steroid psychosis: a case report. Br J Psychiatry. 1974;124:545–546.
109.Brown ES, Stuard G, Liggin JD, Hukovic N, Frol A, Dhanani N, Khan DA, Jeffress J, Larkin GL, McEwen BS, Rosenblatt R, Mageto Y, Hanczyc M, Cullum CM: Effect of phenytoin on mood and declarative memory during prescription corticosteroid therapy. Biol Psychiatry 2005; 57:543–548
110.Roxanas MG, Hunt GE: Rapid reversal of corticosteroid-in duced mania with sodium valproate: a case series of 20 patients. Psychosomatics 2012; 53:575–581
111.Black AC. Biochemical mechanisms of steroid-induced psycho sis. N. Y. State J. Med. 1982; 82: 1024.
112.Gilad GM, Rabey JM, Gilad VH. Presynaptic effects of glu-cocorticoids on dopaminergic and cholinergic synaptosomes. Implications for rapid endocrine-neural interactions in stress. Life Sci. 1987; 40: 2401–2408.
113.Beshay H, Pumariega AJ. Sertraline treatment of mood disorder associated with prednisone: a case report. J. Child Adolesc. Psycho pharmacol. 1998; 8: 187–193.
114.Handley R, Mondelli V, Zelaya F, Marques T, Taylor H, Reinders AATS, Chaddock C, McQueen G, Hubbard K, Papadopoulos A, Williams S, McGuire P, Pariante C, Dazzan P (2016) Efects of antipsychotics on cortisol, interleukin-6 and hippocampal perfu sion in healthy volunteers. Schizophr Res 174(1–3):99–105. https ://doi.org/10.1016/j.schres.2016.03.039
115.Desai S, Khanani S, Shad MU, Brown ES: Attenuation of amyg dala atrophy with lamotrigine in patients receiving corticosteroid therapy. J Clin Psychopharmacol 2009; 29:284–287
116.Brown ES, Wolfshohl J, Shad MU, Vazquez M, Osuji IJ: Attenu ation of the effects of corticosteroids on declarative memory with lamotrigine. Neuropsychopharmacology 2008; 33:2376– 2383
117.Brown ES, Vazquez M, Nakamura A: Randomized, placebocon trolled, crossover trial of memantine for cognitive changes with corticosteroid therapy. Biol Psychiatry 2008; 64:727–729
118.de Quervain DJF, Aerni A, Roozendaal B: Preventive effect of beta-adrenoceptor blockade on glucocorticoid-induced memory retrieval deficits. Am J Psychiatry 2007; 164:967–969
119.Carta MG, Moro MF, Lorefice L, Trincas G, Cocco E, Giudice ED, Fenu G, Colom F, Marrosu MG: The risk of bipolar disorders in multiple sclerosis. J Affect Disord 2014; 155:255–260
120.Thielscher C, Thielscher S, Kostev K: The risk of developing de pression when suffering from neurological diseases. Ger Med Sci 2013; 11:Doc02
121.Yang J, Sun LH, Yang W ,Cui R.J. Bai SK. The Role of BDNF in the Neuroimmune Axis Regulation of Mood Disorders. frontiers in Neurology. June,2019;10:Article 515.
122.Samuel S, Nguyen T, Choi HA. Pharmacologic Characteristics of Corticosteroids. J Neurocrit Care 2017;10(2):53-59
123.Letters to the Editor. Am J Psychiatry June 1999; 156:6
124.Holsboer F. The corticosteroid receptor hypothesis of depres sion. Neuropsychopharmacology 2000;23:477–501. [PubMed: 11027914]
125.Nemeroff CB. The corticotropin-releasing factor (CRF) hy pothesis of depression: new findings and new directions. Mol Psy chiatry 1996;1:336–342. [PubMed: 9118360]
126.Bhangle SD, Kramer N, Rosenstein ED: Corticosteroid-induced neuropsychiatric disorders: review and contrast with neuropsychi atric lupus. Rheumatol Int 2013; 33:1923–1932
127.Fardet L, Flahault A, Kettaneh A, Tiev KP, Généreau T, Tolédano C, Lebbé C, Cabane J: Corticosteroid-induced clinical adverse events: frequency, risk factors, and patient's opinion. Br J Dermatol 2007; 157:142–148
128.Fardet L, Petersen I, Nazareth I: Suicidal behavior and severe neuropsychiatric disorders following glucocorticoid therapy in pri mary care. Am J Psychiatry 2012; 169:491–497
129.Brown ES, Suppes T, Khan DA, Carmody TJ 3rd: Mood changes during prednisone bursts in outpatients with asthma. J Clin Psy chopharmacol 2002; 22:55–61
130.Lieb K, Engelbrecht MA, Gut O, Fiebich BL, Bauer J, Janssen G, Schaefer M: Cognitive impairment in patients with chronic hepa titis treated with interferon α (IFNα): results from a prospective study. Eur Psychiatry 2006; 21:204–210
131.Gift AG, Wood RM, Cahill CA: Depression, somatization, and steroid use in chronic obstructive pulmonary disease. Int J Nurs Stud 1989; 26:281–286
132.Wolkowitz OM, Burke H, Epel ES, Reus VI: Glucocorticoids: mood, memory, and mechanisms. Ann N Y Acad Sci 2009; 1179:19– 40
133.Bender BG, Lerner JA, Kollasch E: Mood and memory changes in asthmatic children receiving corticosteroids. J Am Acad Child Adolesc Psychiatry 1988; 27:720–725
134.Lupien SJ, de Leon M, de Santi S, Convit A, Tarshish C, Nair NP, Thakur M, McEwen BS, Hauger RL, Meaney MJ: Cortisol levels during human aging predict hippocampal atrophy and mem ory deficits. Nat Neurosci 1998; 1:69–73
135.Aulakh R, Singh S: Strategies for minimizing corticosteroid tox icity: a review. Indian J Pediatr 2008; 75:1067–1073

Author

Naisha Deorah is currently studying in the 11th grade at 'The Cathedral and John Connon School' in Mumbai, India. She wrote this paper towards the end of the 10th grade and

went beyond the scope of her school syllabus as she is interested in psychology and biology. She chose to conduct her research on this topic as it perfectly encompasses both these fields and hopes to eventually pursue an MD/PhD.

DOI: 10.36838/v4i5.4

IJHSR
ijhighschoolresearch.org
RESEARCH ARTICLE

Microplastics—A Not So Micro Problem: Prevelence in a North Carolina Freshwater System

Victoria A. Farella,[1] Samantha Faquhar (Mentor)[2]
1. Ardrey Kell High School, 10220 Ardrey Kell Rd, Charlotte, NC 28277 USA; victoria.farella@gmail.com
2. Integrated Coastal Sciences, East Carolina University, Greenville, NC USA

ABSTRACT: While the plastics pollution crisis has remained on the wider global radar, a more recent and seemingly more pervasive type of pollution, known as microplastic pollution, has gained attention by environmentalists. However, there are large gaps in the research of microplastic pollution, especially in freshwater ecosystems. This study seeks to address this gap by investigating the prevalence of microplastics in the Catawba River Basin of North Carolina. The Catawba River Basin is an ideal study location due to its use for recreation, energy, and drinking water for the nearby metropolis of Charlotte, NC. Eighty water samples were collected from five different sites. These sites were characterized by recreated versus non-recreated areas and upstream versus downstream locations. Each sample was vacuum filtered through micron filter paper and then analyzed under a compound microscope for microplastics. Notably, the presence of microplastics in every water sample collected was found. The results showed a 45% increase in prevalence of microplastics in recreated areas compared with less recreated areas, and 25% increase in microplastics downstream of Wastewater Treatment Plants compared with upstream locations. More research is necessary to identify and understand the possible human health and ecological implications of microplastics in the North Carolina area.

KEYWORDS: Earth and Environmental Science; Water Sciences; Environmental Health; North Carolina Freshwater System; Microplastics.

Introduction

Microplastic contamination is recognized as a harmful global environmental problem.[1] Discovered in both aquatic and terrestrial environments, microplastics have been identified as synthetic polymer materials less than five millimeter and greater than one micrometer.[2] Though the highly ubiquitous extent of microplastic pollution can be narrowed down to two major sources categorized as primary versus secondary.[3] Primary sources are those directly manufactured into micro particle sizes, including: fertilizer capsules; fibers that shed from polyester, nylon and vinyl fabrics; unfiltered sewage and sludge from wastewater treatment plants; and industrial abrasives.[4-7] Secondary sources are considered macro particles from everyday plastic items like containers, beverages, packaging, etc., that break down in the environments due to photochemical processes, weathering, erosion, and ultra-violet (UV) radiation.[8] Through the combination of intentional and unintentional waste, these secondary sources are entering the environment on a daily basis, accounting for approximately 69-81% of the microplastic pollution found in the oceans.

Though the implications of microplastics are actively being researched, it is known that microplastics contain chemicals that are toxic and that these alter the development and behavior of organisms.[9-11] These microplastics can also embed themselves into the chemical and physiological makeup of these organisms and consequently become part of the food chain.[12,13] Thus, there is great concern surrounding the human consumption of microplastics especially as it has been estimated that humans consume a credit card's worth of plastic every week.[14] Studies have shown that microplastics exposure, particularly via consumption, in humans may be linked to cancer and liver disease.[15-17,11]

Even with the advanced treatments and filtration systems, freshwater sources can still be contaminated by microplastics. Further research indicates that the most advanced wastewater treatment plants, including activated carbon filtration, reverse osmosis, and membrane technology, can only filter out up to 60% of microfiber particles, and that from a single wash of synthetic clothing material, over 700,000 fibers can shed from garments.[18] Evidence reveals that freshwater organisms, specifically the amphipod species Gammarus duebeni, have the ability to ingest microfibers into their digestive tracts in less than four days.[19]

Biofouling has been seen to increase the risk of ingestion of these plastic particles by marine animals through mistaking them for food using visual and olfactory senses.[20] Additionally, biofouling increases the density of these particles and leads them to sink to the bottom of the ocean where they may remain for years on the deep, cold and less corrosive seafloor, and possibly ingested by benthic organisms.[21]

While much of the microplastic literature has focused on marine environments, there is a growing call to increase research on microplastics in freshwater systems as these are thought to be then entry points of plastic pollution.[22,23] In response to these calls, this study investigates the prevalence of microplastics in a North Carolina freshwater system.

Methods

Study Site :

This study was focused within the Catawba River Basin, located in North Carolina, United States (Figure 1). This river basin is 3,285 square miles and contains water bodies such as Lake James, Lake Hickory, Lake Norman, Mountain Island Lake, and Lake Wylie. Lake Norman is at the northern-most

DOI: 10.36838/v4i5.5

section of the Catawba River and feeds into the river, eventually draining into Mountain Island Lake to the south and eventually Lake Wylie. In particular, Lake Norman is the largest man-made body of water in North Carolina. Today Lake Norman acts as a recreation area, residential area, energy source, and water source for the nearby city of Charlotte. Aside from Charlotte, the Catawba River and Lake Norman provide the primary sources of drinking water to counties across North Carolina and some portions of South Carolina including, Lincoln County, Catawba County, Iredell County, Gaston County, and Mecklenburg County (where Charlotte is located). As of 2022, the population of Charlotte has increased by 26.51% since the most recent census and has obtained the status as the 14th largest city in the United States, as well as the second largest in the Southeastern region.[24] With the reputation as an industrial and highly evolving metropolis, through simultaneous population growth Charlotte is also a central worldwide hub for financial, technological and health care industries, thus stimulating an influx of laborers and white-collar workers from around the country.

Consequently, expanding population, pervasive urban-sprawl, and industrial development all serve to compromise and exasperate the environmental issues prevalent within and around the city. Concerns over air pollution levels, an increase in the frequency of urban heat islands, and sporadic weather patterns due to global warming contributing to stormwater runoff, extreme temperatures, and sedimentation have forced Charlotte city officials and citizens to grapple with the necessity of a healthy environment and the newfound pressures of a continuously growing population. Given these overarching factors, alongside input of thousands of tons of plastics into the environment from the necessary COVID-19 safety measures (masks, gloves, disinfectants, etc.), Charlotte's plastic and solid waste pollution is at the forefront of environmental stressors. Unlike the eight states across the US who have placed bans on single-use plastic bags or the six states who have a moratorium on Styrofoam materials, aside from general recycling measures and a transition towards replacing yard waste plastic bags with paper alternatives, there are not enough county-wide or state-wide measures to combat the threat of plastics pollution and subsequently microplastic pollution in Charlotte's freshwater systems. While wastewater treatment facilities for the Catawba River and Lake Norman are adequate to prevent chemical outbreaks and macroplastics, the growing population of North Carolina counties are proving to be a difficult task for our systems to handle. In addition, several wastewater treatment facilities, like the ones in Gaston County and surrounding Lake Norman, have already reached maximum capacity.[25] Even with the transition towards advanced membrane filtration methods, studies have proven that these systems may allow for the passage of micro and nano-particle plastics to enter into drinking water.[26]

With Charlotte being a sprawling metropolis, industrial power hub, and a sound attraction for financiers and industry workers, it is clear that the environmental risks associated with these conditions are intensifying the concerns related to increased pollution and environmental degradation.

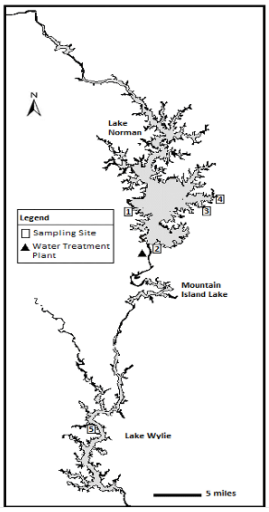

Figure 1: North Carolina Freshwater System Geographic Overview.

Sample Collection :

All samples were collected between June and November of 2021. The sampling sites were chosen based on their proximity to known physical and social characteristics that may influence microplastic contamination. For example, studies have shown that microplastic abundance is more prevalent around wastewater treatment plants and areas with high anthropogenic impact.[27,28] Similarly, sampling sites upstream and downstream of the Mount Holly Wastewater Treatment plant and in highly recreated and low recreated areas were chosen (Table 1). To distinguish recreated versus non-recreated areas, categories were based on proximity to commercial and public activities, including fishing, boating, recreational parks and industries like restaurants or factories for recreational areas, and private residential housing or remote locations without public access for non-recreated areas. An in-depth summary of sampling sites, surrounding characteristics and the number of samples taken from each site can be viewed in Table 1 below.

Table 1: Sample sites and characteristics.

Sampling Site Number	*Geographic Coordinates*	*Site Characteristics*	*Number of Samples Taken*
1	35.35, -80.97	Highly Recreated (Primary Highway NC-16 Intersects / Public Activities Including: restaurants, commercial ventures, boating, industrial factories, public parks)	11
2	35.50, -80.87	Highly Recreated (Public Marina / Commercial Fishing)	4
3	35.50, -80.86	Less Recreated (Private Residential Housing)	15
4	35.33, -80.98	Upstream from Wastewater Treatment Plant	28
5	35.11, -81.22	Downstream from Wastewater Treatment Plant	28

At each sampling site, surface water was collected in 1 liter glass mason jars with latex gloves. Each jar was filled to the halfway mark of the jar. The lid was sealed while submerged in the water to avoid contamination from the outside air. The water samples were all taken in 3-4 feet of water approximately 1.5 feet below the surface. This methodology follows that of grab sampling for microplastics used by

DOI: 10.36838/v4i5.5

Barrows.[29] Additionally, non-synthetic clothing was worn by the sample collector. Geographic coordinates were taken for each sample and the jar was immediately logged for data organization and management purposes.

Water Sample Analysis:

Each water sample was then evaluated for the presence and abundance of microplastics. After sterilizing all equipment with distilled water, the water sample was vacuumed and filtered through a 90 mm Buchner funnel using 11-micron filter paper. This aligned with the laboratory procedure used by Barrows.[29] Microplastics were identified based on their characteristics of durability under hot metal needle point pressure, and the relative unnatural coloration outlined in the Barrows method. To differentiate microfibers from fragments or Styrofoam the characteristics of slenderness, length (average microfibers are 1mm), and coloration were used. The majority of the fragments were transparent or yellowish in color, which was a clear divergence from the royal blue to red coloration of the fibers. Each filter paper contained eight, randomly placed, uniformly sized circles (113 mm²) that were drawn by hand before conducting the filtration process. The filter paper was then placed in a glass petri dish and evaluated under a compound microscope. Microplastic identification and classification was conducted following characteristics outlined by Hidalgo-Ruz.[30] For each filter paper analyzed, the number of and type of microplastics were counted within the eight circles of the filter paper. Given that evaluating an entire filter paper would be time consuming, this allowed for a random subsample to be taken. The raw data found from these analyses can be seen in Appendix A and Appendix B.

Results

It was found that the downstream area had significantly (Student's T-test p=0.03) more microplastics than upstream (Figure 2). Additionally, it was found that highly recreated areas had significantly (Student's T-test p=1.37E-06) more microplastic abundance than low recreation areas (Figure 3). The results of these T-tests can be seen in Appendix C and Appendix D.

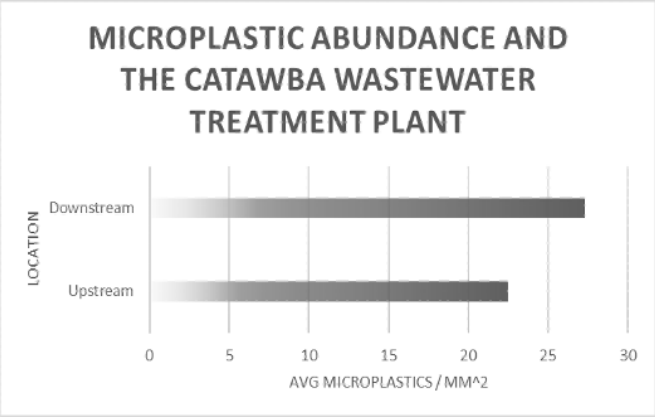

Figure 2: Microplastics prevalence in upstream versus downstream locations of the Catawba River Freshwater System.

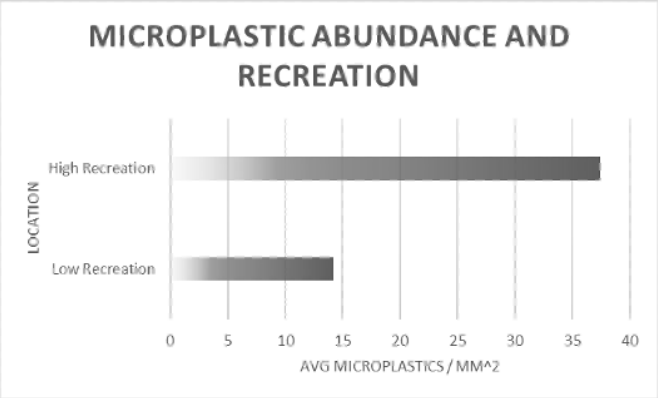

Figure 3: Microplastics prevalence in recreated versus less recreated locations of Lake Norman Freshwater System.

The most common type of microplastics we found were colored microfibers as shown in Figure 4.

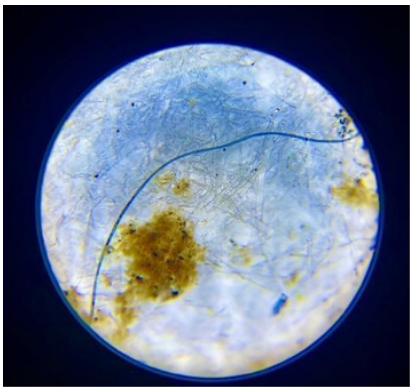

Figure 4: Blue microfiber particle extracted from our Lake Norman Recreated sample site.

However, though rare, over 20 microplastic fragments were identified in the freshwater samples like the one seen below in Figure 5.

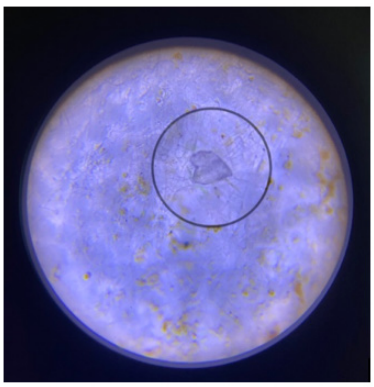

Figure 5: Blue microfiber particle extracted from our Lake Norman Recreated sample site.

In 100% of the samples taken which were identified the presence of microplastic pollution, with a high frequency in microfiber pollution. The average frequency and occurrence at each of the various sites with distinct characteristics can be seen below in Table 2.

Table 2: Sample sites and average number of microplastics.

Sampling Sites (Based on Primary Characteristic)	Number of Samples from Each Site	Average Number of Microplastics per 113 mm^2
High Recreation	15	37.4
Low Recreation	15	14.2
Upstream From Wastewater Treatment Plant	28	22.5
Downstream From Wastewater Treatment Plant	28	27.3

In relation to the recreated versus less recreated data samples, there was a 45% difference in pervasiveness of the microplastic particles, with a major upswing in the amount of microplastics in recreated areas, as seen in Figure 3. This aligned with the assumptions of this study, as when collecting samples visible pollution and secondary macroplastic particles were strewn throughout the environment from restaurants, bars, and retail stores in proximity.

When assessing the differences in prevalence of microplastics between upstream and downstream, downstream samples demonstrated 25% more plastic particles than samples from upstream. This trend was predicted as the technology used during water and wastewater treatment processes in Mecklenburg County, though advanced, are not enough to prevent the flow of micro and nano plastic particles into the freshwater systems as effluent.

Discussion

In an effort to understand the pervasiveness of microplastic pollution in a local urban community, the results of this study compiled from freshwater sampling and analysis of this ubiquitous pollutant indicates that like many other areas, the community of Charlotte must take more decisive action to mitigate and reduce the consumption and waste of plastics pollution. Initially it was shocking that 100% of the samples identified contained some form of microplastic pollution, whether this be the more common microfibers or plastic fragments small enough to allow their absorption and ingestion in marine animals, these findings reinforced the need to comprehend the short- and long-term implications of these substances on the ecosystems and human health.[31] It has been clear for decades that plastics are a staple in consumer culture, yet only now society is starting to really understand the ramifications of this consumption and is now witnessing plastics become part of the human diet too. In the central European lowland river of southwest Poland, a study conducted on freshwater fish and their ingestion and accumulation of microplastics particles revealed that of the 389 sampled gudgeons and freshwater roaches, 54.5% ingested microplastics with the majority of particles being identified as microfibers. Some of these microplastics were entangled in the gills and dug into the mucus of the fins.[32] Though these freshwater animals may not be a common meal for most humans, the concern exists that other primary food sources like salmon, trout, or catfish, are most likely ingesting and accumulating these microplastics on a daily basis, thus demanding the question, what does this mean for humans? Furthermore, gudgeons and roaches are primary food sources for many freshwater and marine life including otters and kingfishers. While preliminary studies are still trying to comprehend the existence and effects of biomagnification of plastic particles up the food chain, it stands to reason that these otters, kingfishers and other marine life that intake plastic infested organisms may suffer negative consequences to their long-term health.

In analyzing high recreational versus less recreational areas, it was concluded that due to the frequency in activities such as commercial and public facilities, which contribute to the likelihood of direct and indirect litter or waste of plastics substances, the increase in plastics within recreated areas is an understandable finding. This mandates policy and action to mitigate future harm. Private areas also have greater access to advanced waste disposal and collection systems, and seem to have a more regular system of trash cleanup. The trends identified were specifically identified in the Lake Norman area, and further studies would need to be done to understand if these patterns align with rivers and streams as well. Similarly, there was a greater presence of biofouling of microplastics, especially fibers, in the Catawba River areas, with darker colored fibers observed having a higher amount of organic or inorganic material adhered to the outside. It is unclear if color or additives to plastics have any effect on whether a material has a greater likelihood of biofouling, but the implications of this are known. When observing samples that came from the middle of the water column, there seemed to be an increase in the amount of microplastics particles, since the density of freshwater is less than that of microplastics, due to the lesser salinity This therefore causing an increase along the bottom of lakes and rivers. Microplastic fragments identified seemed to be discolored, with a yellowish hue, and were irregular shapes. Zero evidence of Styrofoam particles were found, however, there were what seemed to be visible clear films. On cleanups along and near these areas, specifically in the upstream Catawba area, there was a significant presence of secondary Styrofoam macro particles. The general colors of the fibers identified were blue, red, black, and transparent. Although some were green, the validity of these were questioned as they may have been organic material such as algae.

With respect to the upstream versus downstream of wastewater treatment plants study sites, it was clear that although there was not as substantial a difference in the range of microplastics particles found between these locations, there is necessary concern over the contribution of wastewater treatment plants to the accumulation of plastic particles downstream and how this may affect freshwater organisms. The three major treatment facilities for Mecklenburg County include Lee S. Dukes, Vest, and Franklin. Although Charlotte Water Services has clarified in their 2020 Annual Drinking Water Quality Report that they have employed advanced treatment for wastewater treatment including aeration basins, secondary clarifiers, effluent filtration, and disinfection processes, studies have shown that these mitigation techniques still allow for up to 65 millions microplastic particles to be released into water daily, especially microfibers.[33,34] Furthermore, analyzing this study's

DOI: 10.36838/v4i5.5

results of the downstream samples, it is clear that when the wastewater after treatment is released into the surrounding water system of Lake Wylie, there was a significant increase in the prevalence of microplastics as these concentrated particles accumulated downstream. While there are few alternatives for more adequate and effective wastewater treatment solutions, it is necessary that Charlotte and surrounding counties fund and support research and development initiatives towards developing treatment facilities that may prevent and mitigate the dispersal of microplastic infested effluent into water systems.

While out of the scope of this study, it is necessary to note the diversity of factors that contribute to microplastic pollution especially in relation to marine pollution. In 2014 there was a worldwide call for the phasing out and banning of microbeads within cosmetic products as these substances, like microfibers, are understood to escape wastewater treatment and spread into freshwater and marine systems.[35] However, although many countries, including the US, have banned the incorporation of these products, the cosmetic industry is still under scrutiny for the widespread use of single use plastics in their packaging and products, and the dissemination of other microplastic particles within their home care products. Moreover, the cosmetic industry is not the only industrial sector that has some fault for microplastic pollution, but commercial industry and port facilities in general have been classified as major contributors to the prevalence of microplastic pollution near coasts and freshwater systems. In a study taken across Portuguese coasts, resin pellets (primary sources of microplastics) often used as industrial raw materials to be incorporated into goods or to create molds for products, made up 79% of the waste and plastic material collected.[36] The primary and secondary sources of microplastics around the world are boundless, cementing the idea that it may not be a simple feat in lessening the waste and consumption of these items. However, it is a necessary one for the future.

While this study identifies specific trends in the prevalence of microplastic pollution in recreated areas and in proximity to wastewater treatment facilities, future research is needed in understanding the prevalence of microplastics within freshwater organisms and drinking water as well. Though this study collected over 80 samples from various sites, it is necessary further research is conducted to support the trends identified and to have an accurate gauge of the magnitude of plastics pollution in the Catawba River Basin. This study did not get too involved in the intricacies of how and if microplastics act as vectors for harmful pollutants and possibly leach those chemicals into freshwater organisms, yet this is also a necessary step in comprehending the implications of ingesting plastics on human health.

Conclusion

There is clear evidence of microplastics in freshwater systems of the Catawba River Basin. Although the precise implications and extent of the threat may not be fully understood, it is known from prior and current research that microplastics can pose ecological and human health implications over time. It is necessary to gain a greater understanding of this problem. This is especially true given that a major metropolis, the city of Charlotte, uses the Catawba River Basin for drinking water. Although measures have been put into place to try to prevent the expansion of this problem such as Charlotte's initiative to phase out plastic bags for trash collection, there is still extensive contamination of the freshwater systems, as shown in this study. Policy recommendations for microplastic mitigation for the city of Charlotte are provided in Appendix E. Assessing the overall trends in recreated versus less recreated areas it is clear that humans have direct influence on the extent of microplastic pollution as there was approximately a 50% increase in microplastics in recreated than less recreated areas of Lake Norman. Furthermore, the prevalence of microplastics in greater varieties and prevalence downstream than upstream of the Catawba suggests that the wastewater treatment systems may not be having an equal distribution of adequate filtration in these hotspot areas, and that certain communities may be more influenced by this problem than others. Continued research and increased understanding is necessary regarding the toxicology of plastics and chronic health effects that may ensue from ingestion or inhalation of microplastics as this distressing problem continues.

Acknowledgements

We would like to show appreciation to Professor Justin Baumann at Bowdoin College, Maine, for inspiring our ideas for this research. We also want to give thanks to Jennifer Detrano for gracious use of our living space for experimental activities.

Contributions of authors

VF: Collection, data sampling, and evaluation of samples.
SF: Data organization and methodology development.

Conflict of Interest:

Authors report no conflicts of interest for this study. The authors alone are responsible for content and writing of this article.

Funding:

No funds were received from any organization or person to carry out this project.

References

1. Wagner, M. (2022). Solutions to Plastic Pollution: *A Conceptual Framework to Tackle a Wicked Problem* (pp. 333–352). Springer, Cham. https://doi.org/10.1007/978-3-030-78627-4_11 .
2. Shim, W. J., Hong, S. H., & Eo, S. E. (2017). Identification methods in microplastic analysis: A review. *In Analytical Methods* (Vol. 9, Issue 9, pp. 1384–1391). https://doi.org/10.1039/c6ay02558g.
3. Cole, M., Lindeque, P., Halsband, C., & Galloway, T. S. (2011). Mi croplastics as contaminants in the marine environment: A review. *In Marine Pollution Bulletin* (Vol. 62, Issue 12, pp. 2588–2597). Pergamon. https://doi.org/10.1016/j.marpolbul.2011.09.025 .
4. Katsumi, N., Kusube, T., Nagao, S., & Okochi, H. (2021). The input–output balance of microplastics derived from coated fertil izer in paddy fields and the timing of their discharge during the irrigation season. *Chemosphere*, 279, 130574.
5. Carney Almroth, B. M., Åström, L., Roslund, S., Petersson, H., Johansson, M., & Persson, N. K. (2018). Quantifying shedding of synthetic fibers from textiles; a source of microplastics released into the environment. *Environmental Science and pollution research*, 25(2), 1191-1199.
6. Katare, P. Y., Sankhla, M. S., Singhal, M., Ekta, B., Jadhav, K. P., Bh agyashri, T. N., & Bhardwaj, L. (2021). Microplastics in aquatic

environments: Sources, ecotoxicity, detection & remediation. *Bio interface Res. Appl*. Chem, 12, 3407-3428.
7. Qingqing, X., Ge, Z., Yadan, Z., Cheng, L., Yuqing, W., Hao, Z., & Fengmin, L. (2018). Interactions between microplastics and organic pollutants: Current status and knowledge gaps. *Asian Jour nal of Ecotoxicology*, (1), 40-49..
8. Pico, Y., & Barceló, D. (2019). Analysis and prevention of mi croplastics pollution in water: current perspectives and future direc tions. *ACS omega*, 4(4), 6709-6719.
9. Gandara e Silva, P. P., Nobre, C. R., Resaffe, P., Pereira, C. D. S., & Gusmão, F. (2016). Leachate from microplastics impairs larval development in brown mussels. *Water Research*, 106, 364–370. https://doi.org/10.1016/j.watres.2016.10.016.
10. Lönnstedt, O. M., & Eklöv, P. (2016). Environmentally relevant concentrations of microplastic particles influence larval fish ecol ogy. *Science, 352*(6290), 1213–1216. https://doi.org/10.1126/sci ence.aad8828.
11. Sharma, M. D., Elanjickal, A. I., Mankar, J. S., & Krupadam, R. J. (2020). Assessment of cancer risk of microplastics enriched with polycyclic aromatic hydrocarbons. *Journal of Hazardous Materials, 398*. https://doi.org/10.1016/j.jhazmat.2020.122994.
12. Oldenburg, K. S., Urban-Rich, J., Castillo, K. D., & Baumann, J. H. (2021). Microfiber abundance associated with coral tissue var ies geographically on the Belize Mesoamerican Barrier Reef System. *Marine Pollution Bulletin*, 163, 111938. https://doi. org/10.1016/j.marpolbul.2020.111938.
13. Toussaint, B., Raffael, B., Angers-Loustau, A., Gilliland, D., Kes tens, V., Petrillo, M., Rio-Echevarria, I. M., & Van den Eede, G. (2019). Review of micro- and nanoplastic contamination in the food chain. *In Food Additives and Contaminants - Part A Chem\ istry, Analysis, Control, Exposure and Risk Assessment* (Vol. 36, Issue 5, pp. 639–673). Taylor and Francis Ltd. https://doi.org/10.1 080/19440049.2019.158338.
14. Dalberg Advisors, de Wit, W., & Bigaud, N. (2019). No Plastic In Nature: Assessing plastic ingestion from nature to people (AN ANALYSIS for WWF). *World Wide Fund For Nature, 7*. https:// apo.org.au/node/244456?utm_source=APOfeed&utm_medi um=RSS&utm_campaign=rssresearch.
15. Blackburn, K., & Green, D. (2021). The potential effects of micro plastics on human health: What is known and what is unknown. *Ambio*. https://doi.org/10.1007/S13280-021-01589-9.
16. Hu, X., Biswas, A., Sharma, A., Sarkodie, H., Tran, I., Pal, I., & De, S. (2021). Mutational signatures associated with exposure to carcinogenic microplastic compounds bisphenol A and styrene ox ide. *NAR Cancer*, 3(1). https://doi.org/10.1093/narcan/zcab004
17. Palacios-Arreola, M., & Nava-Castro, K. (2021). Environ mental Pollution and Breast Cancer: *The Microplastic Component BPA Regulates the Intratumoral Immune Micro environment and Increases Lung.* https://www.preprints.org/man uscript/202109.0017
18. Mishra, S., charan Rath, C., & Das, A. P. (2019). Marine microf iber pollution: a review on present status and future challenges. Ma rine pollution bulletin, 140, 188-19.
19. Mateos-Cárdenas, A., O'Halloran, J., van Pelt, F. N., & Jansen, M. A. (2021). Beyond plastic microbeads–short-term feeding of cellulose and polyester microfibers to the freshwater amphipod Gammarus duebeni. Science of The Total Environment, 753, 141859.
20. Savoca, M. S., Wohlfeil, M. E., Ebeler, S. E., & Nevitt, G. A. (2016). Marine plastic debris emits a keystone infochemical for ol factory foraging seabirds. *Science Advances*, 2(11).
21. Lusher, A., Hollman, P., & Mendoza-Hill, J. (2017). Microplastics in fisheries and aquaculture: status of knowledge on their occur rence and implications for aquatic organisms and food safety. FAO. Science advances, 2(11), e1600395.
22. Burns, E. E., & Boxall, A. B. A. (2018). Microplastics in the aquatic environment: Evidence for or against adverse impacts and major knowledge gaps. *Environmental Toxicology and Chemistry,* 37(11), 2776–2796. https://doi.org/10.1002/ETC.4268
23. Kallenbach, E. M. F., Rødland, E. S., Buenaventura, N. T., & Hurley, R. (2021). *Microplastics in Terrestrial and Freshwater En vironments* (pp. 87–130). Springer, Cham. https://doi. org/10.1007/978-3-030-78627-4_4
24. World Population Review. (n.d.). Charlotte, North Carolina population 2022. *Charlotte, North Carolina Population 2022* (De mographics, Maps, Graphs). https://worldpopulationreview.com/ us-cities/charlotte-nc-population.
25. Garbrick, K. (2019). *North Carolina's New Era of water qual ity | waterworld*. Retrieved from https://www.waterworld. com/wastewater/treatment/article/14039770/north-caroli nas-new-era-of-water-quality
26. Ding, H., Zhang, J., He, H., Zhu, Y., Dionysiou, D. D., Liu, Z., & Zhao, C. (2021). Do membrane filtration systems in drinking water treatment plants release nano/microplastics?. *Science of the Total Environment*, 755, 142658.
27. Baldwin, A. K., Spanjer, A. R., Rosen, M. R., & Thom, T. (2020). Microplastics in Lake Mead National Recreation Area, USA: Oc currence and biological uptake. *PLoS ONE*, 15(5), e0228896. https://doi.org/10.1371/journal.pone.0228896
28. Estahbanati, S., & Fahrenfeld, N. L. (2016). Influence of waste water treatment plant discharges on microplastic concentrations in surface water. *Chemosphere*, 162, 277–284. https://doi. org/10.1016/j.chemosphere.2016.07.083
29. Barrows, A. P. W., Neumann, C. A., Berger, M. L., & Shaw, S. D. (2017). Grab: Vs. neuston tow net: A microplastic sampling performance comparison and possible advances in the field. *An alytical Methods*, 9(9), 1446–1453. https://doi.org/10.1039/ c6ay02387h
30. Hidalgo-Ruz, V., Gutow, L., Thompson, R. C., & Thiel, M. (2012). Microplastics in the Marine Environment: A Review of the Methods Used for Identification and Quantification. *Environ mental Science and Technology*, 46(6), 3060–3075. https://doi. org/10.1021/ES2031505
31. Pirsaheb, M., Hossini, H., & Makhdoumi, P. (2020). Review of microplastic occurrence and toxicological effects in marine envi ronment: Experimental evidence of inflammation. *Process Safety and Environmental Protection*, 142, 1-14.
32. Kuśmierek, N., & Popiołek, M. (2020). Microplastics in freshwa ter fish from Central European lowland river (Widawa R., SW Poland). *Environmental Science and Pollution Research*, 27(10), 11438-11442.
33. Charlotte Water. (2020). *2020 annual drinking water quality re port ... - charlotte, NC*. charottenc.gov. https://charlottenc.gov/ Water/WaterQuality/Documents/2020%20Consumer%20Confi dence%20Report.pdf
34. Murphy, F., Ewins, C., Carbonnier, F., & Quinn, B. (2016). Waste water treatment works (WwTW) as a source of microplastics in the aquatic environment. *Environmental science & technology*, 50(11), 5800-5808.
35. Anagnosti, L., Varvaresou, A., Pavlou, P., Protopapa, E., & Carayanni, V. (2021). Worldwide actions against plastic pollution from microbeads and microplastics in cosmetics focusing on Eu ropean policies. Has the issue been handled effectively?. *Marine Pollution Bulletin*, 162, 111883.
36. Antunes, J., Frias, J., & Sobral, P. (2018). Microplastics on the Por tuguese coast. *Marine pollution bulletin*, 131, 294-302.

DOI: 10.36838/v4i5.5

Author

Victoria Farella is a high school senior located in Charlotte, North Carolina. Her passions lie in marine and environmental studies of which she hopes to pursue a related major in university. She participates in several conservation projects both locally and internationally. Victoria also started her own initiative called Marine-Clean which focuses on microplastic research and policy analysis.

APPENDICES

Sample Number	Upstream Microplastics 113 mm²	Downstream Microplastics 113 mm²
1	10	24
2	20	17
3	18	24
4	15	21
5	10	33
6	10	36
7	15	44
8	11	21
9	21	33
10	28	17
11	30	36
12	29	16
13	20	21
14	21	30
15	26	42
16	27	30
17	40	21
18	23	33
19	24	21
20	49	28
21	37	20
22	12	31
23	22	28
24	15	32
25	29	24
26	25	17
27	26	28
28	18	36

Sample Number	High Recreation Microplastics 113 mm²	Low Recreation Microplastics 113 mm²
1	22	17
2	30	21
3	23	19
4	42	11
5	41	14
6	32	16
7	36	11
8	45	16
9	31	7
10	37	13
11	64	16
12	53	14
13	28	12
14	34	9
15	43	17

Appendix B: Raw data for microplastics found in samples from high recreated areas and low recreated areas.

	High Recreation	*Low Recreation*
Mean	37.4	14.2
Variance	124.6857	14.31429
Observations	15	15
Pearson Correlation	-0.04092	
Hypothesized Mean Difference	0	
df	14	
t Stat	7.528206	
P(T<=t) one-tail	1.38E-06	
t Critical one-tail	1.76131	
P(T<=t) two-tail	2.76E-06	
t Critical two-tail	2.144787	

Appendix C: Results for the Student T-test between microplastics found in high recreation areas and low recreation areas.

	Upstream	Downstream
Mean	22.53571	27.28571429
Variance	88.18386	59.32275132
Observations	28	28
Pearson Correlation	-0.23775	
Hypothesized Mean Difference	0	
df	27	
t Stat	-1.86362	
P(T<=t) one-tail	0.036642	
t Critical one-tail	1.703288	
P(T<=t) two-tail	0.073285	
t Critical two-tail	2.051831	

Appendix D: · Results of Student's T-test for microplastics found in upstream and downstream locations.

Policy Recommendations:

To confront the issue of microplastic pollution in Charlotte, here we outline seven specific methods we may implement in our county to lower the risks of microplastic pollution.

1. Extended Producer Responsibility (EPR):

Extended Producer Responsibility policies have been adopted in a variety of ways nationally. States across the country have adopted these towards reducing our carbon footprint, making producers responsible for post-production hazardous wastes in wastewater treatment plants or nuclear energy facilities, and to minimize our plastic footprint. However, unlike states such as California, Maine and Maryland, North Carolina has been slow in adopting EPR policies. As the name suggests, policies like these are characterized by holding producers responsible for waste from pre-production materials, the manufacturing process, and post-consumer waste in the form of taxes, fees or government regulations. On July 13, 2021, Maine was the first state to implement an EPR policy towards paper and packaging waste. Producers are responsible for financing "stewardship organizations" who collect and recycle products on the producer's behalf. In this way Maine has cemented their stance on working collectively with producers, consumers and NGOs to foster an environmentally conscious community and reduce their plastic waste. North Carolina, specifically Charlotte, should follow their suit, as they have the means and resources to hold producers in North Carolina responsible for the production of plastic packaging, Styrofoam material in pre- and post- production, and paper cartons, boxes, or other resources. With the help of non-governmental organizations such as the Catawba Riverkeepers, the North Carolina Coastal Federation, and many others, producers across Charlotte should collaborate and help to finance these organizations in relation to waste collection and recycling. At this moment Charlotte and North Carolina as a whole has not implemented any EPR policies, but in order to reduce the risks of plastic pollution it is vital to mitigate plastic production at the source.

2. Taxes/Fees on Textile Companies:

As mentioned above in the description of microplastics as a source of pollution, microfibers are ubiquitous and make up 35% of the microplastic pollution in the world's ocean. Additionally, as only 60% of these microscopic fibers, which are approximately less than 10 micrometers, can be filtered out through wastewater treatment plants, a significant amount of these fibers are released into rivers, streams, and lakes eventually flowing into our ocean. The textile industries situated in North Carolina pose a major threat to the health of our environment, not only in regards to the levels of CO2 emitted during the production process, but the use of synthetic materials such as nylon, polyester and rayon, in the production of textiles has vast implications on the microplastics matter. Trelleborg Engineered Coated Fabrics and Unifi, both located in North Carolina, are the two largest textile industries in the United States. Trelleborg, by their own reports, lists polyester, rayon and nylon as substantial materials which they incorporate into their products. However, Unifi states that their products are made from 100% recycled material and are intent on lowering their plastic byproducts and waste. We should incentivize the production of consumer and industrial goods, such as textiles, which use and produce non-synthetic or recycled material. There should be a cap on the amount of synthetic materials textile companies within and around Charlotte may use in their production, and they must start to transition to incorporating recycled and natural, biodegradable material in their products. If, as mentioned in Section 1, these producers help finance stewardship organizations to recycle and collect material, then there will be greater resources of recycled material for these companies to obtain. It is necessary that there be repercussions for the amount of synthetic material used in the pre-production and production process as well as how it is wasted in post-consumer use. This can take the form of government-initiated fees or taxes on textile companies for the amount of synthetic material used.

3. Banning Polystyrene:

Six states across the US have implemented local bans on polystyrene for the risks it poses towards the environment and human health. As mentioned in the description, polystyrene is persistent, lasting over 500 years in the environment, pervasive, and hazardous, especially if ingested by vulnerable populations like children and adolescents. Maine and California are two states which have led the ban on Styrofoam materials for containers, beverages, and packaging material, and have reaped the benefits of a Styrofoam free community. However, in North Carolina, specifically in Charlotte, which is the 15th largest city by population in the US, consumption and use of Styrofoam material in everyday living is ingrained in our society. This needs to change. Almost every fast-food restaurant, diner and take out options have some form of non-recyclable Styrofoam material within its contents. Antioxidants, UV stabilizers, lubricants, color pigments, nucleating agents, and flame retardants, are all harmful additives included in the production of Styrofoam. It is necessary to have an all-out ban of Styrofoam materials in restaurant facilities, packaging materials, beverage containers, and retail stores in Charlotte, to inspire other cities around North Carolina to act along similar lines. Hopefully, Charlotte's stance will encourage other cities to adopt more progressive environmental policies to lower the risk of endangering our ecosystems and population.

DOI: 10.36838/v4i5.5

4. Phase Out Single Use Bags:

This has been a controversial topic nationally, as states have had to make decisions on how they may phase out single use bags, which invade our environments and subsequently enter our ocean, and find alternatives that are less damaging. Charlotte has taken a step forward, with the initiative towards replacing plastic bags for yard waste with paper bags. However, paper bags use the same amount if not more fossil fuel expenditures than plastic bags. They are often not as durable and unsupported by the local population and additives included during production are just as harmful. Yet, there are solutions to this problem, and we can look at New York's policies towards banning plastic bags, as an example. Eight states so far have banned or phased out plastic bags, but North Carolina is not among this list. New York has banned the sale and dissemination of plastic bags in grocery and retail stores, in restaurants which collect their sales tax for "to-go" items, and for any carry home items that may have gone in a plastic bag previously. To supplement this ban, they have imposed a $0.10 fee on paper bags, and the New York City sanitation department supplies free reusable bags at their local events. Reusable and paper bags are accessible at most retail and grocery stores so that consumers have access to these options and are not left without means to carry their items. The exceptions to this ban include bags used to carry prescription drugs at pharmacies, laundry services and dry cleaners, packaging for raw meat, and newspaper wrapping. We believe Charlotte has the economic means and support from the local community to advance these policies and incorporate phasing out single-use plastic bags in our community. As New York has done, Charlotte should phase out the use of plastic bags for retail, grocery, take-out items from restaurants, and to-go bags, as well as adding fees on paper bag alternatives in these stores. To take this a step further, the proceeds from the fees on paper bags should be administered to local environmental organizations who focus their initiatives on reducing plastic pollution, preserving our natural ecosystems, and implementing recycling initiatives and collection services. We also believe that at local events such as river, stream and street cleanups, like the ones hosted by the Keep Charlotte Beautiful Movement and the City of Charlotte Stormwater Services department, should provide reusable bags to all those who come out and support the cleanups, as a way to foster both collection and environmentally conscious consumer decisions. This phase out transition should be completed by 2024. There should also be access to paper and reusable bags at retail and grocery stores, and the fee should amount to at least $0.10.

5. Circular Economy:

In a city-wide released document, in 2018, Charlotte made a statement regarding transitioning to a circular economy. In this document, the reasons behind the benefits of a circular economy versus a linear, were outlined, highlighting the idea of a zero-waste producing community in which all items are repurposed, reused, and included into the market without losing its value. Transitioning to a circular economy also promotes job growth in the recycling and reusing processes, focuses on preserving biodiversity and promotes equity within a community. Charlotte has clearly taken actions to forward this position, and has cemented their desire towards reducing environmental degradation, however, there are still areas for improvement and growth within this process. Transitioning our economy from linear to circular is not a new initiative, but for this to be effective, as it has been in the European Union, more effort must be put towards proactively reducing the harm and consumption of plastic material. For example, we should start thinking about expanding and advancing our recycling facilities, or advancing our waste collection systems and preventing plastics from entering our aquatic ecosystems. In the Netherlands, scientists and engineers innovated a bubble barricade which prevents plastic materials from entering aquatic ecosystems and can then be easily accessed for waste collection. It is technology like this which demonstrates the possibilities of a circular system. As with the Innovation Barn in Charlotte, we should be incentivizing and raising more community awareness of sustainable innovations, everyday practices, and how we can support local initiatives who foster the reduction of plastic waste and protection of our environment. This can be done through educational programs within schools, specifically lower levels such as elementary, middle and high school education, and should be brought up during council forums to discuss ways in which we can further our sustainability goals and increase our knowledge of the harms of plastics pollution.

6. Funding Research:

California is a leading state in confronting the microplastics crisis. In their Senate Bill 1422: "California Safe Drinking Water Act: microplastics," they proposed a series of investigations on drinking water quality in relations to the presence of microplastic pollution and required under the federal ordinance to regulate the contaminants in public and private water systems. This bill will implement the Safe Drinking Water Act more effectively, and by 2020 will have a concrete definition of microplastics. Although this act is ambitious, and may not fully come to fruition, it demonstrates California's seriousness on the issue of microplastics and will take an active role in reducing its implications. It is necessary that Charlotte acts in a similar manner. Speaking with several NGOs, including the Charlotte Catawba Riverkeeper, CMSWS, the Keep Charlotte Beautiful Movement, and a professor from UNC-Chapel Hill, it is clear that the trends and understanding of microplastics in North Carolina is not being researched thoroughly. With a pervasive issue such as this, it is necessary to have a firm commitment towards understanding and identifying the sources and implications of this issue, as we cannot take proactive steps towards reducing the harm of microplastics if we do not share a consensus that there is a significant problem. It is necessary to fund research and have outreach programs that target all citizens around Charlotte to inform them of the current information and understanding of microplastics around the Charlotte area. This can be done multiple ways. Either by local NGO and NFP organizations who help fundraise for research activities by universities around us, or grants given from state funds to university scholars and local organizations with the intent on researching the prevalence and effects of microplastic pollution in the North Carolina region. We believe we should be taking an active stance towards understanding and identi

fying this problem, especially in our drinking water and food sources, which have a direct impact on our health, instead of neglecting its significance. Researching microplastic pollution is a complex process, especially in regard to understanding how humans are influenced, as there are many other factors that contribute to health risks. This is why it is necessary to have increased funding in universities and local organizations around North Carolina and Charlotte to finance advanced technology, a greater labor force, and gain credibility and support of other states and countries who are also researching microplastic pollution.

7. Cap and Trade:

Using the Cap-and-Trade model for carbon emissions as a guide, we believe implementing Cap and Trade market and government policies for plastic pollution can serve the same purpose and help with our goal towards zero waste. Acting as both an environmental and economic policy, cap and trade incentivizes companies and producers to stay below the carbon emission threshold when they are manufacturing, selling or transporting materials. As the government gives companies allowances for the specific amount of carbon emissions they can release on an annual basis. The allowances are through auctions or given freely depending on whether the company has stayed under their carbon emissions limit. The companies are then able to trade their allowances with other companies on their own terms for those who may have gone over their allowances and need some assistance. This works well under a free market system. We believe the same principle can be used with plastics production and post-consumer waste. There must be a maximum number of plastics that companies cannot go over for pre- production, the process of producing, and post-consumer waste, each set on different terms. For post-consumer waste, the policy should be set so that if their products are not recycled then they must use more of their allowances on the basis that this is entering our environment and causing harm. The limit should become stricter every year with the advancement of having a zero-waste community. The limits may be set differently depending on the type of company or manufacturing facility. For instance, the limits on textile companies for production of materials may be set lower than a plastic packaging company. We believe this can and should fit into the economic system of Charlotte, as this promotes free trade and environmental welfare.

Appendix E: Policy recommendations for the city of Charlotte regarding strategies to mitigate microplastics.

DOI: 10.36838/v4i5.5

IJHSR
ijhighschoolresearch.org
RESEARCH ARTICLE

Use of Mining Waste in Civil Construction

Pedro Valim Hespanha Gonçalves
Colégio Dante Alighieri, Alameda Fernão Cardim, São Paulo, São Paulo (SP), 01403-020, Brazil; pedro.goncalves@colegiodante.com.br

ABSTRACT: Two types of mining waste from the Brazilian mining industry (Samarco), sand waste (RAS) and flotation mud (LFS), were used to manufacture mini bricks. The manufactured bricks were heated in a ceramic furnace at Colégio Dante Alighieri. The products obtained by using RAS became brittle after firing, so they were not used for further studies. The LFS mini bricks presented a consistent appearance and were used in subsequent tests. The selected samples were compared to commercially available blocks of the same size and tested for compressive strength and water absorption. The results showed that the waste brick samples presented water absorption values between 8% and 25%. All mini brick samples also showed compressive strength values greater than 1.0 MPA. Therefore, the LFS bricks followed the standard allowed by the Brazilian legislation for this type of material related to compressive strength and water absorption. The results indicate that these materials could be used in construction works without causing cracking or structural problems. The next step in this study is to perform the same tests, but with waste bricks that present similar standard dimensions as regular bricks. The use of waste in other processes can contribute to the reduction of environmental impacts caused by the mining industries in Brazil. This project also tackles the 8th, 9th, 11th, and 12th sustaintable goals since, if done in large scales, it could provide clean water and sanitation, make cities more sustaintable, and preserve the life on land and below water.

KEYWORDS: ECivil Engineering; Waste Management; Mining Industry; Recovery and Recycling.

Introduction

Recent disasters involving tailing dams reveal the enormous risk that these structures can present. On November 15 of 2015, a dam broke in a Brazilian state called Minas Gerais, generating several environmental impacts in the city of Mariana,[1,2] causing the death of 19 people, burying more than 200 houses, nearly extinguishing 11 species of fish, and contaminating about 680 kilometers of rivers and streams, including the Rio Doce (Figure 1).[3] In addition, the so-called Quadrilátero Ferrífero (a region also located in the state of Minas Gerais that is known for having a large number of mines) has more than 700 waste dams. Moreover, in August 2014, there was a dam disaster by the mining company Imperial Metals Corp. at the Mount Polley mine, which dumped 5 million cubic meters of tailings from copper and gold exploration into the Hazeltine and Cariboo streams in the province of British Columbia in Canada.[4] That accident caused numerous environmental impacts and affected more than 300 homes.[5,6]

In this context, besides the contamination of the environment, mining industries generate large volumes of materials. These materials are often accumulated in piles around the companies themselves, occupying important and necessary physical spaces that could have other purposes, or placed in landfills without generating any profit for the company. An alternative to this problem would be a recycling system, where this material may bring, in addition to environmental benefits, economic return.[7]

As mentioned before, mining waste is usually placed in dams, as this alternative is considered a low-cost method. A survey carried out by a Technological Research Institute (Instituto de Pesquisas Tecnológicas - IPT), located in São Paulo, Brazil, that complements the data generated by the Institute of Applied Economic Research (Ipea), indicates that around 4.86 billion tons of tailings were accumulated between 2009 and 2014 in Brazil, taking into account only 15 minerals out of a total of 70 that the country produces.[8]

Currently, iron is responsible for approximately 80% of the profit generated by the export of ores in Brazil. According to the United States Geological Survey, iron ore production in Brazil was estimated to be 398 million tons in 2013, equivalent to 13.5% of the global total. A number that places the country among the largest iron producers in the world, with an estimated reserve of 31 billion tons of iron ore, behind only Australia, with 35 billion tons.[9]

This project aims to reduce the amount of waste by the use of the mining process' by-products to obtain materials used in the construction industry. The use of waste in the composition of materials for other purposes can lower raw material costs and, consequently, the price of the final product.

One of the most commonly used materials in the construction industry is solid bricks. They are a type of block made of common clay, has no holes, and is molded with straight edges, and can be made by burning the pieces in ovens. It is considered a rustic brick and produces very resistant masonry.[10]

Bricks used in construction can be made from clay, sand, slate, calcium silicate, cement or concrete, as well as other unusual materials. Clay is the most common material to be used. For the manufacture of the brick, initially, a homogeneous mass with the raw material is made, or a mixture of raw materials. Then the material is burned at about 900ºC (in the case of clay) to form the hardened bricks. Common brick typically contains the following components: silica (50 to 60% by weight), alumina (20 to 30% by weight), lime (2 to 5% by

DOI: 10.36838/v4i5.6

weight), iron oxide (5 to 6% by weight), and magnesium oxide (less than 1% by weight).[10]

Solid brick is most commonly used today in the construction of foundations. It also provides thermal and acoustic comfort, which is the reason why it is used on such a large scale. Therefore, using mining waste to produce bricks can minimize the environmental and social degradation caused by activities of this type of industrial process.[11,12]

Once ready, the bricks need to be tested to see if they are suitable for the application. According to Pablos *et al.* (2009), the most suitable tests for bricks are compressive strength, water absorption, air permeability, and solubilization, in which the first two tests are the most important.[12]

Water absorption determination in bricks is essential as it checks the percentage of water absorbed by them, which if it is not ideal can damage the structure. The compressive strength test, on the other hand, verifies the load capacity that the blocks support when subjected to forces exerted perpendicularly on their opposite faces (Figure 2). This test determines if the samples offer adequate mechanical strength and simulates the pressure exerted by the weight of the construction on the bricks. Failure to comply with the minimum normative parameters indicates that the wall may present structural problems such as cracks. Consequently, the failure to comply with a minimum parameter of compressive strength > 1.0 MPa will present risks of collapse in the construction.[13] The limit of compressive strength is calculated by the maximum load divided by the original section of the specimen.

The compressive test can be performed on the universal testing machine by adapting two flat plates, one fixed and one movable. It is between them that the sample is supported and held firm during compression.

This project differs from current literature because, unlike the vast majority of tests, this procedure can be easily done on a larger scale, which can assist in the production of bricks and consequently decrease the amount of mining waste faster than usual.

Methods

Bricks with smaller dimensions than ordinary bricks were used in this study to save the mining waste provided by the Samarco industry. Thus, the original measurements of the common bricks were divided by 4, and the following measurements were obtained: height: 1.3 cm, length: 6 cm, and width: 2.9 cm. After the determination of the dimensions, the drawings were sent to the Dante Alighieri College joinery, which made the plywood molds, with a thickness of 0.5 cm (Figure 3).

The LFS (flotation mud) had a pasty consistency, so it was used directly in the molds. The sand waste was a brittle residue so a binder was required, so that it could be shaped into a brick. The binder used was carboxymethylcellulose, known as CMC. Five grams of the binder was dissolved in water to a volume of 1 liter in a volumetric flask.

The solution was mixed with the sandy residue to form a pasty mixture. The pasty samples of the two residues (LFS and RAS) were placed in the plywood molds. There were six samples of each type of waste, totaling 12 samples (Figure 4).

All bricks dried for 15 days and were then placed to heat in a ceramic kiln (JUNG, Figure 5). The samples were placed in the oven for eight hours until they reached 900ºC. The oven was set to remain at 900 ˚C for 20 minutes and, after that time, the temperature began to decrease, reaching a final temperature of 40 ˚ C. The total time spent in the oven was 16 hours.

Mechanical Tests :

The compressive strength and water absorption tests were performed in partnership with the Pontifical Catholic University of São Paulo - PUC-SP, Marquês de Paranaguá campus (Figure 6). These tests were performed only with the pre-selected bricks.

Compressive Strength Teste:

Firstly, the commercial bricks were cut in the cross-section to have the same dimensions as the mini waste bricks using an AEG Policorte saw, model SMT-355 (Figure 7). The cut bricks can be seen in Figure 8.

A high concentration of BR2 is needed for cancer cell deliverFor the tests of compressive strength and water absorption, the tests were performed following the standard ABNT NBR 8492 (Cement soil brick - Dimensional analysis, determination of compressive strength and water absorption - Test method).[14]

To carry out the compression test, following the previously mentioned standard, 300g of cement (CP II-E32) were weighed on a scale (Mars - AD50K) and mixed with 150 ml of water until a homogeneous paste formed, which was deposited in a porcelain capsule (Figure 9).

For the assembly of the test material, a layer of cement was placed directly on the glass support and then half of the bricks were added under that layer, and so on until it formed a kind of hamburger (Figure 10).

The material was entirely covered by the prepared cement. After that, the bricks dried for 14 days so that it could be tested on the hydraulic press (Figure 11).

Water absorption test:

The water absorption test was also performed following the ABNT NBR 8492 standard. First, the brick mass was determined before and after placing it in a drying oven (Figure 12). Then, the samples were immersed in water (Figure 13), and after twelve hours, the mass of the wet block was measured. The percentage of water absorbed by the sample was determined by the difference between the two values found. At the end of the analysis, the brick was required to have a water absorption between 8% and 25%.[14]

Results and Discussion

Brick rating after heating:

Two types of waste were used by Samarco and were labelled as flotation mud (LFS) and sandy waste (RAS). The chemical composition from both of the samples is shown in Table 1. According to Table 1, both samples had silicon and iron oxides as the main compounds. However, the LFS sample had a 14.8% lower silica content and 9.8% more iron than the

DOI: 10.36838/v4i5.6

RAS sample. Mini bricks molded by using both residues, after heating at 900ºC in a furnace provided by Colégio Dante Alighieri (commonly used for ceramic materials), had the appearance shown in Figure 14.

The bricks obtained by the addition of the bonded RAS had a brittle appearance and therefore were not suitable for use in the manufacture of bricks used in civil construction, as shown in Figure 14. It is believed that the RAS residue was not suitable for the manufacture of mini bricks because its silica content was extremely high (79.3) when compared to the LFS percentage (64.5). However, through research, this solid waste can apply to other areas.

The bricks obtained from flotation mud appeared to be adequate, so they were chosen to continue this study.

The masses of each brick sample before and after heating using the LFS and their respective measurements are shown in Table 2.

The bricks obtained from LFS lost weight after heating at 900ºC due to the loss of water contained in the raw material. The bricks also showed a reduction in length and width after the heating. However, the height measurement was, at times, equal to or greater than the initial measure, showing that the material expanded in the furnace during firing. The percentage of mass loss for samples 1 to 6 was 20.77 g; 21.53 g; 20.44 g; 20.86 g; 21.10 g; 21.0 g, respectively.

Water absorption and compressive strength test results:

The LFS and the common bricks samples presented a cross-section cut at the same dimensions as that of the mini bricks for comparison and were weighed with a scale and measured with a caliper. The data obtained was used to calculate the percentage of water absorption. Water absorption tests were done in duplicate, and the results are shown in Table 3 as well as in Figure 15.

As can be seen in Table 3 and Figure 15, all samples had water absorption values lower than 25%, which is the limit of the standard applied by Inmetro (2019). Thus, the waste bricks met the requirements of the Brazilian law and therefore, when used in a building, would not be damaged by moisture.

The compressive strength tests were performed on four different samples, and the results are shown in Table 4 and Figure 16.

The bricks made by residue presented compressive strength values slightly lower than the values obtained for common bricks, as can be seen in Table 4. All samples presented compressive strength values greater than 1.0 MPa, and therefore meet the requirements of the Brazilian law. 15 A wall formed by the waste bricks would not present cracking problems, and there would be no risk of collapse.

Discussion

Aiming to improve the results in both tests, concrete can be added to the composition of the brick. After that, performing dry curing would be necessary, because this procedure is essential for the concrete to achieve a better performance since it improves the resistance and the durability of the brick. If not done correctly, dry curing can cause cracks and make the surface layer weak, porous, and permeable. The chemical characteristics of mining waste are very close to those required for the production of ceramic products. The manufacturing of pavement and replacement of aggregates for concrete manufacturing are also options for which the chemical composition is not very rigorous. Particle size and strength are characteristics very important for this type of material, and can be evaluated for use in civil construction. Finally, it is possible to measure the application of tailings for the manufacture of cement, since the high content of iron in cement can eliminate the incorporation of powdered iron in conventional cement. Samarco solid waste used in this study has iron in high quantity and could be used for cement production.[6,15]

In aiming for better results, the addition of slate (20%) or chamotte (3%) to the brick making process could improve the results of the resistance tests by, respectively, 41% and 150%, as these residues increase the permeability, improving the drying and firing procedure. Besides, increasing the temperature in the heating process to 1000˚C could improve the results of the absorption tests.[16,17]

Conclusion

Samarco's sandy waste was not suitable for the manufacture of mini-bricks because it was brittle after the heating process. It is believed that the RAS residue was not suitable because its silica content was almost 15% higher than the content of sílica from LFS. The silica content may have been responsible for the brittle appearance of the RAS bricks, so the residue from the flotation step was used for further testing. The bricks obtained from the LFS presented mass loss after burning between 20.44% and 21.53%. The bricks also showed a reduction in length and width during firing. However, the height measurement was, at times, equal to, or greater than the initial measurement. In the water absorption tests, the two samples of waste bricks presented values between 8% and 25%, and, therefore, fit the current Brazilian law. All mini-brick samples had compressive strength values greater than 1.0 MPa, and therefore met the requirements of the law for civil construction in Brazil. These results indicate that LFS residue bricks won't cause cracking or structural problems. The next step of this study will be to perform the same tests but on waste bricks with equal dimensions as ordinary bricks as well as evaluate the addition of other materials to the composition of the bricks.

Acknowledgments

Thanks to Samarco for supplying waste samples, to teacher Lucia for the help in making bricks and burning the samples, to the chemistry lab for help with the entire Project, and to Rodrigo Braga of the Pontifical Catholic University of São Paulo - PUC-SP, Marquês de Paranaguá campus for his assistance in the water absorption and compressive strength tests.

References

1. Izidoro, J.C., Kim, M. C., Bellelli, V. F., Pane, M. C., Junior, A. B. B., Espinosa, D. C. R., & Tenório, J. A. S. (2019). Synthesis of zeolite A using the waste of iron mine tailings dam and its appli cation for industrial effluent treatment. *Journal of Sustainable Mining*, 18(4), 277-286.

2. Freitas, C. M. D., Barcellos, C., Asmus, C. I. R. F., Silva, M. A. D., & Xavier, D. R. (2019). From Samarco in Mariana to Vale in Bru madinho: mining dam disasters and public health. *Cadernos de saude publica*, 35, e00052519.
3. Portal G1 .<http://g1.globo.com/minas-gerais/noticia/2015/11/barragem-de-rejeitos-se-rompe-em-distrito-de-mariana.html> (Accessed May 9, 2018).
4. Baker, P., MS Sweeney, and J. Mcelroy. "Residents calling it an environmental disaster: tailings pond breach at Mount Polley Mine near Likely, BC.", (2014). <https://globalnews.ca/news/1490361/tailings-pond-breach-at-mount-polley-mine-near-likely-bc/> (Accessed February 12, 2020)..
5. De Andrade, Luana Caetano Rocha, Eduardo Antonio Gomes Marques, and Ricardo André Fiorotti Peixoto. "Perspectivas para o reaproveitamento de rejeitos da mineração de ferro como ma teriais de construção." *Revista Geografias* (2017): 32-44. <https://periodicos.ufmg.br/index.php/geografias/article/download/13413/10645> (Accessed October 16, 2019).
6. De Sant'ana Filho, Joaquim Nery. "Estudos de reaproveitamen to dos resíduos das barragens de minério de ferro para uso na pavi mentação de rodovias e fabricação de blocos intertravados." *Cen\tro Federal de Educação Tecnológica de Minas Gerais., Belo Hor izonte* (2013). <http://www.posmat.cefetmg.br/wp-content/uploads/sites/120/2017/08/Disserta%C3%A7%C3%A3o_Joaquim_Nery_Filho.pdf> (Accessed October 16, 2019).
7. Bolzan, Marcelo Veber. "Estudo da utilização de resíduos da mineração de calcário na produção de blocos de concreto para con strução civil." (2015). <http://dspace.unipampa.edu.br/handle/riu/1428> (Accessed October 9, 2019).
8. Piacentini, Patricia. "Existe alternativa para o uso dos rejeitos de mineração?." *Ciência e Cultura* 71.2 (2019): 9-12. <http://cienciaecultura.bvs.br/scielo.php?pid=S0009-67252019000200004&script=sci_arttext&tlng=en> (Accessed April 25, 2018).
9. Instituto Brasileiro de Mineração – IBRAM. Informações e aná lises da economia mineral brasileira. 7ª Edição. 2012. <http://www.ibram.org.br/sites/1300/1382/00002806.pdf> (Accessed February 5, 2020).
10. ECIVIL - <http://www.ecivilnet.com/dicionario/o-que-e-tijolo-macico.html> (Accessed May 16, 2018).
11. Minas Jr Consultoria Mineral - <http://www.minasjr.com.br/do-que-sao-feitos-os-tijolos/> (Accessed on May 16, 2018).
12. Pablos, Javier Mazariegos, Eduvaldo Paulo Sichieri, and Rafaela Lino Izeli. "Reutilização de resíduo sólido industrial, constituído por areias de fundição, na fabricação de tijolos maciços e peças decorativas." *Risco-Revista de Pesquisa em Arquitetura e Urban ismo* 10 (2009): 112-125. <https://www.revistas.usp.br/risco/article/view/44784> (Accessed March 21, 2018).
13. PRACONSTRUIR - <https://blogpraconstruir.com.br/> (Accessed May 16, 2018).
14. Instituto Nacional de Metrologia, Qualidade e Tecnologia - INMETRO - <http://www.inmetro.gov.br/> (Accessed February 15, 2019.)
15. ABNT NBR 8492 - Associação Brasileira de Normas Técnicas. "Tijolo de solo-cimento - Análise dimensional, determinação da resistência à compressão e da absorção de água", (2012). <https://www.abntcatalogo.com.br/norma.aspx?ID=193718#:~:text=Esta%20Norma%20estabelece%20o%20m%C3%A9todo,para%20alvenaria%20sem%20fun%C3%A7%C3%A3o%20estrutural.> (Accessed May 3, 2019).
16. Zhang, Shu-hui, et al. "Current situation and comprehensive utilization of iron ore tailing resources." Journal of Mining Science 42.4 (2006): 403-408. <https://link.springer.com/article/10.1007%2Fs10913-006-0069-9> (Accessed February 12, 2020).
17. PALHARES, L., et al. "A utilização de rejeitos na produção de tijolos para construção civil." Anais do 20º Congresso Brasileiro de Engenharia e Ciência dos Materiais, Joinville–SC. 2012. <http://www.metallum.com.br/20cbecimat/resumos/trabalhos_completos/118-014.doc> (Accessed April 25, 2018)..

Author

Pedro Valim Hespanha Gonçalves is a senior in an Italian private school called Colégio Dante Alighieri. This project was developed in a program called Cientista Aprendiz. He aims to use the knowledge he has obtained for further studies in architecture area and civil engineering.

Figure 1: Area devastated after the rupture of the dam containing mining waste from the Samarco company. Source: https://ferdinandodesousa.wordpress.com/2017/08/17/.

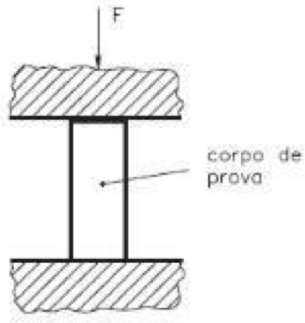

Figure 2: Compression test outline. Source: http://www.inmetro.gov.br/.

Figure 3: Brick molds made from plywood in the Colégio Dante Alighieri's laboratory.

DOI: 10.36838/v4i5.6

Figure 4: Mini bricks made from Samarco waste. On the left: sandy residue (RAS), and on the right: flotation mud (LFS).

Figure 5: Ceramic material oven from Colégio Dante Alighieri.

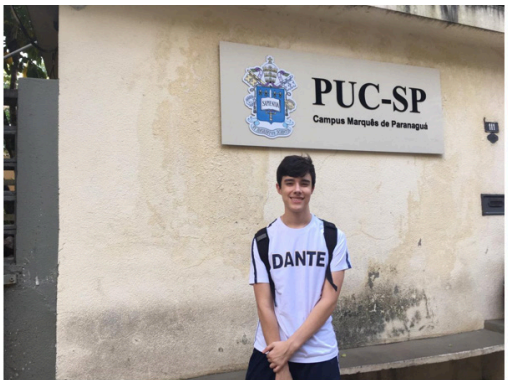

Figure 6: PUC-SP, Marquês de Paranaguá campus.

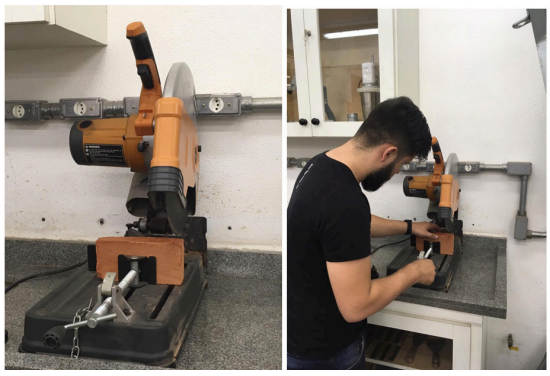

Figure 8: Waste bricks and common bricks after cutting in the civil engineering laboratory at PUC-SP.

Figure 9: Cement being weighed on the scale and the cement mass prepared after adding water.

Figure 10: Cement being weighed on the scale and the cement mass prepared after adding water.

Figure 11: Hydraulic press used for brick compression tests (brand: Solotest).

Figure 12: Determination of the mass of bricks in PUC-SP laboratory analytical balance.

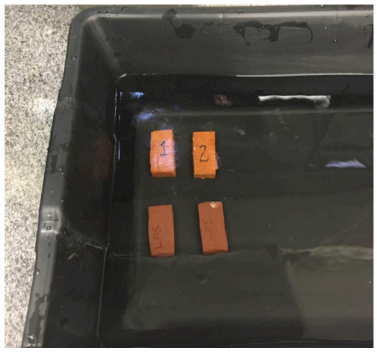

Figure 13: Bricks submerged in water for water absorption testing.

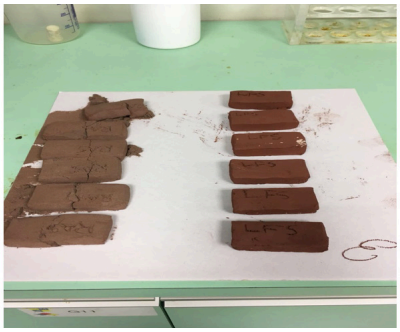

Figure 14: Residue bricks after heating.

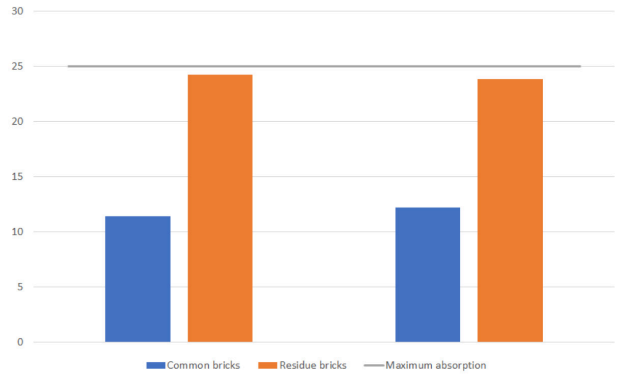

Figure 15: Results of water absorption in percentage.

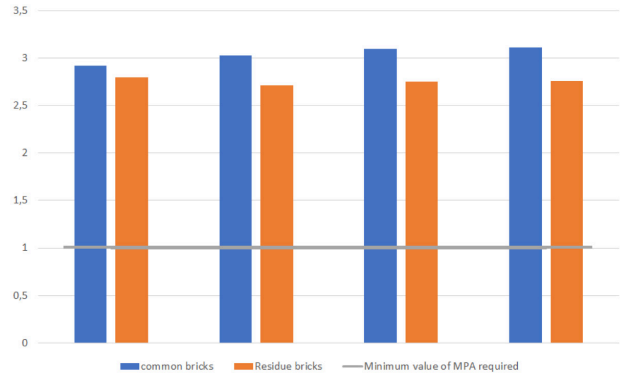

Figure 16: Results of compressive strength tests in MPa.

Table 1: Chemical analysis of the RAS and LFS samples.

COMPONENT	CONTENT % (RAS)	CONTENT % (LFS)
SiO_2(%)	79.3	64.5
Fe_2O_3(%)	19.3	29.1
Al_2O_3(%)	0.46	2.13
Cr_2O_3(%)	0.15	0.051
MgO(%)	0.04	0.040
SO_3(%)	0.04	0.414
P_2O_5(%)	0.03	0.074
K_2O(%)	0.03	0.155
CaO(%)	0.03	0.182
Others	< 0.7	< 3.0
LOI (%)	0.5	2.55

Table 2: Characteristics of the bricks before and after heating.

MINI BRICKS	CHARACTERISTICS BEFORE HEATING				CHARACTERISTICS AFTER HEATING			
	M (g)	L (cm)	W (cm)	H (cm)	M (g)	L (cm)	W (cm)	H (cm)
1	67.45	6.0	2.9	1.3	53.44	5.9	2.6	1.5
2	68.97	6.0	2.9	1.3	54.12	5.8	2.8	1.7
3	69.88	6.0	2.9	1.3	55.60	5.8	2.8	1.4
4	67.13	6.0	2.9	1.3	53.13	5.6	2.9	1.3
5	66.44	6.0	2.9	1.3	52.42	5.7	2.8	1.4
6	66.76	6.0	2.9	1.3	52.74	5.9	2.8	1.4

M = mass; L = length; W = width; H = height.

Table 3: Results of the water absorption test.

TYPE	DIMENSIONS (CM)	DRY WEIGHT(G)	WET WEIGHT(G)	ABSORPTION (%)
CB1*	2.31 x 5.87	37.58	41.85	11.38
CB2*	2.25 x 5.62	33.79	37.90	12.18
RB1**	2.13 x 5.82	55.52	68.95	24.20
RB2**	2.16 x 5.75	53.34	66.04	23.82

*CB = Common brick ; **RB = Residue brick.

DOI: 10.36838/v4i5.6

Table 4: Results of compressive strength tests.

SAMPLE	DIMENSIONS (CM)	AREA (CM^2)	AXIAL FORCE	CHARGE	MPa
CB1	2.43 x 3.03	7.3629	215	29.200	2.920
CB2	2.36 x 2.95	6.962	211	30.307	3.030
CB3	2.24 x 3.07	6.8768	213	30.973	3.097
CB4	2.23 x 3.10	7.3629	229	31.101	3.110
RB1	2.14 x 2.79	5.9706	167	27.970	2.797
RB2	2.07 x 2.83	5.8581	159	27.141	2.714
RB3	2.21 x 2.88	6.3648	175	27.494	2.749
RB4	2.19 x 2.78	6.0882	168	27.594	2.759

IJHSR
ijhighschoolresearch.org
■ REVIEW ARTICLE

Nanotechnology in the Detection and Treatment of Sarcomas

Shreya S. Katuri
River Hill High School, 12101 Clarksville Pike, Clarksville, MD 21029, U.S.A; shreya.s.katuri@gmail.com

ABSTRACT: Current treatments for soft tissue sarcomas primarily involve surgical excision of the tumor with widely negative margins. To further reduce the risk of local recurrence, neoadjuvant or adjuvant treatment with radiation or systemic therapy may be added. Both radiation therapy and systemic therapy may be limited by off-target effects. Advances in nanotechnology aid with intraoperative and postoperative visualization of tumor margins, which improve surgical excisions and offer the opportunity to selectively target tumors with systemic therapy or local adjuvants, reducing off-target effects. Through exploitation of unique attributes of peritumoral vasculature, methods of fluorescence localization and targeted drug delivery, nanotechnology has the potential to transform the surgical management of soft tissue sarcomas.

KEYWORDS: Translational Medical Sciences; Disease Treatment and Therapies; Soft Tissue Sarcomas; Nanotechnology; Targeted Delivery.

■ Introduction

With an estimated 13,130 diagnoses and 5,350 deaths of soft tissue sarcomas in 2020, current treatments for sarcomas have much room for improvement.[1] A majority of these tumors are treated with surgical excision. However, one of the many challenges of excising soft tissue sarcomas, a soft tissue cancer that originates from mesenchymal tissue, is its high recurrence post-surgical excision.[2] In some cases, radiation is added to decrease local recurrence, but this can cause side effects. Similarly, while systemic therapy is not commonly incorporated in the treatment plan for extremity soft tissue sarcomas, these medications are limited by off-target effects, or systemic side effects. Nanotechnology offers the potential to reduce either local recurrence of sarcomas or the side effects of radiation or chemotherapy. The novel technological field aims to reduce the toxic effects of chemotherapy and radiation by taking advantage of the unique attributes of peritumoral vasculature. The use of nanotechnology in cancer detection and treatment can reduce harmful side effects and increase the efficacy of treatments, while providing non-invasive imaging to assist with the surgical removal of sarcomas.[3] This review will discuss current research regarding the use of nanotechnology in the detection and treatment of sarcomas, as well as the future applications of nanotechnology outside of oncology.

The EPR and ELVIS Effect:

One of the most important characteristics of tumors that supports growth is tumor angiogenesis, or the formation of new blood vessels. It has been proven that tumors create vascular endothelial growth factor (VEGF) that increases angiogenesis. The new vasculature in the tumor helps maintain the blood supply to the tissue and keeps it alive. The "...defective vascular architecture; large gaps between endothelial cells in blood vessels; abundant vascular mediators...and vascular endothelial growth factor; and impaired lymphatic recovery" in the peritumoral environment give tumor tissue unique properties including the Enhanced Permeability and Retention (EPR) effect.[4] The EPR effect is a natural phenomenon that occurs in solid tumors as a result of their abnormal vasculature. Normal capillaries allow the diffusion of some small particles. Tumor vasculature, however, is defective and tends to produce an abnormal amount of different permeability factors. Therefore, many solid tumors have an enhanced state of permeability, which helps with the diffusion of nutrients and oxygen into the tissue. The "retention" aspect is accompanied by the retention of the larger particles within the peritumoral environment, though there is a size cutoff for retained particles. Physicians can utilize these characteristics to apply the EPR effect in therapeutic or diagnostic applications.[4] The EPR effect is a fundamental concept in the use of nanotechnology as a targeted drug-delivery system. Because of this phenomenon, nanotechnology proves to be a promising field of research for oncological therapeutics.

The Extravasation through Leaky Vasculature and the subsequent Inflammatory cell-mediated Sequestration (ELVIS) is an alternative mechanism that occurs along with the EPR effect. The initial identification of this effect was observed in inflammatory arthritis animal models. It was noted by Yuan *et al.* that, in inflammatory arthritis animal models, once "the macromolecular prodrug extravasates through the leaky vasculature, it is internalized and sequestered by the synoviocytes."[5] These animal models suggest that the targeted retention of macromolecules at inflamed joints is caused by the selective extravasation, or the leakage of fluids from a blood vessel to surrounding tissue, through the leaky vasculature of the inflamed tissue.[5] Within the peritumoral microenvironment, there are also areas of local inflammatory responses called the reactive zone. These areas of inflammation may result in "leaky" vessels and provide an alternative mechanism for sequestration of the nanoparticles within the tumor through the ELVIS effect.[6] While the EPR effect explains why nanoparticles sequester at tumors, the ELVIS

DOI: 10.36838/v4i5.7

impact of the nanoparticles once they reach the tumor site, since the effect helps with determining the cellular mechanisms utilized once the nanoparticles are in tumor tissue. Understanding this dictate how the nanotechnology properties may be adjusted in order to take full advantage of the characteristics of the tumor.

Nanotechnology:

Nanotechnology describes particle sizes usually between 1 and 100 nanometers. The small size is responsible for its unique properties, which allows for advancements in energy, manufacturing, and medicine.[7] The EPR effect and ELVIS effect utilize nanoparticles ideally between 50 to 150 nanometers, since smaller particles not only clear the body quicker but also diffuse through normal capillaries. In addition to size, the particle shape, charge, and lipophilicity of a nanoparticle all impact its utility and anatomic sites. Combining existing therapeutics with these properties afforded by nanotechnology applications can assist in the detection and treatment of sarcomas through targeted delivery, novel imaging techniques, controlled drug-release, and improved bioavailability.[8]

Fluorescence Localization:

In the last few decades, various imaging techniques, including computed tomography (CT), magnetic resonance imaging (MRI), and positron emission tomography (PET), have assisted in the detection of soft tissue masses as well as preoperative planning. Gadolinium is a contrast agent used in an MRI scan to help show abnormal tissue in the body. This widely utilized agent in magnetic resonance works predominantly by highlighting the localization and timing of vascular flow to the area. Though it is not a nanoparticle in the traditional sense, Gadolinium works as a diagnostic tool in a similar way to nanoparticles, and its size and charge allow the contrast agent to distribute in a similar pattern to that predicted by the EPR effect.[9]

Some tumors are surrounded by a large reactive zone of inflammation which may contain tumor cells. This is perhaps best recognized in myxofibrosarcoma, though inflammatory sarcomas of numerous histopathologic subtypes are recognized. These areas are visually enhanced with gadolinium. As such, a nanosized fluorescence probe may be utilized to identify the area of peritumoral inflammation, using the hyperpermeable vasculature of the inflammatory reactive zone and the properties of the ELVIS phenomena. With intraoperative fluorescence excitation, this technology affords the capability to assist the margin detection during surgical dissections of the soft tissue sarcomas.[10]

One instance of a compound used for intraoperative optical imaging is 5-Aminolevulinic acid (5-ALA). 5-ALA has been extensively studied for neurosurgical applications in managing gliomas. The non-toxic compound was found to be a promising subject of research for Kenan *et al,* who established that 5-ALA can selectively illuminate myxofibrosarcoma and chordoma cells *in vitro*. Since 5-ALA also acts as a photosensitizer, it additionally proved to be a potentially effective compound for photodynamic therapy of myxofibrosarcomas may contain tumor cells, making them susceptible to high rates of local recurrence. 5-ALA's ability to fluorescence at specific wavelengths suggests this as a candidate for fluorescence-guided surgical excisions, and the potential for PDT may further reduce the risk of local recurrence associated with similar tumors.[11]

Another example of a contrast used in intraoperative optical fluorescent detection is Hexa(sulfo-n-butyl)[60]Fullerene (FC_4S).12 FC_4S is a water-soluble molecule that has been known to cause cytotoxic effects on certain microorganisms after light exposure, which is known as photosensitization. Its ability to mediate PDT and water solubility suggests the molecule has the potential to help with the treatment of tumors. Yu *et al* confirmed the photodynamic properties *in vitro,* using fibrosarcoma cells and in murine sarcoma cells. The light irradiation with an argon-ion laser after injection of an FC_4S prevented further growth of the S180 tumors, and the PDT improved hematological and blood biochemistry of mouse models of sarcomas.[12]

Indocyanine Green Dye (ICG) has been used as a guide for carcinoma resections and has proven to greatly improve the results of surgical removals by helping surgeons achieve clear margins. Once injected into the bloodstream, ICG remains in areas of disorganized vasculatures, such as within tumors, and helps identify hepatocellular carcinomas, a common type of liver cancer.[13] Fluorescein angiography is a diagnostic test that uses a yellowish-colored dye called fluorescein to visualize blood vessels generally used by reconstructive surgeons.[14] ICG fluorescence angiography uses ICG instead of fluorescein to take advantage of the dye's attraction to areas of disorganized vasculature. Mahjoub *et al*. conducted research on mouse models of osteosarcoma to determine the effectiveness of ICG as an intraoperative guide during sarcomas resection. The research established that "ICG near-infrared fluorescence angiography signal localized precisely to primary and metastatic OS tumors and not the adjacent microenvironment".[15] The findings prove that the ICG fluorescence angiography can help achieve clear surgical margins, which are essential to ensure the complete removal of sarcomas and decrease local recurrence. Similar to the previously mentioned substances, ICG has the potential, as a nanoparticle, to increase efficacy and prevent positive surgical margins.[15]

Targeted Drug Delivery:

Another potential therapeutic use of nanotechnology, similar to PDT, is the use of a targeted delivery system, which can help decrease toxicity and increase the efficacy of current treatments. It has been found that "local failure rates of 10% to 28% at 5 years have been reported for locally advanced, unresectable sarcomas, due in part to limitations in the cumulative [radiation] dose that may be safely delivered".[16] In other words, radiation is unable to fully treat certain sarcomas due to dosage limitations, similar to chemotherapy. Nanotechnology can greatly improve dosage limitations by using its selective distribution. For instance, cisplatin is an agent that can be used alone or with either radiation or chemotherapy to help fight cancer. The agent is widely used

against many types of solid tumors, including breast, liver, lung, ovarian, testicular, bladder, head and neck, small-cell and non-small-cell lung cancers. However, cisplatin is unable to selectively distribute to tumor tissue, causing dose-limiting side-effects.[17] With the use of nanoparticles, cisplatin can potentially be used without the side effects as the non-selective distribution. The anticancer agent is the ideal example of how nanotechnology can work with both chemotherapy and radiation to provide targeted drug delivery that would reduce the harmful dose-limiting side effects of the treatments. Every radiosensitizer and chemotherapy agent works differently, but nanotechnology can greatly improve the effectiveness of both treatments and offer a more manageable treatment experience for the patient.

One example of targeted delivery systems is ionizing radiation, which treats cancer by forming ions in cells, removing electrons from atoms or forming free radicals and DNA strand breaks. This can activate cell death pathways or prevent cells from growing by changing their genes.[18] Radiosensitizers are substances that increase tumor cells' sensitivity to radiation by increasing the speed at which DNA is damaged.[19] Increasing the sensitivity of tumor tissue to radiation will assist in improving the effectiveness of the limited dosage of radiation against tumors. Nanoparticles can help with the radiosensitization of tumor tissue and provide imaging that may be useful for treatments. For instance, research into gold nanoparticles demonstrates their potential to help improve the efficacy of radiation therapy. Research has shown that radiation, in conjunction with nanoparticle radiosensitizer formulations, increases the effectiveness of radiation treatment. In a mouse model of sarcoma, nanoparticles were able to accumulate in the tumor tissue, providing imaging and possibly radiosensitization. The mice, once treated with gold nanoparticles and radiation, showed improved tumor regression and survival.[16] The small molecules of cisplatin, oxaliplatin, and carboplatin can be made into nanomolecules. The three particles have the ability to kill cancer cells without the use of radiation, and act as radiosensitizers, improving the effectiveness of radiation.[19] Similar to the previously mentioned application of nanotechnology, the use of nanotechnology in therapeutics requires further research to optimize the effects of nanoparticles in the treatment of sarcomas.

An alternative approach towards the use of nanotechnology in oncologic care relates to immunotherapy. One example was the use of N-(2-hydroxypropyl)methacrylamide (HPMA) copolymers, which are water-soluble and biologically stable. Initially, these copolymers were used with arthritis, where HPMA-based anti-inflammatory medications could be selectively delivered to areas of inflammation. Through the same concepts that allow the copolymer to be selectively delivered to sights of inflammation, pro-inflammatory medications can be delivered to extravasate in peritumoral vasculature as an attempt to alter the local macrophage population from a tumor-promoting M2 phenotype to a tumor-suppressing M1 phenotype.[6]

Ultimately, it is important to select the best drugs to work with nanotechnology to detect and treat different inflammatory diseases. Similar to the nanocarrier design, the drugs must be chosen to fit the specific pathophysiology of the disease being treated. Toxic substances with harmful off-target effects could potentially be used in safer and alternative ways if targeted drug delivery can reduce these off-target effects.[6]

Future Applications:

Though research in nanotechnology-based therapeutics has made enormous strides in the treatment of soft tissue sarcomas, there are aspects that require further exploration in order to increase efficacy and safety. More extensive research is needed to investigate the physiological barriers that prevent nanotechnology from working efficiently and avenues to bypass these barriers. Although the design for a nanoparticle will have to be made disease-specific to accommodate for the heterogeneous tumor-microenvironment, this research can help specify design characteristics that optimize the nanoparticle design.[20] Furthermore, nanomaterials will need to be studied to determine their safety in the human body and their effectiveness as a nanoparticle for sarcoma treatment.

Conclusion

Nanotechnology has proven to be an effective tool in medicine. Research in the field of oncology has shown the novel technology to have the potential to detect and treat cancer while also preventing any recurrence. Though further exploration is required in certain aspects of the field, as research continues, nanotechnology's targeting capabilities will revolutionize current soft tissue sarcoma treatments.

Acknowledgments

Shreya Katuri acknowledges and thanks Dr. Adam S. Levin from Johns Hopkins Hospital for donating his time to assist and guide her in writing this paper.

References

1. Key Statistics for Soft Tissue Sarcomas https://www.cancer.org/cancer/soft-tissue-sarcoma/about/key-statistics.html (accessed Mar 13, 2021).
2. Definition of soft tissue sarcoma - NCI Dictionary of Cancer Terms - National Cancer Institute https://www.cancer.gov/publications/dictionaries/cancer-terms/def/soft-tissue-sarcoma (accessed Apr 3, 2021).
3. Susa, M.; Milane, L.; Amiji, M. M.; Hornicek, F. J.; Duan, Z. Nanoparticles: A Promising Modality in the Treatment of Sarcomas. *Pharm Res* **2011**, *28* (2), 260–272. https://doi.org/10.1007/s11095-010-0173-z.
4. Fang, J.; Islam, W.; Maeda, H. Exploiting the Dynamics of the EPR Effect and Strategies to Improve the Therapeutic Effects of Nanomedicines by Using EPR Effect Enhancers. *Advanced Drug Delivery Reviews* **2020**, *157*, 142–160. https://doi.org/10.1016/j.addr.2020.06.005.
5. Yuan, F.; Quan, L.; Cui, L.; Goldring, S. R.; Wang, D. Development of Macromolecular Prodrug for Rheumatoid Arthritis. *Adv Drug Deliv Rev* **2012**, *64* (12), 1205–1219. https://doi.org/10.1016/j.addr.2012.03.006.
6. Purdue, P. E.; Levin, A. S.; Ren, K.; Sculco, T. P.; Wang, D.; Goldring, S. R. Development of Polymeric Nanocarrier System for Early Detection and Targeted Therapeutic Treatment of Peri-Implant Osteolysis. *HSS Jrnl* **2013**, *9* (1), 79–85. https://doi.

DOI: 10.36838/v4i5.7

org/10.1007/s11420-012-9307-7.
7. What is Nanotechnology? – Defining Nanotechnology https://education.mrsec.wisc.edu/what-is-nanotechnology-defining-nanotechnology/ (accessed Feb 10, 2021).
8. Jain, R. K.; Stylianopoulos, T. Delivering Nanomedicine to Solid Tumors. *Nat Rev Clin Oncol* **2010**, *7* (11), 653–664. https://doi.org/10.1038/nrclinonc.2010.139.
9. Chapman, S.; Dobrovolskaia, M.; Farahani, K.; Goodwin, A.; Joshi, A.; Lee, H.; Meade, T.; Pomper, M.; Ptak, K.; Rao, J.; Singh, R.; Sridhar, S.; Stern, S.; Wang, A.; Weaver, J. B.; Woloschak, G.; Yang, L. Nanoparticles for Cancer Imaging: The Good, the Bad, and the Promise. *Nano Today* **2013**, *8* (5), 454–460. https://doi.org/10.1016/j.nantod.2013.06.001.
10. Orbay, H.; Bean, J.; Zhang, Y.; Cai, W. Intraoperative Targeted Optical Imaging: A Guide towards Tumor-Free Margins in Cancer Surgery. *Curr Pharm Biotechnol* **2014**, *14* (8), 733–742.
11. Kenan, S.; Liang, H.; Goodman, H. J.; Jacobs, A. J.; Chan, A.; Grande, D. A.; Levin, A. S. 5-Aminolevulinic Acid Tumor Paint and Photodynamic Therapy for Myxofibrosarcoma: An in Vi tro Study. *J Orthop Surg Res* **2020**, *15* (1), 94. https://doi.org/10.1186/s13018-020-01606-9.
12. Yu, C.; Avci, P.; Canteenwala, T.; Chiang, L. Y.; Chen, B. J.; Ham blin, M. R. Photodynamic Therapy with Hexa(Sulfo- n -Butyl) [60]Fullerene Against Sarcoma In Vitro and *In Vivo*. *j nanosci nanotechnol* **2016**, 16 (1), 171–181. https://doi.org/10.1166/jnn.2016.10652.
13. Hepatocellular carcinoma - Overview - Mayo Clinic https://www.mayoclinic.org/diseases-conditions/hepatocellular-carcinoma/cdc-20354552 (accessed Apr 4, 2021).
14. What Is Fluorescein Angiography? https://www.aao.org/eye-health/treatments/what-is-fluorescein-angiography (accessed Apr 3, 2021).
15. Mahjoub, A.; Morales-Restrepo, A.; Fourman, M. S.; Mandell, J. B.; Feiqi, L.; Hankins, M. L.; Watters, R. J.; Weiss, K. R. Tumor Resection Guided by Intraoperative Indocyanine Green Dye Fluo rescence Angiography Results in Negative Surgical Margins and Decreased Local Recurrence in an Orthotopic Mouse Model of Osteosarcoma. *Ann Surg Oncol* **2019**, 26 (3), 894–898. https://doi.org/10.1245/s10434-018-07114-9.
16. Joh, D. Y.; Kao, G. D.; Murty, S.; Stangl, M.; Sun, L.; Zaki, A. A.; Xu, X.; Hahn, S. M.; Tsourkas, A.; Dorsey, J. F. Theranostic Gold Nanoparticles Modified for Durable Systemic Circulation Effec tively and Safely Enhance the Radiation Therapy of Human Sar coma Cells and Tumors. T*ranslational Oncology* **2013**, *6 (6)*, 722-IN32. https://doi.org/10.1593/tlo.13433.
17. Duan, X.; He, C.; Kron, S. J.; Lin, W. Nanoparticle Formulations of Cisplatin for Cancer Therapy. *Wiley Interdiscip Rev Nanomed Nanobiotechnol* **2016**, *8* (5), 776–791. https://doi.org/10.1002/wnan.1390.
18. The Science Behind Radiation Therapy. American Cancer Society October 27, 2014.
19. Boateng, F.; Ngwa, W. Delivery of Nanoparticle-Based Radiosen sitizers for Radiotherapy Applications. *IJMS* **2019**, *21* (1), 273. https://doi.org/10.3390/ijms21010273.
20. Gadolinium | What Is Gadolinium & What Is It Used for in MRIs? https://www.drugwatch.com/gadolinium/ (accessed June 23, 2021).

Author

Shreya Katuri is a senior at River Hill High School. She is passionate in medicine and interested in how technology can be utilized in the field. Shreya plans to pursue a career in Emergency Medicine. In addition, she loves to dance, volunteer, and cook.

IJHSR
ijhighschoolresearch.org
■ RESEARCH ARTICLE

The Impact Of COVID-19 on Adolescent Anxiety and Depression

Mira R. Kunz
Polygence Research Academy, 720 Serra Street, Suite 413, Stanford, California,94305, USA; mira_kunz@icloud.com

ABSTRACT: COVID-19 has impacted adolescent mental health due to multifarious effects from this pandemic. This study aims to survey how adolescents in Tacoma, Washington have been affected mentally by COVID-19. A survey consisting of 21 different questions based on the DASS-21 scale was conducted in order to assess symptoms of depression and anxiety. In addition, the survey asked participants at the end to give a short description about how the pandemic has impacted them mentally. Overall, there were 124 high school students who participated in the survey with the majority of them being students in 10th and 11th grades. This study showed that multiple students experienced extremely severe levels of stress, anxiety, and depression, from the 2020 quarantine. Overall, the pandemic has had multiple adverse effects on youth and adolescent mental health.
KEYWORDS: COVID-19; Anxiety; Depression; Adolescent; Mental Health.

■ Introduction

The coronavirus disease, also known as COVID-19, has severely impacted the world and not only in China where it originated. Due to the stay-at-home order, which was made by many world leaders in March of 2020, people experienced the loss of jobs, the isolation from people, and having their lives changed drastically. People had to adjust to different lifestyles (ex. working from home), which increased the amount of hardship they experienced by having to alter their lives so quickly.[2] COVID-19 is still an ongoing disease that proves to be unpredictable. So, it is to be understood that this crisis has continued to unfold since it began at the end of 2019.

COVID-19 has caused a widespread concern that mental health in children and adolescents has been negatively impacted due to the effects of the pandemic.[1-5] As such, anxiety and depression symptoms in adolescents have increased since March of 2020.[6] This study specifically targets adolescents and teens in the US, and the levels of anxiety and depression they experienced from March of 2020 to the present day. Nevertheless, there are still limitations to this study mentioned above since it was targeting only one audience in the US and there could have been other outside factors, besides COVID-19, leading to their psychiatric symptoms.

Recent studies have evaluated the impact of COVID-19 on adolescent depression and anxiety. During the spring of 2020 almost all of the states in the Union were in "lockdown" and nearly all education was remote. This lockdown has indeed affected adolescent mental health due to the isolation they felt being confined to their home and having little to no social interaction with the outside world. [2]

A few studies on the effect of adolescent anxiety and depression during COVID-19 pandemic have shown that students' symptoms have increased compared to before the pandemic.[3] Of these two studies only one of them was conducted in the United States.[2] Hawes, Szenczy, Klein, Hajcak, and Nelson all found that at the beginning of COVID-19 adolescents and young adults in Long Island, NY had indeed experienced increased depression and anxiety symptoms due the school and home confinement.[6]

■ Methods

The following study attempts to add to the literature on the impact of COVID-19 on adolescent anxiety and depression. The target audience for this project was high school students ranging from 14-18 years old and was administered in Tacoma, Washington. This survey was limited to this region due to COVID restrictions that were in place throughout the study period. This research was conducted from 1 June - 31 August 2021 and utilized a validated survey to assess participants mental health symptoms during the pandemic. This survey was sent out via email due to COVID-19 restrictions. The participants were chosen by their status as high school students at local schools in Tacoma, WA and were asked to rate and describe their emotional health as it related to the COVID-19 pandemic.

Measures:

The survey used in the study asked the following question: "How has COVID-19 affected your anxiety and depression symptoms?" while using the DASS-21 scale to help measure the participants symptoms. The DASS-21 is the short version of the DASS-42 but with only 21 items on it. Several criteria were used to create the DASS-21 scale and the items that were assessed focused on depression, anxiety, and stress. The participants were asked to pick a number between 1 and 4 to indicate how much the question being asked related to them. 1 equals "never", 2 equals "rarely", 3 equals "sometimes", and 4 equals "almost always". The higher the score in each subcategory the more severe the symptoms are for the respondent answering the question. Each subcategory was further characterized as either mild, moderate, severe, or extremely severe based on their overall score in that subcategory.[14]

DOI: 10.36838/v4i5.8

Procedures:

A survey was emailed out to students in Tacoma, Washington, using an online platform which was google survey. This survey was only given out to the students at private school who were in the age range between 13 and 19. All of the students who participated in the survey were informed about the purpose and objectives of the study and were made aware that their answers would be anonymous but used to conduct further research. The survey consisted of questions asking about age, ethnicity, gender, and sexuality and had a scale adapted from NovoPsych Depression Anxiety Stress Scales - Short Form (DASS-21). It was modified to reflect how the statements used in the survey applied to the participants over their period in quarantine, as opposed to over a one-week period. The DASS-21 scale was used to capture the participants' severity of anxiety, stress, and depression levels of participants taking the survey throughout COVID-19. Additionally, a non-required short answer question was also prompted at the end of the survey to give a better understanding of how COVID-19 quarantine impacted them emotionally. The data collected was between a period of two months from the beginning of July to the end of August 2021. The data was also calculated and analyzed using the online program Excel.

Results and Discussion

The final sample included 120 high school students who completed at least 90% of the survey. They ranged in age from 13-19 years old. 57.5% of the participants were female, 37.5% of the participants were male, and the remaining chose to identify as other. A few participants also preferred not to disclose their gender. All of the participants were from the United States. Participants self-identified as White (62.9%); Asian (15.3%); Hispanic, Latino or Spanish origin (5%); Black or African American (3.3%); Native Hawaiian or other Pacific Islander (3.3%); South Asian (2.5%); Middle Eastern (1.7%). 0.8% of the participants preferred not to say and 4.8% of the participants self-identified as other (Figure 1). Participants identified themselves as (73.3%) Straight, (19.2%) LGBTQ, and the rest preferred not to disclose (Figure 1).

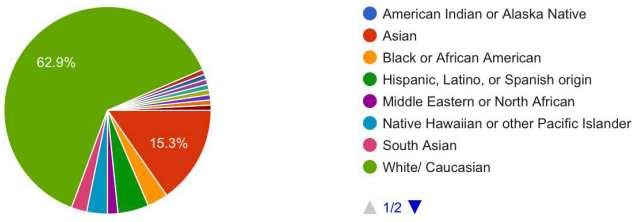

Figure 1: Ethnicity of survey respondents.

Overall, the majority of respondents had features of anxiety, depression, and stress that were rated as "extremely severe" as demonstrated by their scores for these subcategories on the DASS-21 survey (Table 1).

Table 1: Mean (average) Score for each subcategory of the DASS-21 survey.

	Mean Subcategory Score	DASS severity rating
Average Summative Depression Score	36.2	Extremely Severe
Average Summative Anxiety Score	28.5	Extremely Severe
Average Summative Stress Score	36	Extremely Severe

The least frequently endorsed questions (those questions most frequently endorsed as 1, "never") consisted of "There were times where I was aware of the dryness of my mouth" (42.6%) , "I had experienced breathing difficulty" (47.5%) , "I had experienced trembling" (49.2%) , "I felt I wasn't worth much as a person" (37.7%) , I was aware of the action of my heart in the absence of physical exertion" (50.8%) , "There were times where I felt scared without any good reason" (34.3%) , and "I felt that life was meaningless" (45.1%).

The second least frequently endorsed questions (those questions most frequently endorsed as 2, "rarely") consisted of "There were times where I found it hard to wind down" (39.3%), "There were times where I felt that I was using a lot of nervous energy" (32.8%), "There were times where I found it difficult to relax" (29.5%) , "There were times where I felt down-hearted and blue" (30.3%), "I was intolerant of anything that kept me from getting on with what I was doing" (50%), "There were times where I felt I was close to panic" (33.6%), "There were times where I felt like I was unable to be enthusiastic about anything" (34.3%), "I felt that I was rather touchy or very sensitive" (30.3%).

The third least frequently endorsed questions (those questions most frequently endorsed as 3, "sometimes") consisted of "There were times where I found it hard to wind down" (39.3%), "There were times where I couldn't seem to experience any positive feeling at all" (36.9%), "There were times where I tended to overreact to situations" (36.9%), "There were times where I was worried about situations in which I might panic and make a fool of myself" (32%), "There were times where I felt I had nothing to look forward to" (36.1%), "I found myself getting agitated easily" (36.9%), "There were times where I felt down-hearted and blue" (30.3%).

There was only one question where option 4 ("always") was most frequently endorsed. 45.2% of respondents reported "always" to the item, "There were times where I found it difficult to work up the initiative to do things." (Figure 2)

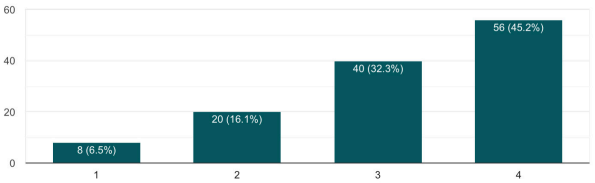

Figure 2: Number of respondents to question "There were times where I found it difficult to work up the initiative to do things."

In the free text response section of the survey, most students specifically commented that their underlying depression or anxiety symptoms worsened during the lock-down and

summer of 2020 prior to the start of school. Additionally, some students commented that these symptoms seemed to worsen despite returning to school and have persisted to the present day. Interestingly, a small number of students surveyed commented that they developed coping skills that helped them deal with their feeling of isolation, depression, and anxiety, and have continued to utilize these skills. The number of students who reported persistent symptoms of depression and anxiety far outweighed the number of students who developed coping skills during the May 2020 quarantine.

Conclusion

Prior studies that have used nationally representative samples have inferred that because of the COVID-19 pandemic, anxiety and depression within adolescents have increased.[7,8] Multiple studies have explored the increased symptoms of depression and anxiety within youth.[9-12] However, only a few studies have been conducted in the U.S. The findings in this study provide insight into how the COVID-19 pandemic has affected adolescents in and out of school in Tacoma, WA, while prior research has been restricted to non-specific measures of increased stress and in regions where the pandemic was not as severe.

The results revealed multiple patterns. First and foremost, the majority of respondents were found to have features of anxiety, depression, and stress that fell within the extremely severe range as demonstrated by their high scores in these subcategories (see Table 1). This illustrates that the pandemic had a severe mental health impact on the students. For questions exploring the lack of motivation in students during the May 2020 quarantine, option 4, "always," was endorsed the most. This demonstrates that multiple adolescents, specifically students, lost their motivation to get tasks done. This was perhaps due to increased depressive symptoms. In other studies, generalized and social anxiety symptoms seemed to increase during the pandemic.[6] This was also illustrated in this study by the extremely severe rates of depression, anxiety, and stress symptoms.

This study had many strengths, including surveying a population of students who were severely affected by the pandemic and who experienced their education during COVID-19 using a combination of in-person and virtual learning environments. However, there were several limitations to this research study. This project was only in one distinct area in the United States and did not include a range of demographics for more well-rounded results. The survey was administered during the summer of 2021, and student summer plans and activities may have impacted responses. Additionally, because the research had to be conducted in a short period of time, only one time-point was assessed in the survey to evaluate their mental health symptoms during the COVID-19 pandemic. Therefore, an additional survey would have to be sent out to examine how students have experienced symptoms at different time points during the pandemic. This study highlights that future research should focus on the relationship between COVID-19 and rates of anxiety and depression, and the impact on high school student motivation.

Across domains, pandemic experiences were associated with mental health and psychiatric symptoms. COVID-19 has had an extremely severe impact on teenage mental health as demonstrated in this study. High school students have also experienced many other mental health symptoms related to COVID-19 which have negatively affected their ability to function and maintain a healthy mind-set. Virtual education and home confinement were associated with these symptoms and compounded by social isolation. In conclusion, this study further highlights the negative impact of COVID-19 on youth and adolescent mental health.

Acknowledgments

I would like to acknowledge The Polygence Research Program Team who facilitated the materials and information necessary for completing this study. I would also like to acknowledge Bellarmine Preparatory School for supporting this study and distribution of this survey throughout Tacoma. Lastly, I would like to thank Ms. Mandy Newman who was my research mentor for this study and helped me overcome challenging and difficult problems that came up throughout the experiment.

References

1. Golberstein, E., Wen, H., & Miller, B. F. (2020). Coronavirus Dis ease 2019 (COVID-19) and Mental Health for Children and Adolescents. *JAMA Pediatrics*. https://doi.org/10.1001/jamapedi atrics.2020.1456
2. Guessoum, S. B., Lachal, J., Radjack, R., Carretier, E., Minassian, S., Benoit, L., & Moro, M. R. (2020). Adolescent psychiatric disorders during the COVID-19 pandemic and lockdown. *Psy chiatry Research*, *291*, 113264. https://doi.org/10.1016/j.psy chres.2020.113264
3. Holmes, E. A., O'Connor, R. C., Perry, V. H., Tracey, I., Wessely, S., Arseneault, L., Ballard, C., Christensen, H., Cohen Silver, R., Everall, I., Ford, T., John, A., Kabir, T., King, K., Madan, I., Michie, S., Przybylski, A. K., Shafran, R., Sweeney, A., Bullmore, E. (2020). Multidisciplinary research priorities for the COVID-19 pandemic: A call for action for mental health science. *The Lan cet Psychiatry*, 7(6),547–560. https://doi.org/10.1016/ S2215-0366(20)30168-
4. Lee, J. (2020). Mental health effects of school closures during COVID-19. The Lancet Child & Adolescent Health, 4 (6), 421. https://doi.org/10.1016/S2352-4642(20)30109-7
5. Racine, N., Cooke, J. E., Eirich, R., Korczak, D. J., McArthur, B., & Madigan, S. (2020).Child and adolescent mental illness during COVID-19: A rapid review. Psychiatry Research, 292, 113307. https://doi.org/10.1016/j.psychres.2020.113307
6. Hawes, M., Szenczy, A., Klein, D., Hajcak, G., & Nelson, B. (2021). Increases in depression and anxiety symptoms in adolescents and young adults during the COVID-19 pandemic. *Psychologi cal Medicine*, 1-9. doi:10.1017/S0033291720005358 https:// www.cambridge.org/core/journals/psychological-medicine/ article/increases-in-depression-and-anxiety-symptoms-in-ad olescents-and-young-adults-during-the-covid19-pandemic/ F10C068F4D7A7AEDF2699A517904C1EB
7. Ettman, C. K., Abdalla, S. M., Cohen, G. H., Sampson, L., Vivier, P. M., & Galea, S. (2020). Prevalence of depression symptoms in US adults before and during the COVID-19 pandemic. *JAMA Network Open*, 3(9), e2019686–e2019686
8. Twenge, J. M., & Joiner, T. E. (2020). US Census bureau-assessed prevalence of anxiety and depressive symptoms in 2019 and during the 2020 COVID-19 pandemic. *Depression and Anxiety*, 37(10),

DOI: 10.36838/v4i5.8

954–956
9. Elmer, T., Mepham, K., & Stadtfeld, C. (2020). Students under lockdown: Assessing change in students' social networks and men tal health during the COVID-19 crisis.
10. Li, H. Y., Cao, H., Leung, D. Y., & Mak, Y. W. (2020). The psy chological impacts of a COVID-19 outbreak on college students in China: A longitudinal study. *International Journal of Environmen tal Research and Public Health*, 17(11), 3933
11. Magson, N. R., Freeman, J. Y., Rapee, R. M., Richardson, C. E., Oar, E. L., & Fardouly, J. (2020). Risk and protective factors for prospective changes in adolescent mental health during the COVID-19 pandemic. *Journal of Youth and Adolescence*, 1–14. Advance online publication. https://doi.org/10.1007/ s10964-020-
12. Saraswathi, I., Saikarthik, J., Kumar, K. S., Srinivasan, K. M., Ar dhanaari, M., & Gunapriya, R. (2020). Impact of COVID-19 outbreak on the mental health status of undergraduate medical stu dents in a COVID-19 treating medical college: A prospective lon gitudinal study. *PeerJ*, 8, e10164.
13. Lee, C. M., Cadigan, J. M., & Rhew, I. C. (2020). Increases in l oneliness among young adults during the COVID-19 pandemic and association with increases in mental health problems. *Journal of Adolescent Health*, 67(5), 714–717
14. Lovibond, S.H.; Lovibond, P.F. (1995). Manual for the Depression Anxiety Stress Scales (2nd ed.). Sydney: Psychology Founda tion (Available from The Psychology Foundation, Room 1005 Mathews Building, University of New South Wales, NSW 2052, Australia
15. Qureshi, A. S. (2020). The Impact of the Covid-19 Pandemic on Mental Health of Teens. *Journal of Emerging Investigators* , 3, 1–6. https://www.emerginginvestigators.org/articles/the-impact-of-the-covid-19-pandemic-on-mental-health-of-teens/pdf

Author

Mira Kunz is currently a senior in high school in Tacoma, WA. She has dedicated most of her time to researching psychology and neuroscience, and how these fields apply to worldwide problems today. She was acknowledged by the Polygence Research Board for her outstanding presentation on this research project during the 2021 Polygence Research Symposium and she continues to advocate for teenage mental health going into her college years.

IJHSR
ijhighschoolresearch.org
RESEARCH ARTICLE

Characterizing γδ T Cell Subtypes to aid in Future Disease Prevention

Ekansh Kushwaha
Westview High School, 4200 NW 185th Ave, Portland, Oregon, 97229, USA; ekansh0308@gmail.com

ABSTRACT: T cells are important to the immune system as they remove foreign pathogens such as bacteria, cancer cells, viruses, and parasites. T cells can change their DNA by undergoing a process called V(D)J recombination. There are two types of T cells: gamma-delta (**γδ**) and alpha-beta (**αβ**). Gamma-delta T cells have been eliciting interest in the past few years as they have an important role in autoimmune diseases, various infections, and cancer. I hypothesized that there are many more gamma-delta T cell subtypes that haven't been characterized yet. Certain subsets of gamma-delta T cells can only be found in the liver as they perform specific functions in liver diseases. Their effect on liver diseases depends on the subset and cytokines produced so characterizing them now can be beneficial in developing vaccines in the future. These new subtypes could have an important role in tumor detection and regression. Cluster 1 had T follicular helper cells, cluster 2 had regulatory T cells, cluster 3 had effector memory cells, cluster 4 had activated tissue memory cells, and cluster 7 had T helper 2-like cells.

KEYWORDS: Computational Biology and Bioinformatics; Cellular immunology; Genomics; gamma-delta T cell; Single-cell RNA sequencing; liver single-cell RNA dataset.

Introduction

The immune system is the body's defense mechanism against foreign and cancerous substances such as bacteria, viruses, parasites, and more. The immune system has many different components that are spread out all over the body.[1,2] Leukocytes, more commonly known as white blood cells, are the cellular mediators of the immune response. They circulate through the body in the blood vessels, and lymphatic vessels, infiltrate tissue and identify any pathogens that might have entered the body.[2] Once they find a pathogen they will multiply and kill it. White blood cells are divided into two main types: myeloid and lymphoid.[2] Many myeloid cells are phagocytic cells that engulf pathogens and display them to other cells of the immune system. Lymphocytes are more targeted in that they not only get rid of any pathogens but also remember them.[2] This is better for the body as now your immune system can quickly remove any pathogen that enters the body for a second time.

Lymphocytes are also further divided into three different subtypes: B cells, T cells, and NK cells.[2] All lymphocytes first develop in the bone marrow. From there some of them move to the thymus and become T cells while the rest remain in the bone marrow and become B cells or NK cells.[2] Some NK cells can also move to the lymph nodes, spleen, tonsils, thymus, or uterus to develop.[3] B cells are responsible for producing antibodies and alerting T cells while T cells are responsible for killing the infected and cancerous cells in the body and alerting other leukocytes.[4] Unlike the B and T cells, NK cells have small particles, or granules, which have enzymes that kill the infected or tumor cells.

Both B cells and T cells can undergo a process called V(D)J recombination which allows the cell to assemble different gene segments and therefore change its DNA in the B and T cell receptors.[5] This allows the T cell receptor to bind to specific peptides that are only found in infected cells.[5] If a cytotoxic T cell receptor binds to the MHC of a cell and detects those proteins, then it will immediately kill that cell.[5] T cells cannot only change their DNA to quickly remove pathogens, but they can also remember all the pathogens that have attacked the body and how to get rid of them quickly.[4] This allows the body to resist diseases much better in the future. This also means that B and T cells can have a near-infinite number of different receptors with each one being able to counter a different type of disease.

The innate immune response is the first line of defense against any invading viruses and is a very general response.[6] This means that it gives a person the same amount of protection against all antigens.[6] Additionally, it keeps no memory of the antigens that have previously attacked. The innate response takes a long time to kill complex pathogens and it does not become any more efficient at killing specific pathogens. The adaptive immune response, as the name suggests, develops a specific gene segment that targets the proteins on the surface of a pathogen and kills it quickly.[6] The adaptive immune response still tends to take longer to respond than the innate immune response since specific cells have to find each other. However, once a pathogen has been identified, the adaptive immune response is much faster at getting rid of it. The memory B and T cells save these targeted gene segments as immunological memory.[4] As one grows up, this memory storage of how to kill different pathogens grows larger and in turn, makes one get sick much less often.

T cells, specifically the **γδ** T cells, that bridge the innate and adaptive immune responses.[7] **αβ** T cells far outnumber the **γδ** T cells, however, currently not much is known about **γδ** T cells and how they work.[8] Not only are there significantly more **αβ** T cells than **γδ** T cells in the blood but **αβ** T cells were also discovered first.[8] **γδ** T cells on the other hand

DOI: 10.36838/v4i5.9

have been gaining a lot of interest in the past few years as they have been discovered to play an important role in autoimmune diseases, various infections, and cancer.[8]

To understand γδ T cells more in-depth, multiple single-cell RNA-seq data sets from the liver were taken from multiple directories. They were then processed through Seurat and clustered into the various cells that were present. After that, the γδ T cell clusters were subsetted out and combined using the Harmony library. They were then clustered again and processed to find if there are any more γδ T cell subsets. Currently, the most well-known γδ T cell subtypes are Vδ1+, Vδ2+, and Vγ9Vδ2+. Other subtypes h been identified but are less characterized such as Vδ3+, Vγ5+, and Vγ6+ but there are still even more subtypes that are undiscovered and uncharacterized. There are certain γδ T cells which can only be that in the liver due to their specific function of removing liver diseases.[1] These include viral hepatitis, autoimmune liver diseases, non-alcoholic fatty liver disease, liver cirrhosis, and liver cancers.[1] The effect of γδ T cells in liver diseases varies but can be determined through subsets and cytokines markers.[1] This makes characterization very important since it can allow the correct γδ T cell to be used for specific disease prevention. The use of diseased liver samples in our study allowed for the analysis of more cytokines which were used to identify γδ T cells which were in the process of fighting against specific diseases.

The V(D)J recombination that T cells can undergo allows for hundreds, if not thousands, of different γδ T cell subtypes so if scientists search for the right genetic markers, then it is possible to find a new subtype or discover more about an already existing one.

Methods

Data collection:

Patient single-cell RNA sequencing data was collected from the Panglao, Human Cell Atlas, NCBI, and single-cell atlas databases (Table 1). The patients were filtered for only liver tissue data and then the data was further filtered into healthy and unhealthy tissues. Five of the datasets chosen had healthy liver tissue while four of the datasets had patients with one of three diseases: hepatocellular carcinoma, primary liver cancer, and non-alcoholic steatohepatitis.

Initial normalization and clustering:

The patient data was imported into RStudio, and the Seurat library was imported into the workflow (Table 2). The different patient datasets were then converted into Seurat objects for further processing following the "Guided Clustering Tutorial" with the following modifications: Cells that either had an expression of over 2500 or less than 200 were removed and the remaining data was normalized using the NormalizeData function (Figure 1). The different features that have the highest cell-to-cell variation got put in a subset for use in downstream analysis using the FindVariableFeatures function. This is an important step to take so that highly expressed ubiquitous genes don't dominate in the downstream analysis. For the final step of the preprocessing workflow, the data was scaled so that the mean expression of each variable gene across cells was 0 and the variance across cells was 1.

Next, cell-cycle scoring, and regression were performed on each of the data sets. Using the CellCycleScoring function, each cell got assigned a score based on the expression of G2/M and S phase markers genes. The data were then scaled again but this time the S and G2/M cell cycle scores were regressed out. Linear dimensionality reduction was done using the RunPCA function. This uses the variable features meta-data that was calculated in the pre-processing workflow. The dimensionalities of the data were defined by the "elbow" of the elbow plot of the principal component variance of each dataset and then clustered them using that information.

Defining gamma delta clusters:

Once the data was clustered, the gamma delta clusters needed to be specifically identified so that they could be subsetted out. This was done using the FIndAllClusters function. This function reads through each of the clusters and finds out the percent exposure of each gene. It stores that data in a table that shows the gene, cluster number, and the percentage expression of that gene. This data then got used in feature plots to see which clusters have the gamma delta T cell markers TRGC1, TRGC2, TRDC, CD3D, and CD3E. If a cluster expressed at least three of these marker genes, each at a minimum percent exposure of 40%, then it was considered a gamma-delta cluster. After confirming that the clusters of interest contain only gamma delta T cells, we subsetted those clusters out of each data set.

Harmony sample integration:

All the different subsets were then combined into a single Seurat object and put through the pre-processing pipeline again. Then we ran harmony on this Seurat object to converge the clusters from different datasets which would allow the processing to work better. This Seurat object was put through the downstream analysis pipeline to find the different gamma delta T cell clusters. To filter the cells even further, another subset was made with the clusters containing mostly gamma delta T cells. We then found the cytokine markers and cell surface receptors to characterize each cell (Figures 2 & 3). We then used this information and compared it with existing literature to find identify each of the cell types.

Table 1: Description of all the datasets used in this study.

Name	Species	healthy/disease	Number of cells	Donors	Read Counts
MacParland SA, Liu JC, Ma XZ, Innes BT, et al. Single-cell RNA sequencing of human liver reveals distinct intrahepatic macrophage populations. Nat Commun 2018 Oct 22;9(1):4383. PMID: 30348985	Homo sapiens	Healthy	30.0k	5	18,519
Zhao J, Zhang S, Liu Y, et al. Single-cell RNA sequencing reveals the heterogeneity of liver-resident immune cells in humans. Cell Discovery. 2020;6:22. DOI: 10.1038/s41421-020-0157-z. PMID: 32351704 PMCID: PMC7186229	Homo sapiens	Healthy	61,144	1	20,007
SRA: SRA716608 SRS: SRS3391629 SRR: SRR7276474	Homo sapiens	Healthy	4,190	Not stated	15,247
SRA: SRA716608 SRS: SRS3391630 SRR: SRR7276476	Homo sapiens	Healthy	4,719	Not stated	18,252

SRA: SRA716608 SRS: SRS3391631 SRR: SRR7276475	Homo sapiens	Healthy	1,425	Not stated	14,431
SRA: SRA716608 SRS: SRS3391632 SRR: SRR7276477	Homo sapiens	Healthy	6,158	Not stated	21,525
The Tumor Microenvironment Shapes Innate Lymphoid Cells in Patients with Hepatocellular Carcinoma SRA: SRP327611	Homo sapiens	Diseased with hepatocellular carcinoma (HCC)	3,800	48	19,923
TNFR2 HnRNPK-YAP Signaling Axis Promotes Primary Liver Cancer Development in Hepatic Progenitor Cells SRA: SRP305905	Homo sapiens	Diseased with primary liver cancer (PLC)	25,189	2	17,991
XCR1+ type 1 conventional dendritic cells drive liver pathology in Non-Alcoholic Steatohepatitis [10x scRNA-seq] SRA: SRP311823	Homo Sapiens	Diseased with Non-alcoholic fatty liver disease (NAFLD) and non-alcoholic steatohepatitis (NASH)	7,829	Not stated	17,727

Table 2: What software was used.

Software	Version
Seurat	4.0.3
Harmony	1.0
R	4.1.1
RStudio	1.4.1717
Bioconductor (biomaRt)	3.13

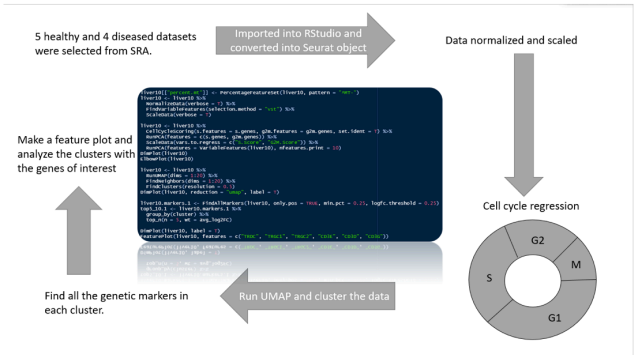

Figure 1: Diagram of workflow before Harmony sample reduction including sample code for one of the datasets. This pipeline was generalized for all datasets.

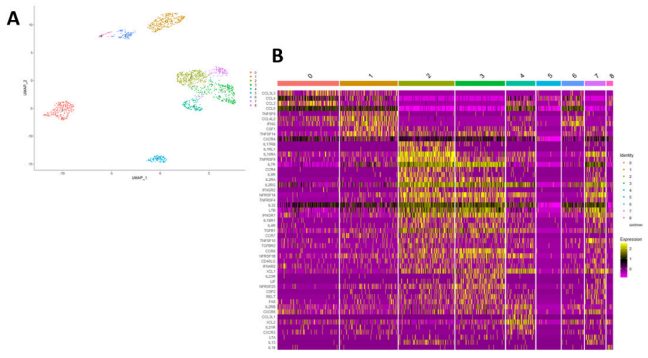

Figure 2: A. Final UMAP of mostly gamma delta T cells. Most clusters represent a different subset of **γδ** T cells that needed to be analyzed. **B**. Heatmap showing the expression of the cytokines in each cluster. This gave us valuable information needed to characterize each cluster. Finds are discussed in the "Results and Discussion" section.

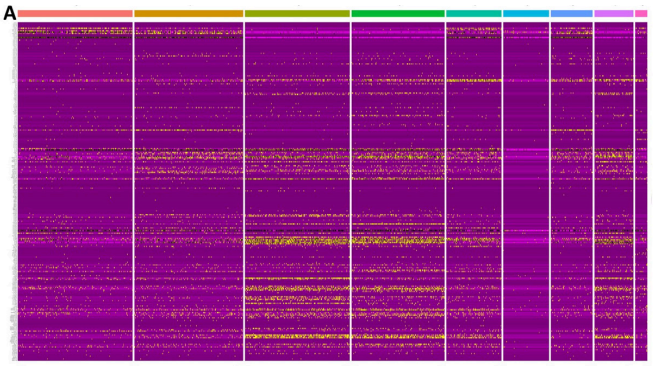

Figure 3: A Heatmap showing the expression of all the cytokine and receptor genes in each cluster. This was the heart of my research and it allowed us to classify what type of gamma-delta T cells were there in all the liver datasets as discussed in the Final Analysis. The colored columns on the top represent the 8 clusters from the post-Harmony UMAP. All the genes in the UMAP are listed on the left and the yellow lines represent the expression of that gene in various parts of the clusters.

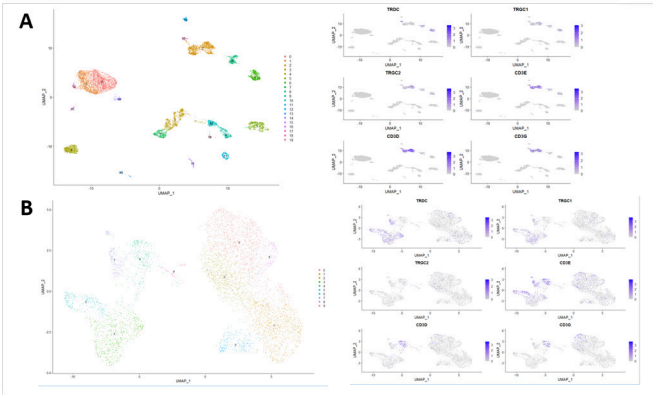

Figure 4: A. UMAP of sc-RNA seq data from PMID: 30348985 with relative gene expression superimposed on a UMAP. Cluster 2 had **γδ** T cells· **B**. UMAP of sc-RNA seq data from SRA: SRP327611 with the relative gene expression superimposed on a UMAP. Clusters 3, 5, and 7 had **γδ** T cells.

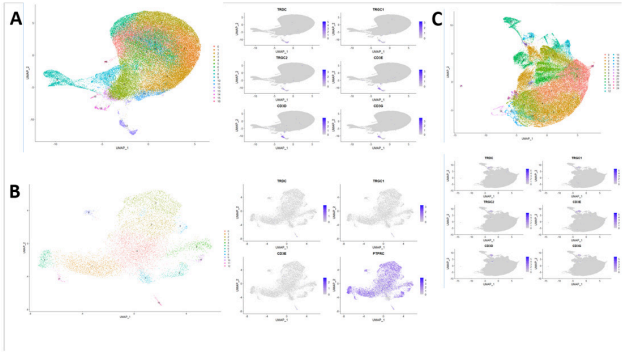

Supplemental Figure 1: A. UMAP of sc-RNA seq data from SRS: SRS3391632 with relative gene expression superimposed on a UMAP. Figure 12 contained some **γδ** T cells and was analyzed further. **B**. UMAP of sc-RNA seq data from SRA: SRP311823 with the relative gene expression superimposed on a UMAP. Cluster 12 contained some **γδ** T cells. **C**. UMAP of sc-RNA seq data from SRS: SRS3391629 with the relative gene expression superimposed on a UMAP. Cluster 14 had the **γδ** T cells.

DOI: 10.36838/v4i5.9

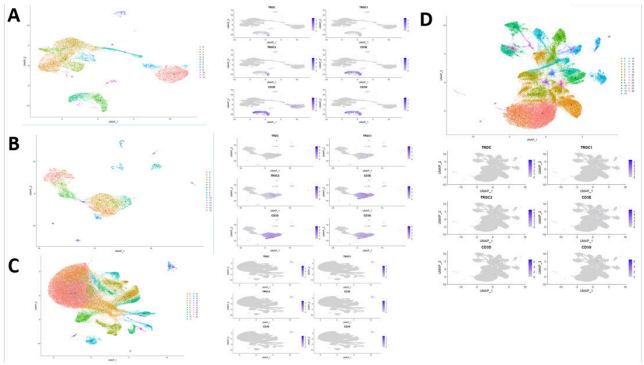

Supplemental Figure 2: A. UMAP of sc-RNA seq data from SRA: SRP305905 with relative gene expression superimposed on a UMAP. Cluster 2 had γδ T cells. **B**. UMAP of sc-RNA seq data from SRA: SRP305905 with relative gene expression superimposed on a UMAP. Clusters 1, 2, 3, and 6 had γδ T cells. **C**. UMAP of sc-RNA seq data from SRS: SRS3391631 with relative gene expression superimposed on a UMAP. Cluster 12 had γδ T cells. D. UMAP of sc-RNA seq data from SRS: SRS3391630 with relative gene expression superimposed on a UMAP. Cluster 7 had γδ T cells.

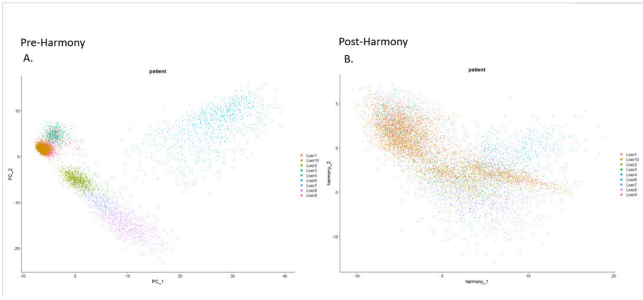

Figure 4: A. PCA plot of the Seurat object with all the subsets before Harmony. B. PCA plot of the Seurat object with all the subsets after Harmony. This merged the subsets making it easier to analyze further.

Results and Discussion

Nine liver scRNA-seq data sets were downloaded from Panglao, Human Cell Atlas, NCBI, and single-cell atlas databases. These were imported into RStudio and converted into Seurat objects to be processed (Methods and Materials). After normalization and data filtering, UMAPs were generated for each data set and were analyzed. To identify the gamma-delta (γδ) T cells, five different markers were used to locate them in the UMAP. A feature plot was used to represent the expression of the genes in each cluster. Clusters that expressed these markers were then further examined to make sure that they contained mostly gamma delta T cells.

Dataset 1:

For dataset 1 we identified 16 different clusters as can be seen in section A of Supplemental Figure 1. The featured plot showed that there was an expression of the genes of interest in cluster 12 (**Methods and Materials**). Closer analysis, however, reveals that not all of cluster 12 has only γδ T cells. This cluster was extracted, and a clustering pipeline was run through it to isolate the γδ T cells in their cluster. After this run, we extracted the cluster with the γδ T cells and created a subtype for this dataset to store these cells. This dataset had only healthy tissue cells.

Dataset 2:

This data set contained 19 different clusters and was unique in that it only contained the immune cells from the liver. This also meant that processing this data was much easier. The feature plots show clearly that the genes of interest are highly expressed in cluster 2 as can be seen in Figure 4, section A. We were able to then conclude that cluster 2 had mostly γδ cells with high certainty. This data set had only healthy tissue cells.

Dataset 3:

This dataset had only 12 clusters and appeared to have γδ cells in cluster 12, as can be seen in Supplemental Figure 1, section B. However, we determined that this was a low-quality dataset and that cluster 12 contained mostly alpha-beta T cells instead of gamma delta T cells. We still extracted this cluster out of this dataset, but it was filtered in post-processing. This dataset had some diseased tissue data.

Dataset 4:

This was one of the bigger datasets as it had 24 clusters, as shown in section C of Supplemental Figure 1, and it had only healthy tissue data. Looking at the feature plot shows clearly that cluster 14 is the γδ cells. The feature plots show high expression of the γδ specific genes as well as the T cell-specific genes.

Dataset 5:

This data was small with only 9 clusters, and it had diseased tissue data. As the UMAP shows in section B of Figure 4, there weren't many cells in this dataset either. The feature plots can be used to show that there was high expression of the genes of interest in clusters 3, 5, and 7. The TRDC and CD3 genes were highly expressed in those areas. We believe that it expressed a different type of TRGC gene because while TRGC1 was highly expressed in those clusters, TRGC2 wasn't.

Dataset 6:

This dataset had diseased cells and 12 clusters overall as shown in section A of Supplemental Figure 2. Based on the expression of the CD3 genes, we knew that clusters 4 and 5 were T cell clusters. Looking closely at cluster 4 we could see that there were γδ cells at the bottom of it. We then isolated cluster 4 and ran it through the clustering pipeline again to extract the bottom part of that cluster to get only γδ cells.

Dataset 7:

This dataset also had diseased cells and had 15 clusters as can be seen in section B of Supplemental Figure 2. This was harder to analyze as the γδ cells were spread throughout multiple different clusters. We couldn't extract clusters 1, 2, and 6 since there would have been a multitude of other cells which we are not looking for. We decided to just extract out cluster 6 since it was the smallest of these clusters and would not contain too many other cells that would need to get filtered out later.

Dataset 8:

This dataset had only healthy cells and had 24 total clusters as is shown in section C of Supplemental Figure 2. It was very faint to recognize but cluster 12 has the highest expression of all the genes of interest. We believe that this cluster does have

the γδ cells but there might also be some alpha-beta T cells that were filtered through post-processing.

Dataset 9:

This dataset had healthy cells and was very big with 26 clusters in total. This can be seen in section D of Supplemental Figure 2. Using the feature plots, we could see the high expression of these genes from mainly cluster 7. Using that information, we believe that some γδ cells in that cluster can be clustered out. We extracted those cells so that they could be further analyzed and filtered in the post-processing.

Harmony:

The harmony package was imported so that the different subsets would cluster together instead of being separate (Figure 4). The new UMAP with the harmony regression was processed again to ensure that there were mostly only γδ cells present. Then we defined the unique characteristics of each cluster such as cytokines and cell surface receptors.

Final Analysis:

We identified cluster 0 as Th2-like and it was also SAA1+ which was interesting as that is not common.[9] This cluster expressed the CCL cytokines such as CCL3L3, CCL4, CCL3, and CCL5. Cluster 1 was identified as a T follicular helper cell.[10] It also highly expressed certain CCL cytokines but it also expressed IFNG, TNFSF14, and CXCR4. We identified cluster 2 as a type of regulatory T cell that expressed SLAMF1 which is also a unique combination.[11] The most commonly expressed cytokine markers were different types of IL1. It also expressed certain CCR, IFNG, and TNF cytokines. Cluster 3 contained effector memory CD8+ T cells but is also highly expressed the gene for an aquaporin.[12] We identified the cluster to be this gene based on the high expression of the CCR6 cytokine. Cluster 3 also expressed high levels of TGFB1, IFNGR1, TNFRSF18, IL2RA, and IL7R. Cluster 4 had activated tissue-resident memory T cells. The highly expressed cytokines for this cluster include XCL2, XCL1, TNFRSF18, and TNFRSF1B. Cluster5 contained dying cells and Cluster 6 had hepatocytes so they weren't further analyzed. Cluster 7 had Th2-like cells and the cytokines it expressed were IL10RA, IL2RG, TNFRSF4, LTB, TNFSF10, and XCL1. Cluster 8 didn't have T cells, so it was not further analyzed.

■ Conclusion

In this paper, we got nine different datasets from a total of four different databases. We then converted everything into Seurat objects so that they could be easily processed. After they were normalized and scaled, they were run through regression to remove any extraneous data. Finally, the cells were clustered and their UMAPs were generated so that they could be analyzed easier. For each dataset, a feature plot was created with the same five genes of interest: TRDC, TRGC1, TRGC2, CD3E, CD3D, and CD3G. The TRDC and TRGC genes are specific to gamma delta T cells and the CD3 genes are specific to all T cells so together they can show where all the γδ cells are in a dataset. Clusters with the γδ cells were extracted out of their original datasets and combined to create a dataset with only γδ cells. Previously discovered gamma delta T cells were researched to find out what signatures they had. Those were then compared to the data that we had extracted, and any new signatures meant that we had discovered a new type of γδ T cell subtype. One big strength of this study was that we used multiple different liver sc-RNA datasets. Other studies usually only analyze 1 dataset, so they get a limited amount of data but by using 9 different datasets as we did, we were able to get a much wider variety of data. We also used both healthy and diseased datasets. This added more cytokine receptors that we could have looked for and could also lead to a discovery of a new γδ T cell subset. A weakness of our study was that we had to rely on a computer program to sort and filter our data so we couldn't make granular changes that we might have wanted. Additionally, the γδ T cell subsets that we created usually had a few other cells, although at very low expression levels. Regardless, this could have added variability to our data and affected our understanding of the results.

The purpose of this study was to identify new gamma delta T cell subtypes and their unique signatures. This would help future studies regarding γδ T cells as these cells will be more easily identifiable and, therefore, researchable. The uses for this kind of cell are numerous as it could be used to treat diseases that may suddenly appear or even cure cancer in a completely natural way. Currently, there are no complete cures to cancer even with modern technology and groundbreaking scientific research. Even though some treatments are present, none of them can guarantee survival. Cancer kills millions of people each year and there is no real way to stop or cure it permanently. CAR-T cell therapy has recently been developed to program T cells so that they can find a specific tumor or cancer cells and kill them immediately.[13] Using γδ cells and their subtypes can allow scientists to try and cure cancer without having to edit the genome of the cell in the first place as the new cells we find might have the DNA sequence already needed to kill that specific cancer. This could save millions of dollars too as editing the genome is very expensive. Additionally, since this method of curing cancer would be completely natural, the side effects would be much less, if there are any at all.

■ Acknowledgements

I thank Zachary Reinstein for his mentorship and the Polygence team for providing the platform and their support. I also would like to thank my parents for their support and encouragement.

■ References

1. Zhou, Q.-H.; Wu, F.-T.; Pang, L.-T.; Zhang, T.-B.; Chen, Z. Role of ΓδT Cells in Liver Diseases and Its Relationship with Intestinal Microbiota. *World J. Gastroenterol.* **2020**, 26 (20), 2559–2569. https://doi.org/10.3748/wjg.v26.i20.2559.
2. Information, N. C. for B.; Pike, U. S. N. L. of M. 8600 R.; MD, B.; USA, 20894. *What Are the Organs of the Immune System?; Insti tute for Quality and Efficiency in Health Care* (IQWiG), 2020.
3. Yu, J.; Freud, A. G.; Caligiuri, M. A. Location and Cellular Stag es of NK Cell Development. *Trends Immunol.* **2013**, 34 (12), 10.1016/j.it.2013.07.005. https://doi.org/10.1016/j. it.2013.07.005.
4. Cano, R. L. E.; Lopera, H. D. E. *Introduction to T and B Lympho cytes*; El Rosario University Press, 2013.
5. Roth, D. B. V(D)J Recombination: Mechanism, Errors, and Fi delity. *Microbiol. Spectr.* **2014**, *2* (6), 10.1128/microbiolspec.

DOI: 10.36838/v4i5.9

MDNA3-0041–2014. https://doi.org/10.1128/microbiolspec.MDNA3-0041-2014.
6. Information, N. C. for B.; Pike, U. S. N. L. of M. 8600 R.; MD, B.; USA, 20894. *The Innate and Adaptive Immune Systems; Institute for Quality and Efficiency in Health Care* (IQWiG), 2020.
7. Meraviglia, S.; El Daker, S.; Dieli, F.; Martini, F.; Martino, A. Γδ T Cells Cross-Link Innate and Adaptive Immunity in Mycobacte rium Tuberculosis Infection. *Clin. Dev. Immunol.* **2011**, 2011, 587315. https://doi.org/10.1155/2011/587315.
8. Kreslavsky, T.; Gleimer, M.; Garbe, A. I.; von Boehmer, H. Αβ versus Γδ Fate Choice: Counting the T-Cell Lineages at the Branch Point. Immunol. Rev. 2010, 238 (1), 169–181. https://doi.org/10.1111/j.1600-065X.2010.00947.x.
9. Smole, U.; Gour, N.; Phelan, J.; Hofer, G.; Köhler, C.; Kratzer, B.; Tauber, P. A.; Xiao, X.; Yao, N.; Dvorak, J.; Caraballo, L.; Puer ta, L.; Rosskopf, S.; Chakir, J.; Malle, E.; Lane, A. P.; Pickl, W. F.; Lajoie, S.; Wills-Karp, M. Serum Amyloid A Is a Soluble Pat tern Recognition Receptor That Drives Type 2 Immunity. *Nat. Immunol.* **2020**, *21* (7), 756–765. https://doi.org/10.1038/s41590-020-0698-1.
10. Crotty, S. T Follicular Helper Cell Differentiation, Function, and Roles in Disease. *Immunity* **2014**, *41* (4), 529–542. https://doi.org/10.1016/j.immuni.2014.10.004.
11. Regulatory T Cell Markers: R&D Systems https://www.rndsystems.com/resources/cell-markers/immune-cells/regulatory-t-cell/regulatory-t-cell-markers (accessed 2021 -09 -30).
12. Kondo, T.; Takata, H.; Takiguchi, M. Functional Expression of Chemokine Receptor CCR6 on Human Effector Memory CD8+ T Cells. Eur. J. Immunol. 2007, 37 (1), 54–65. https://doi.org/10.1002/eji.200636251.
13. Katz, S. G.; Rabinovich, P. M. T Cell Reprogramming Against Cancer. *Methods Mol. Biol. Clifton NJ* **2020**, 2097, 3–44. https://doi.org/10.1007/978-1-0716-0203-4_1.

Author

Ekansh Kushwaha, author of this research paper is a Senior at Westview High School. He has a passion for cell-related research and enjoys working in the vast field of computer science. Due to his passion and interest, he conducted this research and would like to continue research in his future endeavors.

IJHSR
ijhighschoolresearch.org
■ RESEARCH ARTICLE

Addressing Body Image Issues on Instagram: An Intervention-Based Approach

Lauren Sonneborn
The Hotchkiss School, 11 Interlaken Road, Lakeville, CT, 06039, USA; lsonneborn17@gmail.com

ABSTRACT: The negative consequences of Instagram on young adults—in particular, its impact on body image—have become increasingly apparent and difficult to address. This research tested the efficacy of three nudge-style interventions (two moral) designed to ameliorate this issue compared to a non-nudge control. Using a sample of real Instagram posts made by same-gender influencers (*N*= 10, gender-matched), it was tested whether reading subtle nudges prior to scrolling the posts would lead to higher body acceptance, self-esteem, and/or self-compassion among a sample of mainly young adult (age range = 18-62, *M*= 18.69, SD = 3.77) social media users (*N*= 320). A two-way ANOVA revealed that across male-identifying (*N*= 160) and female-identifying (*N*= 160) participants, the interventions were associated with greater body acceptance in participants. The most successful intervention in the study included deontological language, indicating that a moral nudge could be an effective option to address body image issues caused by Instagram at their source.

KEYWORDS: Behavioral and Social Sciences; Sociology and Social Psychology; Social Networking Sites (SNS); Instagram; Body Image.

■ Introduction

Social media has become a critical contributor to mental health issues in young adults.[1-3] One of the primary areas of concern is its impact on body image; the use of social networking sites (SNS) has been linked with body dissatisfaction,[4] eating concerns,[5] and a higher drive for thinness.[6] Controversy is growing about the negative impact of Instagram, in particular, on adolescent body image. An image-based application, Instagram promotes ideals of thinness and unrealistic beauty standards, which in turn raise body image concerns.[7] Researchers have documented the relationship between Instagram use and decreased body image,[8-10] and a recent study reports that 32% of adolescent girls said that when they felt bad about their bodies, Instagram made these feelings worse.[11] This negative body image has been linked with self-esteem and social comparison, factors that contribute greatly to overall emotional well-being.[12,13]

Instagram influencers—people who develop a large following and promote a certain lifestyle, product, or service to their fans—have emerged. Currently, over 500,000 active influencers operate on Instagram.[14] Surpassing traditional aesthetic celebrities (e.g., fashion models) in popularity, Instagram influencers exhibit seeming perfection in their lives and attract a large base of users who wish to imitate their life, inspiring users to follow their endorsements.[15] This new category of celebrities contributes to body concerns through promoting an idealized beauty standard,[16] and scrolling through images of influencers can elicit unhealthy self-comparison and body dissatisfaction.[17] The rampant editing of images posted on Instagram only exacerbates self-comparison and negative body image.[4]

Research on the topic of SNS and body image is extensive, primarily centering on the link between time spent on SNS and decreased body image[6,18] and increased self-comparison.[17,19] However, studies have yet to identify a viable solution to address the issues. One strategy that appears promising is for users to view interventions before they scroll; recent research suggests that interventions can be effective at promoting higher body appreciation, acceptance, and esteem.[20] Further, text-based nudges are tractable, and social media platforms are already implementing them in a variety of arenas, from misinformation to hate speech. Pinterest, a leading social media site, has even blocked content for certain body image related trigger words, and instead links to disordered eating help and resources.[21] Recently, interventions based specifically on moral frameworks have proven effective at influencing users in the context of the COVID-19 pandemic.[22] Ethical frameworks being used in public health is not a new idea—moral language has been implemented across many domains.[23,24] However, research is lacking on whether moral frameworks can be used as a tool for behavioral change in the context of body image concerns online. It is also evident that moral and emotional messages are more likely to spread around social media, suggesting that this morality could be harnessed by the network themselves to support body positivity.[25] Overall, moral messaging has been shown to be more persuasive than nonmoral appeals, leading to the inclusion of moral frameworks in this study.[26]

This study tests whether three different interventions positively impact Instagram users' body image, self-esteem, and self-comparison. Each of these factors have been shown to relate to one another.[12,13] Each one measures a different but related aspect of body image concerns connected to social media use.[27-29] Therefore, it is important to measure each of these factors when exploring how body-image can be intervened upon online. The interventions were given to a group of men (N=160) and women (N=160). Previous work suggests that there are differences in body acceptance, social compar

DOI: 10.36838/v4i5.10

ison and self-esteem across genders, with women generally reporting lower body satisfaction.[30,31] For this reason, participants were shown posts made by same-gender influencers. This enabled testing whether there were differences between men and women in terms of the impact of moral messages on body image. Two of the interventions (deontological and consequentialist) are based on established moral frameworks. Deontology centers on duty and rule-based ideology, defining morality in terms of absolute right and wrong.[32,33] A deontological intervention, therefore, would include a defining statement of duty or obligation in relation to body image. On the other hand, consequentialism asserts that the consequences of an action are the main determinants of its moral worth. Utilitarianism, the most well-known branch of consequentialism,[34] stresses the happiness of the majority as the goal consequence of any action.[35,36] A utilitarian intervention, therefore, might emphasize the widespread beneficial consequences of body positivity.[37] There was also a control intervention and a no-intervention control.

The first hypothesis was that all three interventions will have a positive impact on body acceptance in both men and women. As an additional, exploratory analysis, it was tested whether there were gender differences in the impact of the intervention conditions across the three scales. The next hypothesis was that the interventions based on moral frameworks would be more effective than the control intervention. The hope in exploring these hypotheses was to identify an effective approach to mitigating negative body image effects of Instagram use, thereby contributing to a healthier social media environment for users.

Methods

To test whether body appreciation is positively impacted by moral interventions, a 2x4 experimental design was conducted. A non-random sample of predominantly young adult participants (age range= 18-62, *M*= 18.69, *SD*= 3.77) were provided with a link to the survey (*N*= 320). Approximately half of participants identified as male ("men") and half as female ("women"). All participants were randomly assigned to view a moral or control intervention or to view no intervention at all. Two of the interventions were based on different moral frameworks: one was rooted in deontology, and one in consequentialism (as illustrated in Table 1).

Procedure:

The study was conducted using the Qualtrics (Qualtrics, Provo, UT) platform and distributed through online platforms. Participants were informed that the study was designed to investigate issues around body image on Instagram. The survey began by showing participants one of three interventions (deontological, consequentialist, control) or no intervention. This condition was randomly assigned using Qualtrics. The interventions were displayed to participants as black text on a white background, using the standard Qualtrics text block style. After viewing these interventions, the participants were shown a series of real posts made to Instagram by influencers.[38] Immediately prior to viewing the posts, participants were told that the posts were genuine (i.e., posted to Instagram by platform users). Then participants were asked to complete three scales after viewing the posts. The first scale, the Body Acceptance Scale-2 (BAS-2), measures body acceptance, respect toward their body, and overall favorable opinions of their bodies.[39] The second scale, the Rosenberg Self-Esteem Scale (RSES), assesses general self-esteem.[40] The final scale, the Iowa-Netherlands Comparison Orientation Measure (INCOM), measures the social comparison of participants.[41] Then, demographic data about the participants' basic information and social media habits were recorded, including questions such as "How often do you use Instagram?" and "How many accounts do you follow on Instagram?"

Materials

Table 1: The table outlines the three frameworks used as intervention options as well as the text that was displayed to participants.

Framework	Message
Deontology (moral)	Body positivity promotes an inclusive and ethical online environment. Embrace it as you scroll.
Consequentialism (moral)	Body positivity helps make the world a happier, healthier place for everyone. Embrace it as you scroll.
Control	Comparison is the thief of joy. Enjoy your Instagram experience and focus on uplifting yourself.

Instagram Posts:

Participants scrolled through a series of 10 real posts made to Instagram by influencers. Female participants saw posts made by female influencers and male participants saw male influencers. The posts were adapted from an existing study that identified content published to Instagram by 784 health and wellness influencers in 2020.[38] The 20 most popular posts were sampled, 10 females and 10 males, to present to participants. Following the data-sharing terms of service of Instagram,[42] examples of the posts used cannot be provided here.

Body Acceptance Scale-2:

The BAS-2 consists of 10 items and uses a 5-point Likert scale ranging from 1 (Never) to 5 (Always). Higher scores indicate a higher body acceptance, and to calculate this score item responses are averaged. Items include "I respect my body" and "I am comfortable in my body." Previous research shows strong internal consistency (Cronbach's $\alpha = 0.97$) and test-retest reliability (r= 0.77) in community and college samples of men and women.[39]

Rosenberg Self-Esteem Scale:

The RSES consists of 10 items and uses a 4-point Likert scale ranging from strongly agree to strongly disagree. For items 1, 2, 4, 6, 7: Strongly Agree=3, Agree=2, Disagree=1, and Strongly Disagree=0. For items 3, 5, 8, 9, 10: Strongly Agree=0, Agree=1, Disagree=2, and Strongly Disagree=3. Higher scores indicate higher self-esteem, ranging from 0-30. Items include "I feel that I have a number of good qualities" and "On the whole, I am satisfied with myself." Based on past studies, the scale has adequate internal consistency (Cronbach's $\alpha = 0.77$ to 0.88) and test-retest reliability (r = 0.82 to 0.88).[43]

INCOM Social Comparison Scale:

The INCOM Social Comparison Scale consists of 11 items and uses a 5-point Likert scale ranging from "I disagree strongly" to "I agree strongly." Items 5 and 11 are reverse coded. Items include "I often compare how I am doing socially (e.g., social skills, popularity) with other people" and "I always like to know what others in a similar situation would do." Past research demonstrates consistent Cronbach's alphas ranging from .78 to .85 in 10 American samples.[41]

Results and Discussion

Results:

To test whether reading an intervention before viewing influencer content resulted in improved body image, a one-way ANOVA was conducted. The results suggested that all three of the nudges were associated with higher scores on the BAS-2; consequentialist (M= 19.15), deontological (M= 23.01), and control (M= 18.77) nudges were all associated with average scores that were significantly higher than those recorded by participants in the no-nudge control condition (M= 18.16), $F(3, 316)$= 222.11, p< .001. Post-hoc comparisons of the groups conducted using Tukey's Honestly Significant Difference tests revealed that each condition was significantly different from the others, all ps< .01. This suggests that deontological nudges were associated with the highest body image after exposure to influencer content, followed by consequentialist and then the control nudges (see Figure 1). Again, these results replicated for the two other scales measured (RSES and INCOM), all ps< .05. Means and standard deviations for each of the measures are displayed in Table 2

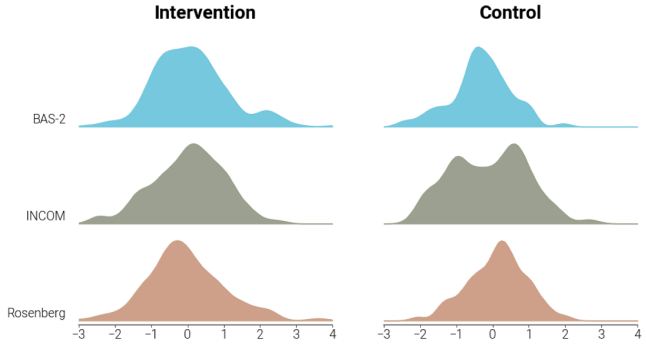

Figure 1: Probability distributions of the z-scored BAS-2, RSES, and INCOM results in relation to the intervention type. The relative distributions of the intervention and control groups highlight that seeing an intervention improved body acceptance across scales.

Although an independent samples t-test revealed that male-identifying participants had a higher average body image across conditions, $t(318)$ = 14.65, p< .01, the pattern of results reported above was observed for both genders when tested separately. Additionally, a two-way ANOVA comparing intervention type (intervention or control) and gender (male or female) did not show a main effect of gender or an interaction between gender and intervention type for any of the three outcome measures, all ps> .05.

These findings were also robust to demographic differences. When participant age, subjective socio-economic status, level of education, and gender were entered into an OLS regression model, condition (entered as a categorical predictor) remained a significant predictor of BAS-2 scores, p< .001. Gender was the only predictive demographic factor, p< .05. When social media use frequency, measured using Guess *et al*'s method,[44] was entered into the model, it was not predictive.

Table 2: Means and standard deviations for each intervention condition.

	BAS-2		INCOM		Rosenberg	
Intervention Type	M	SD	M	SD	M	SD
Deontological	23.01	6.01	44.27	8.63	22.32	3.75
Consequentialist	19.15	4.60	42.22	9.50	20.62	4.19
Control intervention	18.77	3.92	44.99	10.15	20.92	4.49
No intervention	16.16	4.17	40.55	10.17	18.97	3.19

Discussion

In this research, the two hypotheses were that 1) the interventions would positively affect body acceptance across both genders; and 2) the moral interventions would be particularly effective. The results that were obtained and analyzed supported the hypotheses, demonstrating that interventions are an effective and applicable tool to address body image issues. Moreover, the wide-reaching variables of self-esteem and social comparison were positively impacted, indicating the efficacy of interventions in addressing the foundational causes of poor mental health. The results also supported the superiority of moral interventions over the control variables; deontological nudges, in particular, were shown to be the most successful.

While this research yielded new insights and supported the existing literature about interventions, it was limited by certain factors. For example, the lasting effects of the intervention were not tested, and therefore the benefits might only be short-term. The durability of the increased body positivity, self-esteem, and decreased self-comparison was also not measured; outside factors could potentially weaken the intervention's positive effects. Additionally, though real Instagram posts were shown to the study participants, other variables could mitigate the effect of the intervention in a real-life setting.

Future research should focus on measuring the long-term impact and the durability of moral interventions. In addition, more research should be conducted to measure the efficacy of moral interventions on peer posts (non-influencer), with a closer simulation of the Instagram user experience.

All of the outcomes measured were trait-based and the research design did not include any state-based assessment of participants' body image concerns. While it is important to demonstrate changes in trait measures following an intervention, one limitation of the present research which could be addressed by future work is the lack of measurement of any state-level changes brought about by the body image interventions.

A final limitation of the present work is that it did not precisely balance the language of the different interventions. For instance, the deontological intervention includes language which makes the "online environment" immediately salient, whereas the other interventions do not. Similarly, the

DOI: 10.36838/v4i5.10

sentiment of the moral interventions is more positive than in the control intervention. Further work on the topic would benefit from normalizing and balancing the sentiment and content of the interventions.

Thus, although this research does not definitively provide a solution to body image issues on Instagram, it suggests an approach with known markers of success. Recent research corroborates the effectiveness of moral interventions in other realms (specifically, pertaining to a global health crisis).[22]

Conclusion

Negative body image is a widespread problem across society that can be exacerbated by Instagram usage. Ironically, it is necessary to look to Instagram for solutions. This research demonstrates that thoughtfully crafted interventions, particularly moral nudges grounded in deontology, can increase body acceptance among Instagram users. People can be influenced, as evidenced by the thousands of accounts successfully posting product recommendations to their devout followers; Instagram should harness the power of influence to counter negativity and spread positivity among its millions of users.

Acknowledgements

I am grateful to my teacher at The Hotchkiss School, Doron Blake, for fostering my love of philosophy and applied ethics.

References

1. Lup, K.; Trub, L.; Rosenthal, L. Instagram #Instasad?: Exploring Associations Among Instagram Use, Depressive Symptoms, Negative Social Comparison, and Strangers Followed. *Cyberpsychology, Behavior, and Social Networking* 2015, 18 (5), 247–252. https://doi.org/10.1089/cyber.2014.0560.
2. Nesi, J.; Prinstein, M. J. Using Social Media for Social Comparison and Feedback-Seeking: Gender and Popularity Moderate Associations with Depressive Symptoms. *J Abnorm Child Psychol 2015, 43* (8), 1427–1438. https://doi.org/10.1007/s10802-015-0020-0.
3. Balta, S.; Emirtekin, E.; Kircaburun, K.; Griffiths, M. D. Neuroticism, Trait Fear of Missing Out, and Phubbing: The Mediating Role of State Fear of Missing Out and Problematic Instagram Use. *Int J Ment Health Addiction 2020, 18* (3), 628–639. https://doi.org/10.1007/s11469-018-9959-8.
4. Tiggemann, M.; Brown, Z. Attractive Celebrity and Peer Images on Instagram: Effect on Women's Mood and Body Image. *Body Image* 2016, 19, 37–43.
5. Holland, G.; Tiggemann, M. A Systematic Review of the Impact of the Use of Social Networking Sites on Body Image and Disordered Eating Outcomes. *Body Image* 2016, 17, 100–110. https://doi.org/10.1016/j.bodyim.2016.02.008.
6. Cohen, R.; Newton-John, T.; Slater, A. The Relationship between Facebook and Instagram Appearance-Focused Activities and Body Image Concerns in Young Women. *Body Image* 2017, 23, 183–187. https://doi.org/10.1016/j.bodyim.2017.10.002.
7. Grabe, S.; Ward, L.; Hyde, J. The Role of the Media in Body Image Concerns Among Women: A Meta-Analysis of Experimental and Correlational Studies. *Psychological bulletin* 2008, 134, 460–476. https://doi.org/10.1037/0033-2909.134.3.460.
8. Fardouly, J.; Vartanian, L. R. Social Media and Body Image Concerns: Current Research and Future Directions. *Current Opinion in Psychology* 2016, 9, 1–5. https://doi.org/10.1016/j.copsyc.2015.09.005.
9. Hendrickse, J.; Arpan, L. M.; Clayton, R. B.; Ridgway, J. L. Instagram and College Women's Body Image: Investigating the Roles of Appearance-Related Comparisons and Intrasexual Competition. *Computers in Human Behavior* 2017, 74, 92–100. https://doi.org/10.1016/j.chb.2017.04.027.
10. Vendemia, M. A.; DeAndrea, D. C. The Effects of Viewing Thin, Sexualized Selfies on Instagram: Investigating the Role of Image Source and Awareness of Photo Editing Practices. *Body Image* 2018, 27, 118–127. https://doi.org/10.1016/j.bodyim.2018.08.013.
11. Wells, G.; Horwitz, J.; Seetharaman, D. Facebook Knows Instagram Is Toxic for Teen Girls, Company Documents Show. *Wall Street Journal*. https://www.wsj.com/articles/facebook-knows-instagram-is-toxic-for-teen-girls-company-documents-show-11631620739 (accessed October 31, 2021).
12. Laker, V.; Waller, G. Does Comparison of Self with Others Influence Body Image among Adult Women? An Experimental Study in Naturalistic Settings. *Eat Weight Disord* **2022**, 27 (2), 597–604. https://doi.org/10.1007/s40519-021-01196-3.
13. O'Dea, J. A. Body Image and Self-Esteem. I*n Encyclopedia of body image and human appearance*, Vol. 1; Elsevier Academic Press: San Diego, CA, US, 2012; pp 141–147. https://doi.org/10.1016/B978-0-12-384925-0.00021-3.
14. Droesch, B. Is Everyone on Instagram an Influencer? https://www.emarketer.com/content/is-everyone-on-instagram-an-influencer (accessed October 31, 2021).
15. Kapitan, S.; Silvera, D. H. From Digital Media Influencers to Celebrity Endorsers: Attributions Drive Endorser Effectiveness. *Mark Lett* 2016, 27 (3), 553–567. https://doi.org/10.1007/s11002-015-9363-0.
16. Anixiadis, F.; Wertheim, E.; Rodgers, R.; Caruana, B. Effects of Thin-Ideal Instagram Images: The Roles of Appearance Comparisons, Internalization of the Thin Ideal and Critical Media Processing. *Body image* 2019, 31, 181–190. https://doi.org/10.1016/j.bodyim.2019.10.005.
17. Feltman, C.; Szymanski, D. Instagram Use and Self-Objectification: The Roles of Internalization, Comparison, Appearance Commentary, and Feminism. *Sex Roles* 2018, 78. https://doi.org/10.1007/s11199-017-0796-1.
18. Tiggemann, M.; Slater, A. NetGirls: The Internet, Facebook, and Body Image Concern in Adolescent Girls. *International Journal of Eating Disorders* 2013, 46 (6), 630–633.
19. Carey, R. N.; Donaghue, N.; Broderick, P. Body Image Concern among Australian Adolescent Girls: The Role of Body Comparisons with Models and Peers. *Body Image* 2014, 11 (1), 81–84. https://doi.org/10.1016/j.bodyim.2013.09.006.
20. Guest, E.; Costa, B.; Williamson, H.; Meyrick, J.; Halliwell, E.; Harcourt, D. The Effectiveness of Interventions Aiming to Promote Positive Body Image in Adults: A Systematic Review. *Body Image* 2019, 30, 10–25. https://doi.org/10.1016/j.bodyim.2019.04.002.
21. Community guidelines. Pinterest Policy. https://policy.pinterest.com/en/community-guidelines.
22. Everett, J. A. C.; Colombatto, C.; Awad, E.; Boggio, P.; Bos, B.; Brady, W. J.; Chawla, M.; Chituc, V.; Chung, D.; Drupp, M. A.; Goel, S.; Grosskopf, B.; Hjorth, F.; Ji, A.; Kealoha, C.; Kim, J. S.; Lin, Y.; Ma, Y.; Maréchal, M. A.; Mancinelli, F.; Mathys, C.; Olsen, A. L.; Pearce, G.; Prosser, A. M. B.; Reggev, N.; Sabin, N.; Senn, J.; Shin, Y. S.; Sinnott-Armstrong, W.; Sjåstad, H.; Strick, M.; Sul, S.; Tummers, L.; Turner, M.; Yu, H.; Zoh, Y.; Crockett, M. J. Moral Dilemmas and Trust in Leaders during a Global Health Crisis. *Nat Hum Behav* 2021, 5 (8), 1074–1088. https://doi.org/10.1038/s41562-021-01156-y.
23. Cole, P. The Moral Bases for Public Health Interventions. *Epidemiology* **1995**, 6 (1), 78–83.
24. Thomson, R. Moral Rhetoric and Public Health Pragmatism: The Recent Politics of Sex Education. *Feminist Review* 1994, 48 (1),

40–60. https://doi.org/10.1057/fr.1994.41.
25.*Messages with Moral-Emotional Words Are More Likely to go Viral on Social Media*. New York University. http://www.nyu.edu/content/nyu/en/about/news-publications/news/2017/june/messages-with-moral-emotional-words-are-more-likely-to-go-viral-.
26.Luttrell, A.; Philipp-Muller, A.; Petty, R. E. Challenging Moral Attitudes With Moral Messages. *Psychol Sci* **2019**, 30 (8), 1136–1150. https://doi.org/10.1177/0956797619854706.
27.Vogel, E. A.; Rose, J. P.; Roberts, L. R.; Eckles, K. Social Com parison, Social Media, and Self-Esteem. *Psychology of Popular Media Culture* **2014**, 3 (4), 206–222. https://doi.org/10.1037/ppm0000047.
28.Kim, H.; Schlicht, R.; Schardt, M.; Florack, A. The Contributions of Social Comparison to Social Network Site Addiction. *PLoS One* **2021**, 16 (10), e0257795. https://doi.org/10.1371/journal.pone.0257795.
29.Quittkat, H. L.; Hartmann, A. S.; Düsing, R.; Buhlmann, U.; Vocks, S. Body Dissatisfaction, Importance of Appearance, and Body Appreciation in Men and Women Over the Lifespan. *Fron tiers in Psychiatry* **2019**, 10.
30.Muth, J. L.; Cash, T. F. Body-Image Attitudes: What Difference Does Gender Make?1. J*ournal of Applied Social Psychology* **1997**, 27 (16), 1438–1452. https://doi.org/10.1111/j.1559-1816.1997.tb01607.x.
31.Arkenau, R.; Bauer, A.; Schneider, S.; Vocks, S. Gender Differences in State Body Satisfaction, Affect, and Body-Related Attention Patterns towards One's Own and a Peer's Body: An Eye-Tracking Study with Women and Men. *Cogn Ther Res* **2022**. https://doi.org/10.1007/s10608-022-10300-5.
32.Kant, I. *Groundwork for the Metaphysics of Morals*; Oxford Uni versity Press, 1785.
33.Rawls, *J. A Theory of Justice*; Belknap Press of Harvard University Press: Cambridge, MA, US, 1971.
34.Everett, J. A. C.; Kahane, G. Switching Tracks? Towards a Multidimensional Model of Utilitarian Psychology. Trends in Cog nitive Sciences 2020, 24 (2), 124–134. https://doi.org/10.1016/j.tics.2019.11.012.
35.Bentham, J. *The Collected Works of Jeremy Bentham: Deontology. Together with a Table of the Springs of Action and the Article on Utilitarianism*; Clarendon Press, 1983.
36.Mill, J. S. *Utilitarianism*; Parker, Son, and Bourne, 1863.
37.Bellefleur, O.; Keeling, M. Utilitarianism in Public Health; National Collaborating Centre for Healthy Public Policy: Montréal, Québec, 2016.
38.Bak, C.; Priniski, J.; Holyoak, K. *Representations of Health and Wellness on Instagram: An Analysis of 285,000 Posts*; 2020. https://doi.org/10.31234/osf.io/6nxvu.
39.Tylka, T. L.; Wood-Barcalow, N. L. The Body Appreciation Scale-2: Item Refinement and Psychometric Evaluation. *Body Image* 2015, 12, 53–67. https://doi.org/10.1016/j.bodyim.2014.09.006.
40.Rosenberg, M. *Society and the Adolescent Self-Image*; Princeton University Press: Princeton, NJ, 1965.
41.Gibbons, F. X.; Buunk, B. P. Individual Differences in Social Comparison: Development of a Scale of Social Comparison Orien tation. *Journal of Personality and Social Psychology* 1999, 76 (1), 129–142. https://doi.org/10.1037/0022-3514.76.1.129.
42.Instagram Help Center: Data Policy. https://help.instagram.com/519522125107875/?maybe_redirect_pol=0 (accessed 2022-03-10).
43.Rosenberg, M. *Conceiving the Self*; Krieger: Malabar, FL, 1986.
44.Guess, A.; Munger, K.; Nagler, J.; Tucker, J. How Accurate Are Survey Responses on Social Media and Politics? *Political Commu nication* 2019, 36 (2), 241–258. https://doi.org/10.1080/10584609.2018.1504840.

Author

Lauren Sonneborn is a senior at The Hotchkiss School in Lakeville, CT. Her academic interests include applied ethics, social psychology, and literary analysis. Lauren hopes to continue exploring the role of ethics in modern society and institutions, including social media.

DOI: 10.36838/v4i5.10

IJHSR
ijhighschoolresearch.org
RESEARCH ARTICLE

Skin Cancer Patients' Psychological Well-Being: Identifying the Statistically Significant Predictors

Madeleine M. Lepley
Lafayette High School, 401 Reed Lane, Lexington, Kentucky 40503, USA; madeleinelepley@hotmail.com

ABSTRACT: Skin cancer is one of the most frequently diagnosed cancers across the world and studies have shown that patients with low psychological well-being (PWB) may have a poorer disease prognosis. Many factors, including social support, personality, and age, are predictive of cancer patients' PWB. This study aimed to answer the question: Which factors are statistically significant predictors of skin cancer patients' psychological well-being? An anonymous online survey promoted by national and international skin cancer organizations was utilized to answer this question. Four hundred seventy skin cancer patients from 10 countries and 43 U.S. states responded, and 251 responses were complete and analyzed. Multivariate regression, analysis of variance (ANOVA), and t-tests determined the statistically significant predictors of patients' PWB: conscientiousness, social support, stage of skin cancer, neuroticism, agreeableness, and mindfulness. Awareness of these factors by patients and medical teams alike and implementation of the strategies suggested in this paper to improve patients' PWB may ensure that the next wave of incoming skin cancer patients doesn't just survive but thrives.

KEYWORDS: Behavioral and Social Sciences; Physiological Psychology; Skin Cancer; Psychological Well-Being; Significant Predictor.

Introduction

Over many centuries, the word "cancer," a disease caused by the overgrowth of cells and named for the crab-like shape of the tumors it can produce, has developed a connotation distinct from its definition, evoking feelings of pain, grief, and fear in many individuals. Cancer has become one of the most widely feared and infamous diseases across the world.[1-3] Moreover, cancer fatalism, the belief that cancer will inevitably cause death regardless of treatment or intervention, has spread widely in ethnic groups, minorities, and the less-educated demographic.[1,3,4] But these beliefs are not unfounded… In 2018, about 9.5 million people died of cancer globally, with one of the highest death rates in the U.S.[5-7]

This study will focus on skin cancer, the most frequently diagnosed cancer in America.[8] Skin cancer is primarily diagnosed as basal, squamous, or Merkel cell carcinoma or melanoma.[6] More than two people die of skin cancer in the U.S. every hour and one in five Americans will develop the disease by the time they are 70.[8]

Over the past 50 years, there has been a growing focus on patients' mental health, and a field dedicated to the psychological needs of cancer patients has emerged.[9] Psycho-oncology is an interdisciplinary field focused on "the study of psychological, behavioral, and psychosocial factors involved in the risk, detection, course, treatment, and outcome (in terms of survival) of cancer."[12] Psycho-oncologists are less concerned with the outcome of the disease as their main focus is to improve patients' quality of life.[9]

One major component of quality of life (QOL) is well-being, a cornerstone of modern psycho-oncologic research. Well-being has many classifications, including emotional, physical, and social well-being, but the focus of this study was psychological well-being (PWB).[13] Dr. Carol Ryff of the University of Wisconsin-Madison is best recognized for her 6-factor model of psychological well-being, which illustrates PWB as a product of self-acceptance, positive relations with others, autonomy, environmental mastery, purpose in life, and personal growth.[14]

Furthermore, well-being is a state that is associated with higher levels of mental and physical health.[15-17] Therefore, psychological interventions aimed at improving one's PWB could have major implications for the future of oncology. Many longitudinal studies and meta-analyses affirm that psychological well-being, whether defined as "flourishing," positive mental health, etc., correlates with lower mortality rates and optimal disease prognosis.[15-17] On the other hand, depression has been associated with worse survival rates among cancer patients.[18]

There is a clear correlation between a patient's psychological well-being and the outcome of diseases, including skin cancer. However, for psycho-oncologists to make beneficial psychological interventions for patients, they need to know which factors most impact psychological well-being. Prior research has primarily focused on the impact of one factor or group of factors (e.g., solely demographics) on cancer patients' well-being, but no study that the author is aware of has examined them collectively. This gap led to the research question: Which factors are statistically significant predictors of skin cancer patients' psychological wellbeing? As the number of cancer patients and survivors in the U.S. is expected to increase to 26.1 million by 2040, finding the answer to this question is paramount for psycho-oncologists to improve the PWB of skin cancer patients and, potentially, their survival rates as well.[19]

DOI: 10.36838/v4i5.11

Literature Review:

The factors that will be examined can be grouped into five categories: individual, medical, lifestyle, social, and environmental.

Beginning with individual factors, the sub-factors that will be investigated are demographics (gender, ethnicity, and age) and personality. The author is not aware of a study that has examined the impact of gender on cancer patients' PWB specifically. However, women are more prone to anxiety and fear than men, which likely impacts their PWB.[20] Furthermore, a study examining gender differences in mental illnesses and quality of life among 351 cancer patients found that "in general, women experienced more depression, anxiety and poorer QOL (quality of life) than men did."[21] However, some mental health trends in the general population don't apply to cancer patients. Further research illuminated gender differences in depression among cancer patients and the general population in a longitudinal study of 10,317 individuals; men without cancer generally had fewer depressive symptoms than women, while men with cancer generally had more depressive symptoms, which is contradictory to earlier findings.[22] In summary, there isn't a consensus on which gender experiences poorer psychological well-being following cancer diagnosis and the subsequent development of mental illnesses.

While it is unclear how gender impacts PWB, numerous studies have indicated that age is positively correlated with the psychological well-being of cancer patients.[21,23] Thus, older patients generally have higher PWB than younger patients, as these individuals experienced less anxiety and depression and a higher mental QOL.[21] Subsequently, a meta-analysis of 37 studies analyzing the impact of various factors on cancer survivors' QOL also found that cancer patients' PWB improves with age.[23]

Ethnicity has not been directly associated with cancer patients' PWB, but the growth of various ideologies like cancer fatalism in certain ethnic groups may indirectly affect it.[1-4] The prevalence of cancer varies between ethnicities, with non-Hispanic black males having the highest incidence overall, despite having a lower perceived risk and fewer cancer worries.[4,24] An analysis of the prevalence of depression among cancer patients by race and sex found that depression rates were "highest among black men, followed by white women, black women, and white men."[25] Thus, black men's apathy towards cancer may contribute to depression once the reality of their diagnosis sets in. These studies hint that the psychological well-being of black skin cancer patients would be poorer than that of Caucasians due to their fatalistic beliefs and depression rates, but the author is not aware of a study that has directly measured this.[1-4,24,25]

The next individual factor, personality, is defined by the American Psychological Association as "individual differences in characteristic patterns of thinking, feeling and behaving."[26] Research has affirmed that personality impacts a patient's adaptation to cancer and possibly their prognosis.[27] This study will focus on the Big Five personality traits: *extraversion*, being outgoing and sociable; *agreeableness*, being cooperative, trusting, and sympathetic; *openness*, being curious, creative, and imaginative; *conscientiousness*, being organized, diligent, and self-disciplined; and *neuroticism*, being anxious, stressed, and irritable.[56] A 2009 study determined that extraversion, conscientiousness, and neuroticism were correlated with PWB.[28] A later study advanced this notion by analyzing the impact of all Big Five personality traits on an individual's PWB using a survey of 286 Australian individuals.[29] All traits were significantly correlated with PWB, with an individual's lifestyle choices also have significant impacts on their physical and psychological well-being.[35-45] This study will focus on three main lifestyle choices: nutrition, physical activity, and mindfulness practice.

Moreover, certain personality traits like resilience may explain the variation in cancer patients' PWB at different stages of the disease, which leads into the next category of factors: medical. Most types of skin cancer have five stages (0-4) that are classified based on the tumor's size and level of invasiveness.[32] A retrospective observational found that the well-being of early-stage cancer patients is generally lower than that of the general population, while that of late-stage cancer patients is sometimes even higher than that of the general population.[11] These disparities could be attributed to post-traumatic growth (PTG) or the act of benefit-finding (BF), two names for a phenomenon in which resilient individuals who actively cope with traumatic experiences gain a positive outlook on life and undergo personal betterment.[33,34] "Individuals with stage 2 disease had significantly higher BF scores than those with stage 4 or stage 1 cancer. Time since diagnosis [was] not related to BF."[34] Therefore, a patient's stage of cancer is the only medical factor that is currently believed to impact their psychological well-being. Based on the current literature, it can be hypothesized that skin cancer patients in the middle stages (2 and 3) would have the highest PWB.

Cancer Society claims that nutrition is essential to cancer patients' wellbeing.[35] A meta-analysis by Li *et al*. expounded this notion by analyzing 21 studies regarding diet and depression from 10 countries and determining that the Western dietary pattern (consisting of red meat, refined starches and sweets, and high-fat foods) was associated with an increased risk of depression,[37] which suggests that nutrition quality is related to PWB. Conversely, a study involving 100,000 women determined that diet quality has a positive correlation with optimism, which also contributes to PWB.[38,39]

Cancer patients are also encouraged to get physical activity to mitigate symptoms.[36] A 2010 meta-analysis found that exercise interventions improved the QOL of cancer survivors, which is consistent with later findings.[44,45] Thus, patients who exercise are more likely to have higher PWB.

Mindfulness, "the state of being attentive to and aware of what is taking place in the present," has been shown to boost wellbeing and is becoming increasingly implemented in cancer care.[40,41] One study determined that mindfulness was "associated with higher pleasant effect, positive affectivity, vitality, life satisfaction, self-esteem, optimism, and self-actuality" among cancer patients.[41] Furthermore, a study of Japanese breast cancer patients found that mindfulness-based

DOI: 10.36838/v4i5.11

cognitive therapy improved patients' PWB.[43] Thus, mindfulness has a definite impact on cancer patients' psychological well-being, but the relative significance of this variable is unknown.

Numerous studies have shown that social support, "the provision of assistance or comfort to others, typically to help them cope with biological, psychological, and social stressors," improves one's well-being.[46-50] For example, a study conducted using questionnaires and health surveys taken by 351 cancer patients determined that social support was positively correlated with psychological adjustment. and QOL.[47] Therefore, patients with greater social support have higher PWB.

Methods

An online survey was chosen as the research instrument for this study because of its ability to reach a diverse sample of skin cancer patients, its convenience for individuals with internet access, and the relatively short time commitment required to participate.

Measures/Instruments:

The survey included 16 constructs that assessed the factors that could influence a skin cancer patient's PWB. No personally identifiable information was collected in this anonymous survey and respondents were asked for their consent before beginning.

Medical variables were measured using 5 research-developed questions that assessed the patient's time of diagnosis, treatment history, type and stage of skin cancer, and response to treatments.[32,53-55]

Personality types were measured using the Big Five Personality Assessment developed by John and Srivastava in 1999, a 44-item questionnaire that measures extraversion, conscientiousness, agreeableness, openness, and neuroticism using a 5-point Likert scale.[56] Individuals' scores for each item relating to a certain trait were averaged to calculate their overall score for each of the five personality traits.

Nutrition was measured using an assessment developed by the Vitality Group, a global organization that helps individuals live healthier, for use by health insurance companies.[58] The assessment consists of 11 questions that measure various aspects of one's diet, including fruit and vegetable intake, salt consumption, and refined carbohydrate consumption. The question concerning diet satisfaction was omitted. Scores were calculated by summing all items.

Carol Ryff's 18-item psychological well-being scale, developed for the 2004-2006 Midlife in the United States (MIDUS) study, was utilized to measure PWB.[59] This scale measures autonomy, environmental mastery, personal growth, positive relations with others, purpose in life, and self-acceptance (the 6 facets of PWB) using a 7-point Likert scale. Overall PWB scores were calculated by averaging individuals' subscale scores. Cronbach's Alpha was 0.792.

The Perceived Support Scale developed by Krause and Borawski-Clark was used to measure social support.[60] It consists of ten categories of questions on a 4-point scale that measure how often, ranging from "never" or "not at all" to of social support, including "Contact with Family" and "Emotional Support." The questions relating to "Support Provided" and "Satisfaction with Support Received" were omitted. Scores were calculated by averaging all items. The Cronbach's Alpha for this scale was 0.817.

The exercise was measured using a condensed version of the Global Physical Activity Questionnaire (GPAQ), an assessment developed by the World Health Organization that asks questions about exercise related to work, travel, recreational activities, and sedentary behavior.[61] Patients' scores were calculated by summing all items.

The Mindful Awareness Attention Scale (MAAS), developed and validated by Brown and Ryan in 2003, assessed patients' mindfulness.[41] This 15-question instrument evaluates the frequency that one experiences certain incidents or emotions using a 6-point Likert scale. Redundant questions were removed, which condensed the scale to 10 questions. Scores were calculated by averaging all items. The Cronbach's Alpha was 0.836.

Next, respondents were asked questions regarding four aspects of their demographic background: age, gender, ethnicity, and marital status.[62]

Respondents were asked for their zip code to assess the UV index. In the analysis process, Google was used to determine the cities represented by these zip codes. Then, the cities were searched on Weather Atlas (a website with global climate data) to determine the average year-round UV index in each city.[63]

An open-response question was written to conclude the survey: "If you would like, please share what has helped you the most during your skin cancer experience."

Procedures:

Several national and international skin cancer organizations were contacted and asked to promote the survey. The Melanoma Research Alliance, the AIM at Melanoma Foundation, the Melanoma Research Foundation, the Skin Cancer Foundation, and Outrun the Sun posted the survey on at least one of their social media platforms, including Twitter, Instagram, Facebook, and YouTube.

The data were analyzed in SPSS version 26 using multivariate regression, one-way ANOVAs, and independent sample t-tests to determine the statistically significant predictors of skin cancer patients' PWB.

Participants:

Approximately 470 skin cancer patients from 10 countries and 43 U.S. states responded to the survey, 251 of which submitted nearly complete responses and were included in the data analysis. Twenty-four percent of respondents were in each of the age ranges of 30-39, 40-49, and 50-59. In addition, 88% of respondents were female and 11% were male. About 97% of participants were white or Caucasian, 2% were Hispanic or Latino, 1% were American Indian or Alaska Native, and 0.4% were Asian. Most participants (74%) were either married or in a domestic partnership, while the others were never married (15%), separated or divorced (10%), or widowed (1%).

Most respondents (69%) were either diagnosed with skin cancer between the present day and nearly two years ago or over eight years ago. The majority (88%) had melanoma which is likely because three of the organizations that promoted the survey were melanoma-focused. The second-most prevalent type of skin cancer was basal cell carcinoma (25%). Furthermore, stages 1 and 3 patients each represented 26% of survey respondents, while stage 4 patients represented 24%. Respondents received a variety of treatments, with excisional surgery (85%) and immunotherapy (33%) being the most common. Most respondents' tumors exhibited a complete response to treatment (i.e., disappeared completely).

Results

Quantitative:

Multivariate linear regression, a statistic that determines if independent variables are predictive of the dependent variable, was performed comparing 12 quantitative variables to PWB. Variables that were included were conscientiousness, agreeableness, openness, extraversion, neuroticism, social support, nutrition, exercise, mindfulness, UV index, stage of cancer, and time since diagnosis. The questions measuring these variables were grouped into indices, which gave participants a score for each index. Means for each index are displayed in Table 1

The regression analysis shown in Figure 1 indicated that these 12 variables accounted for approximately 48.7% of the variance in respondents' PWB (R^2= .487) and collectively were statistically significant predictors of PWB.

P-values of less than .05 were required to classify an individual variable as significant.[64] After the initial examination of p-values, the regression analysis was trimmed for precision to include only the variables that were shown to be significant in the first analysis. Six factors were shown to be significant predictors of skin cancer patients' PWB (in order of importance): *conscientiousness* (β= .239, p= .000), *social support* (β= .219, p= .000), *stage of skin cancer* (β= -.179, p= .001), *neuroticism* (β= -.188, p= .007), *agreeableness* (β= .145, p= .013), and *mindfulness* (β= .154, p= .019).

ANOVA (analysis of variance) was used to assess differences in mean PWB scores among variables with more than two categorical groups[64]: age, marital status, response to treatment, and type of skin cancer. Independent samples t-tests served the same purpose but for variables with only two possible groups: gender, ethnicity (white vs. non-white), and treatments received (radiation vs. no radiation). Figure 2 shows these factors and the tests used to assess the PWB differences among groups.

Among demographic variables, age, gender, and ethnicity were shown by ANOVAs to not have significant differences in PWB (p > .05). However, marital status was shown to be significant [F(5, 242) = 2.341, p = .042]. Figure 3 shows that married participants had the highest PWB, while widowed patients had the lowest PWB.

Analysis of the medical variables revealed that the amount of time since diagnosis, type of skin cancer, and response to treatment(s) did not show significant differences in PWB (p> .05). In terms of treatments received, chemotherapy, immunotherapy, cryotherapy, excisional surgery, Mohs surgery and photodynamic therapy were all insignificant as well (p> .05). However, radiation treatment was significant to respondents' PWB [t(249)= .324, p= .020]. Figure 4 shows that patients who were treated with radiation experienced lower PWB than those who were not.

Qualitative:

Out of the 470 total responses, 307 responded to the open-response prompt. After each response was analyzed, 28 themes were deduced, each of which was exhibited in at least one response, while some responses displayed more than one. These themes were divided into five categories (shown in Table 2): social, medical, personality, lifestyle, and miscellaneous.

Table 1: Mean index scores.

INDEX	SCALE	MEAN	STANDARD DEVIATION
PWB	1-5	3.91	.51
Conscientiousness	1-5	3.76	.54
Agreeableness	1-5	3.84	.55
Openness	1-5	3.51	.55
Extraversion	1-5	3.05	.74
Neuroticism	1-5	3.12	.76
Social Support	1-4	2.52	.42
Nutrition	N/A	4.38	4.97
Exercise	-2-14	2.98	3.36
Mindfulness	1-5	2.99	.89
UV	1-11	4.11	.95

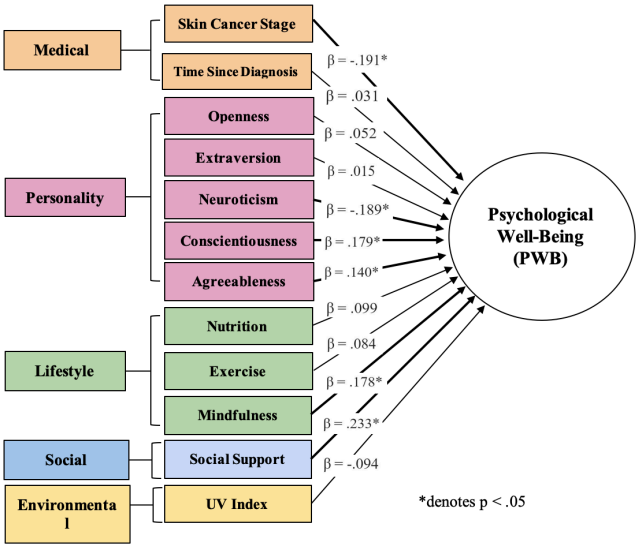

Figure 1: Regression analysis of factors that predict skin cancer patients' PWB.

DOI: 10.36838/v4i5.11

The most frequently expressed theme was family, which included one's immediate and extended family and spouses/partners. A quote that exemplifies this theme is from a

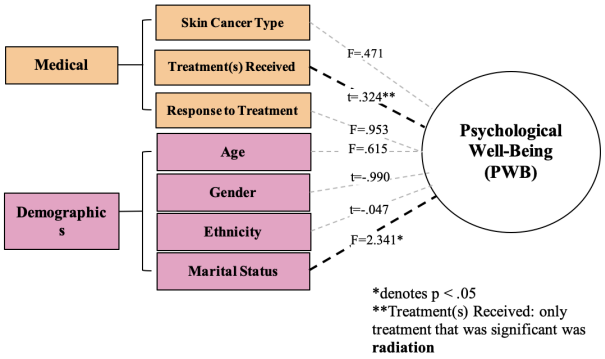

Figure 2: ANOVAs and t-tests.

respondent who claimed that what helped the most was "looking at my daughter and knowing she needs me and I need her." Another wrote, "My wife for her care and concern."

The second most prevalent theme was centered around medical teams, which was mentioned in 44 out of 307 responses and ranged from discussion of oncologists and

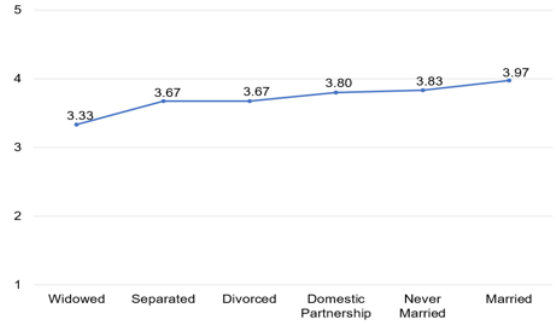

Figure 3: Mean PWB index scores by marital status.

surgeons to nurses and physicians' assistants. Care, skill, honesty, and patience were the most cited characteristics of a good medical team. One respondent wrote, "My oncologist is very thorough, and she seems to care." Another claimed that her "phenomenal Mohs surgeon" had been crucial to her cancer-free status. Though most types of treatment were found to be insignificant to PWB, many respondents mentioned that they were more pleased with medical teams who were "up on all of the latest treatments."

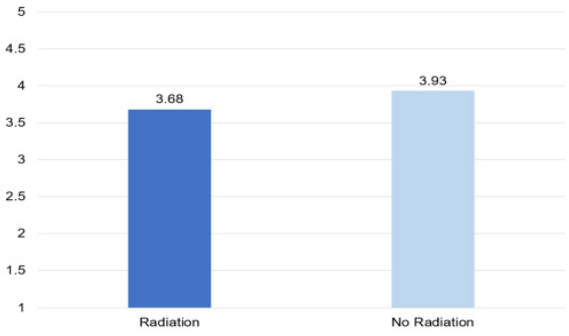

Figure 4: Mean PWB index scores by receipt of radiation treatment.

The next most frequently expressed theme was a community support system, which included friends, co-workers, neighbors, etc. One patient wrote that the most beneficial things were "close people in my life who listened and cared about my experience and fears." Another patient wrote that "having supportive people who didn't see melanoma as 'just skin cancer'…helped immensely as well."

Table 2: Thematic analysis: "If you would like, please share what has helped you the most during your skin cancer experience."

	RESPONSE THEMES	FREQUENCY
SOCIAL	Family (children, siblings, parents, spouses/partners, etc.)	55
	Community Support System (*non-skin cancer patients*: friends, coworkers, church group, neighbors, etc.)	36
	Support Groups (*skin cancer patients/survivors*: in-person and social media)	20
	Religion	19
	Learning from Fellow Skin Cancer Patients (*informally/unintentionally*)	15
	Advocating & Educating Others About Skin Cancer	11
	TOTAL	**156**
MEDICAL	Skilled, Caring & Honest Medical Teams (oncologists, dermatologists, nurses, surgeons, etc.)	44
	Self-Advocacy	5
	Early Diagnosis	5
	Good Healthcare System & Health Insurance	4
	Clinical Trial	2
	TOTAL	**60**
PERSONALITY	Conscientiousness (getting skin checks, wearing sunscreen & hats, taking care of oneself, etc.)	16
	Positivity	10
	Acceptance	10
	Gratitude	3
	Perseverance	2
	Humor	2
	Openness	2
	Curiosity	2
	TOTAL	**47**
LIFESTYLE	Exercise	4
	Mindfulness/Meditation	2
	Balanced Nutrition	1
	TOTAL	**7**
MISCELLANEOUS	Information/Education (and their sources)	22
	Time	4
	Living Life/Not Dwelling on Disease	3
	Handling Personal Problems	2
	Adapting to Physical Limitations	2
	Reading	2
	TOTAL	**35**

Overall, the majority of responses were heavily focused on social support, whether it was from family, friends, or fellow skin cancer patients.

Discussion

The question that this study aimed to answer was: Which factors are statistically significant predictors of skin cancer patients' psychological well-being?

Interestingly, three out of the six significant predictors of skin cancer patients' PWB were personality types (neuroticism, agreeableness, and conscientiousness). Consistent with the previous literature, patients with high levels of agreeableness and conscientiousness had higher psychological well-being, while patients exhibiting high levels of neuroticism had lower psychological well-being.[28-31] However, two out of the five personality traits (extraversion and openness) were not significant to PWB, contradictory to prior research.[29]

Conscientious individuals have a "tendency to be responsible, organized, hard-working, goal-directed, and to adhere to norms and rules."[66] Patients with this personality type may be more likely to follow their treatment plans and

doctor's instructions, get frequent skin checks, and be diligent about wearing sunscreen, hats, and protective clothing to prevent further skin damage. These habits could reduce patients' stress and give them peace of mind.

Agreeable individuals are kind, cooperative, polite, and empathetic.[67] This could contribute to higher PWB because these individuals are more likely to develop positive relationships with others (including their oncologist) and establish a strong support system, which has been shown by this study and numerous others to increase PWB.

Neuroticism, the only Big Five personality trait that is negatively correlated with PWB, contributes to anxiety and depression.[30, 31] Skin cancer patients who are neurotic likely worry about their disease progressing, dwell on their past mistakes, and fear death. Thus, these findings stress the importance of diligence, cooperation, and stability in cancer patients. Fortunately, studies have shown that personality is malleable and capable of being changed over time.[68, 69]

Overall, social support was the statistically significant predictor of PWB with the second-highest Beta coefficient. In the thematic analysis section, most respondents answer the question asking about beneficial aspects of their experience related to social support. Furthermore, ANOVAs illustrated that marital status (a major facet of social support) was significantly related to PWB. The means plot in Figure 3 shows that married skin cancer patients had the highest PWB, which is consistent with prior findings.[48, 49]

Another significant predictor of PWB was mindfulness. Mindfulness is related to higher levels of psychological well-being because it may prevent skin cancer patients from dwelling on the past or thinking too far into the future, which is important for an unpredictable disease like cancer. This conclusion is in line with previous studies that determined the benefits of mindfulness for cancer patients.[40-43]

Consistent with prior findings,[34] stage of cancer was a significant predictor of PWB. However, the trend observed in previous research in which patients in stages 2 and 3 had the highest PWB was not illustrated by the data. In this study, the stage of cancer was negatively correlated with patients' PWB; patients in higher stages had poorer PWB.

Nearly all of the most common skin cancer treatments (excisional surgery, chemotherapy, immunotherapy, cryotherapy, Mohs surgery, and photodynamic therapy) showed no significant differences in PWB. However, patients who received radiation had significantly lower PWB than those who did not. Unfortunately, the word "radiation" has a negative connotation for many cancer patients who have misconceptions about its safety.[70] Thus, patients who receive this treatment may be apprehensive of the outcome, leading to worry and decreased PWB. In reality, radiation is considered a successful treatment for basal and squamous cell carcinomas as 90% of patients who receive it are cured within 5 years.[71] Therefore, healthcare providers should work to amend the reputation of radiation therapy to ensure that patients who receive this treatment are confident in its efficacy and maintain high PWB.

The regression analysis suggested that nutrition, exercise, meditation, UV index, and time since diagnosis were not statistically significant predictors of PWB. Contrary to prior findings,[21,23,25] neither age, gender, nor ethnicity was found to be significantly related to PWB by ANOVAs.

Thematic Analysis:

Many of the factors that participants mentioned in the open-response question were also found to be significant predictors of PWB in the regression analysis. For example, social support, mindfulness, and conscientiousness were all mentioned directly or indirectly by at least one respondent. However, some variables that were not measured in the survey were mentioned in the qualitative section, including religion, gratitude, and humor. This makes sense as the R-squared value of 0.487 indicates that approximately 50% of the variance in skin cancer patients' PWB was accounted for by variables not included in the survey. Thus, future research should attempt to identify the remaining variables that are significant predictors of skin cancer patients' PWB.

Implications:

The findings of this study led to the creation of four strategies that psycho-oncologists could pursue to improve the PWB of skin cancer patients: 1) recognize that patients in higher stages have the poorest psychological well-being and provide these patients with more intense interventions; 2) suggest that cancer patients complete a personality assessment following diagnosis to identify psychological strengths and weakness to tailor their psychological intervention plan around; 3) implement mindfulness-based intervention practices; 4) ensure that patients have adequate social support and recommend support groups to patients who are lacking in this area.

Moreover, patients with mental disorders characterized by neuroticism (anxiety, OCD, etc.) should be referred for psychological assessment and intervention to mitigate the negative effects of this personality type on their psychological well-being.

Limitations:

Due to COVID-19, the distribution of the survey was restricted to skin cancer organizations' social media platforms as opposed to hospitals and cancer centers, which could have reached a larger and more diverse sample of patients.

In addition, the survey could not assess every factor that could be related to PWB since it had to be short enough for a sufficient number of patients to respond to its entirety.

Despite research suggesting that nutrition and exercise may be predictive of patients' PWB,[35-38,44,45] these factors were not shown to be significant in the regression analysis. A possible cause of this could be that the assessment used to evaluate patients' nutrition was not widely used and/or validated in research.

Furthermore, there was a lack of ethnic diversity among respondents as 97% of respondents were Caucasian, which may have prevented PWB differences from being observed based on ethnicity. In addition, 88% of respondents were female, which could explain why gender did not show differences in PWB either. Since the majority of respondents were white

DOI: 10.36838/v4i5.11

females, this study may not be generalizable to the global skin cancer patient population.

Conclusion

Oncology is a field that is constantly evolving, with new advancements in treatments, screening techniques, and surgical methods being discovered rapidly. But the vital aspect of cancer care that is often unacknowledged is tending to patients' psychological well-being. Research in psycho-oncology has greatly ameliorated this relative lack of attention, helping doctors better understand patients' needs. A quote by William Osler, "the father of modern medicine," best exemplifies this philosophy: "The good physician treats the disease; the great physician treats the patient who has the disease."[72, 73]

It is especially important to ensure that cancer patients are conscious and attentive to their psychological well-being due to the likely relationship between PWB and cancer prognosis. Whether or not this theory holds, it is important to prioritize the psychological well-being of skin cancer patients to ensure that these individuals live happy, healthy lives.

The unique holistic approach utilized in this study yielded important findings for skin cancer patients and their providers, addressing a major gap in the field. All skin cancer patients should be aware of the factors that are most predictive of high psychological well-being: high levels of the personality traits of conscientiousness and agreeableness and low levels of neuroticism; earlier stages of cancer; mindfulness; and social support.

Skin cancer is likely never going to disappear. Therefore, all cancer centers have the responsibility to make the experience as stress-free as possible for their patients. With increasing numbers of Americans predicted to develop cancer in the coming years, it is paramount that psycho-oncologists ensure that patients thrive, not just survive. Implementing the interventions proposed in this study to enhance patients' psychological well-being could be a vital step toward ensuring skin cancer patients can achieve equal levels of long-term happiness and well-being as their peers.

Acknowledgements

I would like to thank Dr. Jamie Studts and Ms. Joan Scales for their valuable guidance on survey design and distribution strategies.

I'd like to thank my Advanced Placement (AP) Research teacher, Meredith Dill, for her patience and dedication to teaching my classmates and me to conduct research during the COVID-19 pandemic.

Finally, I would also like to thank my mother, my biggest supporter throughout this process, who helped teach me statistics and research methods while I was at home during the pandemic.

References

1. Vrinten C, Wardle J, Marlow LA. Cancer Fear and Fatalism Among Ethnic Minority Women in the United Kingdom. *British Journal of Cancer*. 2016;114(5):597-604. doi:10.1038/bjc.2016.15
2. Vrinten C, Wardle J. Is cancer a good way to die? A population-based survey among middle-aged and older adults in the United Kingdom. *European Journal of Cancer*. 2016;56:172-178. doi:10.1016/j.ejca.2015.12.018
3. Moser RP, Arndt J, Han PK, Waters EA, Amsellem M, Hesse BW. Perceptions of Cancer as a Death Sentence: Prevalence and Consequences. *Journal of Health Psychology*. 2014;19(12):1518-1524. doi:10.1177/1359105313494924
4. Assari S, Khoshpouri P, Chalian H. Combined Effects of Race and Socioeconomic Status on Cancer Beliefs, Cognitions, and Emotions. *Healthcare*. 2019;7(1):17. doi:10.3390/healthcare7010017
5. Global Cancer Data by Country. World Cancer Research Fund. Published March 20, 2019. Accessed October 23, 2020. https://www.wcrf.org/dietandcancer/cancer-trends/data-cancer-frequency-country
6. Global Cancer Facts & Figures. Cancer.org. Published 2018. Accessed November 27, 2020. https://www.cancer.org/research/cancer-facts-statistics/global.html
7. CDC. An Update on Cancer Deaths in the United States. Centers for Disease Control and Prevention. Published May 29, 2020. Accessed November 27, 2020. https://www.cdc.gov/cancer/dcpc/research/update-on-cancer-deaths/index.htm
8. Skin Cancer Facts & Statistics - The Skin Cancer Foundation. The Skin Cancer Foundation. Published 2018. Accessed October 23, 2020. https://www.skincancer.org/skin-cancer-information/skin-cancer-facts/
9. Lang-Rollin I, Berberich G. Psycho-Oncology. *Dialogues in Clinical Neuroscience*. 2018;20(1):13-22. Accessed October 4, 2020. https://www.ncbi.nlm.nih.gov/pmc/articles/PMC6016045/
10. Smith TG, Troeschel AN, Castro KM, Arora NK, Stein K, Lipscomb J, Brawley OW, McCabe RM, Clauser SB, Ward E. Perceptions of Patients with Breast and Colon Cancer of the Management of Cancer-Related Pain, Fatigue, and Emotional Distress in Community Oncology. *Journal of Clinical Oncology: Official Journal of the American Society of Clinical Oncology*. 2019;37(19):1666-1676. doi:10.1200/JCO.18.01579
11. Sullivan J, Thornton Snider J, van Eijndhoven E, Okoro T, Batt K, DeLeire T. The Well-Being of Long-Term Cancer Survivors. *AJMC*. 2017;24(4):188-195. Accessed October 13, 2020. https://www.ajmc.com/view/the-well-being-of-long-term-cancer-survivors
12. Psycho-Oncology. *American Psychological Association*, dictionary.apa.org. Accessed November 30, 2020. https://dictionary.apa.org/psychooncology
13. Well-Being Concepts. Centers for Disease Control and Prevention. Published 2019. Accessed November 30, 2020. https://www.cdc.gov/hrqol/wellbeing.htm
14. Ryff CD. Happiness is everything, or is it? Explorations on the Meaning of Psychological well-being. *Journal of Personality and Social Psychology*. 1989;57(6):1069-1081. doi:10.1037/0022-3514.57.6.1069
15. Trudel-Fitzgerald C, Millstein RA, von Hippel C, Howe CJ, Tomasso LP, Wagner GR, VanderWeele TJ. Psychological Well-Being as Part of the Public Health Debate? Insight into Dimensions, Interventions, and Policy. *BMC Public Health*. 2019;19(1). doi:10.1186/s12889-019-8029-x
16. Keyes CL M., Simoes EJ. To Flourish or Not: Positive Mental Health and All-Cause Mortality. *American Journal of Public Health*. 2012;102(11):2164-2172. doi:10.2105/ajph.2012.300918
17. Lamers SMA, Bolier L, Westerhof GJ, Smit F, Bohlmeijer ET. The Impact of Emotional well-being on long-term Recovery and Survival in Physical illness: a meta-analysis. *Journal of Behavioral Medicine*. 2011;35(5):538-547. doi:10.1007/s10865-011-9379-8
18. Pirl WF, Greer JA, Traeger L, Jackson V, Lennes IT, Gallagher ER, Perez-Cruz P, Heist RS, Temel JS. Depression and Survival in Metastatic Non–Small-Cell Lung Cancer: Effects of Early

Palliative Care. *Journal of Clinical Oncology.* 2012;30(12):1310-1315. doi:10.1200/jco.2011.38.3166
19. Bluethmann SM, Mariotto AB, Rowland JH. Anticipating the "Silver Tsunami": Prevalence Trajectories and Comorbidity Burden among Older Cancer Survivors in the United States. *Cancer Epidemiology Biomarkers & Prevention*. 2016;25(7):1029-1036. doi:10.1158/1055-9965.epi-16-0133
20. McLean CP, Anderson ER. Brave Men and Timid Women? A Review of the Gender Differences in Fear and Anxiety. *Clinical Psychology Review*. 2009;29(6):496-505. doi:10.1016/j.cpr.2009.05.003
21. Parker PA, Baile WF, Moor C de, Cohen L. Psychosocial and Demographic Predictors of Quality of Life in a Large Sample of Cancer Patients. *Psycho-Oncology*. 2003;12(2):183-193. doi:10.1002/pon.635
22. Pudrovska T. Why is Cancer More Depressing for Men than Women Among Older White Adults? *Social Forces*. 2010;89(2):535-558. doi:10.1353/sof.2010.0102
23. Wu H-S, Harden JK. Symptom Burden and Quality of Life in Survivorship: A Review of the Literature. *Cancer Nursing.* 2015;38(1):E29-54. doi:10.1097/NCC.0000000000000135
24. American Cancer Society. Cancer Facts & Figures 2020. Atlanta: American Cancer Society. Published 2020. Accessed November 28, 2020. https://www.cancer.org/content/dam/cancer-org/research/cancer-facts-and-statistics/annual-cancer-facts-and-figures/2020/cancer-facts-and-figures-2020.pdf
25. Traeger L, Cannon S, Keating NL, Pirl W, Lathan C, Martin MY, He Y, Park ER. Race by Sex Differences in Depression Symptoms and Psychosocial Service Use among Non-Hispanic Black and White Patients with Lung Cancer. *Journal of Clinical Oncology*. 2014;32(2):107-113. doi:10.1200/jco.2012.46.6466
26. Personality. American Psychological Association. https://www.apa.org/topics/personality. Published 2021. Accessed April 25, 2021.
27. Dahl AA. Link Between Personality and Cancer. *Future Oncology*. 2010;6(5):691-707. doi:10.2217/fon.10.31
28. Grant S, Langan-Fox J, Anglim J. The Big Five Traits as Predictors of Subjective and Psychological Well-Being. *Psychological Reports.* 2009;105(1):205-231. doi:10.2466/pr0.105.1.205-231
29. Hicks RE, Mehta YP. The Big Five, Type A Personality, and Psychological Well-Being. *International Journal of Psychological Studies*. 2018;10(1):49-58. doi:10.5539/ijps.v10n1p49
30. van den Bergh RCN, Essink-Bot M-L, Roobol MJ, Wolters T, Schroder FH, Bangma CH, Steyerberg EW. Anxiety and Distress during Active Surveillance for Early Prostate Cancer. *Cancer*. 2009;115(17):3868-3878. doi:10.1002/cncr.24446
31. Den Oudsten BL, Van Heck GL, Van der Steeg AFW, Roukema JA, De Vries J. Predictors of Depressive Symptoms 12 Months after Surgical Treatment of early-stage Breast Cancer. *Psycho-Oncology*. 2009;18(11):1230-1237. doi:10.1002/pon.1518
32. Skin Cancer (Non-Melanoma) - Stages. Cancer.net. Published June 25, 2012. Accessed February 20, 2021. https://www.cancer.net/cancer-types/skin-cancer-non-melanoma/stages#:~:text=There%20are%205%20stages%3A%20stage
33. Seiler A, Jenewein J. Resilience in Cancer Patients. *Frontiers in Psychiatry.* 2019;10(208). doi:10.3389/fpsyt.2019.00208
34. Lechner SC, Zakowski SG, Antoni MH, Greenhawt M, Block K, Block P. Do Sociodemographic and disease-related Variables Influence benefit-finding in Cancer patients? *Psycho-Oncology*. 2003;12(5):491-499. doi:10.1002/pon.671
35. Physical Activity and the Cancer Patient. www.cancer.org. https://www.cancer.org/treatment/survivorship-during-and-after-treatment/staying-active/physical-activity-and-the-cancer-patient.html#references
36. Nutrition for People with Cancer. Cancer.org. Published 2020. Accessed November 20, 2020. https://www.cancer.org/treatment/survivorship-during-and-after-treatment/staying-active/nutrition.html
37. Li Y, Lv M-R, Wei Y-J, Sun L, Zhang J-X, Zhang H-G, Li B. Dietary Patterns, and Depression risk: a meta-analysis. Psychiatry Research. 2017;253:373-382. doi:10.1016/j.psychres.2017.04.020
38. Hingle MD, Wertheim BC, Tindle HA, Tinker L, Seguin RA, Rosal MC, Thomson CA. Optimism and Diet Quality in the Women's Health Initiative. *Journal of the Academy of Nutrition and Dietetics*. 2014;114(7):1036-1045. doi:10.1016/j.jand.2013.12.018
39. Scheier MF, Carver CS. Effects of Optimism on Psychological and Physical Well-Being: Theoretical Overview and Empirical Update. *Cognitive Therapy and Research*. 1992;16(2):201-228. doi:10.1007/bf01173489
40. Mehta R, Sharma K, Potters L, Wernicke AG, Parashar B. Evidence for the Role of Mindfulness in Cancer: Benefits and Techniques. *Cureus*. 2019;11(5). doi:10.7759/cureus.4629
41. Carlson LE, Ursuliak Z, Goodey E, Angen M, Speca M. The Effects of a Mindfulness meditation-based Stress Reduction Program on Mood and Symptoms of Stress in Cancer outpatients: 6-month follow-up. *Supportive Care in Cancer.* 2001;9(2):112-123. doi:10.1007/s005200000206
42. Park S, Sato Y, Takita Y, Tamura N, Ninomiya A, Kosugi T, Sado M, Nakagawa A, Takahashi M, Hayashida T, Fujisawa D. Mindfulness-Based Cognitive Therapy for Psychological Distress, Fear of Cancer Recurrence, Fatigue, Spiritual Well-Being, and Quality of Life in Patients with Breast Cancer—A Randomized Controlled Trial. *Journal of Pain and Symptom Management*. 2020;60(2):381-389. doi:10.1016/j.jpainsymman.2020.02.017
43. Dittus KL, Gramling RE, Ades PA. Exercise interventions for individuals with advanced cancer: A systematic review. *Preventive Medicine*. 2017;104:124-132. doi:10.1016/j.ypmed.2017.07.015
44. Ferrer RA, Huedo-Medina TB, Johnson BT, Ryan S, Pescatello LS. Exercise Interventions for Cancer Survivors: A Meta-Analysis of Quality of Life Outcomes. Annals of Behavioral Medicine. 2010;41(1):32-47. doi:10.1007/s12160-010-9225-1
45. Social Support. American Psychological Association, dictionary. apa.org. Accessed May 19, 2021. https://dictionary.apa.org/social-support
46. Carver CS, Smith RG, Petronis VM, Antoni MH. Quality of Life Among Long-Term Survivors of Breast Cancer: Different Types of Antecedents Predict Different Classes of Outcomes. *Psycho-Oncology.* 2005;15(9):749-758. doi:10.1002/pon.1006
47. Kim HK, McKenry PC. The Relationship Between Marriage and Psychological Well-Being: A Longitudinal Analysis. *Journal of Family Issues*. 2002;23(8):885-911. doi:10.1177/019251302237296
48. Goldzweig G, Andritsch E, Hubert A, Brenner B, Walach N, Perry S, Baider L. Psychological Distress among Male Patients and Male spouses: What Do Oncologists Need to know? *Annals of Oncology: Official Journal of the European Society for Medical Oncology*. 2010;21(4):877-883. doi:10.1093/annonc/mdp398
49. Kim J, Han JY, Shaw B, McTavish F, Gustafson D. The Roles of Social Support and Coping Strategies in Predicting Breast Cancer Patients' Emotional Well-being. *Journal of Health Psychology*. 2010;15(4):543-552. doi:10.1177/1359105309355338
50. U.S. Cancer Statistics Working Group. USCS Data Visualizations. gis.cdc.gov. Published June 2020. Accessed October 28, 2020. https://www.cdc.gov/cancer/dataviz
51. US EPA O. Sun Safety Monthly Average UV Index. US EPA. Published September 3, 2015. Accessed December 2, 2020. https://www.epa.gov/sunsafety/sun-safety-monthly-average-uv-index

DOI: 10.36838/v4i5.11

52.Skin Cancer - Diagnosis and Treatment - Mayo Clinic. MayoClinic.org. Published 2019. Accessed February 20, 2021. https://www.mayoclinic.org/diseases-conditions/skin-cancer/diagnosis-treatment/drc-20377608
53.Types of Skin Cancer. www.aad.org. Accessed February 20, 2021. https://www.aad.org/public/diseases/skin-cancer/types/common
54.Response Evaluation Criteria in Solid Tumors. www.cancer.gov. Published February 2, 2011. Accessed February 20, 2021. https://www.cancer.gov/publications/dictionaries/cancer-terms/def/response-evaluation-criteria-in-solid-tumors
55.The Big Five Trait Taxonomy: History, Measurement, and Theoretical Perspectives. In: *Handbook of Personality: Theory and Research. Guilford Press*; 1999:102-138. Accessed January 29, 2021. https://www.semanticscholar.org/paper/The-Big-Five-Trait-taxonomy%3A-History%2C-measurement%2C-John-Srivastava/a354854c71d60a4490c42ae47464fbb9807d02bf
56.What does Cronbach's alpha mean? | SPSS FAQ. stats.idre.ucla.edu. Accessed May 19, 2021. https://stats.idre.ucla.edu/spss/faq/what-does-cronbachs-alpha-mean
57.*Vitality Health Assessment - Nutrition. Vitality Group*; 2020.
58.Ryff C, Almeida DM, Ayanian JS, Carr DS, Cleary PD, Coe C, Davidson R, Krueger RF, Lachman ME, Marks NF, Mroczek DK, Seeman T, Mailick Seltzer M, Singer BH, Sloan RP, Tun PA, Weinstein M, Williams D. MIDUS - Midlife in the United States, a National Longitudinal Study of Health and Well-being. *wwwmiduswiscedu*. Published online August 2010. Accessed February 3, 2021. http://www.midus.wisc.edu/midus2/project1/
59.Krause N, Borawski-Clark E. Social Class Differences in Social Support among Older Adults. The Gerontologist. 1995;35(4):498-508. doi:10.1093/geront/35.4.498
60.Surveillance and Population-Based Prevention of Noncommunicable Diseases Department, World Health Organization. *Global Physical Activity Questionnaire (GPAQ) Analysis Guide*.;4-5. Accessed January 31, 2021. https://www.who.int/ncds/surveillance/steps/resources/GPAQ_Analysis_Guide.pdf
61.Evans L. *Racial and Ethnic Categories and Definitions for NIH Diversity Programs and Other Reporting Purposes*. National Institutes of Health; 2015. Accessed January 31, 2021. https://grants.nih.gov/grants/guide/notice-files/not-od-15-089.html
62.Weather Atlas | Weather Forecast and Climate Information for Cities All over the Globe. Weather Atlas. Accessed May 19, 2021. https://www.weather-atlas.com/en
63.Beers B. What P-Value Tells Us. Investopedia. Published 2019. Accessed May 19, 2021. https://www.investopedia.com/terms/p/p-value.asp
64.Singh G. Analysis of Variance (ANOVA) | Introduction, Types & Techniques. Analytics Vidhya. Published January 15, 2018. Accessed May 20, 2021. https://www.analyticsvidhya.com/blog/2018/01/anova-analysis-of-variance
65.Conscientiousness | Psychology Today. Psychology Today. Published 2019. Accessed April 25, 2021. https://www.psychologytoday.com/us/basics/conscientiousness
66.Agreeableness | Psychology Today. Psychology Today. Published 2019. Accessed April 25, 2021. https://www.psychologytoday.com/us/basics/agreeableness
67.Soto C. Personality Can Change over a Lifetime, and Usually for the Better. NPR.org. Published June 30, 2016. Accessed April 22, 2021. https://www.npr.org/sections/health-shots/2016/06/30/484053435/personality-can-change-over-a-lifetime-and-usually-for-the-better
68.Personality Changes for the Better with Age. *American Psychological Association*. https://www.apa.org/monitor/julaug03/personality. Published August 2003. Accessed April 22, 2021.
69.Gillan C, Abrams D, Harnett N, Wiljer D, Catton P. Fears and Misperceptions of Radiation Therapy: Sources and Impact on Decision-Making and Anxiety. *Journal of Cancer Education*. 2014;29(2):289-295. doi:10.1007/s13187-013-0598-2
70.Radiotherapy for Malignant Skin Diseases. dermnetnz.org. Accessed April 22, 2021. https://dermnetnz.org/topics/radiotherapy-for-malignant-skin-diseases/#:~:text=Effectiveness%20of%20radiation%20therapy&text=For%20small%2C%20uncomplicated%20basal%20cell
71.Centor RM. To Be a Great Physician, You Must Understand the Whole Story. *Medscape General Medicine*. 2007;9(1):59. Accessed April 22, 2021. https://www.ncbi.nlm.nih.gov/pmc/articles/PMC1924990/#:~:text=Sir%20William%20Osler%20said%2C%20%E2%80%9CThe
72.Biographical Overview. William Osler - Profiles in Science. Accessed April 22, 2021. https://profiles.nlm.nih.gov/spotlight/gf/feature/biographical-overview
73.Centor RM. To Be a Great Physician, You Must Understand the Whole Story. *Medscape General Medicine*. 2007;9(1):59. Accessed April 22, 2021. https://www.ncbi.nlm.nih.gov/pmc/articles/PMC1924990/#:~:text=Sir%20William%20Osler%20said%2C%20%E2%80%9CThe.

Author

Madeleine Lepley is a high school senior from Lexington, Kentucky. Since taking Advanced Placement (AP) Biology her sophomore year, she's had a passion for the medical field and is interested in pursuing a pre-medical school track in college in hopes of one day becoming a surgeon and/or researcher. She also owns a cupcake business that raises money for skin cancer research, runs on the varsity cross country and track teams, and plays on the tennis team.

IJHSR
ijhighschoolresearch.org
REVIEW ARTICLE

The Effect of Dietary Fiber on Asthma Through Cytokine Production

Samyuktha Natesan
Dougherty Valley High School,10550 Albion Rd, San Ramon, CA, 94582, USA ; samyukthanatesan05@gmail.com

ABSTRACT: Asthma is a chronic disease that harms both adults and children, causing symptoms such as debilitating shortness of breath, wheezing, coughing, and in severe cases, even death. There is no cure for asthma, only therapies that can help control asthma symptoms. One significant, under-examined possibility for a supplement to these therapies is dietary fiber. Dietary fiber, found in various everyday foods including grains, fruits, and vegetables, can maintain gut health and a balanced gut micro-biome, which improves the body's immune system and overall health. This paper will review evidence for the relationships between asthma and dietary fiber - specifically how dietary fiber could be used as a supplementary therapy. One of the byproducts of the fermentation of dietary fiber are short-chain fatty acids (SCFAs). One significant function of SCFAs is that they can regulate the production of cytokines. This review paper will examine the benefits of dietary fiber on asthma through SCFA production and the resulting decrease in pro-inflammatory cytokines and increase in anti-inflammatory cytokine. This paper will reveal gaps in knowledge in which clinicians may examine how diet can affect inflammatory diseases like asthma.

KEYWORDS: Biomedical and Health Sciences; Nutrition and Natural Products; Asthma; Dietary Fiber; Cytokines.

Introduction

In 2019, 262,000,000 people were affected by asthma and 461,000 of these people died from the condition.[1] Asthma is a disease in which an inflammatory response causes tightening around the airways, leading to symptoms such as chest tightness, wheezing, coughing, and even death due to asphyxiation. This chronic inflammatory disease affects both adults and children.[1,2] The connection between the inflammatory response in asthma and dietary fiber has not been extensively reviewed when taking cytokine pathways and short-chain fatty acids (SCFAs) into consideration. By further examining this process, dietary fiber can be applied as a supplement to asthma treatments and benefit the many people who suffer from asthma.

Dietary fiber, a soluble or insoluble carbohydrate found in plants, has many health benefits including the maintenance of gut health.[3] Dietary fiber, when fermented in the gut, causes the production of many metabolites. Some of these metabolites are SCFAs, which signal immune cells, and most significantly regulate cytokine levels. Because an excess amount of cytokines can have harmful effects as found in many inflammatory diseases, regulating these cytokines can reduce the severity and symptoms of asthma. This study will review the existing research about dietary fiber, SCFAs, and cytokines in the context of asthma to connect dietary fiber to asthma as a potential supplement for asthma treatment.

Discussion

Asthma:

Asthma is a debilitating disease that comes in different forms, therefore, there are many existing therapies to help control asthma symptoms. For long-term asthma, control medications include inhaled corticosteroids and long-acting beta-agonists (LABAs). Inhaled corticosteroids are anti-inflammatory drugs that reduce the swelling of the airways. This therapy can stunt growth in children, as well as cause irritation in the mouth and throat of patients. LABAs, on the other hand, widen the bronchi, and this therapy can only be used as a supplement to inhaled corticosteroids. Therapies that provide fast relief include oral corticosteroids. Oral corticosteroids are used for very severe and sudden symptoms; they have side effects such as stunted growth, osteoporosis (the thinning of bone), cataracts, etc. For allergic asthma, treatments include allergy shots, which initially, are typically administered weekly.[4] There is a need for more treatment options because these therapies do not work for every patient with asthma, some have adverse effects, and some are inconvenient for patients.

The inflammatory response that defines asthma is driven by certain immune cells, the major players being eosinophils, neutrophils, and macrophages. Eosinophils are granulocytes that are signaled to the site of infection, and they are highly active in allergy and asthma. Too many eosinophils in the blood, lungs, and sputum can lead to eosinophilic asthma, in which the respiratory system and airways are blocked. High levels of eosinophils can also lead to a risk of asthma attacks,[5] which include the exacerbation of symptoms due to the tightening of the muscles around the airways.[6] Neutrophils are also granulocytes, and they are highly active in most immune responses. In asthma, neutrophils are initially recruited when the body is experiencing an allergic reaction. Neutrophils cause broncho-constriction and bronchial hyperreactivity, as well as recruit other immune cells that can aggravate the condition. Because they aggravate asthma, clinicians use neutrophils as inflammatory markers.[7] Macrophages are phagocytes, and they can directly engulf and destroy pathogens. However, they are also able to recruit neutrophils and eosinophils, in addition to other immune cells that can worsen the condition.[8]

DOI: 10.36838/v4i5.12

Other immune cells that drive the inflammatory response in asthma are mast cells and type 2 T helper cells (Th2). Mast cells are recruited by the asthmatic airway smooth muscle and induce bronchial hyper-responsiveness.[9] Th2 cells cause an inflammatory response to harmless particles leading to bronchial hyper-responsiveness.[10] However, one of the driving forces in the inflammatory response of asthma is the role of cytokines, which are chemical messengers for immune cells in asthma.

Cytokines:

Cytokines' effects on inflammation and disease progression are a common topic of discussion in the COVID-19 crisis.[11] Cytokines are peptides that initiate cellular signaling between immune cells and contribute to the immune and inflammatory response. Interleukins (IL), chemokines (CCL), interferon (IFN), and tumor necrosis factor (TNF) are all types of cytokines that function and are secreted differently. Pro-inflammatory cytokines are molecules that signal and recruit immune cells in immune response and inflammation. Though these pro-inflammatory cytokines can help the body fight infection, an excess of these cytokines can harm the body, especially in inflammatory diseases like asthma. Anti-inflammatory cytokines, however, can regulate the secretion and function of pro-inflammatory cytokines and the severity of immune response.[12] Healthy conditions depend on maintaining the proper balance between pro-inflammatory and anti-inflammatory cytokines.

Information about the specific function and role of cytokines in asthma can be found in Table 1. In the lung tissue of patients with asthma, there are increased amounts of cytokines IL-4 and IL-13,[13] and in the sputum, IL-6, IL-8, and IFN-γ are increasingly prevalent.[14] Notably, these cytokines are all proinflammatory. By promoting the growth in eosinophils, neutrophils, mast cells, and histamine, the proinflammatory cytokines trigger the inflammatory response that defines asthma.

Naturally occurring anti-inflammatory cytokines regulate these pro-inflammatory cytokines, but there are also antibody therapeutics that target pro-inflammatory cytokines. Antibody therapeutics allow for the sequestering of pro-inflammatory cytokines, which inhibits these cytokines from reaching their targets and ultimately causing inflammation.

Table 1: The Role, Source and Function of Cytokines in Asthma.

Cytokine	Role in Asthma,[15]	Source,[15]	Function
IL-4	Pro-inflammatory	T cells	Growth in B cells, eosinophils, and mast cells; increase in histamine; histamine-induced Ca2+ mobilization,[13, 15]
IL-5	Pro-inflammatory	Mast cells, Th2 cells	Increased eosinophil production,[15]
IL-6	Pro-inflammatory	Th2 cells and antigen-presenting cells	Increased production of B cells; growth in neutrophils in the sputum; correlation with IL-13 in asthmatics,[15-16]
IL-8	Pro-inflammatory	Macrophages	Attracts T cells and neutrophils,[15]
IL-13	Pro-inflammatory	Th2 cells	Growth in B cells, eosinophils, and mast cells; an increase in histamine; histamine-induced Ca2+ mobilization; increase in neutrophils in the sputum; correlation with IL-6 in people with asthma,[15-16]
IL-33	Pro-inflammatory,[17]	Epithelial cells, macrophages, and dendritic cells,[17]	Activates the Th2 immune response; promotes the growth of eosinophils, macrophages, and pro-inflammatory cytokines,[17]
TNF-α	Pro-inflammatory	Macrophages	Attracts T cells and neutrophils to the site of infection,[15]
INF-γ	Pro-inflammatory	Natural killer and Th1 cells	Activates natural killer cells, macrophages and neutrophils,[15]
CCL5	Pro-inflammatory,[18]	Cytotoxic T cells,[18]	Cytokine production; recruits monocytes, neutrophils, and eosinophils,[18]
CCL17	Pro-inflammatory,[19]	Dendritic cells,[19]	Attracts T cells,[19]
IL-10	Anti-inflammatory	Cytotoxic B and T cells and Th2 cells	Inhibits the production of pro-inflammatory cytokines; increases the production of antibodies; decreases mast cell growth,[15]
IL-35	Anti-inflammatory	Treg, Breg, cytotoxic Treg, and dendritic cells	Inhibits the differentiation of T helper cells; promotes the production of Treg cells,[15]

This table focuses on cytokine activity in asthma specifically. Often, cytokines can have different effects in other disorders that are not described here.[12]

Dupilumab, an anti-4Ra antibody, regulates the function of IL-13 and IL-4, and this has been confirmed to reduce symptoms, delay severe asthma attacks, block the effects of histamine-induced Ca^{2+} mobilization in the bronchi, and increase lung function and forced expiratory volume (FEV%).[20,21] Tralokinumab is a therapy that specifically targets IL-13, and is proven to increase FEV% and lung function.[22] Benralizumab, an antibody for IL-5, reduces the eosinophil count in the airway mucosa, the sputum, bone marrow, and blood of asthma patients.[23,24] These therapeutics help treat asthma by specifically targeting and blocking certain cytokine signaling pathways, but they do not work for every patient with asthma. For example, Tralokinumab, the therapeutic that targets IL-13, cannot be taken along with oral corticosteroids, a treatment that many severe asthma patients take.[22] In addition to being incompatible with some other treatments, there are issues with patient compliance. Tralokinumab, is a home-administered shot; 6 percent of the patients in an initial clinical trial for this therapy discontinued the treatment.[22] These antibody therapeutics also cause various moderate to severe side effects. Dupilumab, the anti-4Ra antibody, causes common symptoms of eye irritation, swelling, burning, and many rare symptoms that can be life-threatening.[21] However, a completely natural, supplementary therapy for asthma, which patients can take without fearing severe risk, is dietary fiber.

Dietary Fiber:

Dietary fiber, which is found in plant foods, has a variety of health benefits. There are two types of fiber, insoluble and soluble, which have different effects. Insoluble fiber is not broken down by water during digestion and it helps maintain regular bowel movements, while soluble fiber, which can be dissolved by water during digestion, is fermentable in the gut and can manage blood sugar, cholesterol, gut health, and more.[25] Fiber is accessible, and there are many sources of fiber including grains, fruits, and vegetables.[3] A fiber-rich diet can increase stool bulk, regulate blood pressure,[26] reduce symptoms of depression,[27] and prevent different types of cancer.[28,29] Regular dietary fiber consumption also leads to a

to a more balanced gut micro-biome which, in turn, improves the body's overall health.[3]

One of the byproducts of the fermentation of soluble dietary fiber in the gut are SCFAs, the most abundant being butyrate, acetate, and propionate. SCFAs affect immune response through signaling to immune cells. For example, dietary fiber is known to up-regulate the messenger RNA (mRNA) of G-protein coupled receptors (GPCRs), such as GPCR41 and GPCR43, which are SCFA receptors.[30] The activation of these SCFA receptors in neutrophils and macrophages by dietary fiber leads to lower inflammation.[31] Notably, SCFAs lead to a modulation of cytokines, and this process potentially reduces the severity of the inflammatory response in asthma.[32]

Dietary Fiber as a Potential Asthma Therapy:

As clinicians have found dietary fiber to benefit inflammatory conditions such as inflammatory bowel disease,[33] and depression,[27] they have started to investigate the connection between dietary fiber and asthma, another chronic inflammatory disease. In a clinical study, which explores the effects of the soluble fiber inulin on asthmatic adults, dietary inulin supplements over the span of 7 days result in a significant improvement in asthma control. This is shown by decreasing levels of airway eosinophils in the sputum in addition to increasing amounts of plasma SCFAs.[34] Within four hours of the consumption of 3.5 grams of inulin, inflammatory markers such as neutrophils, eosinophils, and macrophages significantly decrease in the sputum, while GPCR41 and GPCR43 increase in the sputum.[30] A dust mite-induced asthma model in mice had similar results in which the same inflammatory markers were significantly reduced due to soluble galacto-oligosaccharides (GOS).[35] Insoluble oligosaccharides such as acidicoligosaccharides (AOS) and fructo-oligosaccharides (FOS) mixed with bifidobacterium, a probiotic, reduce airway inflammation, eosinophils, and inflammatory cells in chronic asthma.[36] Multiple clinical studies note better lung function through increased FEV% in people with high fiber intake.[30,37] These studies utilize different types of fiber, such as inulin, GOS, AOS, and FOS, to not only examine the connection between dietary fiber and inflammatory markers, but also the connection between dietary fiber and increased lung function. Therefore, it is evident that fiber improves the condition of asthma.

Cellular signaling by cytokines initiates the inflammatory response that defines asthma. The clinical study by Zhang and Bai evaluated levels of the pro-inflammatory cytokine IL-8 in asthmatic and non-asthmatic patients and found that IL-8 is significantly higher in patients with asthma,[38] and another clinical study showed that inulin decreases the amount of IL-8 in the sputum.[30] Similarly, a mouse model showed that GOS leads to the decrease of the pro-inflammatory cytokines CCL5, CCL17, IL-33, IL-13, and IL-6 in the lung tissue of asthma patients.[35] Additionally, the same pattern occurred in another mouse model with the pro-inflammatory cytokines IFN-γ, IL-5, IL-13, and IL-4.[39] These studies show that fiber intake leads to a decrease in these pro-inflammatory cytokines that help fuel the inflammatory response of asthma. The question remains, how do inulin, GOS, and other dietary fibers lead to a decrease in pro-inflammatory cytokines?

One potential mechanism is through SCFAs, which affect cytokine production by both inhibiting proinflammatory cytokines and increasing the production of anti-inflammatory cytokines. SCFAs are a product of the fermentation of dietary fiber, and it is clinically shown that people with low-fiber diets have a higher white blood cell count and IL-6 levels.[40] Another clinical trial measured SCFA and cytokine levels in the elderly and found that increased butyrate production causes decreasing TNF-α levels.[41] Scientists must consider butyrate, which is gaining recent attention by the scientific community, because by decreasing pro-inflammatory cytokine levels it may help treat asthma.

SCFAs also increase the production of anti-inflammatory cytokines. In an *in vivo* study, 200 mM of the SCFAs acetate and propionate were added to the drinking water of mice three times a week. This method led to an increase in regulatory T cells,[39] which secrete anti-inflammatory cytokines such as IL-35 and IL-10.[43] As acetate and propionate lead to an increase in certain anti-inflammatory cytokines, they are a great therapeutic target for an inflammatory disease like asthma. Similar to previously discussed inflammatory disorders, cereal dietary fiber consumed by obese and overweight people can decrease IL-6 and TNF-α, and increase levels of IL-10, an anti-inflammatory cytokine.[43] By both decreasing pro-inflammatory cytokine levels and increasing anti-inflammatory cytokine levels, SCFAs inhibit the inflammation in asthma (Figure 1).

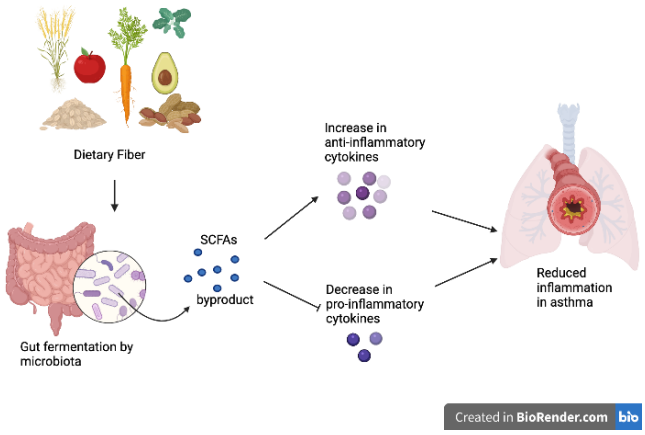

Figure 1: Dietary Fiber Reduces Inflammation in Asthma.

Based on the evidence presented, SCFAs likely decrease levels of the cytokine IL-6 as *in vivo* and clinical data agree.[35,40] However, when examining the cytokine TNF-α, the data are not as clear. An *in vitro* study by Rutting *et al.* shows a decrease in TNF-α when butyrate, propionate, and acetate are present,[44] but in clinical studies, the opposite is seen.[41] The cause of these different behaviors of SCFAs and their relationship with cytokines is evident, yet not explained, making this a gap that should be further examined.

DOI: 10.36838/v4i5.12

Conclusion

Evidence is mounting for the possibility of dietary fiber as a good lifestyle change for patients with asthma through its production of SCFAs, and the resulting regulation of cytokines that leads to anti-inflammatory effects. The *in vitro*, *in vivo*, and clinical data reviewed in this paper support the idea that dietary fiber can benefit patients with inflammatory diseases such as asthma. Recent data indicate that dietary fiber can reduce the number of inflammatory cells, such as eosinophils and neutrophils in the lung airways and sputum.[30, 34-36] Current data also indicate increased lung function (shown by increased FEV%) in cases of asthma treated with dietary fiber.[30, 37]

One mechanism of fiber's effect on inflammation may be through the production of SCFAs as a result of the fermentation of soluble fiber found in legumes, grains, fruits, and vegetables. This is supported by research findings that show increased amounts of plasma SCFAs as well as SCFA receptors in cases of asthma treated with dietary fiber.[30, 34] SCFAs specifically improve asthma in patients through cytokine regulation; studies show that SCFAs decrease pro-inflammatory cytokines and increase anti-inflammatory cytokines. Research supports that proinflammatory cytokines are more prevalent in cases of asthma, but they decrease when the asthma is treated with SCFAs as shown with IL-8.[30, 38] Inversely, anti-inflammatory cytokines are not as prevalent in cases of asthma, yet they increase when an asthma patient is treated with SCFAs, as shown with IL-35 and IL-10.[38, 42]

Current therapies are not sufficient to control asthma in all patients, so clinicians are searching for supplementary therapies. The novel cytokine-targeting antibody therapies proved successful in bettering conditions of asthma in patients, but also carried unintended negative impacts from harmful side effects.[22, 26] Because of the prevalence of these negative side effects, it is crucial to continue to search for effective, low-risk therapies. Thus, the investigation into the significance of dietary fiber and diet as possible supplementary therapies for inflammatory diseases like asthma must continue. These therapies would enhance the success of pre-existing asthma therapies, all while being both low risk and accessible for everyone.

Although basic, mechanistic research linking dietary fiber with asthma exists in animal models, clinical research is limited. Hence, more clinical research is needed to confirm the efficacy of dietary fiber. Additionally, existing clinical research does not investigate long-term implications of dietary fiber in their asthmatic participants. The effect of dietary fiber on asthma in the pediatric population should also be researched, especially considering that about 6 million children currently suffer from asthma. Lastly, many studies consider various types of dietary fiber in the context of inflammation, so the beneficial effects of specific forms of dietary fiber should be studied and compared.

Acknowledgements

Thank you to Chris Ketchum for their help editing this manuscript. Thank you Meenakshi Arunachalam for the editing support. We would also like to acknowledge Polygence Summer Program for their technical support and help connecting the authors.

References

1. Asthma. World Health Organization, 3 May 2021, https://www.who.int/news-room/fact-sheets/detail/asthma (accessed 23 June 2021).
2. Inflammation. National Institute of Environmental Health Sciences, 28 April 2021, https://www.niehs.nih.gov/health/topics/conditions/inflammation/index.cfm (accessed 23 June 2021).
3. Newman, T. Dietary fiber: Why do we need it Medical News Today, 27 April 2020, https://www.medicalnewstoday.com/articles/146935#benefits (accessed 2 August 2021).
4. Asthma medications: Know your options. Mayo Clinic (n.d.), 19 June 2020, https://www.mayoclinic.org/diseases-conditions/asthma/in-depth/asthma-medications/art-20045557 (accessed 19 August 2021).
5. Choi, Y.; Sim, S.; Park, H.-S. Distinct functions of eosinophils in severe asthma with type 2 phenotype: clinical implications. The Korean Journal of Internal Medicine 2021, 35(4), 823. https://doi.org/10.3904/KJIM.2020.022
6. Asthma attack - Symptoms and causes. Mayo Clinic. (n.d.), 2021, https://www.mayoclinic.org/diseases-conditions/asthma-attack/symptoms-causes/syc-20354268 (accessed 10 August 2021).
7. Ray, A.; Kolls, J. K. Neutrophilic Inflammation in Asthma and Association with Disease Severity. Trends in Immunology 2017, 38(12), 942. https://doi.org/10.1016/J.IT.2017.07.003
8. Van der Veen, T. A.; de Groot, L. E. S.; Melgert, B. N. The different faces of the macrophage in asthma. Current Opinion in Pulmonary Medicine 2020, 26(1), 62–68. https://doi.org/10.1097/MCP.0000000000000647
9. Bradding, P.; Walls, A. F.; Holgate, S. T. The role of the mast cell in the pathophysiology of asthma. Journal of Allergy and Clinical Immunology 2006, 117(6), 1277–1284. https://doi.org/10.1016/J.JACI.2006.02.039
10. Lloyd, C. M.; Hawrylowicz, C. M. Regulatory T Cells in Asthma. Immunity 2009, 31(3), 438. https://doi.org/10.1016/J.IMMUNI.2009.08.007
11. Ragab, D.; Eldin, S. H.; Taeimah, M.; Khattab, R.; Salem, R. The COVID-19 cytokine storm; what we know so far. Frontiers in Immunology 2020, 1446(11). https://www.ncbi.nlm.nih.gov/pmc/articles/PMC7308649/
12. Zhang, J.-M.; An, J. Cytokines, Inflammation and Pain. International Anesthesiology Clinics 2007, 45(2), 27. https://doi.org/10.1097/AIA.0B013E318034194E
13. Manson, M. L.; Säfholm, J.; James, A.; Johnsson, A.-K.; Bergman, P.; Al-Ameri, M.; Orre, A.-C.; Kärrman-Mårdh, C.; Dahlén, S.-E.; Adner, M. IL-13 and IL-4, but not IL-5 nor IL-17A, induce hyperresponsiveness in isolated human small airways. Journal of Allergy and Clinical Immunology 2020, 145(3), 808-817.e2. https://doi.org/10.1016/J.JACI.2019.10.037
14. Neveu, W. A.; Allard, J. L.; Raymond, D. M.; Bourassa, L. M.; Burns, S. M.; Bunn, J. Y.; Irvin, C. G.; Kaminsky, D. A.; Rincon, M. Elevation of IL-6 in the allergic asthmatic airway is independent of inflammation but associates with loss of central airway function. Respiratory Research 2010, 11(1), 28. https://doi.org/10.1186/1465-9921-11-28
15. Furukawa, S.; Moriyama, M.; Miyake, K.; Nakashima, H.; Tanaka, A.; Maehara, T.; Iizuka-Koga, M.; Tsuboi, H.; Hayashida, J.-N.; Ishiguro, N.; Yamauchi, M.; Sumida, T.; Nakamura, S. Interleukin-33 produced by M2 macrophages and other immune cells contributes to Th2 immune reaction of IgG4-related disease. Scientific Reports 2017, 7(1), 1–10. https://doi.org/10.1038/srep42413

16.Marques, R. E.; Guabiraba, R.; Russo, R. C.; Teixeira, M. M. Targeting CCL5 in inflammation. Expert Opinion on Therapeutic Targets 2013, 17(12), 1439. https://doi.org/10.1517/14728222.2013.837886
17.Alferink, J.; Lieberam, I.; Reindl, W.; Behrens, A.; Weiß, S.; Hüser, N.; Gerauer, K.; Ross, R.; Reske-Kunz, A. B.; Ahmad-Nejad, P.; Wagner, H.; Förster, I. Compartmentalized Production of CCL17 In Vivo: Strong Inducibility in Peripheral Dendritic Cells Contrasts Selective Absence from the Spleen. The Journal of Experimental Medicine 2003, 197(5), 585. https://doi.org/10.1084/JEM.20021859
18.Ray, A. Cytokines and their Role in Health and Disease: A Brief Overview. MOJ Immunology 2016, 4(2). https://doi.org/10.15406/MOJI.2016.04.00121
19.Dixon, A. E.; Raymond, D. M.; Suratt, B. T.; Bourassa, L. M.; & Irvin, C. G. Lower Airway Disease In Asthmatics With and Without Rhinitis. Lung 2008, 186(6), 361. https://doi.org/10.1007/S00408-008-9119-1
20.Wenzel, S.; Ford, L.; Pearlman, D.; Spector, S.; Sher, L.; Skobieranda, F.; Wang, L.; Kirkesseli, S.; Rocklin, R.; Bock, B.; Hamilton, J.; Ming, J. E.; Radin, A.; Stahl, N.; Yancopoulos, G. D.; Graham, N.; & Pirozzi, G. Dupilumab in Persistent Asthma with Elevated Eosinophil Levels. The New England Journal of Medicine 2013, 368(26), 2455–2466. https://doi.org/10.1056/NEJMOA1304048
21.Dupilumab (Subcutaneous Route) Side Effects – Mayo Clinic. Mayo Clinic 2021, https://www.mayoclinic.org/drugs-supplements/dupilumab-subcutaneous-route/side-effects/drg-20406153?p=1 (accessed 2 August 2021).
22.Busse, W. W.; Brusselle, G. G.; Korn, S.; Kuna, P.; Magnan, A.; Cohen, D.; Bowen, K.; Piechowiak, T.; Wang, M. M.; Colice, G. Tralokinumab did not demonstrate oral corticosteroid-sparing effects in severe asthma. European Respiratory Journal 2019, 53(2), 1800948. https://doi.org/10.1183/13993003.00948-2018
23.Laviolette, M.; Gossage, D. L.; Gauvreau, G.; Leigh, R.; Olivenstein, R.; Katial, R.; Busse, W. W.; Wenzel, S.; Wu, Y.; Datta, V.; Kolbeck, R.; Molfino, N. A. Effects of benralizumab on airway eosinophils in asthma with sputum eosinophilia. The Journal of Allergy and Clinical Immunology 2013, 132(5), 1086. https://doi.org/10.1016/J.JACI.2013.05.020
24.Ferguson, G. T.; Mansur, A. H.; Jacobs, J. S.; Hebert, J.; Clawson, C.; Tao, W.; Wu, Y.; Goldman, M. Assessment of an accessorized pre-filled syringe for home-administered benralizumab in severe asthma. Journal of Asthma and Allergy 2018, 11, 63. https://doi.org/10.2147/JAA.S157762
25.Aleixandre, A.; Miguel, M. Dietary fiber and blood pressure control. In Food and Function. Royal Society of Chemistry 2016, 7(4), 1864–1871. https://doi.org/10.1039/c5fo00950b
26.Swann, O. G.; Kilpatrick, M.; Breslin, M.; Oddy, W. H. Dietary fiber and its associations with depression and inflammation. Oxford University Press: Nutrition Reviews 2020, 78(5), 394–411. https://doi.org/10.1093/nutrit/nuz072
27.Chen, K.; Zhao, Q.; Li, X. Zhao, J.; Li, P.; Lin, S.; Wang, H.; Zang, J.; Xiao, Y.; Xu, W.; Chen, F.; Gao, Y. Dietary fiber intake and endometrial cancer risk: A systematic review and meta-analysis. Nutrients 2018, 10(7). https://doi.org/10.3390/nu10070945
28.Sun, L.; Zhang, Z.; Xu, J.; Xu, G.; Liu, X. Dietary fiber intake reduces risk for Barrett's esophagus and esophageal cancer. Critical Reviews in Food Science and Nutrition 2017, 57(13), 2749–2757. https://doi.org/10.1080/10408398.2015.1067596
29.Huizen, J. Soluble and insoluble fiber: Differences and benefits. Medical News Today, 31 August 2017, https://www.medicalnewstoday.com/articles/319176 (accessed August 2, 2021).
30.Halnes, I.; Baines, K.; Berthon, B.; MacDonald-Wicks, L.; Gibson, P.; Wood, L. Soluble Fibre Meal Challenge Reduces Airway Inflammation and Expression of GPR43 and GPR41 in Asthma. Nutrients 2017, 9(1). https://doi.org/10.3390/nu9010057
31.Sun, M.; Wu, W.; Liu, Z.; Cong, Y. Microbiota metabolite short chain fatty acids, GPCR, and inflammatory bowel diseases. Journal of Gastroenterology 2016, 52:1, 52(1), 1–8. https://doi.org/10.1007/S00535-016-1242-9
32.Lewis, G.; Wang, B.; Shafiei Jahani, P.; Hurrell, B. P.; Banie, H.; Aleman Muench, G. R.; Maazi, H.; Helou, D. G.; Howard, E.; Galle-Treger, L.; Lo, R., Santosh, S.; Baltus, A.; Bongers, G.; San-Mateo, L.; Gilliland, F. D.; Rehan, V. K.; Soroosh, P.; Akbari, O. Dietary Fiber-Induced Microbial Short Chain Fatty Acids Suppress ILC2-Dependent Airway Inflammation. Frontiers in Immunology 2019, 10(2051). https://doi.org/10.3389/FIMMU.2019.02051
33.Wong, C.; Harris, P. J.; Ferguson, L. R. Potential benefits of dietary fibre intervention in inflammatory bowel disease. In International Journal of Molecular Sciences 2016, 17(6) MDPI AG. https://doi.org/10.3390/ijms17060919
34.McLoughlin, R.; Berthon, B. S.; Rogers, G. B.; Baines, K. J.; Leong, L. E. X.; Gibson, P. G.; Williams, E. J.; Wood, L. G. Soluble fibre supplementation with and without a probiotic in adults with asthma: A 7-day randomised, double blind, three way cross-over trial. EBioMedicine 2019, 46. https://doi.org/10.1016/j.ebiom.2019.07.048
35.Verheijden, K. A.; Willemsen, L. E.; Braber, S.; Leusink-Muis, T.; Delsing, D. J.; Garssen, J.; Kraneveld, A. D.; Folkerts, G. Dietary galacto-oligosaccharides prevent airway eosinophilia and hyperresponsiveness in a murine house dust mite-induced asthma model. Respiratory Research 2015, 16(1). https://doi.org/10.1186/s12931-015-0171-0
36.Sagar, S.; Vos, A. P.; Morgan, M. E.; Garssen, J.; Georgiou, N. A.; Boon, L.; Kraneveld, A. D.; Folkerts, G. The combination of Bifidobacterium breve with non-digestible oligosaccharides suppresses airway inflammation in a murine model for chronic asthma. Biochimica et Biophysica Acta (BBA) - Molecular Basis of Disease 2014, 1842(4). https://doi.org/10.1016/j.bbadis.2014.01.005
37.Berthon, B. S.; Macdonald-Wicks, L. K.; Gibson, P. G.; Wood, L. G. Investigation of the association between dietary intake, disease severity and airway inflammation in asthma. Respirology 2013, 18(3), 447–454. https://doi.org/10.1111/RESP.12015
38.Zhang, J.; Bai, C. Elevated Serum Interleukin-8 Level as a Preferable Biomarker for Identifying Uncontrolled Asthma and Glucocorticosteroid Responsiveness. Tanaffos 2017, 4, 260–269.
39.Thorburn, A. N.; McKenzie, C. I.; Shen, S.; Stanley, D.; Macia, L.; Mason, L. J.; Roberts, L. K.; Wong, C. H. Y.; Shim, R.; Robert, R.; Chevalier, N.; Tan, J. K.; Mariño, E.; Moore, R. J.; Wong, L.; McConville, M. J.; Tull, D. L.; Wood, L. G.; Murphy, V. E.; Mackay, C. R. Evidence that asthma is a developmental origin disease influenced by maternal diet and bacterial metabolites. Nature Communications 2015, 6(1). https://doi.org/10.1038/ncomms8320
40.Menni, C.; Louca, P.; Berry, S. E.; Vijay, A.; Astbury, S.; Leeming, E. R.; Gibson, R.; Asnicar, F.; Piccinno, G.; Wolf, J.; Davies, R.; Mangino, M.; Segata, N.; Spector, T. D.; Valdes, A. M. High intake of vegetables is linked to lower white blood cell profile and the effect is mediated by the gut microbiome. BMC Medicine 2021, 19(1). https://doi.org/10.1186/s12916-021-01913-w
41.Macfarlane, S.; Cleary, S.; Bahrami, B.; Reynolds, N.; Macfarlane, G. T. Synbiotic consumption changes the metabolism and composition of the gut microbiota in older people and modifies inflammatory processes: a randomised, double-blind, place

DOI: 10.36838/v4i5.12

bo-controlled crossover study. Alimentary Pharmacology & Thera peutics 2013, 38(7). https://doi.org/10.1111/apt.12453
42. Zhao, S.; Wang, C. Regulatory T cells and asthma. Journal of Zhejiang University. Science. B 2018, 19(9), 663. https://doi.org/10.1631/JZUS.B1700346
43. Vitaglione, P.; Mennella, I.; Ferracane, R.; Rivellese, A. A.; Giacco, R.; Ercolini, D.; Gibbons, S. M.; La Storia, A.; Gilbert, J. A.; Jon nalagadda, S.; Thielecke, F.; Gallo, M. A.; Scalfi, L.; Fogliano, V. Whole-grain wheat consumption reduces inflammation in a randomized controlled trial on overweight and obese subjects with unhealthy dietary and lifestyle behaviors: role of polyphe nols bound to cereal dietary fiber. The American Journal of Clinical Nutrition 2015, 101(2). https://doi.org/10.3945/ajcn.114.088120
44. Rutting, S.; Xenaki, D.; Malouf, M.; Horvat, J. C.; Wood, L. G.; Hansbro, P. M.; Oliver, B. G. Short-chain fatty acids increase TN Fα-induced inflammation in primary human lung mesenchymal cells through the activation of p38 MAPK. American Journal of Physiology-Lung Cellular and Molecular Physiology 2019, 316(1). https://doi.org/10.1152/ajplung.00306.2018

Authors

Samyuktha Natesan is currently a junior at Dougherty Valley High School. Samyuktha is incredibly passionate about research and the biomedical sciences. Samyuktha is also very musically inclined, as she both performs and teaches vocal Indian classical music professionally.

IJHSR
ijhighschoolresearch.org
RESEARCH ARTICLE

An Analysis of Global Indicators Impacting Gender Parity Index in Secondary Education

Arina Oberoi
Pinewood Upper Campus, 26800 Fremont Rd, Los Altos Hills, CA, 94022, USA; arina@cubixon.com

ABSTRACT: Gender equality is a highly discussed topic, especially in regard to education. A standing issue is that there is gender parity in secondary education only in a small minority of nations. With the objective of understanding why gender parity fluctuates and how it can be made equitable, this research analyzes 400-plus social, economic, and political variables from nations across the world using modern data-mining techniques. Using basket-case analysis, Pearson's correlation coefficient, and regression models, the top indicators that affect gender parity are identified. This research found that internet users as a percentage of a population, government-effectiveness index, rule-of-law index, mobile users as a percentage of a population, political violence risk, demographic pressures, displaced persons as a percentage of a population, fragile-state index, and student-to-teacher ratio affect the gender parity index of secondary schools the most. Then the models for each indicator were scored with data from years not included in the model to validate the accuracy of the models. While most nations did support the model predictions, Bangladesh, Rwanda, and Honduras were the few that defied forecasts. Then the factors that allow these nations to achieve gender-parity ratios rivaling first-world economies were investigated. Finally, with insight gained from our regression models and bright-spot analysis, certain policies that improve gender parity were recommended.

KEYWORDS: Education, Gender Parity, Secondary Education, Kashmir.

Introduction

This work began in August of 2019 when the revocation of Article 370 led to high-intensity conflict in the region of Kashmir.[1] This conflict resulted in 1.5 million children being kept out of school and the entire region's population being placed under a strict lockdown.[2] This project partnered with a US-based education non-profit, Kashmir Education Initiative (KEI),[3] and worked under the direct mentorship of Dr. Riyaz Bashir, the president and founder of KEI and a medical professor at Temple University, along with his field staff in the Kashmir Valley. As the work on this topic of investigating gender parity progressed, the work expanded to include other regions affected by political strife. Now some of the policies derived from this are being implemented and related research with a cohort of students is currently being studied with the assistance of KEI in the Kashmir Valley.

The history of the Kashmir Valley provides insight into the diverse population the region sees today. Until 1346, the Kashmir region was ruled by a series of Hindu dynasties. In 1346, the region fell into Muslim control, which lasted until 1819 when the Sikh Kingdom took power. In 1846, the Kashmir Valley was once again switched to the rule of the Dogra kingdom.

As a result of this inconsistent rule, the people of Kashmir are a very heterogeneous population. Religiously, most Kashmiri people practice Islam, Hinduism, or Buddhism. They also speak a variety of languages, including Hindi, Punjabi, Dogri, Balti, and Ladakhi.

The Kashmir region has been a point of contention between India and Pakistan since their 1947 partition. At this time, Hari Singh, the Maharaja of Kashmir, was given the choice to join either India or Pakistan. Hari Singh chose to join India, quickly prompting a violent reaction from Pakistan. The conflict between the neighboring countries eventually reached a point of such intensity that the United Nations was forced to intervene and define a cease-fire line through the region in 1949, which still exists today. This partition divides Kashmir so that Pakistan holds the Kashmir regions of Azad Kashmir, Gilgit, and Baltistan, while the regions of Jammu and Kashmir, and Ladakh lay with India.

In 1962, China even got involved and took part of Ladakh under its control, resulting in tensions erupting in the region once again. In 1971, a cease-fire agreement was signed. The peace didn't last long as, in 1971, Pakistan and India quickly fell into war once again.[4]

Due to the continuous tensions and conflict between the nations of Pakistan and India over Kashmir, the military presence has remained strong in the region of Kashmir.

The region of Jammu and Kashmir of India has remained an autonomous state, as established by Article 370. This protects the region's right to formulate laws and follow a separate constitution. However, in August of 2019, the BJP Government of India revoked Article 370, removing Jammu and Kashmir's self-autonomous status in an attempt to integrate and unify Kashmir with the rest of India. Knowing the effect this revocation would have on the people of Kashmir, the government was quick to send thousands of troops into the region, while simultaneously placing the region under lockdown and house arrest, all to combat the erupting opposition to the revocation.[5] The abrogation of Article 370 launched the region of Jammu and Kashmir into high-intensity conflict, as it added to the already existing tensions of the region.

DOI: 10.36838/v4i5.13

Gender parity in education has long been an integral part of the reach for all-around gender equity. As a result, many have sought to understand how to improve and perfect gender parity in education. Understandably, the causes of low gender parity vary from region to region. A case study in Iran, for example, conducted by Golnar Mehran, concluded that the nation's low gender parity was primarily the effect of the social climate. Thus, to improve gender parity, most of the work would involve promoting the idea of female education to conservative families and making the idea of sending girls to school less daunting, by establishing girls-only dormitories and faculty.[6]

Another case study took place in Chile and yields many different conclusions. A paper by Beatrice Avalos hypothesized that women are generally demotivated to study alongside their male counterparts, knowing that they will not receive equal employment opportunities. Avalos also noted that most women in Chile who are not attending secondary school are from lower-income households. Thus, to promote gender parity, work would need to be done to address these financial issues, such as the creation of scholarship programs.[7]

Another report by Ershad Ali examined the effect of policy on gender parity in Bangladesh. He emphasized the Field Support Services Project (FSSP), a government initiative aimed at encouraging female students to attend school. This initiative worked to provide incentives for both the students and their parents, through loans and guaranteed employment. Though Ali noted the success of this initiative, he also highlighted how the initiative failed to lower the dropout rate of female students, which was already higher than their male counterparts.[8]

As highlighted by these previously conducted case studies, the reasons behind a lower gender parity and the manner in which a nation addresses it varies. This paper seeks to gain a better understanding of, generally, which indicators affect gender parity the most and how lower gender parity can best be addressed.

Methods

To ensure the data was as accurate and applicable to the modern world as possible, all of the data collected was narrowed down the time period 2016 to 2019.

To achieve the goal of this study, the following two goals were focused on for data analysis:

1: Identify the top factors that affect gender parity

2: Identify the rate at which each indicator affects gender parity

All data regarding the gender parity indexes of various nations in secondary education was collected from The World Bank.[9] Then each nation's average gender parity index from 2016 to 2019 was calculated by adding each individual year's value and then dividing the sum by 4. The timeframe of 2016 to 2019 was chosen to ensure that the findings were recent and applicable to the current global state. The data regarding social, economic, and political global indicators were collected from The Global Economy.[11-20] This data was also narrowed down to 2016 to 2019 to match the time frame of the average gender parity, resulting in a total of 404 variables available for use.

Pearson's correlation coefficient was used to calculate which indicators affect gender parity in secondary education the most. Pearson's correlation coefficient,[5] also referred to as Pearson's r, tracks the correlation between two variables and ranges between -1 to 1. The negative value implies inverse correlation, and the higher absolute coefficient value implies a stronger relationship.

Each correlation was plotted with the x-axis as an indicator and the y-axis as the average gender parity. Then, the univariate polynomial regression models were fit to each indicator, using the final model to extrapolate the fluctuation of gender parity according to each indicator. The fluctuation in rates of change in secondary education gender parity according to each indicator was then calculated and modeled in equations.

Results and Discussion

Analyzing Indicators Affecting Gender Parity Ratio:

With the data analysis for this study, the following list of the top global indicators that affect gender parity in secondary education were discovered (Table 1).

Table 1: List of top ten variables and their associated correlation strength (positive and negative) to Gender Parity Index (GPI) for Secondary Education.

Factor	Pearson's Correlation Coefficient
Political Stability	0.3682
Internet users as a percentage of a population	0.2952
Government effectiveness index	0.2910
Rule of law index	0.2872
Mobile users as a percentage of a population	0.2570
Political violence risk	-0.2990
Demographic pressures	-0.3021
Displaced persons as a % of a population	-0.3095
Fragile state index	-0.3152
Student to teacher ratio	-0.3597

Political Stability:

Political Stability Index (PSI)[11] tracks the traditions and institutions by which the country exercises its authority. Computing this involves looking at the country's processes by which it selects its governments, creates and implements policies, and respects the citizens and the institutions. The World Bank ranks countries' PSI index on a scale of -2.5 to 2.5.

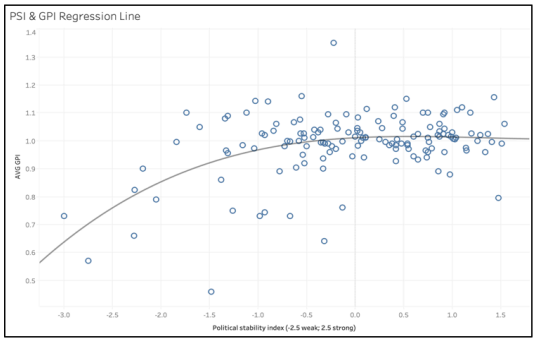

Figure 1: Regression model for GP according to Political Stability. GP and Political Stability have a strong positive correlation.

Gender disparity favoring males appears to be more prominent in politically unstable nations. The more politically unstable a nation appears to be, the higher the disparity is likely to be. Of note is that the country does not need to be a beacon of model governance to achieve good GPI numbers; countries scoring a neutral score of 0 starts achieving equitable GPI (Figure 1).

$y = 0.00506388x^3 + -0.0202883x^2 + 0.0179989x + 1.01063$
R-Squared: 0.231237

Internet Users:

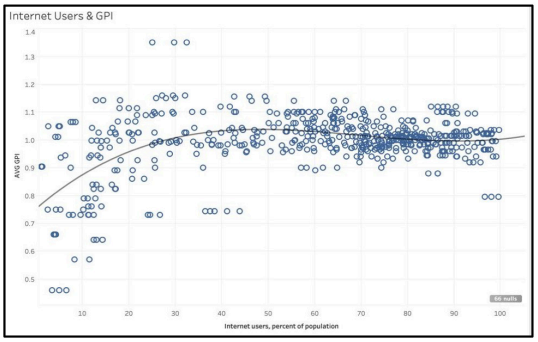

Figure 2: Regression model for GP according to Internet Users, as a percent of population. GP and Internet Users have a moderately strong positive correlation.

This variable tracks the portion of the adult population that has Internet access.[12] When about 50% or more of a population has internet access, gender parity appears to remain consistent at about 1.0 (perfect) (Figure 2).

$y = 1.089e(-0.6x^3) + -0.000227334x^2 + 0.0143416x + 0.75266$
R-Squared: 0.2434

Government Effectiveness:

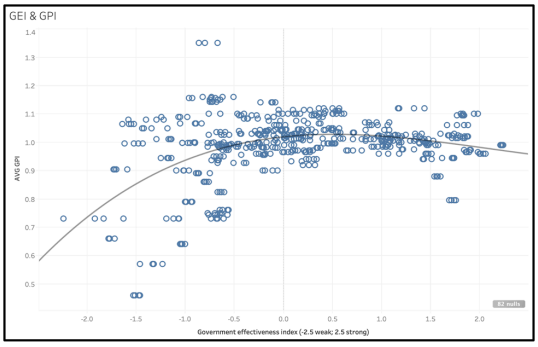

Figure 3: Regression model for GP according to Government Effectiveness Index. GP and Government Effectiveness have a moderately strong positive correlation.

The Government Effectiveness Index (GEI)[13] measures the quality of public services. It is measured on a scale from -2.0 (weak) to 2.0 (strong). Like what is seen with the PSI, countries are likely to see an equitable gender parity ratio when they reach a certain threshold (GEI > -0.5). It is less likely that improving the GEI beyond this threshold (0.5) may meaningfully contribute to an increase in gender parity (Figure 3).

$y = 0.00637171x^3 + -0.0401454x^2 + 0.0363262x + 1.01895$
R-Squared: 0.187606

Rule of Law:

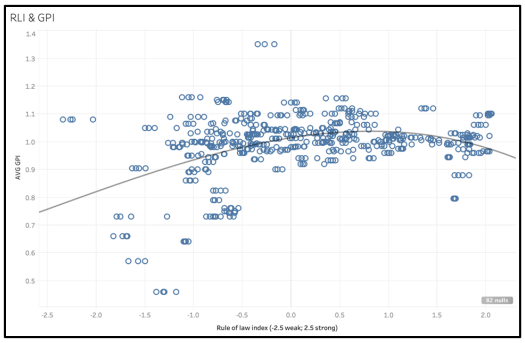

Figure 4: Regression model for GP according to Rule of Law Index. GP and Rule of Law Index have a moderately strong positive correlation.

The Rule of Law Index (RLI)[14] measures across factors such as constraints on government power, absence of corruption, open government, and other factors to assess how a particular county applies the law. The World Bank's RLI ranges from -2.0 to 2.0. Like with previous factors, a significant gender disparity is seen when the country performs poorly on this index. However, once the countries achieve a minimum threshold of rule of law (about 0.0), this particular governance factor does not appear to have a strong positive or negative correlation with GPI (Figure 4).

$y = 6.61748e(-0.8x^3) + -3.94178e(-05x^2) + 0.00692386x + 0.638892$
R-Squared: 0.181936

Mobile Phone Subscribers:

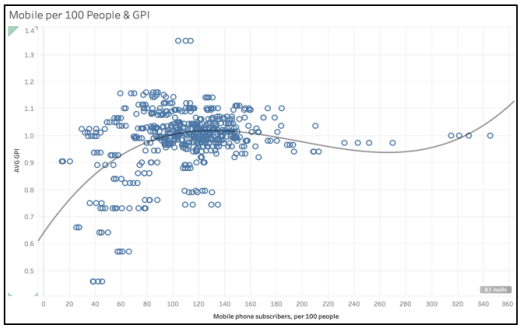

Figure 5: Regression model for GP according to Mobile Phone Subscribers, per 100 people. GP and Mobile Phone Subscribers have a moderately strong positive correlation.

It appears that the more mobile phone subscribers per 100 people,[15] the more likely a nation is to see perfect gender parity. When access to mobile phone subscriptions decreases to be below 80%, GP appears to quickly decrease by about 0.4% per subscriber drop per 100 people (Figure 5).

$y = -0.00379218x^3 + -0.028694x^2 + 0.0547951x + 1.01386$
R-Squared: 0.158001

DOI: 10.36838/v4i5.13

Political Violence Risk:

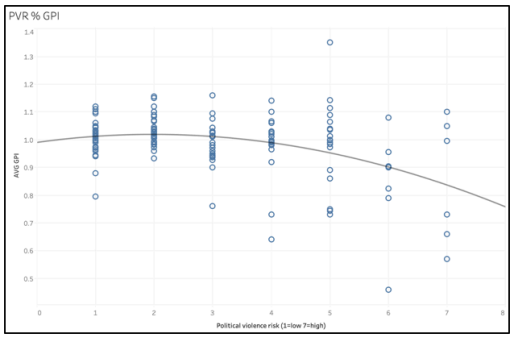

Figure 6: Regression model for GP according to Political Violence Risk. GP and Political Violence Risk have a moderately strong negative correlation.

This indicator measures the likelihood of political instability or politically motivated violence, including terrorism.[16] The World Bank records nations' risk on a scale between 1 (low) to 7 (high). It appears that higher political violence risks are linked to lower gender parity values (Figure 6).

$y = 2.74883e(-0.5x^3) + -0.00752393x^2 + 0.0294145x + 0.990229$
R-Squared: 0.14642

Demographic Pressures:

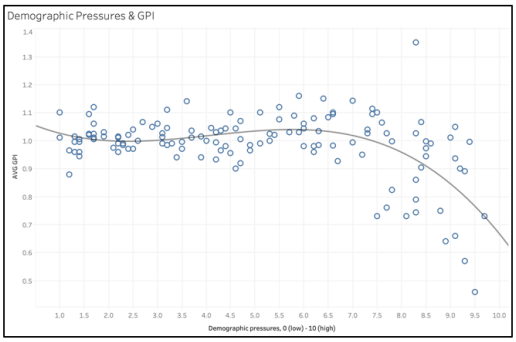

Figure 7: Regression model for GP according to Demographic Pressures. GP and Demographic Pressures have a strong negative correlation.

Demographic pressures,[17] ranging between 1 and 10, is an indicator that measures population pressures related to the food supply, access to safe water, and other life-sustaining resources, or health, such as the prevalence of disease and epidemics. When a nation's demographic pressures are low, less than 4.0, gender parity appears to be linear and close-to-perfect. When demographic pressures become moderate, (between 4.0 and 7.0) gender parity experiences a slight increase in favor of females. Demographic pressures past 7.0 are linked to lower, decreasing gender parity values (Figure 7).

$y = -0.00223279x^3 + 0.0273782x^2 + -0.0930919x + 1.09422$
R-Squared: 0.309687

Fragile State:

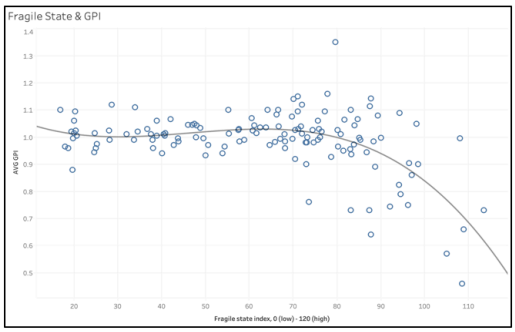

Figure 8: Regression model for GP according to Fragile State Index. GP and Fragile State Index have a strong negative correlation.

The Fragile State Index measures the vulnerability of a state to conflict or collapse.[18] It ranges from 0 to over 120 by summing 12 indicators. When a nation's fragile state index is below 80, it appears that the gender parity is fairly consistent and 1.0 (perfect). At x = 40, however, there appears to be a very slight increase in gender parity. When the fragile state index reaches 80 (moderately high), there is a rapid fall in gender parity at the rate of about 0.012 (Figure 8).

$y = -0.00134662x^3 + 0.015734x^2 + -0.058351x + 1.07948$
R-Squared: 0.233586

Refugee and Displaced Persons:

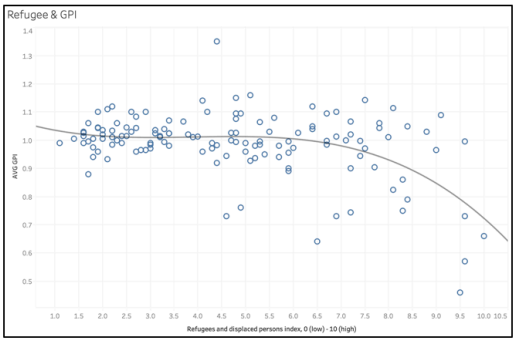

Figure 9: Regression model for GP according to Refugee and Displaced Persons Index. GP and Refugee and Displaced Persons Index have a strong negative correlation.

Gender parity seems particularly sensitive to the Refugee and Displaced Person index (RDP).[19] As the RDP index crosses a threshold (6.5) there is a sharp decrease in gender parity at the rate of about 0.08. While the refugee and displaced persons index is below about 6.5, however, the gender parity appears to be linear and consistent at 1.0 (perfect) (Figure 9).

$y = -1.62533e(-0.6x^3) + 0.000227457x^2 + -0.00930039x + 1.11923$
R-Squared: 0.348468

Student to Teacher Ratio:

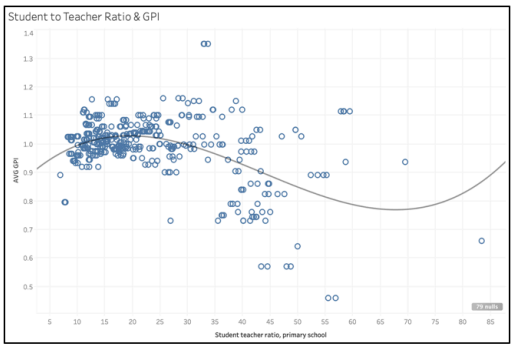

Figure 10: Regression model for GP according to Student to Teacher Ratio. GP and Student to Teacher Ratio have a strong negative correlation.

It was discovered that 25 is the magic number for the student-to-teacher ratio. When the student-to-teacher ratio is between 10 and 25, it appears that the gender parity of the various countries stays consistent close-to or directly at 1.0 (perfect).[20] Once the student-teacher ratio hits 25, however, the gender parity appears to quickly decrease in favor of males (Figure 10).

$y = 4.59474e(-0.6x^3) + -0.000601764x^2 + 0.0182235x + 0.867519$
R-Squared: 0.223758

While the regression models offer insightful statistical analysis on gender parity, it is also useful to speculate the plausible reasons behind each indicator contributing to the Gender Parity Index.

Political Stability, Violence Risk, and Fragile State:

Political stability is defined as the perceptions of the likelihood that the government will be destabilized or overthrown by unconstitutional or violent means, including politically motivated violence and terrorism. The more politically stable the nation, the more likely its gender parity will be closer to 1.00. When a nation is politically weak, the government is often unable to provide for and support its citizens. This may lead to financial instability and overall uncertainty in citizens' lives. As a result, families may resort to pulling their children out of schools, as they may be unable to pay the fees or desperate for another source of income through their children.

There may be many reasons female students are more likely to be pulled out of school compared to their male counterparts, such as prominent cultural beliefs that undermine the importance of female education. In most cultures, women are often designated to tend to household duties and children, while men are left to work, earn, and support the family. With this traditional family structure in mind, many believe that a woman's education is not as important as a man's, as she will likely not have to work. While this belief may even prevent families, in some places, from enrolling their daughters in school, it can also be speculated that it is why families are more reluctant to pull their sons out of school compared to their daughters.

When a nation's government is politically vulnerable, the nation itself becomes especially vulnerable to rebel groups and terrorism. With a weak government and increased conflict amongst citizens, it's likely that the nation's streets will become unsafe. In some nations, rebel groups have taken over schools. As a result, families may feel it is safer to keep their children home from school. Some families may be more protective of their daughters, as they are often more likely to be targets of sexual violence and harassment; thus, when a nation is becoming gradually unsafe, families may be likely to pull their daughters out before their sons.

Internet Access:

The larger the percentage of a population that has internet access is, the more likely it is that the nation will have a gender parity closer to 1.00. With internet access, students are more likely to have open access to resources, such as online educational material, messaging apps, and contact with teachers outside of school. Thus, having access to the internet would likely make it much easier for students to stay engaged with their education as well as support themselves should it be needed.

Internet access is also considered an indicator of a first-world nation. So, this correlation may also simply be a situation of correlation, not causation. It must be considered that internet access does not directly contribute to a gender parity closer to 1.00. Rather, it is plausible that the nation's wealth and resources, which allow it to provide internet access, are rather what results in the nation's perfect gender parity (Table 2; Figure 11)

Government Effectiveness:

Government effectiveness is defined as an index that captures perceptions of the quality of public services, the quality of the civil service and the degree of its independence from political pressures, the quality of policy formulation and implementation, and the credibility of the government's commitment to such policies. As shown in the case studies of Rwanda and Bangladesh, government policies and projects often provide a great deal of support to initiatives and yield significant results. Inversely, families worried about instability and poverty may be less likely to prioritize education. This may be especially true for females, as a daughter is more likely to pulled out of school to aid the family in domestic chores and duties (Table 3; Figure 12).

When government effectiveness is high, a government is effectively engaging with its citizens. As a result, issues amongst citizens are more likely to be addressed and overall satisfaction is likely to be higher. This would likely result in safer environments, as unstable governments and political climates often result in the opposite: rebel groups, terrorist activity, etc.

Rule of Law:

Rule of law index captures perceptions of the extent to which agents have confidence in and abide by the rules of society, and in particular the quality of contract enforcement, property rights, the police, and the courts, as well as the likelihood of crime and violence. When the rule of law is higher, gender parity is more likely to be closer to 1.00. Some cultures and families may be more protective of their daughters, as women are often more likely to be targets of sexual violence and harassment. When a nation is overall safer, families may feel more comfortable sending their children out to school, especially their daughters. Similarly, when a nation is unsafe, families are likely to pull their children out, their daughters, once again, before their sons.

DOI: 10.36838/v4i5.13

Mobile Phones:

The larger the number of mobile phones per 100 people is, the more likely the nation is to have an equitable gender parity index. With mobile phones, students are more likely to have more access to resources, such as online educational material, messaging apps, and contact with teachers outside of school. An example of this would be the situation in Kashmir. When the lockdown was implemented, students with access to mobile phones and devices were more likely to be able to continue their education remotely. Similarly, with Covid-19, students with access to devices were able to continue engaging with their education despite the circumstances. This index can be especially helpful in conflict zones or times of crisis. As illustrated by the events in Kashmir and Covid-19, having access to mobile phones, otherwise simply a device, allows students to continue their education despite the circumstances of the nation.

Refugee Index:

When a nation's refugee and displaced person index (ranges from 0 to 10) is higher, it is likely that the nation's gender parity will decrease substantially. Nations with a higher refugee or displaced person population are also likely to be the nations where the conflict itself is occurring. This explains why nations with a refugee index less than 7.0 on the index have a close-to-perfect GPI, as they may be bordering nations offering asylum to refugees. However, nations above that number are more likely to be the nations harboring the conflict and producing the refugees. In a nation where circumstances are so poor that the country becomes inhabitable, therefore producing refugees, it is likely that education is an afterthought for many. As a result, it is incredibly likely that students will be pulled out of school.

Student-Teacher Ratio:

When a student-to-teacher ratio is smaller, it is more likely that gender parity will be closer to one. When the student-teacher ratio becomes larger, it is likely that gender parity will substantially decrease. A smaller student-to-teacher ratio may be an indicator of more access to resources. For example, underfunded schools cannot afford to hire multiple teachers. Therefore, these schools may allocate more students per teacher. Likewise, wealthier schools are more likely to allocate smaller numbers of students per teacher. Therefore, this ratio may be an indicator of a nation's wealth and prosperity. It may not be the student-to-teacher ratio alone that produces gender parity, but rather the national environment which creates this ratio that produces gender parity.

Validating the Forecasting Accuracy of the Models:

To verify that these models predict gender parity to an acceptable degree of accuracy, two regression models were chosen at random: Internet Users and Government Effectiveness Index. For each model, a nation was chosen at random and plotted on the model, using data from 2010, a year not included when making the models. While this method does not illustrate the full scope of the models' accuracy or inaccuracy, it offers strong evidence that the regression models are accurate.[12,13]

Table 2: Table of values used to predict and compare gender parity in the Internet Users regression model.

Country	Internet Users	Actual GPI	Predicted GPI
Angola, 2010	2.80	0.679	0.80
Albania, 2010	45.00	1.005	1.0367
Germany, 2010	82.00	0.948	1.000

Table 3: Table of values used to predict and compare gender parity in the Government Effectiveness regression model.

Country	Government Effectiveness Index	Actual GPI	Predicted GPI
Serbia, 2010	- 0.05	1.02	1.150
Denmark, 2010	2.10	1.009	0.97

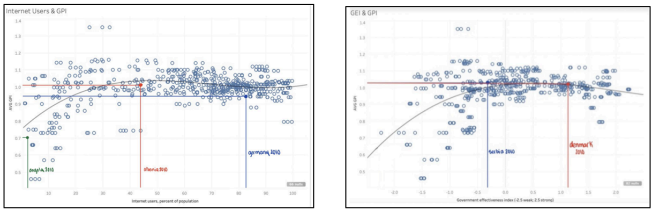

Figure 11 and 12: Statistical comparison of the models to data not included in the given datasets.

Developing a Remediation Path with Bright Spot Analysis:

Another perspective that offers insight into the usefulness of these models is a bright-spot analysis. A bright spot is a positive-deviant measurement. In this case, it was a nation with a perfect or close to perfect gender parity index despite the circumstances that would forecast a lower GPI. These bright spots directly contradicted this model's predictions. The goal of the bright-spot analysis was to identify and understand how certain nations were able to uphold a close-to-perfect or perfect gender parity despite circumstances that normally result otherwise. To make the findings of this analysis as applicable as possible, this analysis focused on finding larger-scale reasons or initiatives that contribute to these nations' exceptional gender parities.

The positive-deviant countries were tracked across the ten indicators and organized by their frequency of deviation from the forecasts (while filtering out extremely small nation-states) (Table 4).

Table 4: List of countries identified as positive deviants with models.

Nation	Frequency
Honduras	6
Bangladesh	3
Nepal	3
Rwanda	3

Honduras is an outlier in six indicators: internet users, government effectiveness index, rule of law index, mobile user, fragile state index, and student-teacher ratio. Even with only about 32% of its population using the internet, a -0.75 on the GEI, a -1.00 on the RLI, 79 per 100 being mobile users, a 77.8 on the FSI, and 27.5 students per teacher, the nation maintains a GPI of 1.16.

Table 5: Table displaying the homicide rate per 100,000 for females and males, as well as gender parity index, secondary, for Honduras, Antigua and Barbuda, El Salvador, and Venezuela.

Country	Homicide Rate per 100,000 (Female)	Homicide Rate per 100,000 (Male)	Gender Parity Index, Secondary
Honduras (2018)	7.8	70.1	1.15
Antigua and Barbuda (2008)	11.2	27.0	0.99
El Salvador (2017)	13.8	115.9	1.15
Venezuela (2018)	10.7	61.9	1.08

Like Honduras, it was found that these nations show a stark difference between the male and female homicide rates. Interestingly, the gender parity for these nations, like Honduras, were all above 1.00. This indicates that the influence of gang violence discourages males from attending school, making the gender parity for these nations extremely high. For this reason, despite extremely poor circumstances which would normally result in a low GPI, these nations with prominent gang activity are able to maintain a high GPI.

Rwanda is an outlier in three indicators: mobile users, fragile state index, and student-teacher ratio. Even with only about 76 per 100 being mobile users, an 87.5 (high) on the Fragile State Index, and 58.5 students per teacher, the nation maintains a GPI of 1.11.

After the Rwandan genocide in 1994, the Rwandan government realized that it must allow its women into the workplace should the nation hope to rebuild itself. Rwanda launched an Education For All Plan of Action (MINEDUC) in 2003,[25] which thoroughly addressed the constraints that discouraged female attendance in schools as well as developed respective plans to address these issues.

A notable objective from the Education For All Plan of Action is Objective 5: Eliminate gender disparities in primary and secondary education by 2005, and achieve gender equality in education by 2015, with a focus on ensuring girls full and equal access to and achievement in basic education of good quality.[25] The plan lists the "Constraints to the elimination of gender disparities in education" as well as their respective, proposed solutions and strategies, some of which include: increasing capacity of schools to take more girls, enhancing policy development on alternative education opportunities for girls, and promoting quality and gender-sensitive learning to reduce dropout and repetition rates for female students.

Rwanda's government intervention narrowed the gender gap in secondary education. Rwanda also rewrote its Constitution in 2003, introducing Article 20, which guaranteed the right to education for all citizens, and Article 80, which allocated 30% of the Senate for women.[26] With strong government initiative and focus to improve the nation's gender parity, Rwanda was able to uplift its female citizens in both the workplace and in schools and, to this day, maintains an exceptional gender parity index given the nation's resources.

Bangladesh is an outlier in three indicators: internet users, government effectiveness index, and fragile state index. Even with only about 15% of its population using the internet, a -0.72 on the GEI, and an 87.7 on the FSI, the nation maintains a GPI of 1.14.

Bangladesh is a predominantly patriarchal society, making its exceptional gender parity index noteworthy. Since 1990, Bangladesh's secondary gender parity index has doubled, going from 0.508 to 1.14. The nation's immense progress despite cultural settings can be attributed to the number of government interventions aimed at promoting girls' education.

In 1994, the Bangladesh Government implemented the Female Stipend Program, [24] an initiative that provided female students with a stipend and tuition fee waiver. This program effectively was modeled and executed similarly to Rwanda's Education For All Plan of Action and, like Rwanda, helped narrow and eventually eliminate the gender gap in secondary education.

In 1983, the Bangladesh government created the Grameen Bank, a financial initiative aiming to alleviate poverty through social and credit intermediation.[27] The initiative especially helped women in Bangladesh who, due to the nation's socio-cultural climate, were often at more risk of poverty than their male counterparts. As a result, the Grameen Bank resulted in an increase in the financial empowerment of the female Bangladeshi population. From 1985 to 1992, the female borrowers of the bank increased by 1,205%, while the male borrowers increased by 67%. In 1992, women received about 80% of the bank's loans. Over the same time period, the number of center-operated schools increased by about 386% and enrollment increased by 583%.[27]

This indicated that encouraging female financial independence may directly result in higher enrollment in schools, and thus a higher gender parity. Though female financial freedom was not an indicator represented in the models above, the Grameen Bank initiative provides convincing evidence that by encouraging gender parity in financial independence, a nation can improve its gender parity in education as well.

Application to Kashmir:

The intention with this paper was to understand the variables that affect gender parity. As the regression models and the bright-spot analysis indicate, government effectiveness and intervention may be one of the more influential variables in gender parity. Therefore, a method can be introduced in which strong government effectiveness can be modeled on a smaller scale, e.g., with non-profits. In nations where the overall state of the nation is not ideal, non-profits have a profound impact, as they often take over the duties the government cannot fulfill.

The region of Kashmir has been a conflict region for dozens of years. Due to this conflict, the region has suffered immensely. If plots were created for Kashmir on the models from Section 3, it is highly probable that the models would predict the region to have a low gender parity index.

To address these challenges, The Kashmir Education Initiative has implemented initiatives along the "Three-Axis of Intervention":

1. Mentoring & Counseling: As illustrated by Figure 11, nations with lower student-to-teacher ratios tend to have better gender parity values. Thus, it can be hypothesized that focusing

DOI: 10.36838/v4i5.13

on decreasing student-to-teacher ratios may improve gender parity. As directly addressing student-to-teacher ratios may be difficult, considering hiring and paying for new teachers, mentorship may be a great alternative. The implementation of mentoring may boost gender parity, as mentors can often take the role of teachers and offer students one-on-one support that might be lacking in larger classroom settings.

2. Financial & Material Assistance: As shown in Figure 3 and 6, access to resources play a significant role in gender parity. Nations, where larger populations have access to mobile phones and the internet, tend to be linked with higher gender parity values. Thus, one way to improve gender parity may be to provide resources to students. In KEI, students not only receive scholarships but also devices with educational software made by Gooru.[28] Gooru's educational software uses artificial intelligence to create a custom learning path for each student based on their proficient and developing skills. By providing students with devices as well as personalized learning plans, this initiative may improve gender parity by providing students with resources they would've otherwise been denied: internet access and mobile devices. The customized learning plan Gooru provides even works to address the student-to-teacher ratio as it provides customized attention without the need of a teacher. The scholarships that KEI provides to students also works to follow the path shown by "positive deviant" countries such as Bangladesh where grass-root level economic support is seen to have an impact on education. These methods of assistance that KEI provides may, as supported by the above research, work to improve their gender parity.

3. Experiential Opportunities: By providing workshops building competency and expertise, and offering full-time and internship opportunities internationally, the Kashmir Education Initiative works to remove the isolation students feel as a result of the lockdown.

The Kashmir Education Initiative's work in Kashmir has been extremely successful at not only providing quality education to students who would otherwise suffer due to the conflict but also improving gender parity. KEI was founded in 2007, and its first batch of students from 2008 - 2013 had a gender parity of 0.67. In 2015, KEI's efforts had successfully boosted their gender parity up to 0.83. [3] It is important to note KEI's method of selecting students. KEI is open to any students who qualify financially and academically. Students who qualify financially are encouraged to take an exam in which top scorers are chosen to join KEI, regardless of gender. Being so, the gender parity ratio is most often determined by the number of male versus female applicants who apply. In years with more male applicants, a larger portion of top-scorers are male, thus resulting in lower gender parity.

KEI's work in Kashmir goes to show that one does not have to wait for sweeping government legislation to improve gender parity. While it does help improve parity on a larger scale, significant change can be made through smaller groups and individuals, as KEI and its efforts have so well demonstrated. While the region of Kashmir's gender parity, as of 2016, was 0.95,[29] the Kashmir Education Initiative was 1.52. [3]

Conclusion

In this paper, indicators that positively or negatively affect the gender parity ratio for nations and communities were identified. Models were developed and validated based on accuracy by testing them on untrained data. Countries that are positive deviants were examined and what they are doing differently to break away was also examined despite scarce resources, poverty, and risk of political violence. All of these have provided insights, for which there is no need to wait for federal or state legislation to improve the conditions of gender equality and education in the world.

Grameen Bank illustrates how a small community development bank changed the course of gender equity and financial independence in a country of 160 million. Rwanda's Education for All Plan of Action showed how a government can successfully work to create and implement initiatives to improve a nation's gender parity and equity. The Kashmir Education Initiative shows how there is no need to wait for legislation to make a significant change in the lives of students. Each person can act -- by volunteering to mentor a student from an underprivileged school, statistically improving the gender-parity ratio. By providing devices with internet connectivity and/or learning curriculums to kids in remote, high-conflict areas of the world, the quality of education can be leveled and, once again gender parity, can be statistically improved. There is no need to discuss legislation with the congresspeople of a nation, though it may help. Each person has the ability to affect the indicators that improve the gender parity index. It may sound cliche, but, as this paper shows, we can be the difference we want to see.

Acknowledgements

I would like to extend my sincere thanks to Dr. Riyaz Bashir, professor at Temple University, for his continuous support and guidance. His insightful suggestions and unparalleled knowledge served as an invaluable contribution to creating this paper.

I must also thank Supreet Singh for his constructive suggestions and unwavering guidance throughout.

I also gratefully acknowledge the assistance of Sana Ghazi, whose extensive knowledge and guidance made this paper possible.

References

1. *India's Constitution of 1949 with Amendments through 2015*. Constitute Project. (n.d.). https://www.constituteproject.org/constitution/India_2015.pdf?lang=en.
2. *Yasir, S., & Gettleman, J. (2019, October 31). Anxious and Cooped Up, 1.5 Million Kashmiri Children Are Still Out of School*. The New York Times. https://www.nytimes.com/2019/10/31/world/asia/kashmir-school-children.html.
3. Kashmir Education Initiative. (n.d.). https://www.kashmirei.org/.
4. *The Editors of Encyclopaedia Britannica. (n.d.). The Kashmir Problem*. Encyclopædia Britannica. Retrieved September 24, 2021, from https://www.britannica.com/place/Kashmir-region-Indian-subcontinent/The-Kashmir-problem.
5. BBC. (2019, August 5). *Article 370: What happened with Kashmir and why it matters*. BBC News. Retrieved September 24, 2021, from https://www.bbc.com/news/world-asia-india-49234708.
6. Mehran, G. (2003). Gender and Education in Iran . *United Nations Educational, Scientific and Cultural Organization*. Retrieved September 25, 2021, from file:///Users/arinaoberoi/Desk

top/10.1.1.550.6578.pdf.
7. Avalos, B. (2003). Gender Parity and Equality in Chile: A Case Study . *United Educational, Scientific and Cultural Organization*. Retrieved September 25, 2021, from file:///Users/arinaoberoi/Desktop/Gender_parity_and_equality_in_Chile_a_case_study.pdf.
8. Ali, E. (2010). Does Scholarship Scheme Contribute to Gender Parity in Female Education?: The Case of Secondary Education in Bangladesh . *Cross-Cultural Communication*, 6(3), 1–9. Retrieved September 25, 2021, from file:///Users/arinaoberoi/Desktop/976-1016-1-PB.pdf.
9. The World Bank. (n.d.). Indicators. https://data.worldbank.org/indicator?tab=all.
10. Correlation Coefficient: Simple Definition, *Formula, Easy Steps*. Statistics How To. (2021, July 1). https://www.statisticshowto.com/probability-and-statistics/correlation-coefficient-formula/
11. *Political stability by country, around the world*. TheGlobalEconomy.com. (2019). https://www.theglobaleconomy.com/rankings/wb_political_stability/.
12. *Internet users by country, around the world*. TheGlobalEconomy.com. (2019). https://www.theglobaleconomy.com/rankings/internet_users/.
13. *Government effectiveness by country, around the world*. The GlobalEconomy.com. (2019). https://www.theglobaleconomy.com/rankings/wb_government_effectiveness/
14. *Rule of law by country, around the world*. TheGlobalEconomy.com. (2019). https://www.theglobaleconomy.com/rankings/wb_ruleoflaw/.
15. *Mobile phone subscribers by country, around the world.* The GlobalEconomy.com. (2019). https://www.theglobaleconomy.com/rankings/mobile_phone_subscribers/.
16. *Political violence risk by country, around the world*. TheGlobalEconomy.com. (2019). https://www.theglobaleconomy.com/rankings/political_violence_risk/.
17. *Demographic pressures index by country, around the world*. The GlobalEconomy.com. (2019). https://www.theglobaleconomy.com/rankings/demographic_pressures_index/.
18. *Fragile state index by country, around the world*. TheGlobalEconomy.com. (2019). https://www.theglobaleconomy.com/rankings/fragile_state_index/.
19. *Refugees and displaced persons index by country, around the world*. TheGlobalEconomy.com. (2019). https://www.theglobaleconomy.com/rankings/refugees_displaced_persons_index/.
20. *Student teacher ratio, primary school by country, around the world*. TheGlobalEconomy.com. (2019). https://www.theglobaleconomy.com/rankings/student_teacher_ratio_primary_school/.
21. *Intentional homicides (per 100,000 people)*. Data. (2018). https://data.worldbank.org/indicator/VC.IHR.PSRC.P5.
22. *Intentional homicides, female (per 100,000 female)*. Data. (2018). https://data.worldbank.org/indicator/VC.IHR.PSRC.FE.P5.
23. *Intentional homicides, male (per 100,000 male*). Data. (2018). https://data.worldbank.org/indicator/VC.IHR.PSRC.MA.P5.
24. Xu, S., Shonchoy, A., & Fujii, T. (2019). Illusion of Gender Parity in Education: Intrahousehold Resource Allocation in Bangladesh. *SSRN Electronic Journal*. https://doi.org/10.2139/ssrn.3386159
25. Ministry of Education, Science, Technology and Scientific Research. (2003). *Education For All Plan of Action*.
26. *Rwanda's Constitution of 2003 with Amendments through 2015*. Constitute Project. (n.d.). https://www.constituteproject.org/constitution/Rwanda_2015.pdf?lang=en.
27. Khandker, S., Khalily, B., & Khan, Z. (1994). *Grameen Bank Sustainable*? - World Bank. Human Resources Development and Operations Policy. https://documents.worldbank.org/curated/en/658601468768006874/pdf/multi-page.pdf.
28. *Navigator is a GPS for Learning. Gooru*. (n.d.). https://gooru.org/about/.
29. Government of India. (n.d.). *Education Statistics at a Glance*. https://www.education.gov.in/sites/upload_files/mhrd/files/statistics-new/ESAG-2018.pdf.

Author

Arina Oberoi is a 12th-grade student at Pinewood Upper Campus. She is interested in pursuing a career involving data analysis and law.

DOI: 10.36838/v4i5.13

IJHSR
ijhighschoolresearch.org
■ RESEARCH ARTICLE

Miniature Submarine using Near-Infrared Spectroscopy to Detect and Collect Microplastics

Brandon Pae, Darson Chen
Horace Mann School, 231 W 246th St, Bronx, NY, 10471, USA; brandon.pae@gmail.com

ABSTRACT: A promising solution to detecting and collecting ocean microplastics is utilizing near-infrared (NIR) spectroscopy. NIR spectroscopy is a cost-effective, safe, and accurate method to determine the chemical composition of unknown materials. However, since it cannot easily function underwater as light cannot penetrate the ocean surface, a submarine drone design developed here will employ near-infrared spectroscopy to differentiate the collected micro-objects. In particular, an experiment was conducted where varying sizes of kombu (edible kelp) and microplastics were scanned by a NIR spectrometer to determine the mass composition of a given sample. A least sum of squares method was used to analyze the spectra data from an unknown concentration of microplastics by comparing the spectra data to stored spectra datasets which were produced from samples of known concentrations. The results showed that least squares analysis was a generally effective method to compare such spectra graphs and deduce the mass composition of a given sample. Although, more improvements including the analysis of the spectra graph's curvature and an increased amount of composition data, are necessary to make the approach more accurate.
KEYWORDS: Materials Science; Computation and Theory; NIR Spectroscopy; R Programming; Least squares Analysis.

■ Introduction

Ocean plastic pollution, which consists of harmful macro and microplastics, is a dire issue that the scientific community must solve. Marine organisms easily mistake microplastics, which are under 5 mm, for food and become polluted, threatening other creatures, like humans, that consume them.[1] Additionally, since microplastics are broken off from macroplastics, they pollute the ocean the same way macroplastics do; stains on microplastics still react in the water to form toxic chemicals. These chemicals can spread anywhere in the ocean as microplastics exist in all ocean depths.[2]

Unfortunately, current solutions to ocean plastic pollution mainly target macroplastics on the ocean surface, which does not address the prevalent microplastic problem. These solutions include the Ocean Cleanup's Interceptor that collects large pieces of plastic and the ESA satellites that detect macroplastics on the ocean surface.[3] There are also reactions and chemicals that have been developed to clean plastics, including ferromagnetic materials, but they cannot be effectively utilized in the ocean environment due to its vast area.

Additionally, there are currently various chemometric techniques that are used to analyze sample compositions with spectroscopy. In particular, a widely used method is the Beer-Lambert Law, which relates the amount of absorption to material concentration.[4] However, one major limitation of this method is that it does not utilize reflectance measurements, which many spectrometers use. The Beer-Lambert Law also requires an optical density coefficient. This coefficient is dependent on the materials in the given sample and must be known in order to execute the chemometric analysis.[4] As a result, if the materials in the given sample are unknown, then their optical density coefficients are also unknown, and the analysis cannot be executed.

One promising solution to detecting and collecting ocean microplastics is NIR reflectance spectroscopy.[5] It is cost-effective, safe, and accurate in determining the chemical composition of unknown materials.[6] However, while the aforementioned ESA satellites utilize NIR light to detect macroplastics, they cannot detect microplastics on the ocean surface because they are too far from the ocean. Furthermore, these satellites cannot detect the widespread ocean microplastics beneath the ocean surface because NIR light cannot penetrate water.

Besides NIR reflectance spectroscopy, Raman spectroscopy can be used for a similar experiment. Raman spectroscopy is a non-destructive technique that gives a chemical analysis of an object. The molecular interaction and chemical structure of a molecule can be identified, making Raman spectroscopy a viable alternative for determining microplastics due to their unique chemical makeup. Moreover, the spectroscopy technique is fundamentally researched and experimented with. However, Raman spectra present units primarily in 1/cm instead of on the micro or nanoscale, making the graph analysis more challenging. Additionally, due to microplastics at times being mixed with toxic chemicals as well as other substances, it is not clear how these possible extra substances may affect or alter the Raman signal and data due to the impurity of the microplastic.

Even with NIR reflectance spectroscopy, an analysis of the intensity peaks of the respective spectra graphs could determine whether a substance contained plastic or not. The peak intensity of a spectra is created by the unique molecule composition of a substance, and a plastic may consistently give a peak intensity that can be read through a machine learning system. Nonetheless, this option was not chosen due to the machine learning algorithm required to analyze the peak in

DOI: 10.36838/v4i5.14

tensities. The algorithm would require extra time to code that the chosen method did not need.

This experiment endeavors to capture the microplastics using NIR reflectance spectroscopy. NIR spectroscopy is employed inside a submarine drone, which is an isolated system without water where NIR light can function. Even if there is no air in the submarine, NIR light would still be able to travel through the vacuum.

The NIR spectroscopy within a submarine drone is highly significant as it opens the possibility of detecting and identifying ocean microplastics autonomously, efficiently, and harmlessly. Due to the detection, the submarine drone can intake the microplastics, leading to a reduced amount of plastic pollution. In addition, the application of the least squares algorithm to compare resulting spectra graphs is a novel and less computationally intensive method to determine the mass composition of a given plastic and algae sample. This method first stores the spectra of samples with known concentrations and then compares the stored graph with new spectra graphs from new test concentrations to find the closest matches. The near-infrared reflectance spectroscopy within a submarine drone could efficiently differentiate the collected microplastics from small pieces of kombu using a least squares analysis method.

Methods

The following materials were used in the experiment: sheets of Polyethylene Terephthalate (PET) and Low-Density Polyethylene (LDPE), kombu (edible algae), a Texas Instruments NIR spectrometer, NIR protective glasses, disposable gloves, protective goggles, a precision scale, a ruler, a stand, a computer with NanoScan installed, scissors, and paper plates. To set up the experiment, the NIR spectrometer was attached to a ruler via tape, so the spectrometer's scan window faced downwards (as pictured in Figure 1; all images are shown on pages 3-5). A ruler was attached to a stand which was then adjusted so the spectrometer's scan window was 1.5 mm away from the floor (as pictured in Figure 1). A spectrometer was connected to a computer in order to send the reflectance data to the NanoScan application. Before preparing the microplastics, the disposable gloves and protective eyewear were worn. The microplastics were made by cutting over 100 pieces of PET, LDPE, and kombu with lengths under 5 mm (as pictured in Figure 3). Afterward, a circular paper plate was cut to have a small rectangle with dimensions 7.5 mm by 3 mm drawn in the center. Next, the data tables (on page 7) were made to record given mass values.

Starting data collection, a piece of kombu that exactly covered the previously drawn rectangle was cut. It was weighed on the precision scale (as pictured in Figure 2) and its mass was recorded. The kombu piece was then placed on the drawn rectangle and slid under the spectrometer so that the kombu was directly under the scan window (as pictured in Figure 4). Before the NIR spectrometer was activated, NIR-protective goggles were worn. The spectrometer was activated, and light shone on the sample (as pictured in Figure 5). Once the reflectance data was sent to the computer and stored in a .csv file, the process with the kombu (cutting, weighing, and scanning it) was repeated with pieces of PET and LDPE that similarly covered the drawn rectangle.

Afterwards, a piece of PET was cut that covered half of the drawn rectangle, and another piece of LDPE was cut that covered the rectangle's remaining half. Their masses were weighed and recorded, and the NIR scanning process was repeated. Then, pieces of PET, LDPE, and kombu were cut such that they each covered about ⅓ of the drawn rectangle (as pictured in Figure 6). The weighing and scanning process was then repeated with this sample. Finally, a piece of PET that covered ¼ of the rectangle and a piece of kombu that covered ¾ of the rectangle were cut and the rest of the data collection process was repeated.

Afterward, a very similar process was repeated to collect the values shown in the second data table. However, instead of uniform macro pieces (as pictured in Figure 6), the small bits of plastic and kombu (< 5 mm) were used instead (as pictured in Figure 7). In addition, in these trials the materials were not separated but instead mixed together (as pictured in Figure 8). However, the approximate ratios of each material in each trial (e.g., LDPE covering ⅓ of the drawn rectangle) were maintained. After this data collection was finished, the disposable gloves, microplastics, and kombu were disposed of within the garbage.

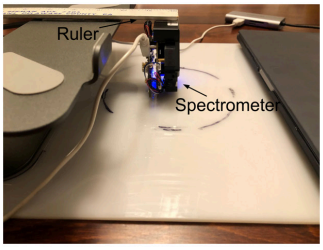

Figure 1: Making the setup.

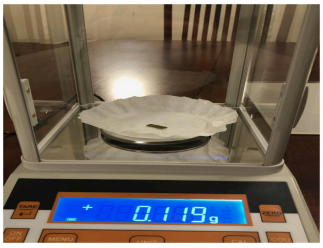

Figure 2: Weighing the kombu.

Figure 3: Cutting the PET, LDPE, and kombu.

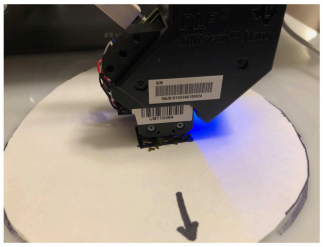

Figure 4: Sample under the spectrometer.

Figure 5: Activating the NIR spectrometer.

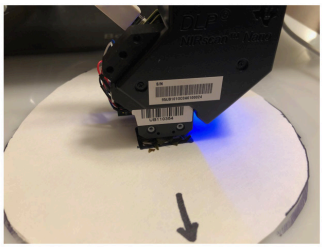

Figure 6: Making a sample that is ⅓ PET, ⅓ LDPE, and ⅓ kombu.

DOI: 10.36838/v4i5.14

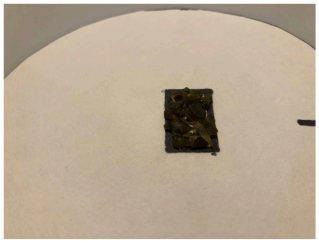

Figure 7: Making a sample with small pieces of kombu.

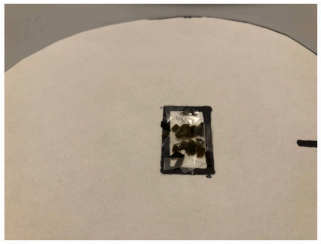

Figure 8: Making sample of small mixed pieces of plastic and kombu.

Engineering Design:

This is a computer aided model of a hypothetical submarine drone to collect microplastics. The drone design consists of an outer hull, an inner hull, and a pressure hull in between the two that holds the water and air. The water and air determine the depth the drone will go in the ocean.

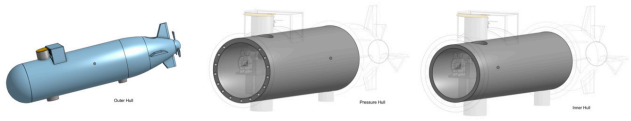

The machinations inside include a pipe that moves the micro-objects outside onto a filter paper where the water passes through, leaving the micro-objects on the filter paper. A motor pushes the micro-objects through while a servo on top of the drone closes the pipe to block water from entering and touching the machines.

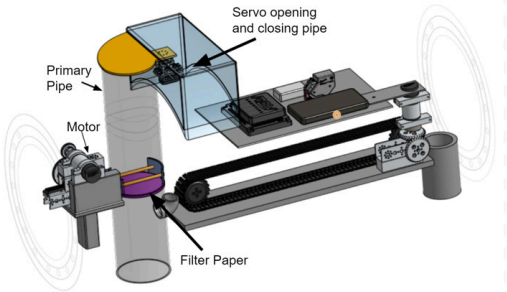

Micro-objects are pushed onto the conveyor belt that moves them under the spectrometer to be scanned. The scan determines whether they are microplastics or not. If the sample is not more than 10% microplastics, the conveyor belt reverses and drops everything down a pipe that is connected back to the first pipe where the water is flowing out. If there are sufficient microplastics, they will be dropped into the microplastic container.

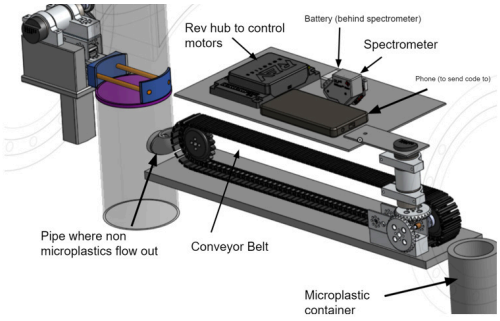

Data Analysis:

The R programming language was used in RStudio. The spectrometer returned information on the percentage of each wavelength, from 900 to 1700 nm, that is reflected from the sample. Therefore, after preparing samples of the kombu and microplastics with known mass concentrations of microplastics and obtaining the spectra data, the information was organized into a data table with the wavelength as the independent variable and the reflectance value as the dependent variable. After conducting multiple trials, spectra graphs were generated that represented various compositions (e.g., 50% plastics, 50% kombu).

Afterward, multiple samples were created with different concentrations of microplastics. After recording the reflectance values from these six new test samples and producing spectra graphs accordingly, it was determined which previous spectra graph (from the initial six trials) best represented the new test graph in question. To quantify the best fit, a least sum of squares approach was utilized, such that the difference between the two spectra graphs (the test graph and an initial spectra graph) for each wavelength was squared and summed together. After completing the analysis between the given test graph and each of the initial six graphs, the initial spectra graph that produced the smallest sum of squares value (which means that it has the highest similarity to the given test graph) was chosen. Since this initial spectra graph was produced from a known concentration of PET, LDPE, and kombu, the associated concentrations were also used to indicate the concentrations of the test graph in question.

The full code developed for this experiment can be found in a GitHub Repository:

https://github.com/paeb/ISEF-Code.

Data Tables:

In Table 1, the mass of PET, LDPE, and Kombu in each sample were recorded to calculate the sample's unique mass composition. The compositions were used to identify the respective NIR spectra graphs.

Table 1: First set of trials (stored cases).

PET Mass (g)	LDPE Mass (g)	Kombu Mass (g)	Total Mass (g)	PET Percent Mass (%)	LDPE Percent Mass (%)	Kombu Percent Mass (%)
0	0	0.393	0.393	0	0	100
0.073	0	0	0.073	100	0	0
0	0.033	0	0.033	0	100	0
0.038	0.013	0	0.051	75	25	0
0.024	0.008	0.118	0.15	16	5	79
0.021	0	0.116	0.137	15	0	85

In Table 2 the trials contained the samples which were cut up and mixed. Then the mass of the PET, LDPE, and Kombu in each sample were recorded to calculate the sample's unique mass composition for the respective NIR spectra graph.

Table 2: Second set of trials (test cases).

PET Mass (g)	LDPE Mass (g)	Kombu Mass (g)	Total Mass (g)	PET Percent Mass (%)	LDPE Percent Mass (%)	Kombu Percent Mass (%)
0	0	0.258	0.258	0	0	100
0.077	0	0	0.077	100	0	0
0	0.017	0	0.017	0	100	0
0.044	0.012	0	0.056	79	21	0

0.044	0.012	0	0.056	79	21	0
0.033	0.008	0.077	0.118	28	7	65
0.018	0	0.167	0.185	10	0	90

Results and Discussion

In analyzing the results, certain compositions were accurately compared from the least squares algorithm, while others were not. In particular, the spectra graphs from the test samples (from the second set of trials) in Figure 8 (0% PET, 0% LDPE, and 100% kombu), Figure 9 (0% PET, 100% LDPE, and 0% kombu), and Figure 10 (10% PET, 0% LDPE, and 90% kombu) fit very closely with the spectra graphs from the first stored trials that have the most similar mass percentages. There was not an exact match in composition for Figure 10 because there was no composition from the first set of trials that had 10% PET and 90% kombu; however, the closest composition from the first set of trials (0% PET and 100% kombu) was accurately matched as the closest spectra graph.

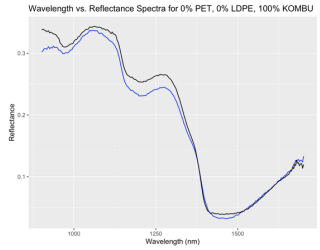

Figure 8: 0% PET, 0% LDPE, 100% KOMBU best fits the spectra graph of: 0% PET, 0% LDPE, 100% KOMBU; peak intensity in the 1150 nm range. The NIR spectrometer can accurately detect 100% KOMBU substances.

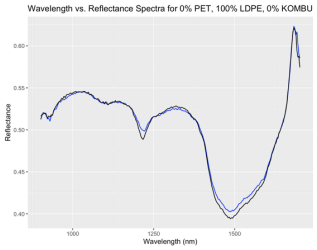

Figure 9: 0% PET, 100% LDPE, 0% KOMBU best fits the spectra graph of: 0% PET, 100% LDPE, 0% KOMBU; peak intensity in the 1700 nm range. The NIR spectrometer can accurately detect 100% LDPE substances.

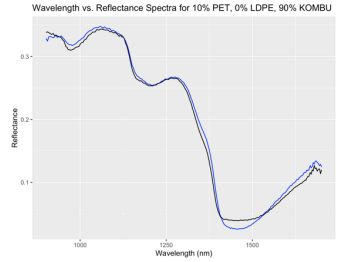

Figure 10: 10% PET, 0% LDPE, 90% KOMBU best fits the spectra graph of: 0% PET, 0% LDPE, 100% KOMBU; peak intensity in the 1150 nm range. The spectrometer correctly determined the mixture was mostly KOMBU.

Blue: new test data (second set of trials)

Black: previously stored data (first set of trials)

However, for Figures 11, 12, and 13, there were some discrepancies in the matched graphs. For Figure 11, the test composition was 28% PET, 7% LDPE, 65% kombu, but was matched with the composition 0% PET, 0% LDPE, 100% kombu. While there is no exact composition from the first set of trials that matches this test composition from Figure 11, it was expected that the initial composition of 16% PET, 5% LDPE, 79% kombu would produce the closest spectra graph. Even so, it was within the range of expected possibilities because the kombu in the test graph occupied 65% (a vast majority) of the mass in the sample and the associated composition had a kombu percentage of 100%. However, in Figures 12 and 13, there were more unexpected errors. In Figure 12, the test composition of 79% PET, 21% LDPE, 0% kombu was paired with 0% PET, 100% LDPE, and 0% kombu, and in Figure 13, the test composition of 100% PET, 0% LDPE, 0% KOMBU was matched with 0% PET, 100% LDPE, 0% kombu. In each of these instances, the entire sample was filled with one material, but that single material was incorrectly identified with the least squares algorithm.

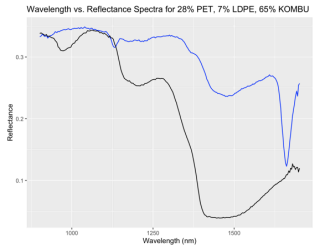

Figure 11: 28% PET, 7% LDPE, 65% KOMBU best fits the spectra graph of: 0% PET, 0% LDPE, 100% KOMBU; peak intensity in the 1150 nm range. The spectrometer inaccurately determined the contents of the 28% PET, 7% LDPE, 65% KOMBU substance.

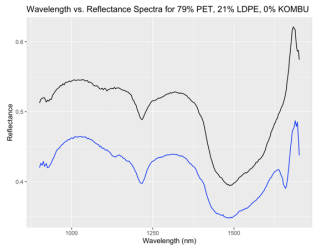

Figure 12: 79% PET, 21% LDPE, 0% KOMBU best fits the spectra graph of: 0% PET, 100% LDPE, 0% KOMBU; peak intensity in the 1700 nm range. The spectrometer inaccurately determined the contents of the 79% PET, 21% LDPE substance.

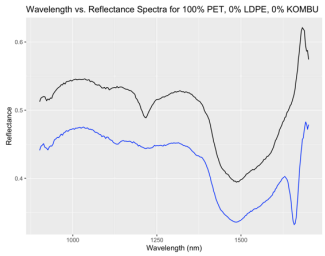

Figure 13: 100% PET, 0% LDPE, 0% KOMBU best fits the spectra graph of: 0% PET, 100% LDPE, 0% KOMBU; peak intensity in the 1700 nm range. The spectrometer inaccurately determined the contents of the 100% PET substance.

There are two main reasons for these false identifications. The first and largest error is that there were not enough trials conducted. Since each composition was tested once in each set of trials, there were probably inaccuracies in the reflectance percentages received for certain wavelengths. Therefore, in the future, many more trials will be conducted for each mass composition and the average spectra values will be taken in order to minimize any false identifications due to errors. Furthermore, more spectra for diverse sample compositions will be obtained. The second reason for the error is because of the least squares method in the algorithm. In particular, Figure 14 shows the spectra graph of 100% PET, 0% LDPE, 0% kombu, with the shredded small pieces, from the second set of trials compared with the spectra graph of 100% PET, 0% LDPE, 0% kombu, with the full uncut pieces, from the first set of trials (this difference in material size in the first versus second dataset is also a small reason for these discrepancies). Even these two graphs were not matched by the least squares

DOI: 10.36838/v4i5.14

algorithm because the overall distance between the two graphs was not the smallest, yet the graphs appear more identical in terms of their shape (relative minima and maxima, rates of change). Similarly, in Figure 15, while the two graphs that had the most similar mass composition were not matched together, their overall shapes are more similar than the associated match in Figure 13. One reason behind this is because in the samples from the second set of trials, the samples were composed of various small pieces; as such, there were gaps between them and not as much light of each wavelength was reflected back in comparison to their counterparts from the first set of trials. Therefore, one crucial addition to the algorithm will be to compare the relative extrema and rates of change in various sections of the two graphs, using derivatives, in addition to comparing the distance between them.

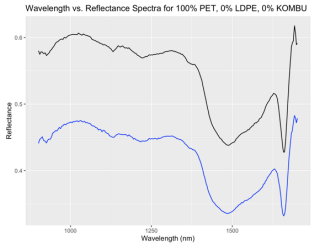

Figure 14: 100% PET, 0% LDPE, 0% KOMBU compared to the spectra graph of: 100% PET, 0% LDPE, 0% KOMBU; peak intensity in the 1700 nm range. The spectrometer accurately detected but misaligned the graph for 100% PET, 0% LDPE, 0% KOMBU.

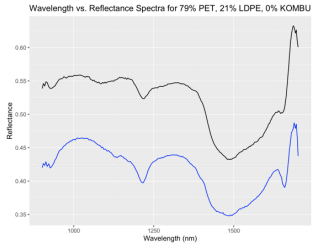

Figure 15: 79% PET, 21% LDPE, 0% KOMBU compared to the spectra graph of: 75% PET, 25% LDPE, 0% KOMBU; peak intensity in the 1700 nm range. The spectrometer accurately detected but misaligned the graph for 79% PET, 21% LDPE, 0% KOMBU.

In future experimentation, these errors will be limited to confirm that NIR spectroscopy is a valid method of detecting microplastics compared to existing methods, namely those that use the Beer-Lambert Law.

Future Research:

The following topics should be further researched and developed: the process through which factory systems physically sort plastic after detection, a system to separate kombu into smaller bits so kombu cannot clog up the conveyor belt, and more cost-effective materials to build a submarine. One key addition that will be incorporated into the algorithm is machine learning, especially once more trials of the experiment are conducted and the number of compositions for which data is collected is increased. In this case, machine learning will be key to sort through the large amounts of data and identify trends that can be used to compare different compositions' spectra. With machine learning, identifying the corresponding graphs will be faster, causing the drone to detect microplastics with elevated accuracy.

Additionally, sonar detection can be implemented to detect microplastics in waters that are not rich in microplastics.[7] If added, the drones can help clean all the waters at various depths compared to the current drones that are deployed in ocean garbage patches to clean up the rich microplastic density there. Sonar detection does not have an impact on human activity, so long as high frequency transducers are used so humans and marine species cannot hear the sound.[8] The sonar transducer would be a part of the outer hull, where it would fire at a fixed angle to cover the most water.[9] A sonar-proof casing will protect the transducer from the ocean whilst letting sonar frequencies enter and leave. A coding program will be implemented where if the sonar transducer obtains a signal from an object, the boat will be positioned so the current pushes the micro-objects into the PVC pipe and it will use the existing methods to determine whether the micro-objects were microplastics or not.

■ Conclusion

The results showed that least squares analysis was an overall effective method to compare such spectra graphs and deduce the mass composition of a given sample. However, there were errors in the experiment regarding half of the test cases, as the samples in Figures 11, 12, and 13 were not correctly identified. More improvements including the analysis of the spectra graph's curvature and an increased amount of data are necessary to make the algorithm more accurate.

■ Acknowledgements

We thank the following individuals for their support and time: Mr. George Epstein; Dr. Christine Leo. We offer our sincere appreciation for their exceptional guidance throughout our project.

■ References

1. Moore, C. J.; Moore, S. L.; Leecaster, M. K.; Weisberg, S. B. https://ftp.sccwrp.org/pub/download/DOCUMENTS/AnnualReports/1999AnnualReport/10_ar11.pdf (accessed Oct 11, 2021).
2. Long, M.; Moriceau, B.; Gallinari, M.; Lambert, C.; Huvet, A.; Raffray, J.; Soudant, P. Interactions between microplastics and phytoplankton aggregates: Impact on their respective fates. https://www.sciencedirect.com/science/article/abs/pii/S0304420315000766 (accessed Oct 11, 2021).
3. Allen, L. How satellites and machine learning are being used to detect plastic in the Ocean. https://www.forbes.com/ sites/alenelizabeth/2020/04/27/how-satellites-and-machine-learning-are-being-used-to-detect-plastic-in-the-ocean/?sh=240a9fb64fd1 (accessed Oct 11, 2021).
4. Nicolas Coca, P. D. Classical least squares method for quantitative spectral analysis with python. https://towardsdatascience.com/classical-least squares-method-for-quantitative-spectral-analysis-with-python-1926473a802c (accessed Oct 11, 2021).
5. Corradini, F.; Bartholomeus, H.; Lwanga, E. H.; Gertsen, H.; Geissen, V. Predicting soil microplastic concentration using vis-nir spectroscopy. https://www.sciencedirect.com/science/article/pii/S0048969718335435 (accessed Oct 11, 2021).
6. Zhu, S.; Chen, H.; Wang, M.; Guo, X.; Lei, Y.; Jin, G. Plastic solid waste identification system based on near infrared spectroscopy in combination with support Vector Machine. https://www.sciencedirect.com/science/article/pii/S2542504818300113 (accessed Oct 11, 2021).
7. Galceran, E.; Djapic, V.; Carreras, M.; Williams, D. P. A Real-time Underwater Object Detection Algorithm for Multi-beam Forward Looking Sonar. http://robots.engin.umich.edu/~egalcera/papers/galceran_ngcuv2012.pdf (accessed Oct 11, 2021).
8. Active sonar - springer. https://link.springer.com/chapter/10.1007/978-0-387-30441-0_96 (accessed Oct 11, 2021).
9. Selecting a sonar transducer. https://www.westmarine.com/WestAdvisor/Selecting-a-Sonar-Transducer (accessed Oct 11, 2021).
10. Pelletier, M. J. (n.d.). Quantitative Analysis Using Ra

man Spectrometry. https://journals.sagepub.com/doi/pdf/10.1366/000370203321165133. Retrieved February 17, 2022, from https://journals.sagepub.com/doi/full/10.1366/000370203321165133?url_ver=Z39.88-2003&rfr_id=ori%3Arid%3Acrossref.org&rfr_dat=cr_pub++0pubmed https://doi.org/10.1152/ajplung.00306.2018

Authors

Brandon Pae is a senior from the Horace Mann School who wants to protect the environment through technology. As such, he has created a company, Cypol Technologies, with Darson Chen to clean up the oceans with plastic-collecting drones. In college, he plans to study environmental engineering.

Darson Chen is a senior from the Horace Mann school who passionately studies nanoparticles, nanotechnology, and environmental issues. He co-founded Cypol Technologies, designed plastic-collecting drones, and wrote papers detailing nanotechnology's method to combat plastic pollution in the future. In college, he plans to study material science and engineering.

DOI: 10.36838/v4i5.14

IJHSR
ijhighschoolresearch.org
■ RESEARCH ARTICLE

HSPB1 as a Novel Genetic Marker for Predicting Poor Survival of Stomach Cancer Patients

Aileen Daeun Ryu
The Lawrenceville School, 2500 Main St, Lawrenceville, NJ 08648, USA; Corresponding author email: gosyber1@gmail.com

ABSTRACT: The *HSPB1* gene encodes heat shock proteins and acts as a chaperone by regulating processes and maintaining competent proteins induced in response to stresses and injuries. The expression or alteration of this HSPB1 gene can be associated with poor survival rates by promoting and proliferating metastasis. Although this gene enhances tumor growth in various cancers, gene alteration of *HSPB1* has not been reported for stomach cancer. DNA, mRNA, and clinical data of 1512 patient samples were analyzed from seven stomach cancer studies by cBioPortal. The data showed that gastric cancer patients with the HSPB1 amplified gene had a significantly lower survival rate (median survival = 14.3) than the patients with the HSPB1 non-amplified gene (median survival = 31.0) (p = 0.033). The median survival month of the patient group with high expression of HSPB1 (21.2 months) was lower than the group with a low expression of the *HSPB1* gene (107.7 months). Overall, patients with a non-amplified *HSPB1* gene had a higher percentage of papillary stomach adenocarcinoma.

KEYWORDS: Biology; Genetics; *HSPB1* gene; Stomach Cancer; Survival Rate.

■ Introduction

Stomach cancer starts when cells in the stomach grow out of control. A tumor can be malignant or benign. A malignant tumor is threatening, which can develop and spread to different organs. A benign tumor implies the tumor can grow but would not spread. Cancer can start in any part of the stomach. The cause of gastric cancer is multifactorial.[1]

Heat shock proteins are proteins induced in response to environmental, physical, and chemical stresses, and they limit damage and help the recovery of cells. They protect protein substrates against damage to promote the function of the proteins, prevent aggregation, and prevent the formation of toxic inclusion bodies.[2]

Heat shock proteins strengthen healthy cells by protecting cells against stress and injuries, making them more resistant to diseases. They are significant regulators of cell proliferation and differentiation and implicated in cancer development and progression as they are well-established oncoproteins in many tumor types.[3]

The *HSPB1* gene provides the necessary information for making heat shock proteins; it functions as a chaperone by regulating processes and maintaining competent proteins. Additionally, it helps cells stay secure from many conditions such as injuries and disease. The *HSPB1* gene can enhance or proliferate cell growth and cancer progression. It can also display help in tumor growth and can be found in breast cancer, colorectal cancer, cervical cancer, liver cancer, and lung cancer, in addition to gastric or stomach cancer.[4]

This research aims to find the association between the genetic alterations of the heat shock protein gene *HSPB1* and the overall survival rate of these stomach cancer patients. Because stomach cancer is a common type of cancer with one of the highest death rates, the analysis of both the genetic alteration of the heat shock protein gene and the survival rate can help predict the survival of stomach cancer patients. Therefore, this research would aim to aid these stomach cancer patients by using the *HSPB1* heat shock protein gene as a novel genetic marker.

■ Methods

Patient survival analysis by cBioPortal:

cBioPortal is an open-source cancer genomic database.[5] This database provides a patient's genomic data set published from previous studies. In this study, seven previous studies with stomach cancer patients' data were analyzed for survival. The query "*HSPB1*" was typed for the input command. Then, the selected studies were divided into two groups: the HSPB1 amplified group and the *HSPB1* non-amplified group. The Kaplan Meier plot analyzed the overall survival.

Patient clinical analysis by cBioPortal:

The clinical attributes were analyzed in different categories: cancer type, 15q status, and 19p status. In clinical analysis, seven studies from the previous studies were selected, and the stomach cancer patients were divided into two groups: HSPB1 amplified group vs HSPB1 non-amplified group.

Kaplan-Meier plot survival analysis :

Gene expression data from 875 stomach cancer patients were downloaded from GEO, EGA, and TCGA. The database was analyzed by a PostgreSQL server, which integrates gene expression and clinical data. The prognostic value of the *HSPB1* gene was analyzed by splitting the patient samples into two groups by quantile expression of the *HSPB1*. Two groups (low vs high expression) were compared by Kaplan-Meier survival plot with 95% confidence intervals, and log-rank p-value was calculated. The databases and clinical data are updated regularly in http://kmplot.com.[6]

DOI: 10.36838/v4i5.15

Results and Discussion

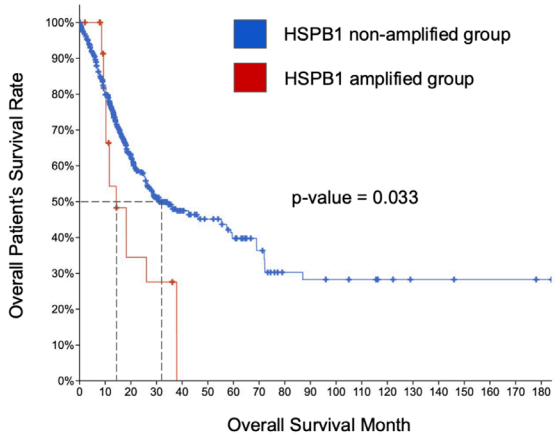

Figure 1: Overall survival rate of *HSPB1* non-amplified (n=1093) and amplified (n=29) stomach cancer patients. The dotted line indicated the median survival month: *HSPB1* non-amplified (median survival month= 31.0) and amplified group (median survival month= 14.3). A log-rank statistical test calculated statistical significance (p= 0.033).

First the copy number variation of the *HSPB1* gene with an amplified and non-amplified group was determined, showing the difference in the survival rate of patients with gastric cancer between the two groups (Figure 1). Because gastric cancer is a type of cancer with a low survival rate, this study decided to evaluate whether there is a correlation between survival in months and amplifications of the *HSPB1* heat shock protein gene. A significant difference according to the given data in this figure was observed, where the patient group with an amplified *HSPB1* gene had a much lower survival rate. In contrast, the non-amplified group had a higher one. In summary, this led to the conclusion of an existing association between the *HSPB1* gene amplification and survival rates of patients affected by gastric cancer.

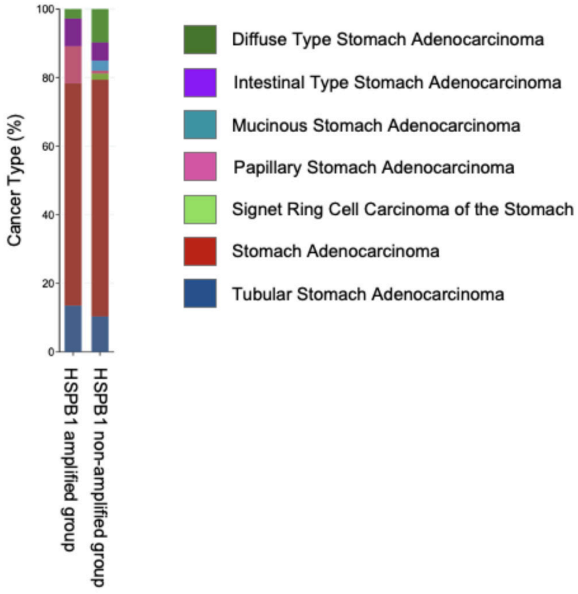

Figure 2: A comparative analysis of *HSPB1* non-amplified and amplified patients based on cancer type. A chi-squared test was used to calculate statistical significance. ($p= 6.12e^{-5}$)

First the difference in types of stomach cancer of patients with an amplified *HSPB1* gene and a non-amplified *HSPB1* gene with the data was determined (Figure 2). The goal was to find an association between amplifications of the heat shock protein gene and specific types of gastric cancer it causes. A notable difference was observed, where 10.8% of patients with the amplified *HSPB1* gene had papillary stomach adenocarcinoma while only 0.81% of patients with the non-amplified *HSPB1*. Papillary gastric adenocarcinoma is a rare histologic entity among gastric adenocarcinomas. Although the 5-year survival rate for the PGC did not differ significantly, death caused by papillary stomach adenocarcinoma was more frequently associated with liver metastasis (62%) than with peritoneal dissemination (5%).[7] This result indicates that both *HSPB1* amplification and papillary stomach adenocarcinoma may be associated with decreased survival rates.

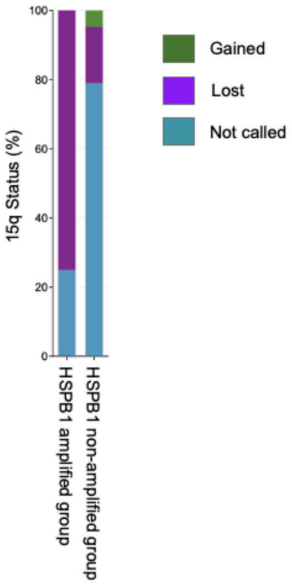

Figure 3: A comparative analysis of *HSPB1* non-amplified and amplified patients based on 15q chromosome status. A chi-squared test was used to calculate statistical significance. ($p= 9.15e^{-5}$)

Next, the 15q status from both *HSPB1* amplified and non-amplified patients was analyzed because chromosomal imbalances in gastric cancer are often correlated with tumor progression. 75% of *HSPB1* non-amplified patients lost chromosome 15q, whereas only 16.27% of *HSPB1* amplified patients lost chromosome 15q (Figure 3). The deletion of 15q has been reported in various steps of cancer, such as ovarian carcinoma and breast cancer.[8] The loss of 15q is known to be discovered in a late event in most high-grade tumors and metastatic breast carcinomas.[9] This result suggested that both 15q loss and *HSPB1* amplification are associated with the decreased patient survival rate.

Additionally, this data set of 19p chromosome status of both the *HSPB1* amplified and non-amplified patients was analyzed with the goal of seeing an association between the 19p status and cancer development. It was observed that 77.78% of patients with the non-amplified *HSPB1* gene lost the 19p chromosome, while only 27.27% of the

DOI: 10.36838/v4i5.15

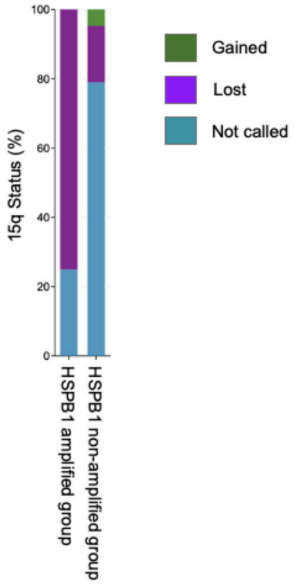

Figure 4: A comparative analysis of *HSPB1* non-amplified and amplified patients based on 19p chromosome status. A chi-squared test was used to calculate statistical significance. ($p= 4.60e^{-3}$)

amplified gene lost chromosome 19p. The data also shows that the *HSPB1* gene amplified group gained 5.43% of the chromosome. Similar losses of this chromosome 19p can be found in different types of cancer, such as ovarian cancer, lung cancer, breast cancer, and neuroblastoma.[10] Chromosome 19p plays a vital role in ovarian carcinogenesis, correlates with poor prognosis in neuroblastoma, and lung oncogenesis or remote metastasis in breast cancer.[11] The result of this figure shows an association between the loss of chromosome 19p and decreased patient survival (Figure 4).

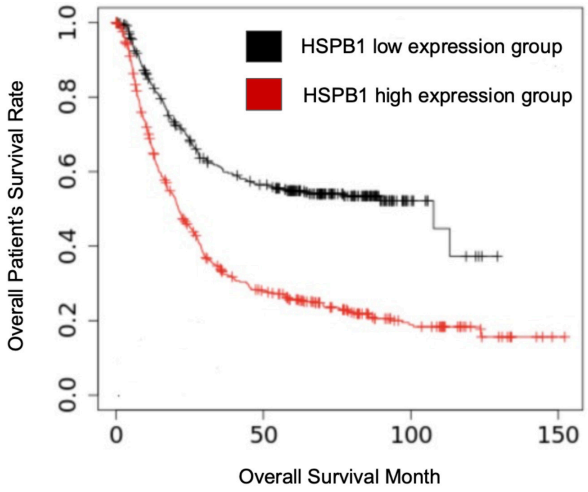

Figure 5: The overall survival rate of low (n= 557) and high (n=665) HSPB[1] mRNA expression of stomach cancer patients. The median survival of the low *HSPB1* expression group was 107.7 months. The median survival of the high *HSPB1* expression group was 21.2 months. A log-rank statistical test was used to calculate statistical significance. (p< 1e-16)

Since gene amplification promotes over-expression of genes, the patient survival rate was further analyzed among two different *HSPB1* expression groups: high and low *HSPB1* expression groups. These two groups were selected according to various quantile expressions of *HSPB1*. The public databases provided these patient survival cohorts: GEO, EGA, and TCGA, and compared by a Kaplan-Meier survival plot (kmplot.com). As shown in Figure 5, stomach cancer patients with high *HSPB1* mRNA expression levels had significantly poorer survival rates than patients with low *HSPB1* expression levels.

Conclusion

Accurately predicting the prognosis of cancer states and identifying cancer stages may benefit cancer patients. For example, molecular markers with clinicopathological parameters are often used to predict cancer patients' survival rates. However, due to the complexity of cancer, the molecular marker for predicting the survival of cancer patients has not been well established. This research identified that amplification of the heat shock protein gene, *HSPB1*, can be used as a novel marker for predicting a patient's overall survival rate. When the *HSPB1* amplified patient's clinical status was further analyzed, they were also associated with a high percentage rate of papillary cancer type and chromosomal loss on 15q and 19p. It was also expected that an increased mRNA expression level of *HSPB1* may decrease patient survival. This expectation was consistent with the survival analysis performed by the Kaplan-Meier survival plot (Figure 5).

Some overexpressed genes in stomach cancer are the HER-2/neu oncogene, the TOP2A gene, the EGFR gene, and chromosome 17q, which decrease survival rates.[12] The amplification of the HER-2/neu oncogene affects the progression of gastric cancer, as it amplifies the amount of tumor tissue and therefore reduces the survival rate. There is also a correlation between gene amplification and protein overexpression of the TOP2A gene shown in gastric cancer.[13] Additionally, the overexpression of the EGFR gene has been implicated in the process of tumor cell motility and metastasis, which is associated with decreased patient survival. Chromosome 17q also is frequently amplified in patients with gastric cancer. The increased copy number of many genes with high expression levels within this chromosome has been identified.[14]

Many studies indicate that heat shock protein (Hsp) overexpression in many types of cancer cells. This phenomenon can be associated with the tumor microenvironment's various stress conditions, including low pH, high oxidative stress conditions, and low glucose levels. Cancer cells reprogram many biological pathways to survive harsh tumor microenvironments in response to this stress condition. Hsps prevent protein aggregation, which is induced by cellular stress.[15] Recently, *HSPB1*, one of the small Hsps groups, has been described as ATP-independent molecular chaperones. Many studies indicate that HSPB1 interacts with many pro-oncogenic proteins that play an essential role in human cancer progression. The high expression level of *HSPB1* usually results in a poor survival rate in many cancers: stomach, uterine, breast, ovarian, and kidney.[16]

Overexpression of *HSPB1* has been identified in both lung and breast cancer. The overexpression of the *HSPB1* gene can also be found in lung cancer, where *HSPB1* helps lead to tumor invasion and metastasis by enhancing the EMT in

lung cancer. The *HSPB1* gene may cause deleterious effects by allowing cancer cells to evade immune surveillance. The overexpression of the *HSPB1* gene has also been identified in breast cancer. It can enhance cell proliferation, tumor development, and the growth of breast cancer cells. It is also associated with resistance to apoptosis in human breast cancer cells; high levels of *HSPB1* expression affect tumor susceptibility to cancer treatments and therefore decrease survival rates.[17]

The next goal of this research is to find the functional role of a high expression level of *HSPB1* on cancer cell progression. *In vitro* experiments will be performed to find the novel function of *HSPB1* on stomach cancer. These findings may lead to the development of a novel stomach cancer therapy.

Acknowledgements

I want to thank Dr. Woo Rin Lee from the University of Suwon in South Korea. His guidance and advice were helpful.

References

1. Carcas, L. P. Gastric Cancer Review. *J. Carcinog.* **2014**, *13*, 14.
2. Tutar, L.; Tutar, Y. Heat Shock Proteins; an Overview. *Curr. Pharm. Biotechnol.* **2010**, *11* (2), 216–222.
3. Wu, J.; Liu, T.; Rios, Z.; Mei, Q.; Lin, X.; Cao, S. Heat Shock Proteins and Cancer. *Trends Pharmacol. Sci*. **2017**, *38* (3), 226–256.
4. Acunzo, J.; Katsogiannou, M.; Rocchi, P. Small Heat Shock Proteins HSP27 (HSPB1), AB-Crystallin (HspB5) and HSP22 (HspB8) as Regulators of Cell Death. *Int. J. Biochem. Cell Biol*. **2012**, *44* (10), 1622–1631.
5. Cerami, E.; Gao, J.; Dogrusoz, U.; Gross, B. E.; Sumer, S. O.; Aksoy, B. A.; Jacobsen, A.; Byrne, C. J.; Heuer, M. L.; Larsson, E.; et al. The CBio Cancer Genomics Portal: An Open Platform for Exploring Multidimensional Cancer Genomics Data. *Cancer Discov.* **2012,** *2* (5), 401–404.
6. Nagy, Á.; Munkácsy, G.; Győrffy, B. Pancancer Survival Analysis of Cancer Hallmark Genes. *Sci. Rep*. **2021**, *11* (1), 6047.
7. Yasuda, K.; Adachi, Y.; Shiraishi, N.; Maeo, S.; Kitano, S. Papillary Adenocarcinoma of the Stomach. *Gastric Cancer* **2000**, *3* (1), 33–38.
8. Richard, F.; Pacyna-Gengelbach, M.; Schlüns, K.; Fleige, B.; Winzer, K. J.; Szymas, J.; Dietel, M.; Petersen, I.; Schwendel, A. Patterns of Chromosomal Imbalances in Invasive Breast Cancer. Int. *J. Cancer* **2000**, *89* (3), 305–310.
9. Wick, W.; Petersen, I.; Schmutzler, R. K.; Wolfarth, B.; Lenartz, D.; Bierhoff, E.; Hümmerich, J.; Müller, D. J.; Stangl, A. P.; Schramm, J.; et al. Evidence for a Novel Tumor Suppressor Gene on Chromosome 15 Associated with Progression to a Metastatic Stage in Breast Cancer. *Oncogene* **1996**, *12* (5), 973–978.
10. Wang, X.; Zhang, Y.; Nilsson, C. L.; Berven, F. S.; Andrén, P. E.; Carlsohn, E.; Horvatovich, P.; Malm, J.; Fuentes, M.; Végvári, Á.; *et al*. Association of Chromosome 19 to Lung Cancer Genotypes and Phenotypes. *Cancer Metastasis Rev*. **2015**, *34* (2), 217–226.
11. Yu, W.; Kanaan, Y.; Bae, Y. K.; Gabrielson, E. Chromosomal Changes in Aggressive Breast Cancers with Basal-like Features. Cancer Genet. *Cytogenet*. **2009**, *193* (1), 29–37.
12. Pilarsky, C.; Wenzig, M.; Specht, T.; Saeger, H. D.; Grützmann, R. Identification and Validation of Commonly Overexpressed Genes in Solid Tumors by Comparison of Microarray Data. *Neoplasia* **2004**, *6 (6)*, 744–750.
13. Terashima, M.; Ichikawa, W.; Ochiai, A.; Kitada, K.; Kurahashi, I.; Sakuramoto, S.; Katai, H.; Sano, T.; Imamura, H.; Sasako, M.; *et al*. TOP2A, GGH, and PECAM1 Are Associated with Hematogenous, Lymph Node, and Peritoneal Recurrence in Stage II/III Gastric Cancer Patients Enrolled in the ACTS-GC Study. *Oncotarget* **2017**, *8* (*34*), 57574–57582.
14. Noguchi, T.; Wirtz, H. C.; Michaelis, S.; Gabbert, H. E.; Mueller, W. Chromosomal Imbalances in Gastric Cancer. Correlation with Histologic Subtypes and Tumor Progression. *Am. J. Clin. Pathol*. **2001**, *115* (*6*), 828–834.
15. Feder, M. E.; Hofmann, G. E. Heat-Shock Proteins, Molecular Chaperones, and the Stress Response: Evolutionary and Ecological Physiology. *Annu. Rev. Physiol*. **1999**, *61*, 243–282.
16. Xiong, J.; Li, Y.; Tan, X.; Fu, L. Small Heat Shock Proteins in Cancers: Functions and Therapeutic Potential for Cancer Therapy. *Int. J. Mol. Sci*. **2020**, *21* (18).
17. Arrigo, A.-P.; Gibert, B. HSPB1, HspB5 and HspB4 in Human Cancers: Potent Oncogenic Role of Some of Their Client Proteins. *Cancers (Basel)* **2014**, *6* (*1*), 333–365.

Author

Aileen Daeun Ryu is a freshman in The Lawrenceville School. She is interested in biological science and medical science. She wants to study medical and health science in college and become a doctor in the future.

DOI: 10.36838/v4i5.15

IJHSR
ijhighschoolresearch.org
RESEARCH ARTICLE

Exosome Encapsulation of Curcumin Blocks TNF-α and IL-2 Dependent Cytokine Storm

Seongwon Park
Branksome Hall Asia, 234 Global edu-ro Daejeong-eup, Seogwipo-si, Jeju-do, 63644, Republic of Korea; gosyber1@gmail.com

ABSTRACT: Severe acute respiratory syndrome coronavirus 2 (SARS-COV2), a highly contagious virus, has caused a pandemic of a respiratory disease named coronavirus disease 2019 (COVID-19). The disease can be fatal because of a systematic cytokine storm that causes excessive inflammatory responses in the lungs. However, no drugs are available to calm severe inflammatory responses that cause lung injury. Through its antioxidant activity and ability to release different anti-inflammatory cytokines, curcumin could be used as a therapeutic drug for COVID-19. Also, cancer-derived exosomes, which can carry biological molecules inside the cell, induce immunosuppression within the tumor microenvironment. Previous research indicated that curcumin does not inhibit *TNF* and *IL-2* in COVID-19 patients and has a limited effect on inhibiting cytokine storms. To solve this limitation of curcumin treatment, we hypothesized that exosome encapsulated curcumin would enhance the inhibiting effect on cytokine. We tested a total of 12 conditions using curcumin and exosomes in different concentrations and ratios on T-cells (Jurkat), finding the optimal condition for inhibiting *TNF* and *IL-2*. As a result, we found that the 1:3 ratio (curcumin: exosome) treatment most efficiently inhibits the expression of *TNF* and *IL-2* in Jurkat cells. Our result indicates that encapsulating the curcumin with an exosome can be used as a therapeutic application on calming the cytokine storm for COVID-19 patients.

KEYWORDS: Biology; Cell biology; Curcumin; Exosome; Cytokine Storm; COVID-19.

Introduction

At the end of 2019, Severe acute respiratory syndrome coronavirus 2 (SARS-CoV-2) emerged in Wuhan, China, and caused an outbreak of an unusual viral pneumonia.[1] This novel coronavirus disease, known as coronavirus disease 2019 (COVID-19), has spread fast worldwide. The ongoing epidemic of COVID19 still threatens global public health in 2022.[2]

While COVID-19 has caused a million deaths worldwide, approximately 15% of the patients developed respiratory failure from acute respiratory distress syndrome (ARDS), a product of inflammatory cytokine storm.[3] Notably, COVID-19 has a broad spectrum of disease severity for the patients, including ARDS. Previous research showed that ARDS and cytokine storm is a causative syndrome of death in over 70% of fatal COVID-19 cases, where inflammatory responses occur aggressively.[4] As respiratory disorder caused by ARDS is the leading cause of death from COVID-19, many immune cells resulting from the cytokine storm are activated in the lungs.[5]

Curcumin is a polyphenol pigment derived from the perennial plant *Curcuma longa L.*, commonly known as the turmeric spice. It inhibits tumor cell proliferation, regulates anti-inflammation, and induces a neuroprotective effect on brain cells.[6] A previous study aimed to evaluate the efficacy of curcumin (dose- 160 mg in four 40 mg capsules daily for 14 days) on regulating the levels of inflammatory cytokines IL-1β, IL-6, TNFα, and IL-18.7 They found out that decreased expression and secretion of IL-1β and IL-6 were achieved in COVID-19 patients.[7] However, there was no positive effect on TNFα concentration and *IL-2* expression with curcumin treatment.

To solve this limitation of curcumin treatment on inhibiting cytokines, we used cancer-derived exosomes to encapsulate the curcumin. Many research papers indicated that cancer-derived exosomes have an immunosuppressive effect in the tumor microenvironment.[8] Tumor-derived exosomes from glioma (brain cancer) decreased the expression level of TNFα, IL-2, IFN-γ, IL-4, IL-5, IL17, GM-CSF of Jurkat cells.[9]

As TNFα and *IL-2* are present in the blood and disease tissues of patients with COVID-19, it acts as an amplifier of inflammation and is essential in acute inflammatory reactions.[10] Moreover, excessive production of both *TNF* and *IL-2* is involved in inducing cytokine storms, which may cause severe damage to lung tissue.[11] Therefore, in this experiment, we tested a total of 12 conditions using curcumin and exosomes in different concentrations and ratios on T-cells (Jurkat), analyzing its potential effect on inhibiting *TNF* and *IL-2*.

Methods

Cell culture and maintenance:

Jurkat and A172 cells were purchased from Korea Cell Line Bank. The cells were maintained in RPMI 1640 media (Gibco) in a 5 % CO2 incubator at 37 °C (Eppendorf). The cells were subcultured into a new plate every three days to maintain the cells in healthy condition.

RNA Extraction from cultured cell:

After adding 400 µL RB Buffer (lysis buffer) to the cell pellet and 300 µL ethanol (80%) to the cell samples, transfer the samples to the 2 mL collection tubes. The cells were centrifuged at 14,000 rpm for 20 seconds. Repeat the centrifuging process after adding each 700µl RWA1 Buffer (washing buffer 1) and 500 µl RWA2 Buffer (washing buffer 1). The

DOI: 10.36838/v4i5.16

ethanol was completely removed from the tube by centrifuging the tube once more at 14,000 rpm for 1 minute. 50~200 µL of ER Buffer (elution buffer) was added to the new tube after transferring the cells. After waiting 1 minute at room temperature (15~25 °C), centrifuge the tubes at 10,000 rpm for 1 minute to elute.

cDNA synthesis:

For each cDNA synthesis reaction sample, we added 1 µL RT Buffer, 0.5 µL RT enzyme, 1 µL dNTP mixture, 0.5 µL T primer, and 7 µL of RNA, with a total of 10 µL. This step was repeated 13 times to make 13 samples for cDNA synthesis. Then, the reaction sample was placed inside a thermocycler machine to synthesize cDNA from extracted RNA. The following temperature and time conditions were used: 1) 25 °C for 10 min 2) 45 °C for 60 min 3) 95 °C for 5 min 4) 4 °C for sample storage.

Polymerase Chain Reaction (PCR):

PCR reaction was performed to amplify cDNA of TNFα, IL-2, and GAPDH. For each PCR reaction sample, we added 0.5 µL synthesized cDNA, 17.5 µL water, 1 µL primer-F, and 1 µL primer-R, with a total of 20 µL. Pre-mixed PCR reaction tubes (Bioneer) were used, and the premix solution contains DNA Polymerase, dNTP, and buffer mixture. The process was repeated 13 times to make 13 samples for PCR reaction. The following primer sequences were used to amplify TNFα, IL-2, and GAPDH. TNFα Forward: CCTCTCTCTAATCAGCCCTCTG, TNFα Reverse: GAGGACCTGGGAGTAGATGAG. IL2- Forward: TCCTGTCTTGCATTGCACTAAG, IL2- Reverse: CATCCTGGTGAGTTTGGGATTC. GAPDH Forward: GGAGCGAGATCCCTCCAAAAT, Reverse: GGCTGTTGTCATACTTCTCATGG. The following temperature and time conditions were used: 1) 95 ˚C for 3 min 2) 95 ˚C for 30 sec 3) 61 ˚C for 30 sec 4) 72 ˚C for 25 sec 5) repeat step 2 to 4 for 34 times 6) 72 ˚C for 5 min 7) 12 ˚C for sample storage.

Agarose gel electrophoresis:

Agarose gel was prepared to visualize the amplified cDNA of TNFα, IL-2, and GAPDH. To prepare the gel, 1.3 g agarose was added to 100 mL of TBE Buffer. After microwaving for 3 minutes until the mixture is completely solubilized, we added 5 µL of Red Safe (Intron) DNA staining solution. For the gel to be completely solidified, we poured the solution into the gel caster and wait for 20 minutes. After the gels were solidified, the gel was placed inside the gel tank. The TBE buffer was poured until the gel was completely submerged. Then, 7 µL of amplified cDNA sample was carefully loaded into the empty well of the agarose gel. The gel was run for 20 minutes and placed on the blue illuminator to visualize the amplified DNA band. Then, the photo was taken to analyze the band intensity. The band intensity was quantified using the ImageJ program.

Statistical test analysis:

An unpaired t-test was used to calculate the statistical significance. Prism 8 program was used to calculate the p-value, and a p-value less than 0.05 was considered to be statistically significant.

Results and Discussion

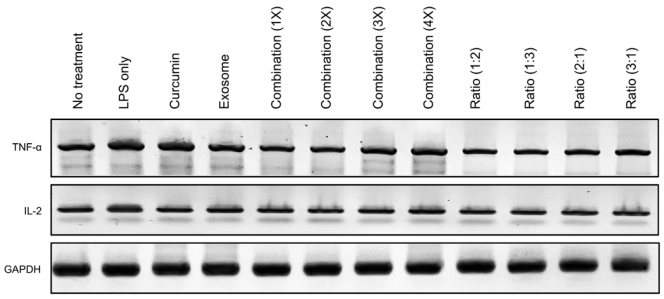

Figure 1: The expression level of TNF-α, IL-2, and GAPDH on Jurkat cells using 12 different treatment conditions: 1) no treatment (negative control), 2) LPS only, 3) LPS+ Curcumin, 4) LPS + Exosome, 5) LPS+ Combination (1X), 6) LPS+ Combination (2X), 7) LPS + Combination (3X), 8) LPS + Combination 4X), 9) LPS + Ratio (1:2), 10) LPS+ Ratio (1:3), 11) LPS + Ratio (2:1), 12) LPS +Ratio (3:1)

We prepared 12 different treatment conditions in this experiment. We used lipopolysaccharide (LPS), which is a natural adjuvant synthesized by gram-negative bacteria to activate the human T-cell (Jurkat). The high expression level of TNF-α and IL-2 represents the cytokine storm phenotype. GAPDH was used to normalize the expression level of TNF-α and IL-2. This experiment aims to find the optimal condition for inhibiting the expression level of both TNF-α and IL-2. As we expected, when we compared the band intensity of TNF-α and IL-2 between no treatment and LPS only condition, LPS treatment increased the band intensity of both TNF-α and IL-2 on Jurkat cells (Figure 1). Also, the individual treatment of both curcumin and exosome decreased the band intensity of TNF-α and IL-2 compared to the LPS only condition. This result indicates that both curcumin and exosome inhibit TNF-α and IL-2 dependent cytokine storms.

Next, we tested the combination treatment of curcumin and exosomes. We investigated four different combination conditions by increasing the concentration of both curcumin and exosomes up to four times. The combination treatment of 1X and 2X showed lower band intensity of both TNF-α and IL-2. However, combination treatment of 3X and 4X showed increased band intensity compared to 1X and 2X. In addition, we also tested four different ratios of curcumin to exosome. All four combination treatments with different ratios decreased the band intensity of both TNF-α and IL-2 compared to LPS only condition. In conclusion, our result indicates that combination treatment effectively inhibits the expression level of both TNF-α and IL-2, which may block the cytokine storm on T-cells.

To find the optimized condition that efficiently inhibits TNF-α dependent cytokine storm, we quantified the gene expression level of TNF-α in all twelve conditions. Compared to LPS only condition, we found that Ratio (1:3) significantly decreased the expression level of TNF-α in Jurkat cells (Figure 2). Since an increased expression level of TNF-α is commonly found in the COVID-19 patient's blood with severe cytokine storm, this treatment condition may calm the overexpression of TNF-α, inhibiting inflammation in patients' lung tissue.

DOI: 10.36838/v4i5.16

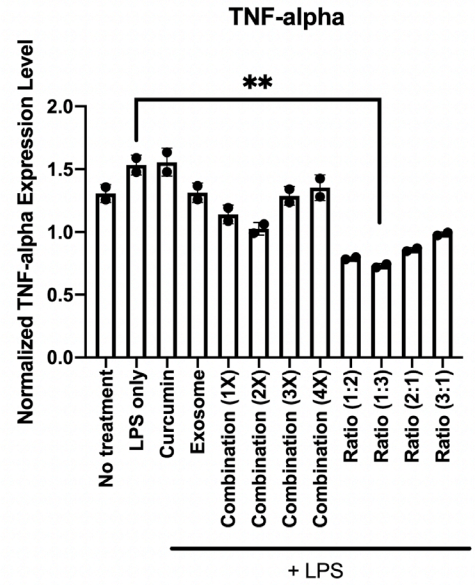

Figure 2: The ratio (1:3) treatment condition significantly decreased the expression level of TNF-α compared to LPS only condition. Normalized TNF-α expression level was calculated using the following equation: (band intensity of TNF-α) / (band intensity of GAPDH). The mean and standard deviation is graphed. (n= 2), Unpaired t-test, ** P< 0.01.

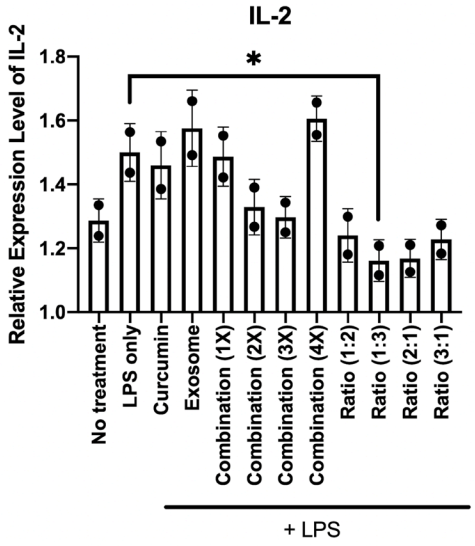

Figure 3: The ratio (1:3) treatment condition significantly decreased the expression level of IL-2 compared to LPS only condition. Normalized TNF-α expression level was calculated using the following equation: (band intensity of IL-2) / (band intensity of GAPDH). The mean and standard deviation is graphed. (n= 2), Unpaired t-test, * P< 0.05.

To find the optimized conditions that efficiently inhibit IL-2 dependent cytokine storm, we quantified the gene expression level of IL-2 in all twelve conditions. Compared to LPS only condition, we found that Ratio (1:3) significantly decreased the expression level of IL-2 in Jurkat cells (Figure 3). A high expression level of IL-2 is found in COVID-19 patients since it induces a severe cytokine storm in COVID-19 patients' lungs. Previous studies indicated that curcumin treatment did not effectively suppress IL-2 in COVID-19 patients. However, our result showed that this Ratio (1:3) treatment would efficiently prevent the cytokine storm induced by IL-2.

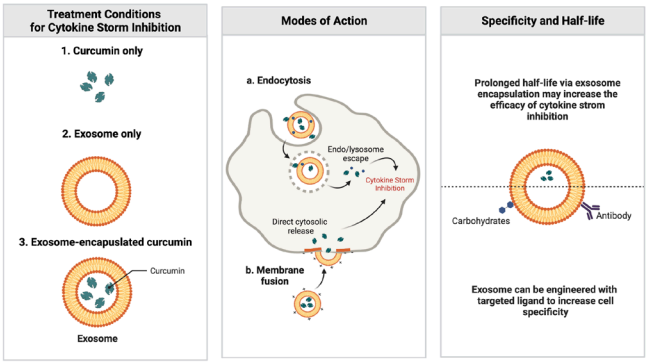

Figure 4: The proposed model for exosome encapsulated curcumin delivery that inhibits cytokine storm. Three treatment conditions were listed: 1) curcumin only, 2) exosome only, 3) Exosome-encapsulated curcumin.

Previous research indicated that curcumin alone did not inhibit TNF-α and IL-2 dependent cytokine storm. Therefore, our experiment aimed to find an optimal condition that efficiently inhibits TNF-α and IL-2 dependent cytokine storm on T-cells. In this study, we tested three treatment conditions with varying curcumin and exosome concentrations and ratios; a total of twelve conditions were investigated in this study. Since exosomes efficiently deliver the cargo into target cells, we expected that exosome encapsulated curcumin would be delivered more efficiently rather than curcumin treatment alone. As a result, combination treatment with a ratio (1:3) demonstrated the most efficiency in inhibiting both TNF-α and IL-2 expression on T-cells. The prolonged half-life and increased delivery efficiency via exosome encapsulation may enhance the stability and activity of curcumin to block the cytokine storm (Figure 4).

Conclusion

COVID-19, which is caused by SARS-CoV-2, is expressed by diverse symptoms ranging from moderate fatigue to life-threatening problems, including cytokine storm and multiorgan failure.[12] Importantly, cytokine storm was also found in patients with SARS and often led to poor outcomes. Previous studies indicated that cytokine blockades improved the survival rate of patients with COVID-19 who are at risk of respiratory failure.[13] However, since many cytokines induce inflammation in the lungs, current cytokine blocking treatment is limited. Also, previous studies showed that high serum IL-2, IL-6, IL-8, and TNF-α levels at the time of hospitalization were strong and independent predictors of low patient survival rates.[14] Therefore, our study aims to find the effect on blocking TNF-α and IL-2.

We focused on curcumin treatment, which has shown blocking inflammation effects on COVID-19 patients. However, curcumin alone cannot block IL-2 and TNF-α dependent inflammation.[15] To increase the efficacy of blocking both IL-2 and TNF-α, we encapsulate the curcumin with human brain cancer cell exosomes, which are known to change the cytokine molecules in T-cell. As we hypothesized, the combination treatment of curcumin and exosomes with 1:3 ratio showed the most effective blocking of cytokines of IL-2 and TNF-α. This result indicates that our new method can be applied to patients with COVID-19 dependent

inflammations for calming the cytokine storm. We speculate that 1:3 ratio (curcumin:exosome) efficiently delivers the curcumin to the T-cell and may exhibit the most effective blockage of cytokine storm-related genes. Also, there is a possibility that the exosome itself has the blocking effect of the cytokine storm. However, further experiments are needed to confirm how 1:3 ratio efficiently blocks the cytokine storm.

One of the limitations of our study is that only Jurkat T-cell was used during the experiment. More types of immune cells (T-cells) should be used to validate our experimental results. Moreover, a mouse model should also be tested to confirm our results, while our study only performed cell experiments. In the future, clinical studies comparing control groups to exosome encapsulated curcumin treatment groups should be performed. Another limitation is that our experiment only investigated blocking IL-2 and TNF-α. As cytokine storms can be induced by hundreds of genes depending on growth factors and hormones, we should explore more types of cytokine genes that can be controlled by exosome encapsulated curcumin.

Acknowledgements

I would like to express my special thanks to my primary supervisor who guided me throughout this project in terms of research and experiments. I would also like to show appreciation to my family who supported me and allowed me to extend my insight into the study.

References

1. Dhama, K.; Khan, S.; Tiwari, R.; Sircar, S.; Bhat, S.; Malik, Y. S.; Singh, K. P.; Chaicumpa, W.; Bonilla-Aldana, D. K.; Rodriguez-Morales, A. J. Coronavirus Disease 2019-COVID-19. *Clin. Microbiol. Rev.* **2020**, *33* (4)..
2. Van Kerkhove, M. D. COVID-19 in 2022: Controlling the Pandemic Is within Our Grasp. *Nat. Med.* **2021**, *27* (12), 2070.
3. Tang, Y.; Liu, J.; Zhang, D.; Xu, Z.; Ji, J.; Wen, C. Cytokine Storm in COVID-19: The Current Evidence and Treatment Strategies. Front. *Immunol.* **2020,** *11*, 1708.
4. Hojyo, S.; Uchida, M.; Tanaka, K.; Hasebe, R.; Tanaka, Y.; Murakami, M.; Hirano, T. How COVID-19 Induces Cytokine Storm with High Mortality. *Inflamm. Regen.* **2020,** *40*, 37.
5. Conti, P.; Caraffa, A.; Gallenga, C. E.; Ross, R.; Kritas, S. K.; Frydas, I.; Younes, A.; Ronconi, G. Coronavirus-19 (SARS-CoV-2) Induces Acute Severe Lung Inflammation via IL-1 Causing Cytokine Storm in COVID-19: A Promising Inhibitory Strategy. J. Biol. Regul. Homeost. *Agents* **2020**, *34* (6), 1971–1975..
6. Hewlings, S. J.; Kalman, D. S. Curcumin: A Review of Its Effects on Human Health. *Foods* **2017**, *6* (10).
7. Ahmadi, R.; Salari, S.; Sharifi, M. D.; Reihani, H.; Rostamiani, M. B.; Behmadi, M.; Taherzadeh, Z.; Eslami, S.; Rezayat, S. M.; Jaafari, M. R.; et al. Oral Nano-Curcumin Formulation Efficacy in the Management of Mild to Moderate Outpatient COVID-19: A Randomized Triple-Blind Placebo-Controlled Clinical Trial. *Food Sci. Nutr.* **2021**, *9* (8), 4068–4075.
8. Olejarz, W.; Dominiak, A.; Żołnierzak, A.; Kubiak-Tomaszewska, G.; Lorenc, T. Tumor-Derived Exosomes in Immunosuppression and Immunotherapy. *J. Immunol. Res.* **2020**, *2020*, 6272498.
9. Domenis, R.; Cesselli, D.; Toffoletto, B.; Bourkoula, E.; Caponnetto, F.; Manini, I.; Beltrami, A. P.; Ius, T.; Skrap, M.; Di Loreto, C.; et al. Systemic T Cells Immunosuppression of Glioma Stem Cell-Derived Exosomes Is Mediated by Monocytic Myeloid-Derived Suppressor Cells. *PLoS ONE* **2017**, *12* (1), e0169932.
10. Luo, W.; Zhang, J.-W.; Zhang, W.; Lin, Y.-L.; Wang, Q. Circulating Levels of IL-2, IL-4, TNF-α, IFN-γ, and C-Reactive Protein Are Not Associated with Severity of COVID-19 Symptoms. J. *Med. Virol.* **2021**, *93* (1), 89–91.
11. Costela-Ruiz, V. J.; Illescas-Montes, R.; Puerta-Puerta, J. M.; Ruiz, C.; Melguizo-Rodríguez, L. SARS-CoV-2 Infection: The Role of Cytokines in COVID-19 Disease. *Cytokine Growth Factor Rev.* **2020**, *54*, 62–75..
12. Coperchini, F.; Chiovato, L.; Croce, L.; Magri, F.; Rotondi, M. The Cytokine Storm in COVID-19: An Overview of the Involvement of the Chemokine/Chemokine-Receptor System. *Cytokine Growth Factor Rev.* **2020**, *53*, 25–32.
13. Jose, R. J.; Manuel, A. COVID-19 Cytokine Storm: The Interplay between Inflammation and Coagulation. Lancet Respir. *Med.* **2020**, *8* (6), e46–e47.
14. Del Valle, D. M.; Kim-Schulze, S.; Huang, H.-H.; Beckmann, N. D.; Nirenberg, S.; Wang, B.; Lavin, Y.; Swartz, T. H.; Madduri, D.; Stock, A.; et al. An Inflammatory Cytokine Signature Predicts COVID-19 Severity and Survival. Nat. *Med.* **2020**, *26* (10), 1636–1643.
15. Zahedipour, F.; Hosseini, S. A.; Sathyapalan, T.; Majeed, M.; Jamialahmadi, T.; Al-Rasadi, K.; Banach, M.; Sahebkar, A. Potential Effects of Curcumin in the Treatment of COVID-19 Infection. Phytother. *Res.* **2020**, *34* (11), 2911–2920.

Author

Seongwon Park is a junior in Branksome Hall Asia. She plans to major in biochemistry at her future university. With an interest in the biochemistry field, she is currently in various science clubs in school. She also gave a talk related to this field in the TEDx event held in her school. Moreover, she is a member of the varsity volleyball team..

DOI: 10.36838/v4i5.16

IJHSR
ijhighschoolresearch.org
■ RESEARCH ARTICLE

Poacher Activity Detection Device for Wildlife Conservation

Shreya Kakhandiki
Lynbrook High School, 1280 Johnson Ave, San Jose, CA 95129, USA; shreya.kakhandiki@gmail.com

ABSTRACT: The scale of the wilderness makes it extremely difficult to constantly patrol for poaching activity. Consequently, there is an urgent need for an effective automated tool to curb poaching. The goal of this project was to build a low-cost device that can be installed in wilderness areas as well as on surveillance drones and can send real-time alerts of poaching activity to park officials. The device hardware consists of a Raspberry Pi computer with a power bank, camera, and an antenna. The test data mainly consisted of publicly available images of wild animals and humans in the wilderness. An image classification algorithm was built using a set of pre-trained AI models to detect the presence of humans, weapons, and animals in a photo; this algorithm was implemented on a device that can be used to notify officials of possible poaching activity. The device successfully meets all engineering goals. The design costs about US$100, takes about 5 minutes to run per image, is over 90% accurate in recognizing humans, weapons, and animals in all the test images, and can generate notifications. The poacher activity detection device may help rangers monitor large areas and decrease poaching activity.

KEYWORDS: Ecology; Camera Trap; Poacher Detection; Wildlife Conservation; Artificial Intelligence; Machine Learning; Facial Recognition; Raspberry Pi.

■ Introduction

Wildlife poaching poses an ongoing, significant threat to global biodiversity.[1,2] Numerous studies have demonstrated that poaching is causing significant population declines in several more common species[3-5] and benefits insurgent groups and criminal networks around the world.[3]

Preventative action requires significant resources and constant monitoring. Moore *et al*.[8] looked at the effect of ranger posts and patrols in detecting and mitigating poaching threats, examining factors influencing the spatio-temporal dynamics of these threats, and testing the efficiency of management actions. This study highlights the need to increase patrol resources. Unfortunately, they require significant budget expansion which is often an intractable problem in developing countries. Furthermore, depending on the geographical region, the size and scale of reserve land makes it extremely hard for constant human patrolling. There is an inherent human safety issue as well; hundreds of rangers and volunteers have been killed by poachers.[9,10] As a result of this, poaching is often only recognized after the fact, at the risk of both animals and rangers. We have a clear and urgent need for an automated real-time tool to detect and curb poaching.

The goal of this project is to introduce a low-cost, scalable approach to wildlife conservation by developing a wildlife monitoring device that can alert the appropriate agency in real-time when poaching activity is detected. The entire system needs to be easy to install and maintain, widely deployable in any geographical region, offers one of the lowest cost solutions, and is based on standard components widely available today to promote a self-serve approach for anyone who wishes to deploy such devices in mass quantities. Releasing the device designs publicly will ensure that a maximum number of people will be able to build and deploy these devices rapidly and extensively for immediate impact on our planet's dwindling wildlife.

The project leverages recent innovations in computing hardware and software, motion sensors, AI-based image classification algorithms, solar cells, and satellite technology. This is packaged into a reference architecture design that anyone can reproduce, complete with hardware specifications, assembly instructions, and software components for rapid deployments anywhere in the world.

Related work:

Current preventative efforts and solutions to poaching can be classified into the following three main categories: risk prediction, wildlife monitoring, and threat monitoring.

Risk prediction:

Poaching risk prediction techniques have evolved from statistical analyses in the past to current approaches based on artificial intelligence (AI). The goal of these solutions is to predict where the poaching threat is greatest so appropriate resources can be mobilized in these areas. A potential shortcoming of this class of solutions is that poachers can simply move to other areas to avoid detection.

Risk prediction techniques can be further divided into two categories: statistical and GIS-based techniques, and AI-based techniques.

Statistical and GIS-based risk prediction

These techniques use statistical analyses incorporating geospatial elements of the physical environment to create risk maps indicating the highest areas of risk.[11] Typical high-risk areas occur near roads or water features that make it easy for poachers to haul animals to their destination.

AI-based risk prediction

These techniques use AI to predict when and where poachers are most likely to strike. Protection Assistant for Wildlife Security (PAWS)[12] is an AI system that predicts poaching

DOI: 10.36838/v4i5.17

risk levels in different areas of a wildlife preserve and helps rangers patrol more efficiently.[13] PAWS's machine-learning algorithm uses data from past patrols to predict where poaching is likely to occur in the future. It also uses a game-theory model to generate randomized, unpredictable patrol routes so poachers can't see any patterns to dodge rangers.

Wildlife Monitoring using image analysis:

Wildlife monitoring techniques consist of identifying animal populations and even individual animals. Such techniques help gauge the decline of specific species in a region. These techniques are effective when supported by wider regional coverage and a large number of images taken from several different vantage points. A great example of this is the Wildbook project,[14] which identifies individual animals in images uploaded by conservation scientists, rangers, and tourists.

Threat monitoring:

Monitoring of poaching threats via aerial surveillance

These techniques typically use manned planes or unmanned drones for aerial surveillance, taking pictures and videos that can be analyzed, often using computer-vision-based analysis to recognize animals and humans.[15] A potential drawback of aerial surveillance is that it requires ultra-high-resolution cameras (due to long distances to the subjects) that are very expensive. Photos from the above may miss capturing important features needed for species detection. Another downside to this technique is that it only works with large species in open habitats (i.e., savannas and whales in the ocean). Manned planes are expensive besides leaving a large carbon footprint impacting the very environment that wildlife relies on to survive. Consequently, these techniques are very difficult to scale worldwide.

Monitoring of poaching threats via camera traps

Camera traps are a relatively inexpensive method for capturing high-quality photos of animals and can be installed on a large scale for wide regional coverage. Due to these characteristics, camera traps are a useful tool in combating poaching. Examples of these include the Resolve organization, which, with Intel, has developed TrailGuard AI,[16] an anti-poaching camera trap system. While it has a long battery life and is capable of running AI models on the device, it still costs around $800 to manufacture. Maintenance costs are relatively high due to the lack of modular, replaceable components.

Methods

Device requirements:

The project goals can be translated into specific requirements for the poacher activity detection device prototype. The requirements include cost requirements (cost to assemble, cost to replace/repair), physical requirements (weight, form factor), performance requirements (accuracy, power consumption), to functional requirements (motion detection, animal and human detection, alerting authorities based on different conditions). These requirements were formulated such that the devices can be deployed practically with fairly high density in high-risk poaching areas.

Cost requirements:

The device should be low-cost, preferably costing less than US $100 to make it viable to deploy in arrays to cover large areas of wildlife preserves and parks. It should consist of standard, widely available components that can be individually replaced in case of malfunction or failure to reduce the cost of maintenance.

Physical requirements:

The device needs to weigh less than 500 grams to make it very portable and install it in hard-to-reach places and can be carried by small drones. It also needs to have a compact form factor (not bigger than 10cm x 10cm) that makes it easy to camouflage for discrete installations that can go undetected by poachers to prevent vandalism and theft.

Power requirements:

The device should run on natural renewable power sources such as solar so it can be installed in remote areas as well as surveillance drones that may not have access to regular power supplies. It should be efficient in power consumption to continuously run on small solar panels. It should also incorporate motion sensors and take pictures only when motion is detected, thereby reducing the volume of data to be transmitted over long distances. In habitats where daylight is limited, such as dense forests, the devices could run on battery power, and they would need to be maintained by park rangers.

Functional requirements:

The device should be able to run AI algorithms locally and should leverage widely available, commodity hardware.

Software on the device should be able to process images and detect animals, humans, or weapons, analyze these images for conditions that indicate a poaching threat, and notify appropriate authorities. To differentiate between rangers and possible threats, the device should be able to perform facial recognition on any humans in the frame. Based on the threat level it detects, the device should be able to send near-real-time alerts (within 10 minutes) to park rangers so they can respond quickly and effectively. It should be capable of detecting animals and humans with at least 90% accuracy to be an effective tool.

Device design:

We elected to use a Raspberry Pi with GSM / GPRS / GNSS modem (Figure 1) as the device hardware since it meets the requirements of being low-cost, small, low-power (10 watts), and sufficiently compute-capable (1.5 GHz, quad-core CPU) to run AI models. The Raspberry Pi is widely available at a cost of US $35. Other devices were considered but rejected either due to insufficient computing power to run AI models, higher costs, or insufficient connectivity options. The Raspberry Pi also has some key advantages in creating a device that is optimized for performance and functionality. It can run Linux, which has a good cadence of security and functionality updates that can be applied remotely. It also has a set of pins that can be easily connected to a wide variety of sensors and programmed. Storage is on standard SD cards which are available widely and cheaply. SD cards can be imaged from the internet for instant-on capability for the system. The Raspberry Pi can run Python development and

DOI: 10.36838/v4i5.17

runtime environments along with all the associated AI libraries and models that are necessary for training and automated detection.

Figure 1: Raspberry Pi board

After deciding to use a Raspberry Pi as the device's computer, a prototype was built with a small solar power bank, a camera, an infrared motion sensor, and a GPRS modem. This entire prototype setup (Figure 2) weighed less than 500 grams and can be reduced with further prototyping. The exposure of the motion sensor and the camera can also be reduced greatly as we fine-tune the prototype. Smaller camera form factors are currently being explored for this purpose. The size of the structure could be substantially reduced as well in future iterations.

Figure 2: Device set-up.

The next step was camouflaging the device (Figure 3). The prototype was placed in a structure that looks like a bird's nest. The entire device was hidden inside with only the motion sensor and the camera exposed, and the "bird's nest" was placed on a tree branch and further camouflaged with foliage from the tree. The overall system can be hidden inside a tree trunk or among rocks by covering an optional enclosure in some soil etc. Of all the aspects of the device, camouflaging is perhaps the easiest to improve on, as we can change the outer casing of the device to match any environment.

Figure 3: Camouflaged device.

Algorithm design:

The core algorithm of the device consists of various components working together based on certain trigger events and the contents of the photos taken by the camera. Details of the overall workflow combining the algorithms can be found in Figure 4 below. A high-level description of the algorithm is as follows:

1. A photo is taken by the camera when the motion sensor is triggered due to motion in the environment.
2. The photo is analyzed for the presence of animals and/or humans as well as for the presence of any weapons.
3. Further analysis is done to classify the animal species and check whether the human is a local park ranger or an unknown individual.
4. The appropriate alert level is set triggering a potential alert to park/preserve authorities, e.g., if an unknown human with a weapon is detected, this triggers the highest poaching threat level (see detailed description of alert logic in a later section).

Software components:

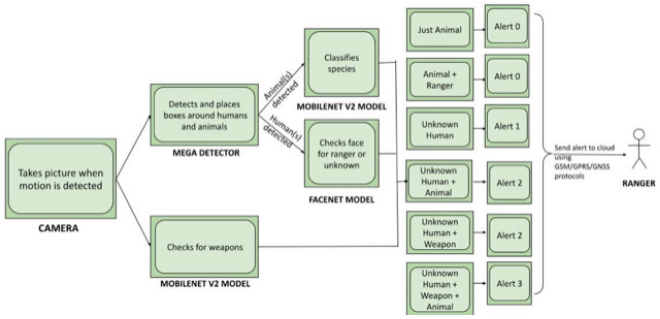

Figure 4: Device set-up.

Once this approach was decided on, the appropriate AI libraries needed to be pinpointed for each of the four components.

Human/animal/vehicle detection:

The MegaDetector[17] model was found to be best suited for detecting humans, animals, and vehicles in images. The MegaDetector model is specially trained for conservation biologists to identify humans and animals in camera trap images from a variety of ecosystems. MegaDetector is used in the current system to avoid running species classification and ranger identification on empty images, as well as to crop the relevant objects from the image to speed up downstream analysis (Figure 5).

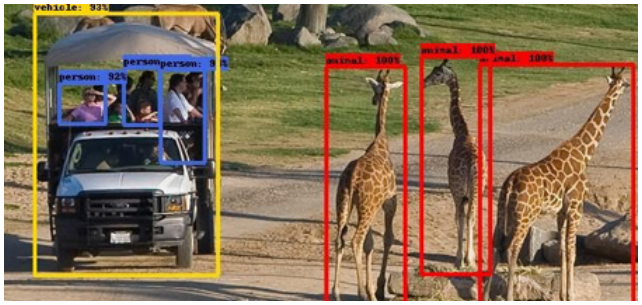

Figure 5: Detection of animals, humans, and vehicles with *MegaDetector*.

Weapon detection and species classification:

MobileNetV2 is a lightweight model pre-trained on weapons and animal species from the ImageNet database and is highly suited for our device here. Given the constraints of the high speed and low memory of the Raspberry Pi device, we selected the MobileNet v2[18] classifier based on an analysis done by Bianco *et al.*[19] Some of the other networks that were evaluated did not have versions compatible with the Raspberry Pi and were hence ruled out.

MobileNetV2 also serves the purpose of classifying animal species (Figure 6). It has very good accuracy for detecting a variety of animal species and new species are being added on an ongoing basis by researchers worldwide. At this time, MobileNetV2 was chosen for this purpose as it is widely available and is actively being enhanced by a large number of stakeholders.

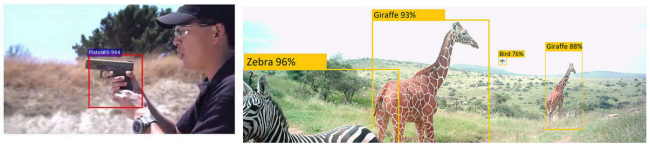

Figure 6: Detection of weapons and classification of species with MobileNetV2

Poacher/non-poacher classification:

To detect whether the human in the photo is a ranger or a potential poacher, we must perform face recognition. Identifying individual poachers is difficult since there is no readily available database of poachers. Even if such a database existed, it would become obsolete rapidly since one would need to add new poachers promptly.

To overcome these real-world constraints, we decided to train a face recognition system for known rangers, and mark everyone else as unknown. The database of rangers and other associated park personnel is much more reliable and can be kept up to date easily. The device identifies humans that are not poachers (rangers and other park officials). An alert is generated if the human is not recognized by the device, indicating a possible poacher. This approach can be further augmented in the future by adding photos of known poachers who pose a high threat to alert police authorities quickly in case such poachers are found by the device in a wildlife preserve.

For facial detection, the well-known FaceNet[20,21] model (Figure 7) was selected. FaceNet uses MTCNN with triplet loss for improved accuracy over other existing models. It is lightweight and only needs 2-3 images/person to train it to recognize the person. Furthermore, it is compatible with Raspberry Pi, making it highly suited for the poaching detection device.

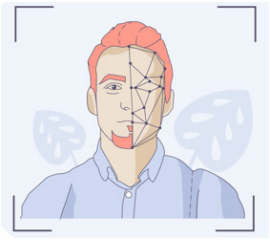

Figure 7: Detection of weapons and classification of species with MobileNetV2

Alert rules:

An important part of the overall design of the poaching detection device was designing the rules that would establish the threat levels and send out appropriate alerts (Figure 8). The logic for the alerting rules is based on the threat level perceived by the device per its analysis of the photo taken. It is as follows:

- If the photo contains only an animal, the threat level is 0, no alert needs to be sent.
- If the photo contains a human that is recognized as a ranger, the threat level is still 0, no alert needs to be sent.
- If the photo contains only a human that is unknown, the threat level is 1 and an alert needs to be sent that an unknown person is on the park / preserve land.
- If the photo contains an animal and an unknown human, the threat level is 2 and an alert needs to be sent that an unknown person is close to an animal and represents a poaching threat.
- If the photo contains an unknown human with a weapon, the threat level is 2 and an alert needs to be sent that an unknown person with a weapon is on the park / preserve land and represents a hunting / poaching threat.
- If the photo contains an animal with an unknown human with a weapon, the threat level is 3. This is the highest threat level, and an alert needs to be sent immediately that there is an imminent poaching threat.

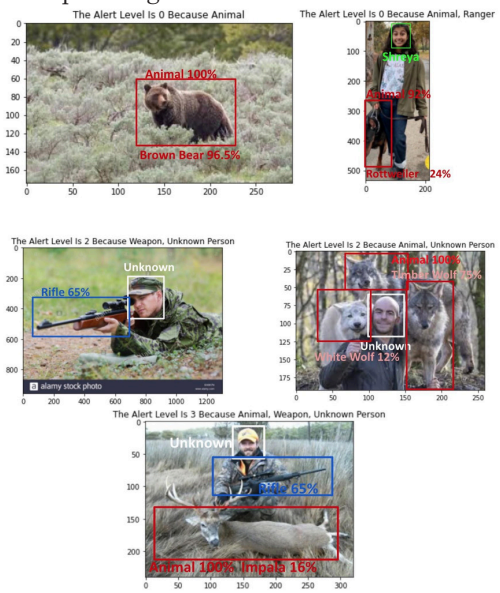

Figure 8: Examples of alert levels.

Results and Discussion

Each of the three components (MegaDetector, MobileNetV2, FaceNet) of the Protego device were separately tested for performance accuracy. The entire device was then tested for overall end-to-end performance. Performance metrics were chosen as appropriate for each component and are described in each section below.

Animal and human detection:

The MegaDetector network has been developed to detect three classes: animals, humans, and vehicles. It is used in our device for detecting the first two classes. Each class detection

DOI: 10.36838/v4i5.17

was tested separately, and three metrics were calculated for each:

- ROC-AUC (Receiver Operating Characteristics – Area Under the Curve), is created by plotting the true positive rate (TPR) against the false positive rate (FPR) at various threshold settings. The AUC measures the degree of separability between the classes being distinguished.
- Sensitivity or true positive rate refers to the proportion of positives correctly identified by the detector to the actual number of positives. It is a measure of how well a classifier can identify true positives.
- Specificity or true negative rate refers to the proportion of negatives correctly identified by the detector to the actual number of negatives. It is a measure of how well a detector can identify true negatives.

Testing was done on 204 negative images (no animals or humans in image), 58 images containing animals, and 35 images containing humans. These images were obtained from open-source images (including day/night captures from various angles) on the internet and were manually labeled. As seen in Figure 9, the ROC curves for both the animal and human classes are near perfect, with corresponding area under the curve (AUC), sensitivity, and specificity values shown below the plot.

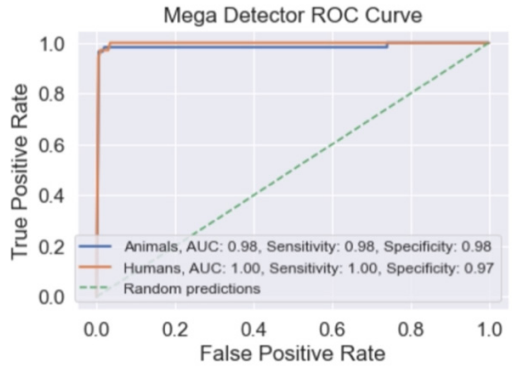

Figure 9: Mega Detector Test Results.

Weapon detection:

MobileNetV2 has been thoroughly tested for weapons detection accuracy by Mohebban[22] in the context of improving surveillance systems to address mass shootings. He tested the MobileNet detector on 152 images with no weapons, 152 images containing handguns, and 137 images containing rifles. Figure 10 shows the ROC curves plotted for all three classes. The AUC shows as greater than 90% for all classes indicating very good performance in detecting common weapons.

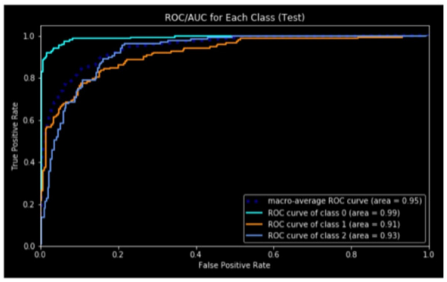

Figure 10: Weapons Detection Test Results.

Ranger identification:

The FaceNet code was tested on 25 "ranger" images (facial images of the author). When tested on a single image at a time, the FaceNet algorithm shows relatively poor accuracy (percent of images correctly identified). Hence a temporal filter was added which ran FaceNet on multiple consecutive images and the maximum detection value over those images is chosen as the final value. For example, if FaceNet identifies two out of three images as Ranger A, then the final output is set to Ranger A. Applying such a temporal filter significantly improves the accuracy of the algorithm as shown in Figure 11. Temporal filtering also improves robustness when there is target motion. An accuracy of over 90% was observed with multiple camera images. Device setting ensures successive capture of 5+ images to get to the highest accuracy.

Test Accuracy		
Single	Max of 3	Max of 5
72%	92%	96%

Figure 11: FaceNet test results.

Results

Finally, we measure the end-to-end performance of the entire device. Since the Protego device is built to classify the input image into four classes (alert levels), we use the confusion matrix as a metric to measure its performance.

A confusion matrix is a summary of prediction results on a classification problem. The number of correct and incorrect predictions are summarized with count values and broken down by each class. This is the key to the confusion matrix. The confusion matrix shows how a classification model can be confused when it makes predictions. It gives one insight not only into the errors being made by your classifier but more importantly the types of errors that are being made.

Figure 12 shows the confusion matrix generated for the Protego device. A set of 40 images were used to test the device, evenly divided among the four classes or alert levels (10 images per class). As seen in the figure, the device performed extremely well on the test images. Average accuracy came in at 92.5%. The most reassuring aspect of the results is that in cases where the device failed to correctly generate the alert level, it was only off by one level, thus not significantly impacting the outcome.

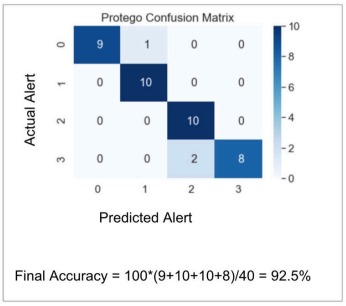

Figure 12: Overall device test results (92.5% accuracy).

Conclusion and future work

The proof of concept was successful: all design requirements were met, and accuracy was high under test conditions. This work sets up the foundation for a low-cost, open platform that can be greatly expanded upon by others. There is tremendous scope for improvement in the areas of performance and accuracy, which can be achieved by innovation and field testing of the device. We hope to build on and improve this device in the future.

For example, one of the future goals is to expand the algorithm to detect snares and other poaching tools so that rangers can remove them before any animals are caught. In addition to that, a night vision camera would help catch nighttime and low light poaching activities. While this will be more expensive than just an ordinary webcam, it will catch a much higher percentage of poachers. Other ideas include estimation of the proximity of poacher to animal and include information in the alert sent and connecting to the systems like Wildbook to effectively detect and identify individual animals to protect.

From the field deployment perspective, work needs to be done in deploying the device to high poaching risk areas and partnering with wildlife protection organizations to test the device.

Acknowledgements

I would like to thank Mr. Lester Leung, my Chemistry teacher and the school science fair coordinator for giving me the opportunity to conduct this research and represent my school at the Synopsis Science Fair. I would like to thank Prof. Tanya Berger-Wolf at the Ohio State University. She is the director and co-founder of the non-profit organization Wild Me, which utilizes computer vision for wildlife conservation. Dr. Berger-Wolf gave me the opportunity to work on a Wild Me project, which led to my inspiration to do this research. I would like to thank Prof. Charles Stewart at RPI for guiding me with my hypothesis and overall design goals.

References

1. The Devastating Effects of Wildlife Poaching - One Green Planet https://www.onegreenplanet.org/animalsandnature/the-devastating-effects-of-wildlife-poaching/ (accessed Nov 6, 2021)
2. 52 Eye-Opening Poaching Statistics You Must Know in 2021 https://petpedia.co/poaching-statistics/ (accessed Nov 6, 2021)
3. Anderson, B.; Jooste, J. Wildlife Poaching: *Africa's Surging Trafficking Threat, Africa Security Brief*, No. 28, May 2014
4. Everatt, K. T.; Kokes, R.; Lopez Pereira, C. Evidence of a Further Emerging Threat to Lion Conservation; Targeted Poaching for Body Parts. *Biodivers. Conserv.* **2019**, *28*, 4099–4114
5. Linkie, M.; Martyr, D. J.; Holden, J.; Yanuar, A.; Hartana, A. T.; Sugardjito, J.; Leader-Williams, N. Habitat Destruction and Poaching Threaten the Sumatran Tiger in Kerinci Seblat National Park, Sumatra. *Oryx* **2003**, *37*
6. De Sadeleer, N.; Godfroid, J. The Story behind COVID-19: Animal Diseases at the Crossroads of Wildlife, Livestock and Human Health. *Eur. j. risk regul.* **2020**, *11*, 210–227
7. Karesh, W. B.; Cook, R. A.; Bennett, E. L.; Newcomb, J. Wildlife Trade and Global Disease Emergence. *Emerging Infect. Dis.* **2005**, *11*, 1000–1002
8. Moore, J. F.; Mulindahabi, F.; Masozera, M. K.; Nichols, J. D.; Hines, J. E.; Turikunkiko, E.; Oli, M. K. Are Ranger Patrols Effective in Reducing Poaching-Related Threats within Protected
9. Over One Thousand Park Rangers Die in 10 Years Protecting Our Parks and Wildlife | News | Global Conservation https://globalconservation.org/news/over-one-thousand-park-rangers-die-10-years-protecting-our-parks/ (accessed Nov 6, 2021)
10. O'Grady, C, The Price Of Protecting Rhinos: Conservation has become a war, and park rangers and poachers are the soldiers, *The Atlantic*, **2020**
11. Shaffer, M. J.; Bishop, J. A. Predicting and Preventing Elephant Poaching Incidents through Statistical Analysis, GIS-Based Risk Analysis, and Aerial Surveillance Flight Path Modeling. *Tropical Conservation Science* **2016**, 9, 525–548
12. Outsmarting poachers https://www.seas.harvard.edu/news/2019/10/outsmarting-poachers (accessed Nov 6, 2021)
13. Fang, F.; Nguyen, T. H.; Pickles, R.; Lam, W. Y.; Clements, G. R.; An, B.; Singh, A.; Schwedock, B. C.; Tambe, M.; Lemieux, A. PAWS — A Deployed Game-Theoretic Application to Combat Poaching. *AIMag* **2017**, 38, 23–36
14. Home | Wild Me https://www.wildme.org/#/ (accessed Nov 6, 2021)
15. Chalmers, C.; Fergus, P.; Wich, S.; Montanez, A. C. Conservation AI: Live Stream Analysis for the Detection of Endangered Species Using Convolutional Neural Networks and Drone Technology. *arXiv* **2019**
16. Trailguard - RESOLVE https://www.resolve.ngo/trailguard.htm (accessed Nov 6, 2021)
17. CameraTraps/megadetector.md at master · microsoft/CameraTraps · GitHub https://github.com/microsoft/CameraTraps/blob/master/megadetector.md (accessed Nov 6, 2021)
18. Sandler, M.; Howard, A.; Zhu, M.; Zhmoginov, A.; Chen, L.-C. Mobilenetv2: Inverted Residuals and Linear Bottlenecks. *In 2018 IEEE/CVF Conference on Computer Vision and Pattern Recognition*; IEEE, 2018; pp. 4510–4520
19. Bianco, S.; Cadene, R.; Celona, L.; Napoletano, P. Benchmark Analysis of Representative Deep Neural Network Architectures. *IEEE Access* **2018**, 6, 64270–64277
20. Face Recognition with FaceNet and MTCNN – Ars Futura https://arsfutura.com/magazine/face-recognition-with-facenet-and-mtcnn/ (accessed Nov 6, 2021)
21. GitHub - R4j4n/Face-recognition-Using-Facenet-On-Tensorflow-2.X https://github.com/R4j4n/Face-recognition-Using-Facenet-On-Tensorflow-2.X (accessed Nov 6, 2021)
22. GitHub - HeeebsInc/WeaponDetection https://github.com/HeeebsInc/WeaponDetection (accessed Nov 6, 2021)

Author

Shreya Kakhandiki is a senior at Lynbrook High School in San Jose, CA. She is passionate about wildlife conservation, computer science, and public policy. She is fascinated by how these fields intersect and would like to pursue a career in wildlife conservation advocacy.

DOI: 10.36838/v4i5.17

IJHSR
ijhighschoolresearch.org
■ RESEARCH ARTICLE

Trends in Chronic Liver Disease Mortality Rates during the COVID-19 Pandemic

Shashvath Srivatsan
Oyster River High School, 55 Coe Drive, Durham, NH, 03824, USA; shashuvatsan@gmail.com

ABSTRACT: This study was performed to analyze trends in chronic liver disease and influenza during the COVID-19 pandemic. The CDC VSRR database and the CDC NHSS Pressroom Database were used to analyze chronic liver disease mortality rates from 2014 to 2020. Secondary, state level data was analyzed to look for potential correlation between mortality rates and "strictness" of COVID-19 restrictions. From 2014-2020, there was a slight increase in national yearly deaths with a large increase seen between 2019 and 2020. When analyzing 2019 to 2020 quarterly data, rates appear to increase rapidly after 2019 Q4. In the state-wide analysis, it was found that states with less restrictive COVID-19 guidelines had higher mortalities and mortality rates of chronic liver disease; Iowa saw the highest increase from 2019 Q4 to 2020 Q4 in chronic liver disease/cirrhosis mortality rates at 38.6%, followed by Nevada at 23.1%, and by Virginia at 22.1%. During the COVID-19 pandemic, national chronic liver disease mortality rates significantly increased. There seems to be an association between mortality rates and the "strictness" of COVID-19 restrictions at a state level.

KEYWORDS: Translational Medical Sciences; Disease Prevention; COVID-19; Pandemic; chronic liver disease.

■ Introduction

Chronic liver disease is the 9th leading cause of death in the US, and the 11th leading cause of death in the world.[1,2] It is in the top 20 causes of disability-adjusted years of life lost, and accounts for roughly 2% of the worldwide burden. It's yearly economic burden in the US is approximately 2.5 billion dollars.[3] The healthcare cost was $17,277 for non-cirrhosis patients, $22,572 for compensated cirrhosis patients, and $59,995 for patients in the final stages of liver disease, with an estimated national healthcare cost of 32 billion dollars annually.[4] Liver cirrhosis is the final stage in liver disease, which is the progressive deterioration of liver functions, caused by scar tissue replacing healthy tissue in the liver.[5,6] Although mortality rates vary, those in the moderate stages of liver disease have a 60% chance of survival over a two year period.[7] Those with compensated liver disease have a median life expectancy of 12 years, while those with decompensated liver failure have a median life expectancy of 2 years.[8] Most people afflicted by this condition in the US are ages 45-54.[9] Although there is no definitive cure for chronic liver disease, common treatments include: general lifestyle changes (reduced alcohol consumption, losing weight, changes in diet), certain medications, and in extreme cases, liver transplants.

On January 21st, 2020, the first case of COVID-19 in the contiguous 48 states was confirmed.[10] As of October 2021, there have been 44.9 million cases and 724,000 deaths due to COVID-19 in the United States.[11] The estimated projected total economic burden of COVID-19 is $16 trillion.[12] This is including but not limited to: economic losses due to cumulative and premature deaths, long-term complications, and mental health symptoms. It caused states to impose lockdowns, close schools, and enforce curfews, all of which negatively affected the population. During the ongoing COVID-19 pandemic, influenza rates have dropped significantly.[13] This study has explored the trends observed in chronic liver disease mortalities compared to influenza during the COVID-19 pandemic. It analyzed the effect of distinct levels of statewide COVID-19 restrictions on that state's liver disease mortality levels. By doing this, provided new insight into the direct correlation between chronic liver disease and COVID-19.

■ Methods

Data Source:

Data were acquired from the CDC VSRR Mortality Database, the CDC NCHS Pressroom Database, and the United States Census Bureau.[14-17] The CDC VSRR Mortality Database collects quarterly mortality data by age, state, sex, and cause of death from 2019-2020. The Census Bureau has been collecting population data since 1903 and was used to collect yearly populations from 2014-2020. Quarterly populations were not available, so quarterly mortality rates were derived using yearly populations. The data was divided into yearly deaths and mortality rates from 2014-2020, as well as quarterly mortality rates from 2019-2020 due to the lack of available quarterly data (for both deaths and mortality rates) from 2014-2018. Because this study used publicly available de-identified data, the study was determined to be exempt from Institutional Review Board review.

Inclusion Criteria:

Chronic liver disease/cirrhosis (abbreviated as LD) deaths as defined in the CDC VSRR Mortality Database were included. Influenza/pneumonia (referred to as influenza going forward) deaths were also extracted as a control. For each disease, yearly death counts and crude mortality rates are reported with quarterly data presented for only 2019-2020. Deaths were examined at a national level with secondary analysis including three specific states selected based on the

DOI: 10.36838/v4i5.18

severity of that state's COVID-19 restrictions. The included states were Iowa, Nevada, and Virginia, listed in order of increasing COVID-19 restrictions.[18]

Statistical Analysis:

The crude rates per 100,000 people were calculated using the CDC VSRR mortality data, the CDC NHSS mortality data, and the US Census Bureau population data. Linear regression analyses with Pearson correlation were performed to study mortality trends from 2014-2020. For the quarterly percent difference between 2019 Q4 and 2020 Q4, the CDC VSRR database has already calculated the statistical significance so additional analysis of the yearly Q4 difference from 2019-2020 was not performed, and the provided results were used.[15]

Results and Discussion

Both death counts and mortality rates as a result of COVID-19 were analyzed nationally and in three individual states (Iowa, Nevada, Virginia). This data is presented both yearly (from 2014-2020) and quarterly (from 2019 Q1-2020 Q4). According to Becker's Hospital Review, Iowa had the least restrictions, Nevada was ranked 29th least strict, and Virginia was the strictest of the states in terms of COVID-19 restrictions and policies.[18]

Chronic Liver Disease/Cirrhosis Mortality Rate Trends:

From 2014-2020, there was a slight increase in national yearly deaths with a large increase seen between 2019 and 2020 (Figure 1).

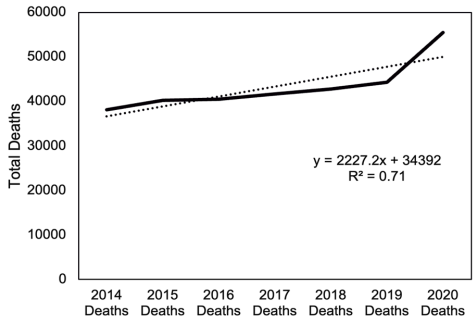

Figure 1: 2014-2020 yearly liver disease/cirrhosis crude deaths, β = 2227.2 deaths per year; R^2 = 0.71.

A similar trend is seen for mortality rates for 2014-2020, with a steady yearly increase, followed by a large spike in mortality rates in 2019-2020 (Figure 2).

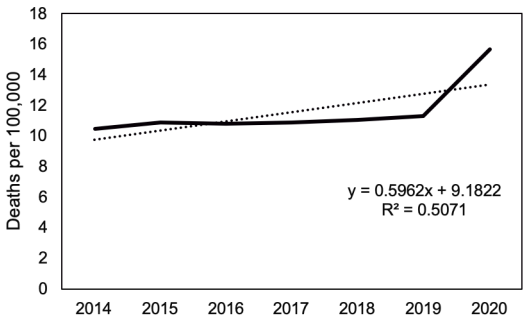

Figure 2: 2014-2020 yearly chronic liver disease/cirrhosis crude mortality rates, β = 0.5962 deaths per 100,000 per year.

When analyzing 2019 to 2020 quarterly data, rates appear to increase rapidly after 2019 Q4, corresponding with the start of COVID-19 (Figure 3).

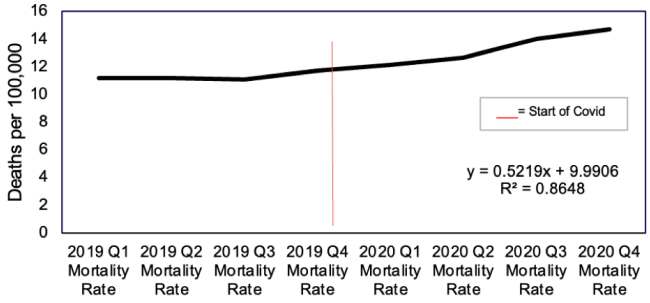

Figure 3: 2019-2020 quarterly chronic liver disease/cirrhosis crude mortality rates.

There is a statistically significant difference between 2019 Q4 and 2020 Q4 according to the CDC VSRR database, with a national percent increase of 22.0% (Table 1).[15]

Table 1: 2019 Q^4 to 2020 Q^4 chronic liver disease/cirrhosis crude mortality rate change by state.

	2019 Q4 Mortality Rate (Deaths per 100,000)	2020 Q4 Mortality Rate (Deaths per 100,000)	Percent Change from 2019 Q4 to 2020 Q4
Iowa	11.4	15.8	38.6*
Nevada	16.0	19.7	23.1*
Virginia	11.6	14.9	22.1*
US	14.1	17.2	22.0*

*Denotes statistical difference between 2019 Q4 and 2020 Q4 ($P < 0.05$) according to the CDC VSRR database.

The data from the three states showed that the total percent increase was inversely proportional to how strict that state was; Iowa saw the highest increase in chronic liver disease/cirrhosis mortality rates at 38.6%, followed by Nevada at 23.1%, and by Virginia at 22.1% (Table 1). This was although stricter states like Nevada and Virginia both maintained overall mortality rates that were higher than the least strict state - Iowa. The interquartile fluctuations in the data were represented by the quarterly mortality rates of each state (Figure 4).

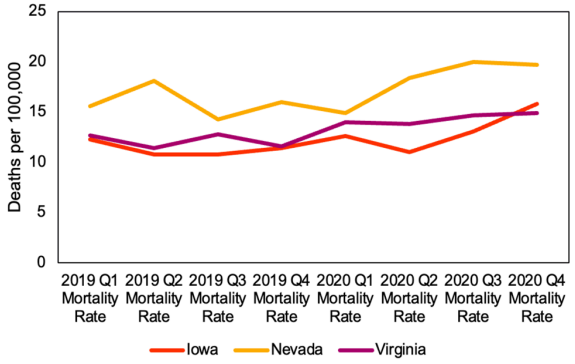

Figure 4: 2019-2020 quarterly chronic liver disease/cirrhosis crude mortality rates by state.

Influenza/Pneumonia Mortality Rate Trends:

During 2014-2020, there was an average annual decline in the national mortality rate of influenza/pneumonia. (Figure 5).

DOI: 10.36838/v4i5.18

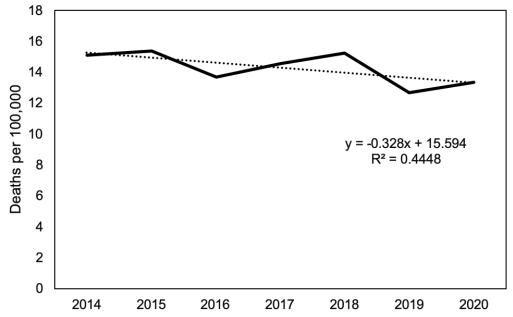

Figure 5: 2014-2020 yearly influenza/pneumonia crude mortality rates, β= -0.328 deaths per 100,000 per year.

Upon closer examination, the national mortality rate reached its minimum in 2019 Q3 and 2020 Q3, separated by a large peak in 2020 Q1, as well as a rapid increase and decrease in 2019 Q4 and 2020 Q2 respectively (Figure 6).

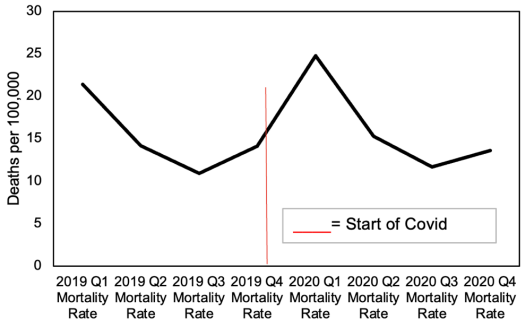

Figure 6: 2019-2020 quarterly influenza/pneumonia crude mortality rate.

This pattern of rapid increase and decrease was also present in the state data, as data from all three states (Iowa, Nevada, Virginia) showed a sharp incline in 2019 Q4, followed by a peak in 2020 Q1, and a sharp decline in 2020 Q2 (Figure 7).

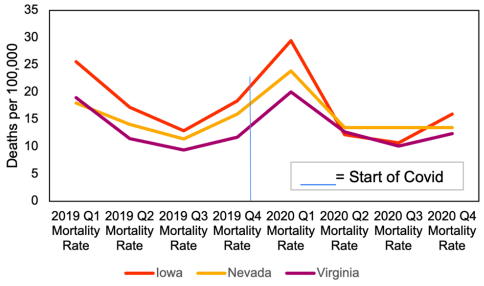

Figure 7: 2019-2020 quarterly influenza/pneumonia crude mortality rate by state.

The national mortality rate was 14.1 in 2019 Q4, and 13.6 in 2020 Q4, resulting in a percent decrease of 3.7%, a change that has statistical significance, as stated by the CDC VSRR database (Table 2).[15]

Table 2: 2019 Q4 to 2020 Q4 pneumonia/Influenza Crude Mortality Rate Change by State.

	2019 Q4 Mortality Rate (Deaths per 100,000)	2020 Q4 Mortality Rate (Deaths per 100,000)	Percent Change from 2019 Q4 to 2020 Q4
Iowa	18.4	16.0	13.0*
Nevada	16.0	13.5	15.6*
Virginia	11.7	12.4	6.0
US	14.1	13.6	3.7*

*Denotes statistically difference between 2019 Q4 and 2020 Q4 (P < 0.05) according to CDC VSRR database.

Iowa and Nevada had percent decreases of 13.0% and 15.6% respectively (both of which were statistically significant as stated by the CDC VSRR database), while Virginia had a percent decrease of only 6.0% (not statistically significant).[15]

In this comparative study of national and statewide chronic liver disease/cirrhosis and pneumonia/influenza trends over a 7-year period, it was found that LD mortalities followed a slightly upward sloping trend, followed by a sudden rise in 2019-2020. Influenza mortality numbers repeated a triannual pattern in which they rose to a peak, and then declined, which continued even after the start of COVID-19.

For example, LD increased by 22%, and influenza decreased by only 3.7% from 2019 Q4 to 2020 Q4. It has widely been discussed that influenza numbers were at an all-time low during the pandemic. Studies hypothesize that this was caused by precautions taken to slow the spread of COVID-19, such as practicing social distancing and wearing masks.[19] While literature points to reasons such as these for the decrease in influenza, there may be other reasons contributing to the significant increase in LD mortality rates. The abrupt increase in LD seems to line up with when COVID-19 first started (2019 Q4), indicating that there may be some association there. Three potential explanations for the increase in LD deaths arise: 1) direct impact of COVID-19 virus on the liver, 2) increased alcohol consumption during pandemic, 3) restricted availability of healthcare facilities during the pandemic and likely all 3 of these contributed to the 22.0% increase in LD deaths between 2019 Q4 and 2020 Q4.

Patients that have been hospitalized due to COVID-19 have been tested, and often show an increased level of liver enzymes such as alanine aminotransferase (ALT).[20] The buildup of enzymes like these temporarily damages the liver for the entire duration of the illness. For people unaffected by liver disease, this may not be a problem. But, for patients whose livers are already compromised due to a pre-existing condition such as chronic liver disease or cirrhosis, this may accelerate the progression of their illness. Following the infection of COVID-19, patients are at risk of increased rates of hepatic decompensation, acute liver failure, and death due to respiratory failure.[21]

After the initial progression of COVID-19 in early 2020, worldwide lockdowns and restrictions were implemented, resulting in an extended period of extreme stress and disconnectedness from other people. Around 60.1% of people have said that their alcohol consumption increased during the pandemic, 45.7% of whom quoted increased stress, and 30.1% of whom quoted increased boredom.[22] Unhealthy eating habits and disorders have seen reemergence during the pandemic, another potential cause of increasing LD mortalities. A second potential explanation for the increase in LD deaths was the restricted availability of healthcare facilities for those with non-COVID-19 related ailments. A pulse survey conducted in February 2021 by the US Department of Health and Human Services (HSS) found that surges in COVID patients caused most hospitals to restrict the number of patients with non-COVID related illnesses they could treat.[23] A lack of available nearby medical facilities may have prevented some LD patients from receiving treatments that they normally would have received in the

absence of a pandemic like this one. In addition to this, those with LD might have chosen to skip regular checkups for their liver condition out of the fear of the coronavirus itself, since hospitals themselves were flooded with COVID-19 patients. Unfortunately, it is not possible to tease out which and how much each of these three factors affected/caused the increase in LD deaths seen.

A state level analysis of LD deaths was also conducted. Out of the three states (Iowa, Nevada, Virginia) analyzed, COVID-19 restrictions of each state appear to influence the number of LD mortalities. Data from the three states show that states with less strict COVID-19 restrictions had higher percent increases of LD mortality rates from 2019 Q4 to 2020 Q4 (Iowa-38.6%, Nevada - 23.1%, Virginia- 22.1%). Iowa had the least restrictions and had a significantly higher percent increase in LD mortality rates from 2019 Q4 to 2020 Q4.[15] Although Virginia was the strictest in terms of COVID restrictions, its percent increase was only significantly lower than Iowa, not Nevada. This difference in COVID-19 restrictions between Iowa and Virginia shows the efficacy (and inefficacy) of the guidelines in stopping the increase of LD mortalities. In late 2020, Iowa lifted all bar/restaurant curfews, as well as social gathering limitations, which explains the increase in the mortality rate of Iowa in 2020 Q3 and 2020 Q4.[24] Until March 1st of 2021, Virginia residents had a mandatory curfew from midnight to 5 AM, indoor and outdoor gathering limits of 10 people, as well as 30% capacity for both indoor and outdoor entertainment.[24] This change in restrictions offers an explanation for the gradual increase in the LD mortality rate throughout the entirety of 2020 Q2. These restrictions, as well as how late Virginia eased up on restrictions compared to Iowa, highlight a connection between the LD mortality rate of a state with the severity of its COVID-19 guidelines. Las Vegas is Nevada's largest tourist attraction, and with borders closed, and statewide lockdowns enforced, tourism rates decreased notably. Specifically, visitor volume decreased by 55% compared to 2019, so a decrease in LD deaths was to be expected, offering a potential explanation for why Nevada and Virginia have similar mortality rate percent increases from 2019 Q4 to 2020 Q4 despite differences in COVID restrictions.[25]

Despite the associations reported here, there were some limitations that must be acknowledged. This data was collected using national databases, and with some numbers being self-reported by states, there is a level of internal bias to be expected, to preserve the stature of the state. Here, it was assumed that the differences in mortality rates of the states of interest is directly associated with the strictness of that state's COVID-19 restrictions, however there may be some overlooked variable(s) that may also be responsible for this finding. Although states were selected based on their COVID-19 guidelines, other variations between the states may be responsible for these numbers.

Conclusion

During COVID-19 pandemic, national chronic liver disease mortality rates significantly increased. There seemed to be an association between mortality rates and the "strictness" of COVID-19 restrictions at a state level. As new variants emerge and the pandemic continues, patients with chronic liver disease should be closely monitored and states should better incorporate this high-risk patient population into public health decision making.

Acknowledgements

I want to thank Shashwat Tripathi, my mentor, for his guidance throughout the process of my research. This would not have been possible without the assistance of my family members, to whom I extend my sincere gratitude.

References

1. Asrani, S. K.; Devarbhavi, H.; Eaton, J.; Kamath, P. S. Burden of Liver Diseases in the World. *Journal of Hepatology* **2019**, 70 (1), 151–171. https://doi.org/10.1016/j.jhep.2018.09.014.
2. What are the mortality rates for cirrhosis in the US? https://www.medscape.com/answers/185856-109599/what-are-the-mortality-rates-for-cirrhosis-in-the-us.
3. Desai, A. P.; Mohan, P.; Nokes, B.; Sheth, D.; Knapp, S.; Boustani, M.; Chalasani, N.; Fallon, M. B.; Calhoun, E. A. Increasing Economic Burden in Hospitalized Patients with Cirrhosis: Analysis of a National Database. *Clinical and Translational Gas troenterology* **2019**, *10* (7), e00062. https://doi.org/10.14309/ctg.0000000000000062
4. Economic cost of advanced liver disease https://www.sciencedaily.com/releases/2011/11/111107160142.htm.
5. Chronic Liver Disease/Cirrhosis https://www.hopkinsmedicine.org/health/conditions-and-diseases/chronic-liver-disease-cirrhosis.
6. Sharma, A.; Nagalli, S. Chronic Liver Disease https://www.ncbi.nlm.nih.gov/books/NBK554597/.
7. Holland, K. How Does Cirrhosis Affect Life Expectancy? https://www.healthline.com/health/cirrhosis-of-the-liver-life-expectancy.
8. Prognosis in Decompensated Chronic Liver Failure https://www.mypcnow.org/fast-fact/prognosis-in-decompensated-chronic-liver-failure/.
9. Definition & Facts for Cirrhosis | NIDDK https://www.niddk.nih.gov/health-information/liver-disease/cirrhosis/definition-facts.
10. AJMC Staff. A Timeline of COVID-19 Developments in 2020 https://www.ajmc.com/view/a-timeline-of-covid19-developments-in-2020.
11. Centers for Disease Control and Prevention. COVID Data Tracker https://covid.cdc.gov/covid-data-tracker/#datatracker-home.
12. CDC Library: COVID-19 Science Updates https://www.cdc.gov/library/covid19/scienceupdates.html?Sort=Date%3A%3Adesc.
13. Rubin, R. Influenza's Unprecedented Low Profile during COVID-19 Pandemic Leaves Experts Wondering What This Flu Season Has in Store. JAMA 2021. https://doi.org/10.1001/jama.2021.14131.
14. Bureau, U. C. State Population Totals: 2010-2019 https://www.census.gov/data/tables/time-series/demo/popest/2010s-state-total.html.9
15. Quarterly Provisional Estimates for Mortality Dashboard https://www.cdc.gov/nchs/nvss/vsrr/mortality-dashboard.htm#.
16. Stats of the States - Chronic Liver Disease/Cirrhosis https://www.cdc.gov/nchs/pressroom/sosmap/liver_disease_mortality/liver_disease.htm.
17. Stats of the States - Influenza/Pneumonia Mortality https://www.cdc.gov/nchs/pressroom/sosmap/flu_pneumonia_mortality/flu_pneumonia.htm.
18. States ranked by COVID-19 restrictions https://www.beckershospitalreview.com/rankings-and-ratings/states-ranked-by-covid-19-restrictions.html.

DOI: 10.36838/v4i5.18

19.Boston, 677 H. A.; Ma 02115 +1495-1000. A sharp drop in flu cases during COVID-19 pandemic https://www.hsph.harvard.edu/news/hsph-in-the-news/a-sharp-drop-in-flu-cases-during-covid-19-pandemic/.
20.Your Liver and (COVID-19) Coronavirus https://www.webmd.com/lung/coronavirus-liver-disease#:~:text=Link%20Between%20COVID%2D19%20and%20Your%20Liver.
21.Marjot, T.; Webb, G. J.; Barritt, A. S.; Moon, A. M.; Stamataki, Z.; Wong, V. W.; Barnes, E. COVID-19 and Liver Disease: Mechanistic and Clinical Perspectives. *Nature Reviews Gastroenterology & Hepatology* **2021**, 1–17. https://doi.org/10.1038/s41575-021-00426-4.
22.Grossman, E. R.; Benjamin-Neelon, S. E.; Sonnenschein, S. Alcohol Consumption during the COVID-19 Pandemic: A Cross-Sectional Survey of US Adults. *International Journal of Environmental Research and Public Health* **2020**, *17* (24), 9189. https://doi.org/10.3390/ijerph17249189.
23.Grimm, C. *Office of Inspector General Hospitals Reported That the COVID-19 Pandemic Has Significantly Strained Health Care Delivery Results of a National Pulse Survey*; **2021**.
24.Hargrove, A.; Graff, H. Gov. Northam announces changes to coronavirus restrictions, lifts stay-at-home curfew https://www.nbc12.com/2021/02/24/gov-northam-give-update-vaccine-rollout/.
25.CNN, B. K. F., Jessie Yeung and Adam Renton. Iowa governor lifts bar and restaurant curfews and removes social gathering limitations https://www.cnn.com/world/live-news/coronavirus-pandemic-vaccine-updates-12-16-20/h_ae605e4e12461155eb526ce5e1ccd6c1

Author

Shashvath Srivatsan is currently a senior at Oyster River High School in Durham, New Hampshire. He is interested in researching epidemiology and microbiology and aspires to pursue a career in medicine.

IJHSR
ijhighschoolresearch.org
RESEARCH ARTICLE

Smoking Associated Cancer Mortality Trends in Select Countries

Siddharth Srivatsan
Oyster River High School, 55 Coe Drive, Durham, NH, 03824, USA; siddhuvatsan@gmail.com

ABSTRACT: The objective of this paper was to examine potential factors contributing to smoking-related cancer mortality trends. Smoking associated cancer mortality data from 1970 to 2016 was extracted from the IARC Cancer Mortality Database and WHO Mortality Database. Data from the United States, Greece, Norway, Chile, and Colombia were analyzed due to variance in annual cigarette consumption per capita, the prevalence of current tobacco use, and geographical similarity. Norwegian males, Chilean males and females, and Colombian males and females saw decreases in cancer mortality rates during the study period; on the other hand, Greek males and females showed unchanged mortality rates, and Norwegian females showed a very slight increase in cancer mortality rates. United States age-standardized mortality rates (ASR) rose from 180.75 deaths per 100,000 persons in the year 1970 to the early 1980s before showing a steady and significant decline to 90.46 deaths per 100,000 persons in 2016. This study shows a strong correlation in developed countries (United States, Norway, and Greece) between advances in cancer therapies, early detection techniques, health screening, and public and legal health initiatives with a decrease in smoking-related cancer mortality rates. In developing countries (Chile and Colombia), widespread *H. pylori* testing, and treatment advances were found to be the main drivers of decreasing cancer mortality rates.

KEYWORDS: Translational Medical Sciences; Disease Prevention; Cancer Mortality; Smoking Related Cancer Mortality Trends; Causes of Smoking Related Cancer Mortality.

Introduction

Cancer continues to be one of the leading causes of death in the United States, being the 2nd leading cause of death in 2019 with 600,000 deaths or 21% of total deaths in the United States.[1] Cancer not only is a devastating disease, but it also carries a set of many economic burdens. In the United States alone, in 2017, cancer healthcare spending was 161.2 billion dollars, productivity loss from morbidity was 30.3 billion dollars, and the cost of premature mortality was 150.7 billion dollars.[2] Other countries such as China and South Africa face an average loss of 108,320 dollars per cancer mortality due to productivity losses.[2] These drastic economic burdens in the United States and other countries show the medical severities and economic effects of cancer.

An extreme risk factor for cancer is smoking, which results in bodily exposure to more than 70 proven carcinogenic chemicals that spread not only to the lungs but to other parts of the body.[3] The buildup of these carcinogenic chemicals can damage parts of the DNA that protect against cancer, increasing cancer risk.[3] Quitting smoking can significantly reduce one's risk of cancer by approximately 30-50% after ten years compared to smokers who continue to smoke.[4] Specifically, cancer of the lungs, trachea, and bronchus (cancers associated with smoking) was responsible for a staggering 139,682 of those deaths or roughly 5% of all deaths in the United States. The goal of this paper is to analyze certain smoking-related cancer mortality trends in select countries and their potential causes. This paper will provide better insight into the progression of cancer mortality in different countries. This research paper differs from other scientific literature as it examines potential historical, medical, and scientific factors contributing to smoking-related cancer mortality trends in several countries.

Methods

Data Source:

The data were collected from the IARC Cancer Mortality Database extracted from the WHO Mortality Database.[5] The Cancer Mortality data was sorted by type of cancer(s), sex (male or female), country, period, and age range. The database calculated yearly ASR per 100,000 persons based on the different search criteria including sex, country, and range. The periods of the data collected for all countries except Colombia were restricted from 1970 to 2016 due to inconsistencies in recorded cancer mortality data; the period for Colombia was restricted from 1984 to 2015 due to a lack of data before 1984 and after 2015. The age range for all the data from the IARC Cancer Mortality Database was restricted to ages 45 to 69 due to fully available data for that age range.[5] Data on the prevalence of current tobacco use among persons aged 15 years and older were also collected from the GHO health database.[6] The data were sorted by gender and different periods: 2000, 2005, 2010, and 2013 to 2017. Data on Annual Cigarette Consumption per person aged 15 or older were collected from *The Tobacco Atlas - 6th edition*, a report on various tobacco and smoking-related data and graphics.[7] Availability of data and statistics collected from the IARC Cancer Mortality Database, GHO Health Database, and The Tobacco Atlas were used to identify select countries.[5-7] The ICD-10 codes C00-14 (Lip, Oral Cavity, and Pharynx Cancer), C15 (Oesophagus Cancer), C16 (Stomach Cancer), and C33-34 (Lung Cancer) were extracted. Because this study used pub

DOI: 10.36838/v4i5.19

licly available deidentified data, the study was determined to be exempt from Institutional Review Board review.

Inclusion Criteria:

Countries were selected based on sufficient data availability and consistency, annual national cigarette consumption per capita rates, national tobacco usage statistics, and geographical proximity in the same continent. The five selected countries included the United States, Greece, Norway, Chile, and Colombia. Greece and Norway were selected based on the variance in prevalence of current tobacco use and geographical proximity in the same continent. Chile and Colombia were selected due to differences in annual tobacco usage and cigarette consumption per capita, and geographical proximity in the same continent. Annual mortality rates were grouped by sex (male or female), age (45 years to 69 years), and cause of death (type of cancer). Countries were generally classified by "low", "medium", and "high" smoking rates relative to the other country in the same continent in the selection process. Chile was classified as a high smoking rate country with 44.7% of its population aged above 15 years using tobacco and Colombia was classified as a low smoking rate country with 7.9% of its population aged above 15 years using tobacco. Similarly, Greece was classified as a high smoking rate country with 39.1% of its population aged above 15 years using tobacco and Norway was classified as a low smoking rate country with 18.4% of its population aged above 15 years using tobacco. Lastly, the United States was classified as a medium smoking rate country with 25.1% of its population aged above 15 years using tobacco.

Statistical Analyses:

Mortality rates were calculated by year, sex (male or female), and age (45 to 69 years). Linear regression analyses with Pearson correlation were performed to study mortality trends from 1970 to 2016 for the United States, Chile, Greece, and Norway and from 1984 to 2015 for Colombia.

Results and Discussion

Male smoking-related cancer deaths in the United States slightly increased from 180.75 ASR mortalities in 1970 to 201.34 ASR mortalities in 1986 and decreased to 90.46 ASR mortalities in 2016. A negative association was indicated by the line of best fit (Figure 1A). Female-smoking related deaths in the United States increased from 1970 to 1992 and gradually decreased from 1992 to 2016 (Figure 1B).

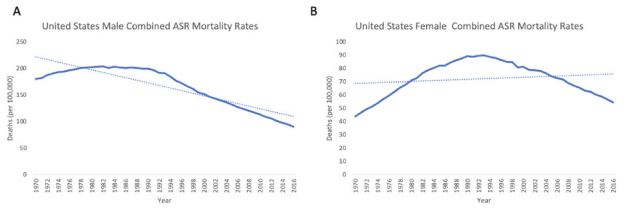

Figure 1: A) Male ASR Mortality rates per 100,000 for the United States are displayed from 1970 to 2016 (β= -2.445 ASR/year: R^2 = 0.7897). B) Female ASR Mortality rates per 100,000 for the United States are displayed from 1970 to 2016 (β= 0.1545 ASR/year: R^2 = 0.0263).

Male smoking-related cancer deaths in Greece stayed constant from 1970 to 2016, as shown by the strong association of the line of best fit (Figure 2A). Female-smoking related deaths in Greece showed a slight decline from 1970 to 2000 and an increase from 2000 to 2016 (Figure 2B). Male smoking-related cancer deaths in Norway showed a general decrease from 1970 to 2016, but female smoking-related cancer deaths in Norway showed a general increase from 1970 to 2016 (Figures 2C and 2D).

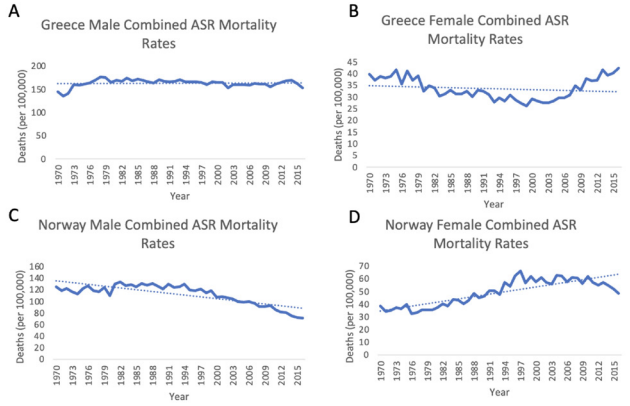

Figure 2: A) Male ASR Mortality rates per 100,000 Greece are displayed from 1970 to 2016 (β= 0.0255 ASR/year: R^2= 0.0019). B) Female ASR Mortality rates per 100,000 for Greece are displayed from 1970 to 2016 (β= -0.0585 ASR/year: R^2= 0.0298). C) Male ASR Mortality rates per 100,000 for Norway are displayed from 1970 to 2016 (β= -1.0204 ASR/year: R^2 = 0.6332). D) Female ASR Mortality Rates per 100,000 for Norway are displayed from 1970 to 2016 (β = 0.6247 ASR/year: R^2 = 0.7038).

Male and female smoking-related cancer deaths in Chile showed a general decrease from 1970 to 2016 (Figures 3A and 3B). Male and female smoking-related cancer deaths in Colombia also showed a general decrease from 1984 to 2015 (Figure 3C and 3D).

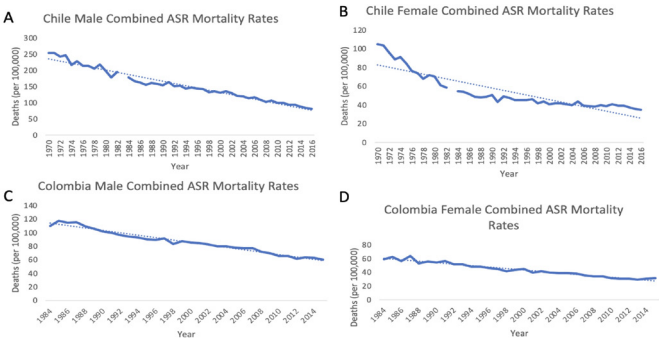

Figure 3: A) Male ASR Mortality rates per 100,000 for Chile are displayed from 1970 to 2016 (β= -3.4742 ASR/year: R^2= 0.9601). B) Female ASR Mortality rates per 100,000 for Chile are displayed from 1970 to 2016 (β= -1.2324 ASR/year: R^2= 0.7807). C) Male ASR Mortality rates per 100,000 for Colombia are displayed from 1984 to 2015 (β= -1.7672 ASR/year: R^2 = 0.9697). D) Female ASR Mortality Rates per 100,000 for Norway are displayed from 1984 to 2015 (β = -1.0636 ASR/year: R^2 = 0.9555).

The analysis of trends in the figures showed different periods of increasing and decreasing cancer mortality rates in the United States for both genders (Figure 1). The observed trends for Greece showed a steady cancer mortality rate for males and a decrease from 1970 to 2000 followed by an increase from 2000 to 2016 for females (Figure 2). The cancer mortality rate trends in Norway decreased for males and increased for females (Figure 2). Both male and female cancer mortality rate trends in Chile and Colombia showed a general decrease. Numerous factors including, but not limited

to, public health initiatives, improved cancer treatment in target areas, advertisement targeting of certain groups, and the prevalence of other medical issues may have had an impact on certain trends.

Smoking Associated Cancer Mortality Rates in the United States:

In general, in the United States, male cancer mortality rates showed a slight increase from 1970 to 1986 followed by a general decrease after 1986. However, notable negative trends were observed from the mid-1990s until 2016 in both males and females. This decreasing trend could be explained through the development of smoking public health initiatives that could have contributed to the significant decline in cancer mortality rates. In 1998, California became the first US state to pass a law banning smoking in bars; combined with other laws that banned smoking in restaurants and public places, California became the first US state to pass a statewide smoke-free air law that lowered the overall risk of secondhand smoke exposure.[8] The passing of this law was controversial but approval ratings for this law significantly increased within several years. Public statewide surveys in the state of California showed that the percentage of adults who supported the law 3 months after it passed was 46% and the percentage of adults who approved the law 2.5 years after it was passed was 62%.[9] After the passing of a similar smoke-free law in New York in 2003, various surveys showed that the number of all adults in New York who supported the law increased from 64% to 80% within 2 years of its implementation.[9] The overall increased support of smoke-free laws could have contributed to the decreasing smoking-related mortality rate in the United States.

Other contributing factors for the decreasing cancer mortality rates in the United States are the improvements in pre-existing cancer treatments, the development of new cancer treatments, and the improvements in cancer diagnosis. Chimeric antigen receptor T cells (CAR T cells) are genetically designed T cells that can be used as an immunotherapy cancer treatment that supplements the immune system. The first effective CAR T cells were developed in the early 2000s and developments through the 21st century have led to the creation of "armored" CAR T cells that can produce other molecules that suppress cancerous tumors.[10] Other improved cancer treatments include certain targeted therapies like Bevacizumab which can be used to treat non-small cell lung cancer (NSCLC), which makes up approximately 85% of all lung cancers, by inhibiting angiogenesis.[11] The usage and development of CAR T cells and Bevacizumab could have significantly contributed to the decline in smoking-related cancer mortality rates in the United States (Figure 1).

Lastly, improved lung cancer screening has contributed to reduced mortality rates in the United States. Low-dose helical computed tomography (LDCT) scans were shown in the National Lung Screening Trial, from 2002 to 2004, to reduce a lung cancer patient's chance of mortality by 15% to 20%.[12] The study showed that 3 fewer deaths occurred per 1000 people screened using LDCT scans, a significant statistic.[12] This dramatic breakthrough in lung cancer screening has continued to decrease potential smoking-related cancer mortality in the United States.

Female Smoking Associated Cancer Mortality Rates in the United States:

Female smoking-related cancer mortality rates had a significant increase from the 1970s to mid-1990s compared to male smoking-related cancer mortality rates during that period (Figure 1). A potential cause of this increase is advertisement and campaign targeting of women for smoking. Starting in the 1920s, tobacco companies created women-oriented cigarettes through the promotion of cigarettes as a form of weight control and femininity.[13] Furthermore, tobacco companies created tobacco products that gained popularity through association with the Women's liberation movement, such as the Virginia slims brand. Studies have shown that during the late 1960s and early 1970s, when these products were introduced, smoking rates in females significantly increased.[13] Since then, cigarette companies have launched cigarettes with reduced levels of tar, "reduced" nicotine, and even "purse" packs that specifically targeted women. This increased level of advertising and campaign targeting have affected women throughout the 20th century and could have been a significant factor affecting the increase in smoking-related cancer mortality rates for females from 1970 to the mid-1990s (Figure 1).

Smoking Associated Cancer Mortality Rates in South America – Chile and Colombia :

In the continent of South America, countries like Chile and Colombia have seen a dramatic decrease in smoking-related cancer mortality from the 1980s to 2016 (Figure 3). These decreasing smoking-related cancer mortality rates could have been significantly influenced by the improvement of cancer treatment in rural areas and the initial prevalence of *Helicobacter pylori* bacterial infections in South American countries. *H. pylori* bacteria can live in the digestive tract for many years and when it infects the stomach, it can cause painful stomach ulcers. To treat *H. pylori* infections, proton pump inhibitors (PPIs) can be used along with antibiotics like amoxicillin, clarithromycin, or metronidazole to have a high eradication rate of the *H. pylori* infection.[14] However, a combination of high rates of *H. pylori* and high smoking rates, as in Chile and Colombia, and a lack of proper treatment in the rural areas of South America could have contributed to the high stomach cancer mortality rates. Advances in *H. pylori* infection diagnosis tests such as the urea breath test and the HpSA test could have improved *H. pylori* diagnosis and infection recurrence in patients in Chile and Colombia, leading to reductions in smoking-related cancer rates. The urea breath test and HpSA tests are simple, non-invasive tests that can be used to diagnose *H. pylori* infections as well as to manage the recurrence of such infections.[15] Both tests have been used in combination with PPIs and antibiotics to provide a safer and more manageable approach to *H. pylori* infections in Latin America.[15] These improvements in diagnostic tests reduced the risk of *H. pylori* infection and could have potentially caused a decrease in smoking-related

DOI: 10.36838/v4i5.19

cancer mortality in Chile and Colombia from the 1980s to 2016 (Figure 3).

Smoking Associated Cancer Mortality Rates in Europe – Greece and Norway:

Countries in Europe, such as Greece and Norway, seem to show varying trends in cancer mortality rates which could be due to the different public responses to smoking legislation. While Norway shows a slight mortality rate decline for males and a slight mortality rate increase for females, Greece shows a constant trend for males and a curved trend for females (Figure 2). These trends may be due to the more restrictive smoking legislation in Norway and the public criticism and disobedience of smoking legislation in Greece. In 2009, Greece banned smoking in indoor places and started to institute fines, however, this was met with criticism due to the influence of smoking culture in Greece.[16] The legislation was weakly enforced and smoking still exists in many common places such as restaurants and bars in Greece, potentially contributing to the constant and curved trends of cancer mortality rates in Greece (Figure 2).[16] Tobacco control legislation has existed in Norway for over 40 years starting with the Norwegian Tobacco Act in 1975 that banned tobacco advertising and required health warnings on tobacco packaging.[17] Since then, other strict legislation was enacted that banned retail advertising of tobacco, totally banned smoking in restaurants and bars, and increased restrictions on tobacco product advertising.[17] Such strong legislation in Norway could have potentially contributed to the decreasing smoking mortality trend in Norway and the constant and curved mortality trends in Greece (Figure 2).

Limitations:

Limitations include the varied availability of statistical cancer mortality data, internal bias, and confounding variables. The extracted cancer mortality data was based on the overall cancer mortality of a certain type of cancer, not exclusively cancer caused by smoking. For example, it is predicted that 80-90% of lung cancer mortalities are linked to smoking, so the extracted lung cancer mortality data is assumed to have been caused primarily by smoking, although it is not possible to separate the exact causes of the mortality data.[18] Lastly, confounding variables could be responsible for the presented trends in the results. While factors such as public health initiatives, smoking legislation and smoking advertisement targeting of women may be potential factors affecting cancer mortality trends, there may be other confounding variables that are not accounted for in this paper.

Conclusion

From 1970 to 2016, the selected countries showed declining or unchanging cancer mortality rates. This study shows a strong correlation in developed countries between advances in cancer therapies, early detection techniques, and screening and public and legal health initiatives and the decrease in smoking-related cancer mortality rates. In developing countries, widespread *H. pylori* testing, and treatment advances were found to be the main drivers of decreasing cancer mortality rates. The application of similar factors in other cancers could give clinicians and researchers insight into potential mechanisms to decrease non-smoking-related cancer mortality rates.

Acknowledgements

I would like to thank Shashwat Tripathi for his guidance and mentorship in authoring this research paper and my parents for all their encouragement and support. Additionally, I would like to thank all my teachers for their guidance and inspiration throughout high school.

References

1. Centers for Disease Control and Prevention. Leading Causes of\\ Death https://www.cdc.gov/nchs/fastats/leading-causes-of-death.htm
2. The Economic Burden of Cancer https://canceratlas.cancer.org/taking-action/economic-burden/.
3. Cancer Research UK. How does smoking cause cancer? https://www.cancerresearchuk.org/about-cancer/causes-of-cancer/smoking-and-cancer/how-does-smoking-cause-cancer.
4. Cigarette Smoking: Health Risks and How to Quit (PDQ®)–Patient Version - National Cancer Institute https://www.cancer.gov/about-cancer/causes-prevention/risk/tobacco/quit-smoking-pdq#:~:text=People%20who%20quit%20smoking%20cut.
5. WHO cancer mortality database (IARC) https://www-dep.iarc.fr/WHOdb/WHOdb.htm.
6. GHO https://www.who.int/data/gho.
7. Tobacco Atlas https://tobaccoatlas.org/.
8. Cancer Progress Timeline https://www.asco.org/research-guidelines/cancer-progress-timeline./
9. CDCTobaccoFree. Smokefree Policies Reduce Smoking https://www.cdc.gov/tobacco/data_statistics/fact_sheets/secondhand_smoke/protection/reduce_smoking/index.htm.
10. CAR T Cells: Timeline of Progress https://www.mskcc.org/timeline/car-t-timeline-progress. 2019;37(19):1666-1676. doi:10.1200/JCO.18.01579
11. Targeted Drug Therapy for Non-Small Cell Lung Cancer https://www.cancer.org/cancer/lung-cancer/treating-non-small-cell/targeted-therapies.html.
12. National Lung Screening Trial (NLST) - National Cancer Institute https://www.cancer.gov/types/lung/research/nlst.
13. A Lifetime of Damage; 2021. https://www.tobaccofreekids.org/assets/content/press_office/2021/womens-report.pdf
14. Sugiyama, T. Proton Pump Inhibitors: Key Ingredients in Helicobacter Pylori Eradication Treatment. Proton Pump Inhibitors: A Balanced View 2013, 32, 59–67. https://doi.org/10.1159/000350631.
15. Rollan, A. Management of Helicobacter Pylori infection in Lat in America: A Delphi Technique-Based Consensus. World Journal of Gastroenterology 2014, 20 (31), 10969. https://doi.org/10.3748/wjg.v20.i31.10969.
16. Rafenberg, M. In Greece, smoking is alive and kicking despite bans https://medicalxpress.com/news/2019-05-greece-alive.html.
17. LTobacco Control in Norway https://www.helsedirektoratet.no/english/tobacco-control-in-norway.
18. What Are the Risk Factors for Lung Cancer? | CDC https://www.cdc.gov/cancer/lung/basic_info/risk_factors.htm#:~:text=Smoking.

Conclusion

Siddharth is a senior at Oyster River High School in Durham, New Hampshire. He is extremely interested in biology and biotechnology and hopes to have a career in science or medicine in the future.

IJHSR
ijhighschoolresearch.org
■ RESEARCH ARTICLE

Effects of Different Music Genres on Concentration Time of Children with Learning Disabilities (LD)

Krittin Hirunchupong, Nannaphat Suwannakul,
Ruamrudee International School, 6 Soi Ramkhamhaeng 184, Khwaeng Min Buri, 10250, Thailand; krittinh23@gmail.com

ABSTRACT: This study aimed to introduce new treatment options through investigating the type of music that is the most effective in extending the concentration time of students. Four groups were established in this study: control, instrumental music, classical music, and pop music groups. The qualitative data was obtained through an online questionnaire assessed by an art teacher monitoring the students, while the quantitative data was collected through photographs of each child's drawings under different experimental group stimulus. Then, they were interpreted by Dr. Supalak Khemthong, an assistant professor with a doctoral research degree in occupational therapy at Mahidol University, Bangkok. All the interpretations were based on The Individualized Music Therapy Assessment Profile (IMTAP), an in-depth assessment protocol developed by Holly Baxter. The results from this study suggested that the three genres of music impacted students in different ways. Overall, instrumental music was the most effective tool to increase the concentration time, while pop music was the least effective and led to some deterioration in concentration.

KEYWORDS: Behavioral and Social Sciences; Physiological Psychology; Music Therapy; Children; Learning Disabilities.

■ Introduction

The number of students with learning disabilities (LD) has been continuously increasing for the past decade in Thailand.[1] Although it is well established that LD cannot be cured, students can seek therapy to manage and alleviate symptoms.[2,3] LD are a set of disorders that affect a child's ability to understand instructions, speak or write fluently, perform mathematical calculations, coordinate movements, or concentrate on a task for a certain amount of time.[3] Students with LD often struggle to interact with others and to perform with their peers academically. In Thailand, the number of students with learning disabilities in schools increased substantially from approximately 60,000 in 2015 to an estimate of 250,000 in 2021. Furthermore, these numbers only accounted for the children enrolled in schools. There are many neglected children that have parents who cannot afford their education nor the special care that they need.[1]

However, music and art activities can be utilized to help those children to a certain extent. For people with LD, music therapy has been proven useful in language, speech, auditory, and learning recovery.[3] Similar psychological studies corroborate that music therapy has the potential to improve the communication, behavior, and emotional skills of neuro-diverse adolescents.[4] Additionally, further case studies that investigate the effectiveness of music therapy consistently agree that music therapy enables prolonged attention span and an overall positive behavior.[5] Despite this, the effect of various types of music have yet to be robustly examined. Hence, the purpose of this study is to compare the effectiveness of instrumental, classical, and pop music on extending the concentration time of children with LD.

■ Methods

Study group:

The study group consisted of 5 children residing at Camillian Home for Disabled Children with learning disabilities (LD) medical diagnosis. Every participant's name was abbreviated to protect their privacy as seen in Table 1.

Table 1: Patient identification and general information

Name	Age	Gender
C.P.	22	Female
P.P.	16	Male
Pi.P.	16	Male
A.P.	18	Male
C.S.	9	Male

Media:

The music content utilized in this study was produced by a group of fifteen student volunteers. All volunteers were informed that the contents would be used to investigate the impact of music on concentration time of children with LD.

Instrumental Musics:

Instrumental music utilized in the study were piano recordings of Thai pop songs that were slow in tempo (performed slower than 100BPM) and consisted of a small dynamic range (performed between mezzo piano to mezzo forte). The recordings were posted on the Musical.Remedy__ youtube channel (https://www.youtube.com/channel/UCoXFy8RRxf5T1pdliaOf21A). The instrumental music did not contain lyrics but did contain a melody. The duration of the record-

DOI: 10.36838/v4i5.20

ings was 45 minutes. They were played for the entire time duration when the children were completing their assigned tasks.

Classical Music:

Classical music utilized in the study were piano and cello recordings of classical pieces. They ranged in tempo (performed from below 100BPM to above 150BPM) and dynamics (performed between pianissimo and fortissimo). The recordings were posted on the Musical.Remedy__ youtube channel (https://youtube.com/playlist?list=PL2gm7sWK2oiSH04p5UI1CkEpBeBErJ6DR). The classical music did not contain lyrics but did contain a distinct melody. The duration of the recordings was 45 minutes, and each instrument had approximately equal duration of performance time. They were played for the entire time duration when the children were completing their assigned tasks.

Pop Music:

Pop music utilized in the study included vocals, drums, electric and acoustic guitar recordings of Thai pop songs. They were fast in tempo (performed above 120 BPM) and consisted of a large dynamic range. The pop music recordings were posted on the Musical.Remedy__ youtube channel (https://youtube.com/playlist?list=PL2gm7sWK2oiQci5G-9dX-H2Bh1MPwyJDyt). The pop music recordings did contain lyrics and had a distinct melody. The duration of the recordings was 45 minutes, and each instrument had approximately equal duration of performance time. They were played for the entire time duration when the children were completing their assigned tasks.

Art Activity:

Each child in the study was assigned to draw and color an image of their choice. The approximate time for this task was 30-40 minutes. The art activity was kept as a controlled variable while the music played for each art session was instrumental music, classical music and pop music, respectively. Then, the drawings were collected and analyzed by a therapist later in the study.

Control Group:

The first music and art session conducted was a control group. Each child was assigned to draw and color an image of their choice in an art room. However, they were working without music playing. Drawings from those sessions were collected for further analysis by Dr. Supalak Khemthong, using IMTAP as reference.

Experimental Groups:

The second, third, and fourth music and art session conducted were experimental groups 1, 2, and 3, respectively. In all of the experimental groups, each child was assigned to draw and color an image of their choice in the same art room. Then, the art teacher played an instrumental, classical, and instrumental pop music recording for children in the order listed above while they were completing the tasks. Their changes in concentration span, behavior, and artwork were documented.

Data Collection:

The qualitative data of the experiment were the interpretations of each child's drawings from the control group, experimental group 1, experimental group 2, and experimental group 3 in comparison to each other in a single-blind study.

The quantitative data for the experiment was collected through a survey, in which the caretaker took for each child. Following the questions that asked for the child's name, age and medical condition(s), questions asked to assess the improvement in concentration time included:

a. Did the child complete the task assigned?

This question investigated the child's ability to maintain concentration to achieve a task.[6] An improvement in task completion was reflected when the child did not complete the task assigned in the control group but completed the task in any experimental group.

b.Did the child change their activity while completing the tasks assigned?

The question investigated whether the child is multitasking, which was a sign of low concentration in the assigned activity. An improvement in concentration was reflected when the child changed activity in the control group but did not change their activity while completing the tasks assigned in the experimental group.[6]

c. What is the total time in minutes that the child spent on the tasks assigned?

The question investigated an increase in concentration span of each child. An improvement in concentration was reflected when the child's total time spent on the tasks in the control group was less than the child's total time spent on the tasks in the experimental group.[6]

Results and Discussion

Control group:

All of the children completed their tasks even in the control group. However, 60% of the children multitasked when they completed the activity without background music, which was a sign of concentration loss. The total time spent on their tasks varied, which could be influenced by other factors such as their age and their stages of LD.[4,7,8] Hence, the total concentration time was not compared between children, but compared between the same child in different experiment groups.

The qualitative data interpretations from the control group by Dr. Supalak Khemthong were translated and reported as seen in Table 2.

Table 2: Qualitative data interpretations from the control group.

Student	Interpretation	Positive or Negative Emotions
C.P.	The drawing reflected her positive emotions. The picture included 2 people and a clear blue sky which indicated optimism.	Positive
C.S.	The picture included a military officer, weapons and people, which indicated a sign of worry and stress.	Negative
P.P.	There were traces of erasing which indicated a fear of failure in this child. There were also repetitive lines over the same area which indicated stress.	Negative
Pi.P.	Similarly, there were repetitive lines, mostly repeated over the same area which indicated stress. The drawing was unfinished, which indicated over-thinking and a sensitive emotion.	Negative
A.P.	There was an imbalance of body parts in the drawing (disproportionate arms to legs) which indicated over-thinking and stress.	Negative

Instrumental music:

All of the children completed the tasks assigned both in the control group and experimental group 1. Hence, there was no difference in the children's ability to maintain concentration to achieve a task. Sixty percent (60%) of the children showed less multitasking when they were exposed to instrumental music compared to the control group, which was a sign of higher concentration (Figure 1). Eighty percent (80%) of the children showed a 15–20-minute increase in the total time spent on their assigned tasks when exposed to instrumental music compared to the control group, which reflected an improvement in attention span (Figure 2).

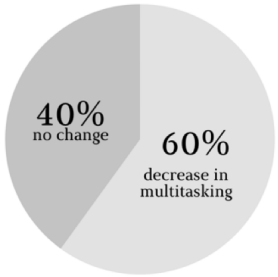

Figure 1: A pie chart illustrating a decrease in multitasking.

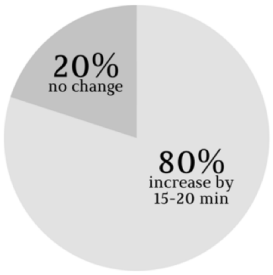

Figure 2: A pie chart illustrating an increase in the total time children spent on their assigned tasks by 15-20 minutes.

The qualitative data interpretations from the instrumental music session by Dr. Supalak Khemthong were translated and reported as seen in Table 3.

Table 3: Qualitative data interpretation from instrumental music sessions.

Student	Interpretation	Positive or Negative Emotions
C. P.	The drawing reflected her positive emotions. There were colorful flowers which indicated optimism.	Positive
C. S.	The drawing reflected his fearful, stress and worried emotions.	Negative
P. P.	The drawing was clearer and there was less traces of erasing visible. It can be interpreted that he had a clarity of thought. Additionally, less erasing meant that he planned ahead, which indicated that he had an optimistic, positive and effective approach to his task.	Positive
Pi. P.	Similarly, the drawing was clearer and there were less traces of erasing visible. It can be interpreted that he had a clarity of thought. Additionally, less erasing meant that he planned ahead, which indicated that he had an optimistic, positive and effective approach to his task.	Positive
A. P.	The drawing was heavily skewed to one side, which reflected over-reasoning and over-thinking. The drawing reflected loneliness, lack of self-confidence and poor self-esteem.	Negative

Classical music:

All of the children completed the tasks assigned both in the control group and experiment group 2. Hence, there is no difference in the children's ability to maintain concentration to achieve a task. Sixty percent (60%) of the children showed less multitasking when they were exposed to classical music compared to the control group, which was a sign of higher concentration (Figure 3). Eighty Percent (80%) of the children showed a 5–10-minute increase in the total time that they spent on their assigned tasks when exposed to classical music compared to the control group, which reflected an improvement in attention span (Figure 4).

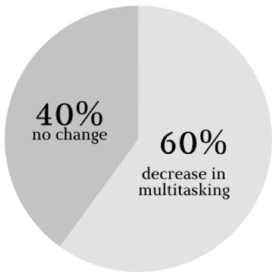

Figure 3: A pie chart illustrating a decrease in multitasking.

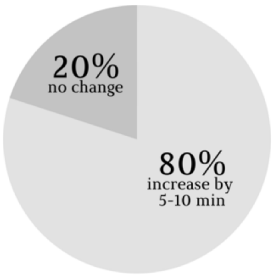

Figure 4: A pie chart illustrating an increase in the total time children spent on their assigned tasks by 5-10 minutes.

The qualitative data interpretations from the classical music session by Dr. Supalak Khemthong were translated and reported seen in Table 4.

Table 4: Qualitative data interpretation from classical music sessions.

Student	Interpretation	Positive or Negative Emotions
C.P.	The drawing was hyper focused on a single person. The sky depicted in the image was unclear. There were dust pathogens floating around a person. The elements combined indicated worry and stress during the pandemic.	Negative
C.S.	The blue color utilized in the drawing indicated that he felt supported and had a hopeful emotion.	Positive
P.P.	Similarly, the blue color utilized in the drawing indicated that he felted supported and had a hopeful emotion.	Positive
Pi.P	The drawing was very similar to previous ones, indicating major artistic limitations. The harsh lines indicated he was coloring in a fast and accentuated manner. It indicated a sensation of worry and stress.	Negative
A.P.	The drawing was very rigid, robotic and lack flexibility. This reflected his limited creativity and could be interpreted as a lack of self-confidence.	Negative

Pop music:

All of the children completed the tasks assigned both in the control group and experimental group 3. Hence, there is no difference in the children's ability to maintain concentration to achieve a task. Twenty Percent (20%) of the children showed more multitasking when they were exposed to pop music compared to the control group, which was a sign of

DOI: 10.36838/v4i5.20

lower concentration (Figure 5). Forty Percent (40%) of the children showed a 5 to10-minute increase, while 20% showed a 10–15-minute increase in the total time that they spent on their assigned tasks when exposed to pop music compared to the control group, which reflected an improvement in attention span. However, 40% of the children showed a 5–10-minute decrease in the total time spent on their assigned tasks, which reflected a deterioration in attention span (Figure 6).

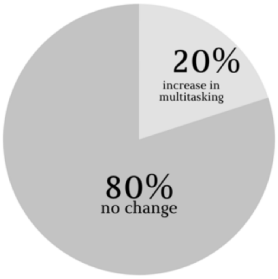

Figure 5: A pie chart illustrating an increase in multitasking.

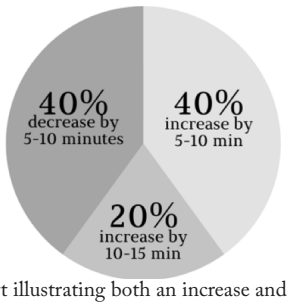

Figure 6: A pie chart illustrating both an increase and decrease in the total time children spent on their assigned tasks.

The qualitative data interpretations from the pop music session by Dr. Supalak Khemthong were translated and reported as seen in Table 5:

Table 5: Qualitative data interpretation from pop music sessions.

Student	Interpretation	Positive or Negative Emotions
C.P.	Birds flying towards the horizon indicated that she felt liberated and free. However, the unfinished ship that was drawn on the same level as the coconut tree indicated some signs of stress.	Negative
C.S.	The drawing was unclear, the lines were thin and there was very light color accentuation. The drawing indicated sensations of loneliness, lack of self-confidence and poor self-esteem.	Negative
P.P.	There were only two colors in the drawing: red and black, which depicted an imbalance of emotions. It indicated that he felt too distracted.	Negative
Pi.P.	The drawing was very similar to previous ones, indicating major artistic limitations. The drawing was also in black and white, which indicated close-mindedness.	Negative
A.P.	The drawing was very similar to previous ones, indicating major artistic limitations. The drawing was skewed to the left, which indicated over-reasoning and over-thinking. The isolation of the person in the drawing indicated loneliness, lack of self-confidence and poor self-esteem.	Negative

■ Conclusion

In this study, it was determined that different types of music played impacted the concentration time, some positively and some negatively, of children with LD. Quantitative data clearly reflected that instrumental music extended the concentration time of 80% of the children by 15-20 minutes, the most out of the three music genres. The results from the qualitative data corroborated to the findings to a certain extent because two out of five children shifted from reflecting negative emotions to positive ones in their drawings based in Dr. Supalak Khemthong's interpretations. This concludes that instrumental music can be an effective tool to increase the concentration time of children with LD when they need to focus on a task for 30-40 minutes.

The quantitative data reflected that classical music extended the concentration time of 80% of the children by 5-10 minutes, the second most out of the three music genres. The results from the qualitative data were highly individualized. Ms. C.P. deteriorated from expressing positive emotions in the control group to negative ones in the classical music group. However, two other children shifted from reflecting negative emotions to positive ones in their drawings. Hence, the quantitative data and the qualitative data did not corroborate. Additionally, the study's population size was highly limited which could lead to uncertainty with the results and the inability to eliminate outliers. This concludes that classical music can be an effective tool to increase the concentration time of some children with LD, but each child's response to classical music is highly individualize and need to be taken into consideration.

The quantitative data reflected that pop music both extended and decreased the concentration time of the children by 60% and 40%, respectively. Thus, the effectiveness in increasing the concentration time of children of pop music ranked last among the categories. The results from the qualitative data also corroborated to the findings because four out of five children's drawings reflected negative emotions for both the control group and the pop music group. Additionally, Ms. C.P. deteriorated from expressing positive emotions in the control group to negative ones in the pop music group. This concludes that pop music was not an effective tool to increase the concentration time of most children with LD and should be avoided when a child needs to focus on a task for 30-40 minutes.

■ Acknowledgements

The authors would like to express sincere gratitude to Asst. Prof. Dr. Supalak Khemthong for his qualitative data interpretations for this research. We also would like to thank Dr. Somrak Choovanichvong for her guidance and mentorship in the experimental design throughout this research.

■ References

1. Tongsrirag, T. Learning Disorder (ความบกพร่องในการเรียนรู้). Bangkok, Thailand: Siriraj Hospital Publishing, 2018.
2. Watson, T. Music Therapy with Adults with Learning Disabilities. New York, NY: Taylor & Francis, 2007.
3. White Swan Foundation. Learning Disability. New York, NY. https://www.whiteswanfoundation.org/disorders/neurodevelopmental-disorders/undiagnosed-autism-in-adulthood, 2015.
4. Brodeur, J. Music as a therapeutic tool to increase social skills in the learning disabled child. Proceedings from the sixteenth annual conference of the Canadian Association for Music Therapy (pp. 112-114). Sarina, Ontario: Canadian Association for Music Therapy, 1990.
5. Calussen, D., & That, M. Music as a mnemonic device for children

with learning disabilities. Canadian Journal of Music Therapy, 1997..
6. Gold, C., Voracek, M., & Wigram, T. *Effects of music therapy for children and adolescents with psychopathology: A meta analysis.* Journal of Child psychology and Psychiatry, 2004..
7. Hyde, K.L., Lerch, J., Norton, A., Forgeard, M., Winner, E., Evans, A.C., & Schlaug,G. *The Effects of Musical Training on Structural Brain Development: The New York Academy of Science*s, 2009.
8. Kemp, P., Smith, M., Segal, L. *Learning Disabilities and Disorders*. Massachuseetts, MA: Harvard Health Publishing, 2020.

Author

Krittin Hirunchupong is a 11th grade student studying at Ruamrudee International School (RIS) located in Bangkok. He is a multi-instrumentalist and has a diploma (ATCL) in both piano and cello. He wants to utilize his talents and his knowledge of music to help those with mental disabilities.

Nannaphat (JaJar) Suwannakul is a junior at Ruamrudee International School (RIS) who is especially passionate about science and music. She wants to combine both of her interests to help underprivileged members of society. Hence, she initiated the Musical Remedy Project to open-up new treatment opportunities for neurodiverse children.

DOI: 10.36838/v4i5.20

IJHSR
ijhighschoolresearch.org
REVIEW ARTICLE

Chinese Media Representations of Chinese Women during COVID-19: Implications, Impacts, and Future

Caibinfen Wu
Shenzhen College of International Education, 1301,4, Zhenshanfu, Futian District, Shezhen, Guangdong, 518000, China;
s5011.wu@stu.scie.com.cn

ABSTRACT: As COVID-19 threw the world into uncertainty, countries' public health responses, as well as how the media presented them, drew widespread public attention. By analyzing a specific incident in which female nurses in Gansu, China were filmed having their heads shaved before going into the Wuhan frontline, this paper examines Chinese media's nationalist rhetoric, and questions the techniques used in this kind of propaganda, which focuses excessively on individual sacrifices. My research demonstrates a close relationship between media representations of symbolized women's bodies and social responses. This connection at least affects people psychologically, while it can also lead to abusive behavior. News sources and social media are taken into account to analyze the implications and impact of the Gansu incident. In conclusion, this paper demonstrates the incident's dehumanizing nature for the women involved, but also interprets it as a social ritual that raised awareness on the status of gender equality in China among the public.

KEYWORDS: Public health; Media representation; Gender equality; Coronavirus; China.

Introduction

Pandemics are feared because of their devastating power to cause death and fear. For example, the 1918 flu killed almost 5 percent of the global population--an estimated 100 million people --and lowered the overall life expectancy by over 10 years during the course of a single year.[1] Pandemics are also "hailed" because of their stimulating effect on disease control and medical development. For instance, in 2005, a collaborative group of scientists from several universities and research centers recreated the 1918 virus and produced a specific vaccine that would protect populations in the event that a similar strain develops naturally or is somehow created as a bioterrorism agent.[2] COVID-19 is commonly feared because of both its physical damage (painful breathing, and potential for heart attack, kidney failure, and coagula dysfunction, etc.) and its economic devastation which can cause lingering pain and perhaps even deeper scars – far larger than the other post-war pandemics.[3] However, inevitably, marginalized groups, such as women and children, are often more affected because they endure both the physical and social discrimination of disease due to unequal access to power

This is especially true in the case of Covid-19 where Chinese women have experienced the virus along with sexism. Being a socially-conservative communist country, China restricts its media in a self-laudatory way in order to achieve national stability. This produces a generally under-informed population and can even be viewed as the main cause of the outbreak of COVID-19 in China. For example, initially the Wuhan government concealed the fact that hospitals had taken in several patients who had the same undiagnosed symptoms. Moreover, provincial TV stations even reported on doctors who tried to spread the news as scaremongers and admonished them. Still worse, this inaccurate and regulated reporting can lead to misinterpretations of issues such as the true contribution women made during the pandemic. China's tightly controlled media, in conjunction with ingrained patriarchal ideas including "proper" gender roles and sexuality, have ultimately made the road to gender equality extremely difficult. In the following paper, I will examine how media representations of women during the most recent pandemic—COVID-19—affects the progression of gender equality in China. Specifically, I will review images, videos, and texts from various Chinese newspapers' websites and social media. Building on existing research and available media records from publisher, this article reviews how media represent women, what responses they arouse, and to what extent they catalyze or hamper equality. Sources such as Wuhan Evening News are employed because they reflect authentic official Chinese media milieu.

Historical Context and Background:

As early as the 19th century, there was evidence that gender was a site where people who suffered from epidemics tried to rationalize or explain diseases. For example, The Contagious Disease Acts passed in 1864 by the British Parliament assumed carriers of syphilis were female.[4] Stigmatizing them as "fallen women" that threatened civil and family life, both local and central government enacted legislation that regulated prostitution, locking prostitutes in quarantine hospitals.[5]

Women's bodies were also seen as symbols of socio-cultural status.[6] Different representations of how women themselves or others "used" their bodies, linked with perceptions from various standpoints towards these visual embodiments, had both negative and positive impact on the perpetual pursuit for most of the women—equality. One of the standpoints in fact equated the nation itself to a woman, by referring to it as "mother country" or using the pronoun "her". Maternalizing the country can be seen as early as 16th century France when politicians who advocated national community used the

DOI: 10.36838/v4i5.21

the metaphor, "France is a mother whose body is split by her children's religious conflict."[7] This visualization signifies the relationship between the nation and its people as mutually protective and intimate. The very first shift in image of Chinese women occurred 100 years ago, when the Republic of China was established in 1911. Grand President Zhongshan Sun repealed the infamous rule of "bound feet" under the new ideal of modernity of the new nation. This custom once embodied patriarchal ideals about sexuality in a way that physically confined women, preventing their escapades, so that women were better used as domicile breeders/householders, even as objects.

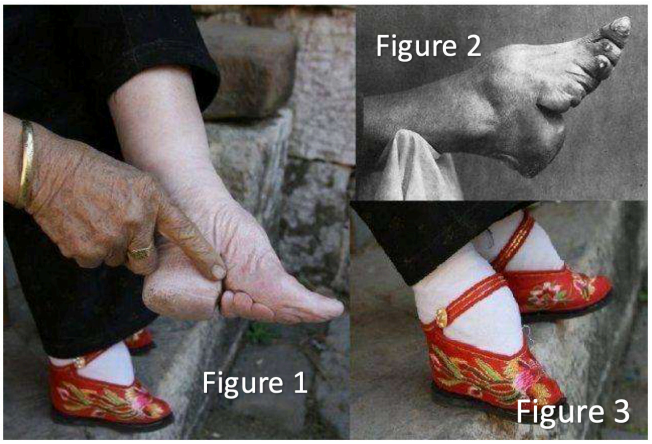

Figure 1 & 2: The distorted feet after binding for years.
Figure 3: Specially designed shoes (approximately 10 cm in length), hand made by women themselves. Source: http://www.ladywu.net/qiwenjiemi/2018/112227581

In the 1920-30s, after foot binding's repeal, reformist intellectuals such as Qichao Liang went further and urged magazines to focus on women's themes, and print advertisements with female models "boldly" displaying their beauty in order to consolidate the idea of "modern women", who were patriotic, politically aware, and educated.[8]

This idea of "modern women" was advocated simultaneously as the newly created Republic of China tried to show its people and the world that it was independent, glamorous, and confident. Women in Wuhan also facilitated the process by holding a naked pageant in 1927 to "break shame and get freedom". As a positive result, numerous local and national Women's Associations were established afterwards.[9] However, as these positive representations were either commercial in nature, or politically motivated - spearheaded by elites and members of the middle class under male dominance in order to intervene and assert a political agenda, or arouse patriotism, they can hardly be considered as having solid utility for advancing gender equality/encouraging feminist movements.

Although a leap from 100 years ago, women's status in China nowadays is still incomparable to that of men. This is shown by a 1-1.18 female to male ratio discrepancy[10], which exceeds the standard ratio of 1.03-1.08 set by the United Nations. This lower status is also shown by lower mean salaries: 75.4% of mens'.[11] Luckily, the equality awareness of both genders in China is progressing, which can be seen by the fact that more pro-women proposals were brought up during the National People's Congress and the Chinese Political Consultative Conference. In the case of the pandemic, the manifestation of Chinese women's bodies in media brings its significance to the fore of gender equality in China.

Gender and Media:

According to an online survey conducted 16-20 March 2020 by Amy Watson, 40% of the 1003 Chinese respondents said that they spend more time-consuming news coverage than they did before the pandemic, while 22% of the respondents specifically consume news on social media.[12] Knowing this, insidious Chinese media overemphasized individual sacrifices of people—particularly female nurses—in order to arouse patriotism and a sense of solidarity. One example was propaganda of nurses from Gansu getting their heads shaved by a team of male barbers before they were dispatched to Wuhan, 15th February. Videos recorded them crying while barbers "triumphantly" showed the nurses their shaved hair. Media users--regardless of gender--were angered by this portrayal of women.

The public was angered because hair has significant historical meaning for Chinese people. Confucian culture took hair seriously as exemplified by the saying, "Body hair skin, received by the parents, dare not to damage" that links hair to filial and ethical values. In the 1910-30s, hair was symbolized as a holdover from feudalism by innovators from Republic of China. However, none of hair's multiple implications were related to patriotism or solidarity. Although large groups of women cutting their hair short were not uncommon in Chinese history, this 2020 occasion was particularly infuriating because it seemed to annihilate women's autonomy and agency. "Women are essential, as part of the nation, are owned by the country, but not by family or men, have their independent identity."[14] Opinions like this prevailed at that time, leading many female students to voluntarily advocate for hair cutting as an "independent choice". In that historical context, this body transformation was endowed with utmost feminist symbolism--as well as

DOI: 10.36838/v4i5.21

nation-building expectations.[15] Nowadays, cutting women's hair is again being used as a vehicle to convey assigned meanings, as well as to grab public attention. Ironically, from the videos of the nurses' hair cutting, there are no signs of independent determination from the nurses' expressions, only sadness and unwillingness, which sharply contrasts with the mood of those early female students. Although later clarified by the hospital that the nurses did this voluntarily, the fact that male barbers are doing the job for them still communicates a sense of deprivation and oppression.[16] This largely departs from the origins of female hair cutting—beneficial for self-identification. The public responded indignantly towards these videos and photos, condemning both the Gansu government and the media publishers for excessive formalism and the overwhelming patriarchal messages it carried.

To see this hair cutting in a positive light, the event drew a significant amount of social attention toward issue of gender. Countless queries it drew such as "Why not shave male nurses' hair as well?" and "why overly report on female's bodies instead of reporting on female expertise?" were raised and posted online. Well-written arguments by both feminists and politically neutral people aroused over 10,000 retweets and spurred numerous critiques discussing Chinese gender issues as well. Moreover, reputed celebrities such as Yuchun Lee, a female singer, and Hesu Yang, a male rapper, wrote songs called To girls and Harley Quinn (an unconventionally fierce female comic character) respectfully in order to show support. Over 25,000 active users on NetEase Cloud Music, the most popular China-based music platform among Chinese users, commented on, or "liked" each of the song. It is therefore evident that beginning with discussions about media representations of female bodies, the sense of gender equality is awakening in China.

However, to see the hair cutting in a more pessimistic way, the event actually lowered women's status. To begin, even though the nurses' body images were exploited in propaganda to arouse sympathy and supposedly patriotism, we still don't even know the fifteen nurses' names. This neglect of individuality yet overemphasis on "being a part of something greater" again reduced women's' values---their sacrifices as "attractive women" had overshadowed their contributions as medical professionals. This again fits the long-existing patriarchal ideals that perceive women mainly by appearance and exaggerate their roles as "mothers" and "wives" instead of their other roles like "protectors" or "fighters". Moreover, this representation also contrasted sharply with the diminishment of nurses' material needs in Wuhan. When asked about how many menstrual pads were needed to support nurses on their periods, for example, a male authority from Jinyintan Hospital refused this help by indicating, "This is not a necessity. We need more masks and protection suits."[17] Propaganda about artificial female heroism and their muffled requests go hand in hand, materializing women's bodies into dehumanized tools that arouse patriotism.

Finally, there might be an association between burgeoning domestic abuse rates and this head shaving event. Recordings of women crying after having their heads shaved delivered the implicit message that women were fragile and were not in control of their own bodies. "Reports of domestic violence in February were two to three times higher than the same month last year." Wan, leader of an anti-domestic violence organization WanHuWuBao, said. From January 23 to March 6, the public security bureau in Jianli and Qianjiang (both are cities in Hubei Province) received more than 300 reports of domestic violence. Wan offers one explanation, "Many cases occurred between ex-couples, who initially only temporarily reunited for their children during the Chinese New Year, were now forced to stay under one roof because of the pandemic. Their past and present resentment towards each other accumulated and triggered violence."[18] Could it be then that the recordings of women crying after having their heads shaved provided additional legitimacy to overarching patriarchal ideas that men - rather than women - control women's' bodies?

Conclusion

The representation of nurses' bodies by Chinese media during the COVID-19 pandemic indicated many historical and cultural implications. While it revealed the cruel reality of the status quo of gender inequality in China, it also drew much social attention toward this issue, and promoted calls for improvement in future media representations.

Looking Ahead:

Overall, this exposure of nurses getting their hair shaved should be cherished, not because the behavior itself is valuable, but for the extent of reflection it called upon people, and its awakening effect on the issue of gender equality in China. Unprecedentedly, educated and thoughtful responses about gender-discriminating were evoked from the masses, which encouraged more feminists to continue their activism, and spurred more people to devote interest in feminism. As discussed, historical media such as literature and commercials had characterized China as a mother. People accordingly adopted their "mother's" idiosyncrasies from "weak", "deprived", and "desolated" to "strong", "independent" and "protective" as she walked from foreign invasions to gaining a place in the world (1920-30s).[19]

As China develops faster materially, its future media certainly has a role in representing its moral development, which includes the pursuit of gender equality. Future media should direct people in the same way it did 100 years ago, depicting stronger women instead of posting their seemingly oppressed images online. In order to optimize the media's positive effects, publications and propaganda should no longer focus on women's bodies, or their individual sacrifices. Therefore, everyday woman who haven't made such sacrifices such as "going onto the frontline 10 days after miscarriage" could be treated as nobly as those who had. Otherwise, completely ordinary women would be seen as "not deserving of a place in media reports" even though they contribute no less. I look forward to a good media environment in China that reports on subjects as inclusively as possible. In conclusion, the best result is that we can learn lessons from media representations of women during the COVID-119 crisis, so that we can find a way to navigate future media

wisely in order to improve the general gender environment in China.

Acknowledgements

Supervisor: Scholar Launch

References

1. Loomis. J. Epidemics: The Impact of Germs and Their Power over Humanity, 1st ed.; PRAEGER: Santa Barbara, **2018**; pp 194.
2. Loomis. J. Epidemics: The Impact of Germs and Their Power over Humanity, 1st ed.; PRAEGER: Santa Barbara, **2018**; pp 217
3. Baldwin. R.; Mauro. B. Economics in the Time of COVID-19, 1st ed. ; CEPR : London, **2020**; pp 2
4. Walkowitz. J. R., Prostitution and Victorian Society: Women, Class, and the State, Cam: Cam.Uni P., **1982**
5. Worboys.M, Spreading Germs: Disease Theories and Medical Practice in Britain, 1865–1900, Camb: Cam.Uni. P. **2000**, 51–60
6. Zhou. H.Y; Zhou. N. Metaphorical Body: The "Haircut Problem" of women in Schools during the Republican China J.E.C.Nor.Uni. Edu.Sci. **2016**, 4, 1
7. Pan.X.H. "Motherland": the transmission and the origin of a political metaphor, J.H. **2018**, 1, 2-4
8. Edwards, L. Policing the Modern Women in Republican China. Mo.Ch. [online] **2000**, 26, 116. http://www.jstor.org/stable/189430 (accessed July 20, 2020)
9. SH.Pic **1927**, 225.
10. The sixth National population census http://www.stats.gov.cn/tjsj/pcsj/rkpc/6rp/indexch.htm
11. Lin.X; Gunderson.M (January 2013). Gender Earnings Differences in China: Base Pay, Performance Pay, and Total Pay. C.E. P. [online] Feb 27, **2012**, p 235–254. Wiley Online Library https://onlinelibrary.wiley.com/doi/abs/10.1111/j.1465-7287.2011.00307.x (accessed Sept 7, 2020)
12. Watson. A. Statista. https://www.statista.com/statistics/1106766/media-consumption-growth-coronavirus-worldwide-by-country/
13.
14. Gao S.S. Resolution of women's problem, N.Y. **1917**, 3, 104-108 11.Lin.X; Gunderson.M (January 2013). Gender Earnings
15. Yang. Z.D. Hair cutting trend during the Northern Expedition (1926-1927), W.S.C.Q. **2011**, 1, 61
16. Social Latitude and longitude. https://baijiahao.baidu.com/s?id=1658973468596537982&wfr=spider&for=pc
17. Sina Weibo. https://weibo.com/u/1306934677?from=feed&loc=nickname&is_hot=1
18. KuaiBao. https://kuaibao.qq.com/s/20200308A07JP100?refer=spider
19. Pan.X.H. "Motherland": the transmission and the origin of a political metaphor, J.H. 2018, 1, 3

Author

Caibinfen Wu is a high school student from Shenzhen College of International Education. She is interested in exploring social dynamics and interpersonal relationships, as well as their implications. She aims to major in Sociology/Anthropology in further education.

DOI: 10.36838/v4i5.21

IJHSR
ijhighschoolresearch.org
RESEARCH ARTICLE

Effects of Urbanization on a North Carolina Piedmont Stream

Yasmine P. Ackall, Katherine M. Lopez, Pristine C. Onuoha, Micah E. van Praag
East Chapel Hill High School, 500 Weaver Dairy Rd, Chapel Hill, NC, 27514, USA; yasmine.ackall@gmail.com

ABSTRACT: Bolin Creek, located in Chapel Hill, North Carolina, a highly urbanized town, has been listed on the NC 303 (d) list of impaired waters since 2003. The objective of this study was to investigate potential connections between urbanization and the declining water quality of Bolin Creek. Data were collected on the water chemistry and benthic macroinvertebrates of Bolin Creek and two reference streams. A strong negative correlation was found between the percentage of developed land around the stream sites and stream water quality. Correlational data on conductivity, turbidity, and nutrient concentration indicated that urban runoff, associated with the high percentage of impervious surface cover in Chapel Hill, largely contributed to the degradation of the water quality of Bolin Creek. The results suggest the need for further action to improve the water quality of the stream. The researchers of the present paper suggest the following actions to help restore the water quality of Bolin Creek and create a more resilient watershed plan for the community: restoration of the riparian buffer along Bolin Creek, policy and educational changes in Chapel Hill, street cleaning, green roofs, the use of the Clean Water State Revolving Fund (CWSRF) revenue, and relevant public engagement.

KEYWORDS: Environmental Effects on Ecosystems; Ecology; Urban Runoff; Impervious Surfaces; Benthic Macroinvertebrates.

Introduction

Significance of Water Quality:

The present study concerns water quality and how urbanization affects it. Freshwater is essential for life and scarce, as freshwater constitutes only 2.5% of the surface water of the Earth and is predominantly found in ice.[1] Presently, agricultural and urban development threatens the health of freshwater bodies, and population growth is decreasing freshwater accessibility.[1] In 2020, 26% of the world's population lacked clean drinking water and water services, and 2.3 billion people currently live in "water-stressed" environments.[2] Lower water quality increases the resources necessary to treat drinking water.[3] Studies reviewed by Carpenter *et al.* (2011) highlight that water quality is a major indicator of human health, and that decreased habitat biodiversity is associated with increased diseases in humans.[1]

Streams purify water, control flooding, decompose waste,[4] and remove contaminants and added nutrients.[5] Studying streams such as Bolin Creek is also important because streams and other water bodies are part of a complex, connected network of ecosystems. Ecosystems are fragile and more sensitive to stressors than individual organisms.[6] Currently, anthropogenic factors such as agriculture, urbanization, climate change, and invasive species synergistically threaten ecosystems globally.[1] Ecosystem services form the foundation of human life and the basis of human economic activity.[7,8] They provide ecosystem goods, such as timber and biomass fuels; support the life humans depend on; purify air and water; stabilize climates; and provide support and regulation services such as pollination, the dispersal of seeds, and control of pests.[7] Predicting the extent of the effects of anthropogenic stressors on ecosystems is complicated in that human impacts on ecosystems can affect societies elsewhere.[8]

Urbanization:

Currently, more than 4 billion people live in urban areas, and global urbanization is projected to further increase.[9] High probability estimates show an increase of 1.2 million km^2 in urban land cover by 2030.[10] The effects of urbanization remain complex and our knowledge of its effects remains limited.[11] There are benefits to urbanization; for example, the high-density development in urban areas could decrease total energy use and greenhouse gas emissions compared to suburban areas.[10] However, urbanization affects water quality, as well as ecosystem services derived from water bodies.[12] Below, two specific ways by which urbanization affects water quality are described: contaminated runoff and thermal pollution.

Runoff:

Urbanization increases the amount of impervious surface cover (ISC) in a watershed, which decreases infiltration rates.[13-16] Impervious surfaces are made of impermeable materials such as asphalt and concrete, and they are found in rooftops, parking lots, roads, and other works of infrastructure.[17] Increased ISC can increase stream channel erosion because impervious surfaces are hydrologically active, meaning that they can generate runoff that flows directly into the stream channel.[17] Together with increased artificial drainage systems (e.g., pipe drains and ditches), urbanization and ISC have large effects on the amount and intensity of runoff.[11,18-20] Sun and Caldwell (2015) have demonstrated the existence of a strong exponential correlation between imperviousness and runoff (R^2= 0.92).[12]

Stormwater runoff can directly contribute to the pollution of water bodies, and if stormwater drains into treatment facilities through pipes, overloads wastewater treatment facilities and impair sewer systems.[21] In addition, the increased intensity of the flowing water of runoff entering streams increases

DOI: 10.36838/v4i5.22

erosion in the stream channels, which degrades stream water quality[22] and increases sedimentation.[20] While runoff has physical effects on water bodies and streams, the most important way that runoff harms aquatic life is the toxins that runoff carries into freshwater ecosystems.[23] Runoff can contain contaminants washed off cars and from roads, chemicals used by industry and by the public, and chemicals deposited from the atmosphere. Atmospheric inputs of pollution (e.g., from industry or automobiles) also affect water bodies through direct transfer to water bodies, even without runoff.[1, 21] Runoff and municipal waste can contain organic compounds; heavy metals; acids; alkalis; pesticides such as insecticides, herbicides, fungicides; DDT and other banned substances; polychlorinated biphenyls (PCBs), even though their use has been outlawed; petroleum-based organic compounds; phosphorus and nitrogen from fertilizers; and chlorides; all entering water bodies and potentially poisoning aquatic organisms.[1,5] Water in urban areas can also contain human medication, including antibiotics, narcotics, psychotherapeutic drugs, and chemotherapeutic drugs.[12,5] Instead of infiltrating into the ground, the pollutants and solids accumulate in water bodies and the severity of this process are further accelerated as ISC increases the flow of runoff, leaving less time for the pollutants to infiltrate into the ground.[15, 20] When the runoff does infiltrate, urban pollutants then pollute groundwater. One indication of increased dissolved chemicals in water bodies is electrical conductivity (EC).[5] EC is measured by the ability of an electric charge to pass through a water sample.[24] EC is an indicator of human disturbances to water.[25] Another indicator, turbidity, is a measure of the solids suspended in water and is measured by the amount of light absorbed and scattered by a water sample.[26,27] Measurements of EC and Turbidity were used in this study.

Urbanization, ISC, runoff, and the resulting pollution have impacts on aquatic ecosystems, which include fish, macrophytes, and macroinvertebrates.[15,5] Ephemeroptera, Plecoptera, and Trichoptera (EPT) are examples of orders of aquatic insects sensitive to change in water quality and are useful as bioindicators because they are easily negatively affected by water pollution.[23,28,29] Gresens *et al*. (2006) found that EPT taxa numbers were lower in urban sites than rural sites.[23]

Benefits of Macroinvertebrate Use:

Pollution is broadly defined in Britannica as "the addition of any substance (solid, liquid, or gas) or any form of energy (such as heat, sound, or radioactivity) to the environment at a rate faster than it can be dispersed, diluted, decomposed, recycled, or stored in some harmless form." Pollution "can have negative effects on the environment and wildlife and often impacts human health and well-being." The extent of pollution can be assessed by examining damage to aquatic organisms.[30]

Monitoring organisms in aquatic ecosystems is essential in evaluating the effects of pollution on water quality. One way to notice how the changes in water quality affect aquatic organisms is to monitor and identify the benthic macroinvertebrates (BMI) populations in waterways.

Monitoring BMI survival has many benefits; they can be found in most aquatic habitats, they are affected by the physical and chemical conditions of the waterway, and they are generally sedentary in nature due to limited mobility, so they cannot escape acute water pollution events,[31] and thus they can be used to indicate changes in water quality over the course of months and years.[32]

Thermal Pollution and the Urban Heat Island Effect :

Urbanization is associated with thermal pollution. The Urban Heat Island Effect (UHI) is the process of urban areas heating up more rapidly than the surrounding areas due to decreased vegetation, increased heat-absorbing infrastructure, and increased heat-generating infrastructure.[11,33] Bornstein (1968) found an average UHI intensity of 1.6 °C in his studies of New York City.[33] Magee *et al*. (1999)[34] studied two areas in Alaska from 1949 to 1997: Fairbanks, which underwent urbanization and population growth, and Eilson, which had similar geographic features but less urbanization and a steady population. The authors found a substantial difference between the heating of Fairbanks and Eilson, and that ⅕ of the heating of Fairbanks was attributed to the UHI. Thermal inversions, typical in the winter, cause heat and pollution to be trapped in urban areas,[34] and previously mentioned atmospheric pollution can enter stormwater runoff.[1] Furthermore, layers of anthropogenic chemicals and air pollutantss, such as sulfur dioxide, water vapor, and smoke, also further re-radiate heat back to urban surfaces exacerbating the UHI.[33]

Stormwater runoff can heat up significantly due to the heat conducted into the runoff by ISC,[17] thereby transferring the heat into receiving water bodies.[18] According to the United States Environmental Protection Agency (EPA; 2020),[18] thermal pollution stresses aquatic life in a variety of ways. Fish increase their metabolism in proportion to temperature, and large temperature increases can have fatal effects when the thermal tolerances of aquatic organisms are exceeded.6 Additionally, warm water holds less DO than cold water due to entropy, reducing oxygen available to aquatic organisms and further degrading water quality.[35] Because fish are important members of, and even regulators of, aquatic ecosystems,[1] harm to fish can be inferred to affect many other organisms, including benthic macroinvertebrates.

Channelization :

Channelization is an example of anthropomorphic changes in aquatic ecosystems. The deepening and widening of streams by channelization destroy benthic habitats; straightening streams increases flow rates, affecting species and habitat quality.[36] Other species may decrease as channelization removes needed turbulent and rocky areas in streams with high oxygen contents.[37] Studies reviewed by Brooker (1985) show that bankside trees and stable soils are often decreased due to channelization.[38] The removal of riparian buffer zones can increase the sunlight entering headwaters which can increase water temperature and alter the normal tenets of the River Continuum Concept described by Vannote *et al*. (1980).[37, 39]

History of Bolin Creek:

This study analyzed the water quality of Bolin Creek, which is located in Orange County, North Carolina, in the Cape Fear

DOI: 10.36838/v4i5.22

river basin. It runs for 14½ km (9mi) through the cities of Carrboro and Chapel Hill and has an area of about 31 km^2 (11.98 mi^2).[40,41] The land cover of the Bolin Creek watershed is 16.9% impervious.[20] Bolin Creek converges with Booker Creek to form Little Creek.[41] Little Creek eventually flows into B. Everett Jordan Lake,[40] a source of water for hundreds of thousands of people.[42]

Bolin Creek has had a history of troubled water quality. It is listed on the state of North Carolina's 303 (d) list as a result of the excess sedimentation found in the creek.[40,41,43] This indicates that the creek has been unable to sustain the normal amount of biodiversity of a healthy stream.[40] The investigations by Beggs *et al.* (2012) of the North Carolina Department of Environmental Quality (NCDEQ) concluded that the water quality of Bolin Creek worsened as it traveled downstream into a denser urban environment, starting at Carrboro and flowing into Chapel Hill.[40] As seen on the NCDEQ Benthic Monitoring Data website, the site nearest to the headwaters of Bolin Creek near Homestead Road had a bioclassification of "Good-Fair" while the site furthest downstream was classified as "Poor".[44]

Recently, multiple developments have accelerated the degradation of Bolin Creek. In 2009, the Town of Carrboro, as part of its Bicycle Plan, proposed the replacement of the nature trail along Bolin Creek with a 10-foot wide paved path, eliciting a negative response from the community.[42,45] Similarly, according to a report done by the North Carolina Department of Environmental and Natural Resources (NCDENR), both Bolin Creek and its neighboring Booker Creek were channelized downstream of East Franklin Street to allow for straighter roads, railroads, and sewer and water lines.[41]

Broader Purpose:

The present study focused on the effects of urbanization and ISC on water quality in Bolin Creek, to aid organizations in removing Bolin Creek from the 303(d) list and mitigate the impacts of urbanization. We hypothesized that increased development around Bolin Creek would be correlated with a decrease in the water quality of the creek as determined by biological analyses on BMI assemblages, and measurements of physical and chemical parameters.

Materials and Methods

Overview:

This study researched the water quality of three sites at Bolin Creek as well as of two reference streams. The five sites were found using the NCDEQ Benthic Monitoring Data online interactive website.[44] Each site was chosen to represent a different bioclassification rank ranging from excellent to poor based on previous work (Figure 1). The "Excellent" reference site was at Pokeberry Creek (35.7742°, –79.1200°; Site ID: BB320). The "Good" site was at Morgan Creek (35.92361°, –79.11556°; ID: BB146). The "Good-Fair" site was located near State Road and Homestead Road (35.9436°, –79.08833°; ID: BB330). The "Fair" site was located at Bolin Creek near Village Road (35.92278°, –79.06667°; ID: BB449). The "Poor" site was located at Bolin Creek near East Franklin Street (35.92778°, –79.035°; ID: BB071). The research team tested riffles, areas of fast-moving shallow water passing over rock or sand that are optimal environments for aquatic organisms and BMI to inhabit.[46]

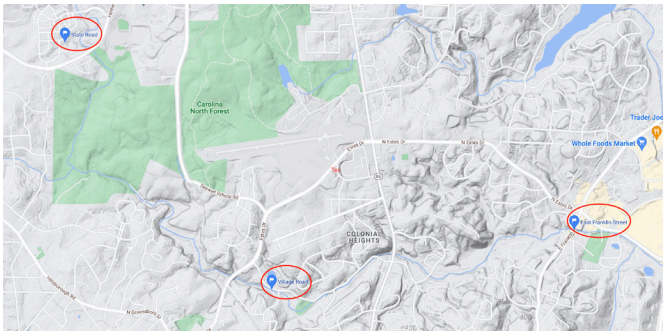

Figure 1: A Google Maps depiction of Bolin Creek. The three tested sites (upstream to downstream) are marked with red circles: State Road, Village Road, and East Franklin Street.

Macroinvertebrate Collection:

In order to collect the BMI, the team followed the 2016 NCDEQ Standard Operating Protocol (SOP) for the Collection and Analysis of Benthic Macroinvertebrates, specifically, the Qual-4 method.[32] The Qual-4 method involved four steps: a riffle-kick, sweep, leaf pack, and visual search. The riffle kick involved kicking the benthos (3m2) for 2min and letting BMI flow into a 1m wide net (with 1000µm mesh) downstream. A D-Net was used to sweep BMI from roots and undercut banks. All BMI were removed from leaf packs, and the visual searches involved BMI collection from riffle rocks, woody debris, and other features not previously sampled. Approximately 10–15 minutes were allocated to each step. All collected BMI were preserved in >70% ethanol solutions and stored in glass vials. After collection, the BMI were morphotyped using handheld magnifying glasses and identified to family using the Atlas of Common Freshwater Macroinvertebrates of Eastern North America as a reference.[47] In addition, previous NCDEQ BMI collection data were provided to the team by Mr. Eric Fleek from the NCDEQ as a reference to the taxa collected by the state of North Carolina.[48] Knowledge of previous BMI collections allowed the researchers to deduce the type of BMI, sometimes even identifying species.

North Carolina Biotic Index:

After identification (to family-level taxonomic group) and enumeration of each taxon, the BMI assemblages were used to determine the NCBI values of the stream sites. The NCBI score (equation 1) uses the abundance values and family-level tolerance values (mean of all reported NC species in the family) of BMI taxa to determine a quantitative value of water quality, the mean tolerance value of the sample. The outputs range from 0.0–10.0, where the lower values indicate less tolerance for pollution and higher water quality. An abundance of pollution-intolerant species (e.g., EPT taxa) would indicate better water quality, whereas an abundance of pollution-tolerant species would indicate poorer water quality. The following equation for calculating a mean (e.g., from the NCDEQ SOP) was used to determine the NCBI:[32]

$$B = \frac{\sum(Ti)(ni)}{N} \quad (1)$$

The North Carolina Biotic Index where:
B = the Biotic Index
T_i = the Tolerance Value (TV) for the i^{th} taxon
n_i = the abundance category value (1, 3, or 10) for the i^{th} taxon
N = the sum of all abundance category values

A lower value of the Biotic Index (B) signifies greater water quality with lower mean tolerance values. The resulting NCBI scores were compared to the bioclassification criteria according to the NCDEQ SOP Table 8 and ranked based on the scale from "Excellent" to "Poor" using the Piedmont area classifications.

Biodiversity Indices:

To prevent solely relying on the Biotic Index to determine the water quality of the stream sites, biodiversity was also quantified using two indices: Simpson's Diversity Index (equation 2) and Shannon-Wiener Diversity Index (equation 3), which produced results in ranges of 0–1 and 0–5, respectively. These indices indicate the level of biodiversity and evenness within a sample. For the Simpson's Diversity Index, which takes into account the dominance of species, numbers nearing the lower limit of the range represent relatively lower biodiversity and evenness whereas numbers nearing the upper limit represent relatively higher biodiversity and evenness. For the Shannon-Weiner Diversity Index, numbers nearing the lower limit of the range represent lower biodiversity while numbers nearing the upper limit of the range represent higher biodiversity. The formulas are displayed below:

$$DI = 1 - \Sigma\left(\frac{n}{N}\right)^2 \quad (2)$$

Simpson's Diversity Index where
n = total actual abundance of organisms of a certain species
N = the total actual abundance of organisms of all the species

$$H = -\Sigma\left[\left(\frac{n_i}{N}\right) \cdot ln\left(\frac{n_i}{N}\right)\right]$$
$$E = \frac{H}{H_{max}} \quad (3)$$

Shannon-Wiener Diversity Index where
n_i= actual abundance of individual species
N= total actual abundance
H_{max}= maximum diversity possible

Water Chemistry and Physical Water Properties:

Eight measurements of water chemistry and physical water properties were collected at the five sites. The Vernier LabQuest® 2 probes and monitors were used to measure turbidity in Nephelometric Turbidity units (NTU), dissolved oxygen (DO, mg/L), conductivity in microsiemens per centimeter (μS/cm), pH, and water temperature (°C). All probes were "plug-and-play" with the exceptions of the turbidity probe, which required calibration before each use, and the DO probe, which also required occasional calibration. A LaMotte Earth Force® Low-Cost Water Monitoring Kit was used to test approximate nitrate (NO_3, ppm) and phosphate (PO_4, ppm) concentrations, as well as the presence or absence of mammalian fecal coliform (*Escherichia coli*).

BEHI:

A modified Bank Erosion Hazard Index (BEHI) was used to assess the extent of bank erosion at each site. The specific BEHI procedure used, developed by Dave Rosgen of Wildland Hydrology, Inc., was written and explained by Rathbun (2008). Factors that affected BEHI scores49 included root depth, root density, surface protection, bank angle, and the presence of various types of rock/soil and stratification.

Discharge:

Baseline discharge, or the amount of water usually flowing through a river at any given point and measured in ft3/s, was determined and recorded at each of the five sites. The team followed the protocol created by the National Great Rivers Research and Education Center for the calculations.[50] Briefly, this entaileds determining the cross-sectional area of the stream site in ft^2 multiplied by the water flow rate in ft/s.

Land Coverage Data:

Land coverage data for each of the areas around the watersheds that drained into their respective stream sites were collected through QGIS software with data retrieved from the USGS National Map as well as the National Land Cover Database (NLCD).[51] The NLCD is a product of the Multi-Resolution Land Characteristics (MRLC) Consortium, a federal collaboration.[52] The MRLC consortium uses Landsat satellite imagery as part of their data collection procedure. These data allowed for the categorization of urbanized land cover. The authors categorized the land use upstream to sampling sites into "low", "medium", and "high" groups based on the percentage of ISC in each watershed.[51] "Low" entails 20–49% ISC, "medium" entails 50–79% ISC, and "high" entails 80–100% ISC. For the purposes of the study, low, medium, and high land uses were combined into one measurement of "developed land coverage". In addition, the same methods were used to determine the percentage of agricultural and forested land cover. However, these data were not used in correlation calculations.

Results

North Carolina Biotic Index (NCBI) values ranged from 4 to 7 and increased as Bolin Creek flowed further downstream, indicating decreasing water quality (Figure 2). State Road is upstream from Village Road, and Village Road is upstream from East Franklin Street. Developed land cover increased from State Road to East Franklin Street, but Village Road had a lower percentage of developed land cover than State Road (Table 1). Notice that the percentage of developed (impervious) land cover at the "Poor" site at E. Franklin Street was approximately six times greater than that of the "Excellent" site at Pokeberry Creek. Strong positive correlations were found between developed land cover and NCBI (Figure 3) as well as developed land cover and conductivity (Figure 4). Conductivity was moderately positively correlated with NCBI values (Figure 5). Turbidity was strongly positively correlated with NCBI (Figure 6). Nitrate and phosphate concentrations strongly positively correlated with developed land cover (Figure 7) and with NCBI values (Figures 8–9). In comparing

DOI: 10.36838/v4i5.22

biodiversity scores determined using the Simpson's Diversity Index (SDI) and the Shannon-Wiener Index, it was found that Pokeberry Creek had the highest level of biodiversity and Morgan Creek had the lowest level of biodiversity (Figure 10). From furthest upstream (State Road) to furthest downstream (East Franklin Street), Bolin Creek's biodiversity decreased. Both biodiversity indices agreed on the relative biodiversity scores. It may appear that the SDI detected no difference between the biodiversity of Bolin Creek at State Road and Village Road (Figure 10), but closer analysis of the values indicated that it did. A moderately strong, positive correlation was found between SDI and dissolved oxygen (DO; Figure 11).

A moderate negative correlation was found between nitrate concentration and DO (R^2= 0.60; not shown). A weak–moderate positive correlation was found between DO and the number of EPT found at the sites (R^2= 0.39; not shown). A strong but chemically unexpected correlation was found between DO and temperature (R^2= 0.84; not shown).

Correlations with R^2 values below 0.40 were not considered meaningful. However, a correlation approaching R^2> 0.40 was found between temperature and SDI (R^2= 0.38). No meaningful correlations (not shown) were found between discharge and DO; turbidity and SDI; turbidity and the abundance of EPT; discharge and NCBI values; discharge and SDI; pH and NCBI values; temperature and NCBI; nitrates, phosphates, and SDI; or pH and SDI. No correlation was found between temperature and developed land cover (not shown).

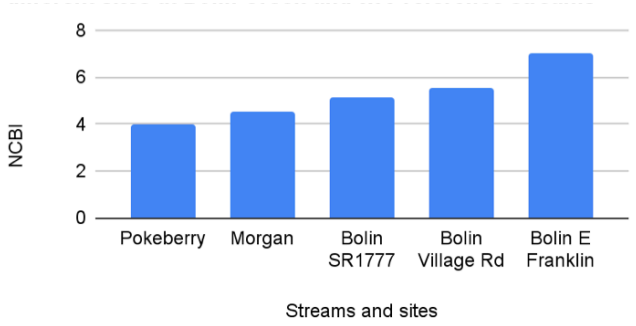

Figure 2: North Carolina Biotic Index values for three different sites at Bolin Creek and two reference streams (Pokeberry and Morgan Creeks).

Table 1: Percentage of developed, forested, and agricultural land in the area that drains into each of the five study sites. Notice that the percentage of developed (impervious) land cover at the "Poor" site at E. Franklin Street was approximately six times greater than that of the "Excellent" site at Pokeberry Creek.

Site name	% Developed land	% Forested land	% Agricultural land
Pokeberry Creek	3.08	70.06	12.09
Morgan Creek	0.76	69.39	18.79
Bolin Creek—SR1777	7.61	64.17	5.22
Bolin Creek—Village Rd	4.67	38.80	3.21
Bolin Creek—E. Franklin	18.10	45.84	4.02

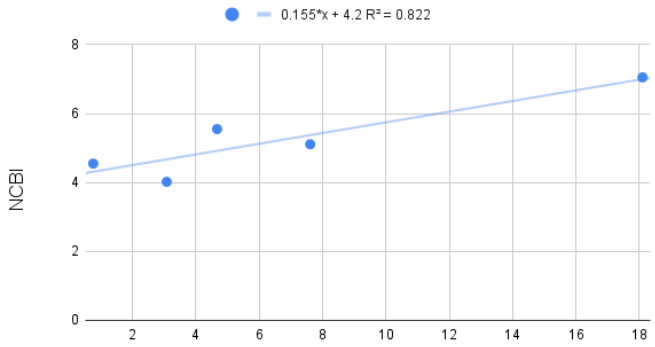

Figure 3: The relationship between the percentage of developed land cover and the North Carolina Biotic Index value.

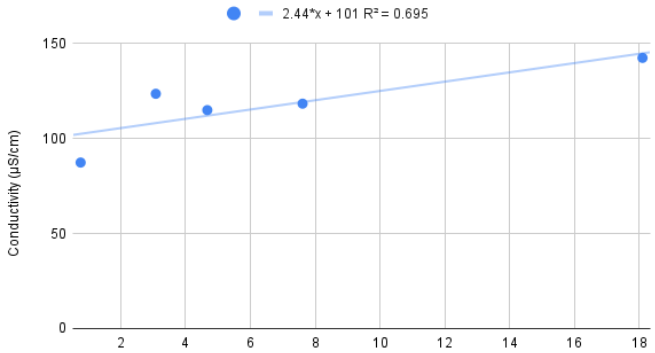

Figure 4: The relationship between the percentage of developed land and conductivity.

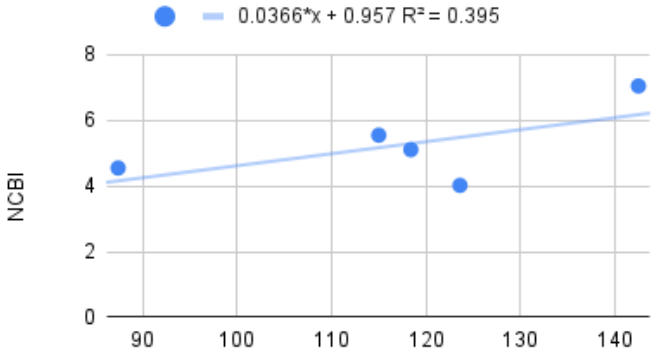

Figure 5: The relationship between conductivity and North Carolina Biotic Index scores.

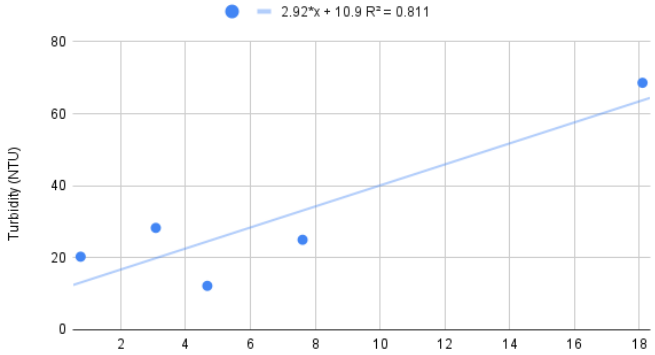

Figure 6: The relationship between the percentage of developed land cover and turbidity. Turbidity was measured in Nephelometric Turbidity Units, NTUs.

Water Chemistry and Physical Water Properties:

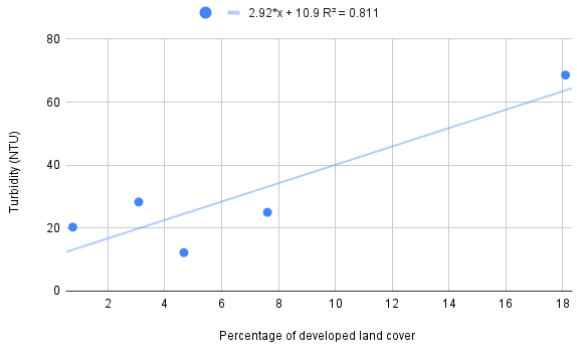

Figure 7: The relationship between the percentage of developed land cover and nitrate and phosphate concentrations. The red data points and red line-of-best-fit correspond to the correlation between the percentage of developed land and nitrate concentrations. The blue data points and line-of-best-fit correspond to the correlation between the percentage of developed land and phosphate concentrations.

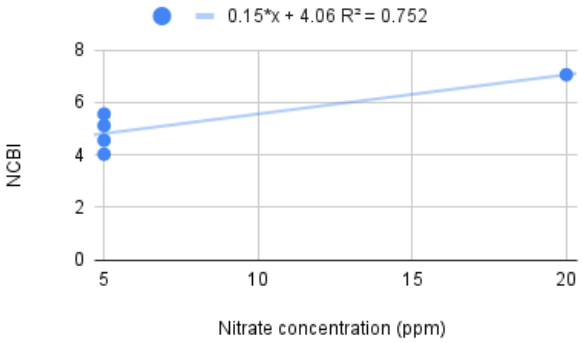

Figure 8: The relationship between nitrate concentration and North Carolina Biotic Index (NCBI) value.

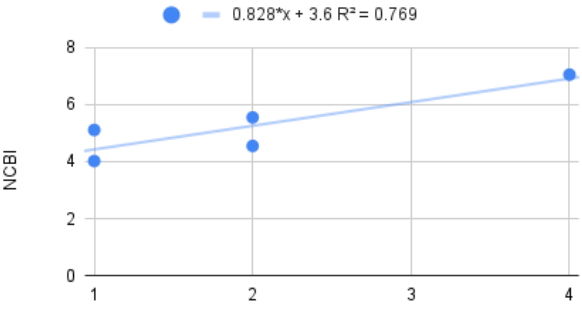

Figure 9: The relationship between phosphate concentration and North Carolina Biotic Index (NCBI) value.

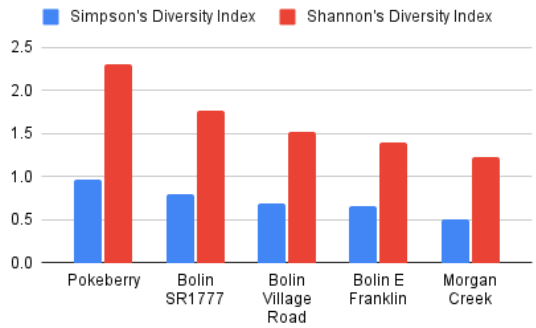

Figure 10: Biodiversity scores for the five tested sites as measured by both the Simpson's Diversity Index (blue bars) and the Shannon-Wiener Diversity Index (red bars).

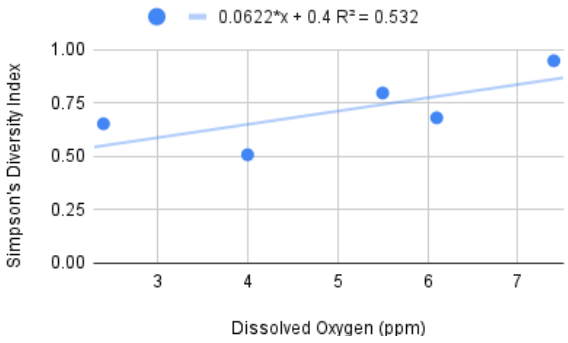

Figure 11: The relationship between Simpson's Diversity Index scores and dissolved oxygen (ppm).

Temporal Changes:

Figures 12–14 show changes in the water quality of the Bolin Creek sites at State Road, Village Road, and East Franklin Street over time, respectively. The water sites and graphs thereof are ordered from best to worst quality in terms of NCBI score. In each graph, the red bar indicates the data recorded by this study. The remaining data is taken from Lenat Consulting Services (2015) as well as data from the North Carolina Department of Water Resources (NCDWR), retrieved from the report by Lenat Consulting Services (2015).53 This study's data were calculated using the "Qual-4" method. Lenat Consulting Services (2015) mentioned other methods as well, such as the Standard Qualitative Method, so the comparisons may not be exact. However, since the NCBI takes the total abundance of species into account, the comparisons are nonetheless valuable. Compared to 2015, the water quality of the site of Bolin Creek at State Road has increased (Figure 12). Since 2002, the water quality of Village Road has increased, but the water quality is still lower than in 1998 (Figure 13). From March 2001 to July 2001, the water quality of Bolin Creek at East Franklin Street improved, but since July 2001 it worsened and remains at the same level as in March 2001 (Figure 14).

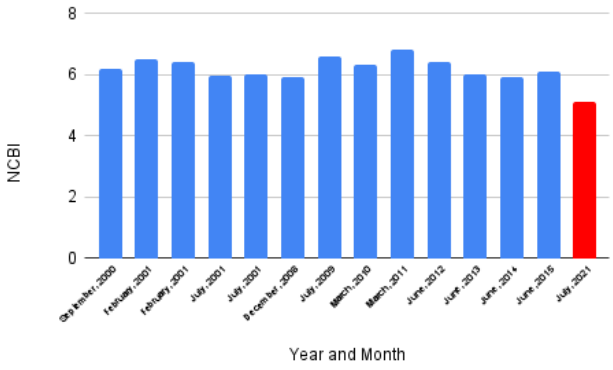

Figure 12: The change in the Biotic Index values of Bolin Creek at State Road 1777 over time.

DOI: 10.36838/v4i5.22

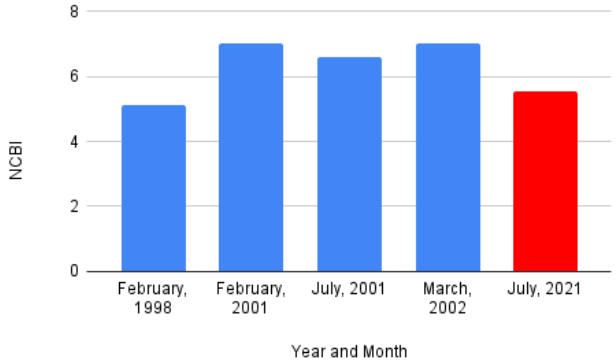

Figure 13: The change in Biotic Index values of Bolin Creek at Village Road over time.

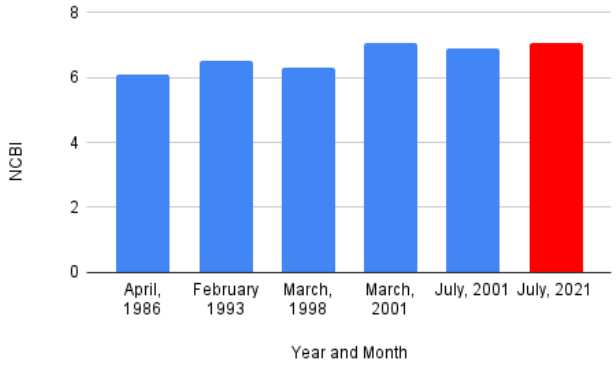

Figure 14: The change in Biotic Index values of Bolin Creek at East Franklin Street over time.

Discussion

Previous Studies and Observations:

Observations of NCDEQ data and previous studies show that the water quality of Bolin Creek does not decline uniformly, and upstream sites may be improving in water quality over time (Figures 12–13). However, as the creek flowed further into Chapel Hill, the bioclassifications changed into "Fair" near Estes Drive and Village Road; then, it flowed to a "Poor" rating at Bolinwood Drive and East Franklin Street.[44] The Watershed Assessment Restoration Project (WARP) determined urbanization and its effects as causes for the impairment, linking "habitat degradation, riparian degradation, [...], and toxicity" as primary stressors of the Bolin Creek watershed,40 as well as the possible stressors of extreme temperatures, high oxygen demand, and high nutrient levels.[40] The Bolin Creek Greenway, built in 1992, contributed to habitat and riparian degradation, as well as increased erosion along the banks of the river because of reduced vegetation to maintain bank stability, resulting in increased sedimentation in the stream substrate.[41] The installation of paved paths creates impervious surface cover (ISC) by which stormwater runoff can flow directly into the river.[54] Unpaved paths also create problems for the river as most unpaved paths are created in a "dip" shape which can erode and drain into the stream adjacent to the greenway, increasing sedimentation in the water.[55]

Bolin Creek has also had multiple sewage failures. The North Carolina Department of Water Quality (NCDWQ) non-discharge compliance unit data and the Orange Water and Sewage Authority (OWASA) recorded 4 sewage spills in the span of January 2000 to December 2002.[41]

Some efforts have been made to restore Bolin Creek. As a result of being on the 303 (d) list of impaired creeks, it qualified for an EPA 319 grant as part of the Clean Water Act.[56] The grant allowed the Bolin Creek Restoration Project (BCRP) to focus on repairing and controlling stream bank erosion, improving the overall water quality, and eliminating invasive species.[57] The BCRP included bank reshaping to reduce further erosion; removing and replacing invasive species; creating "step-pools" to reduce erosion and create riffles for aquatic life; and building multiple bioretention cells to redirect stormwater drainage, reduce erosion, recharge groundwater, and filter pollution.[57,58]

The Findings of this Study:

The findings of this study supported the conclusion made by the NCDWQ Watershed Assessment Report that the water quality of Bolin Creek declines as it flows further downstream (Figure 2).[40] The site of Bolin Creek at East Franklin Street, furthest downstream of the sites tested, has more urban development than the site of Bolin Creek at State Road, the site of Bolin Creek furthest upstream of the tested sites (Table 1). The site at East Franklin Street also had the poorest water quality in the study (Figure 2). In comparison, the site at State Road had the best water quality among the tested sites of Bolin Creek (Figure 2). Before the data collection, a decline in the water quality of Bolin Creek further downstream, as well as an increase in urbanized surroundings further downstream were observed, suggesting a correlation between urbanization and the declining water quality of Bolin Creek. The site of Bolin Creek at Village Road lies between State Road and East Franklin Street. According to the hypothesis that urbanization and poor water quality co-occur, Village Road's water quality would measure between those of State Road and East Franklin Street. This study showed that this is indeed the case (Figure 2). However, the site of Bolin Creek at Village Road had lower levels of development (ISC) than State Road (Table 1). This may be because Village Road has a lower percentage of forest land (Table 1).

The strong correlations found between developed land cover and declining water quality support the hypothesis that urbanization co-occurs with the declining water quality of Bolin Creek (Figure 3). The differences in development between the reference sites and the Bolin Creek sites in terms of ISC and development were associated with the decreased water quality of Bolin Creek. BMI populations were adversely affected in successive downstream sites on Bolin Creek (Figure 2). Sensitive BMI species' population densities decreased, while densities of tolerant species increased.

It was seen that electrical conductivity (EC) is an important effect of urbanization influencing water quality (Figures 4–5). EC was positively correlated with development (Figure 4) and declining water quality (Figure 5). Urban runoff can pick up pollutants,[17,23] as well as total dissolved solids (TDS).21 For example, Sartor et al. (1974) measured a weighted mean of 1,400 pounds of TDS per curb mile in their study of 12 cities.[21] Through urban and agricultural runoff, as well as sewage, TDS can accumulate in water bodies.[59] TDS, which also measures ions,[24] increases the EC of water. While the relation

ship between EC and TDS is more complex in wastewater, the correlations between TDS and EC in natural water are significant,[24] further explaining the associations found between developed land cover, EC, and declining water quality.

Turbidity was shown to be a factor of development associated with declining water quality, ISC, and runoff (Figure 6). Sedimentation is correlated with turbidity,[27] and sediments and nutrients can harm habitats and benthic aquatic organisms.[60] Higher turbidity levels lead to decreases in photosynthesis levels and resulting dissolved oxygen concentrations, and vegetation density.[60] This may explain the decrease in biodiversity as Bolin Creek flowed further downstream into more developed land (Figure 10) as DO was correlated with biodiversity (SDI; Figure 11). Algal growth increases turbidity,[61] and in the events of algal blooms, turbidity measurements can inversely correlate with DO because of increased algal metabolic activity at night and increased aerobic bacterial decomposition of dead algae.[62]

Nitrate and phosphate levels were correlated with development and ISC (Figure 7). Increased nitrate and phosphate levels may cause higher turbidity and EC levels, as the nutrients cloud water. Urban areas are sources of nitrogen (N), found in nitrate ions, and phosphorus (P), found in phosphate ions, to aquatic ecosystems, for example from fertilized laws.[63] When runoff is insufficiently slowed, increased amounts of N and P can enter streams, providing essential nutrients for algal growth.[64] Growing human populations increase runoff and discharges of pollutants and sewage (including pet sewage), leading to cultural eutrophication, which entails pollution of water bodies by nutrients and toxic algal blooms.[63,65] Algal populations increase in proportion to the amount of N and P, essential nutrients, in water bodies. A study of the Belgian Coastal Zone found a meaningful relationship between nitrate concentration in water and the growth of *Phaeocystis globosa*, a harmful algal bloom species, and an indicator of eutrophication.[66] Algae blooms can increase turbidity and algal toxin concentrations, and cause deoxygenation due to the decay and cellular respiration of excesses of algae.[62] While nutrient pollution may lead to eutrophication, it is also important to consider that metals, toxins, and turbidity increases due to urban development can negatively affect algae biodiversity and biomass, as shown by studies reviewed by Paul and Meyer (2001).[5] It is clear, however, that nutrient pollution, similar to increased sediment and suspended matter, was associated with development, runoff, and declining water quality.

Similar to the correlations found between development and nutrient pollution (Figure 7), Kim et al. (2016),[67] in their studies of 47 sub-watersheds over 5 years in the Han River Basin in Korea found a strong correlation between ISC and P levels. Ballasiotes *et al*. (2015) showed that in Bolin Creek, there was a higher level of N at East Franklin Street, which has 15.58% ISC, than at a site they tested with 14.23% ISC.[20] The site with 14.23% ISC had higher levels of N than another site they tested with an even lower ISC percentage of 9.23%. They found that N was "generally increasing" further downstream in Bolin Creek.

Bolin Creek at East Franklin Street, the most developed site tested, has continually proved to have the poorest water quality of the three sampled sites at Bolin Creek (Figure 2). Comparisons between this study's data and those of the NCDWR show that the water quality at East Franklin Street has not improved since 2001 (Figure 14). Chapel Hill currently has dangerously high levels of ISC.[20]

The bioclassifcations determined by the NCBI scores calculated were relatively consistent with the data from the NCDEQ, but there were some differences. The NCDEQ rated Bolin Creek at State Road (BB330) and Village Road (BB449) "good-fair" in 2001 and "fair" in 2002, respectively. This study, however, rated them as "good" and "good-fair," respectively. These findings may indicate that the water quality of the two sites has improved.

The hypotheses that the UHI effect and that pH impact Bolin Creek were not supported. The correlation found between temperature and DO was the opposite of what would be expected chemically. The short time span of the data collection likely contributed to inconsistent findings on temperature. Further studies should be conducted to investigate the relationship between temperature and land cover at Bolin Creek. In addition, further research is needed to clarify the relationships between the pH of the water of Bolin Creek and development in its watershed.

Limitations:

Among the limitations encountered in this study, the most challenging was a lack of complex and precise equipment. The nitrate and phosphate tests provided a rounded measurement in ppm. The coliform (*E. coli*) test provided only qualitative results in the form of "positive" or "negative"; hence, there was a lack of precision in the density of coliform present in the streams. Another limitation encountered was the use of BMI to assess water quality. Although they are useful, BMI does not respond to all types of pollutants. The presence or absence of a species may be due to factors other than pollution, such as unfavorable water currents, type of substrate, or drought, and their abundance and distribution may vary seasonally. Our tools for BMI identification, such as handheld magnifying glasses, did not have enough magnifying power to allow specific morphotyping of all BMI into genera and species. Another limitation of this study was the researchers' general lack of experience and expertise in the collection and identification of BMI. However, the data collected in this study were considered sufficient enough to support this study's hypothesis and are consistent with NCDEQ findings. If this study were to be repeated with more sophisticated equipment, the results could be subject to small changes, but it is inferred that the overall conclusion would remain the same. Future research should be conducted to corroborate this study's conclusions over a longer time span, a larger number of samples, and in different weather conditions and seasons.

Broader Issues and an Orientation to the Future:

The continued study of urbanization, ISC, and water quality are crucial, both as it relates to Bolin Creek and water quality and ecosystems in general. Runoff is the third largest cause of water impairment in tested lakes, according to the National

DOI: 10.36838/v4i5.22

Water Quality Inventory.[68] Chapel Hill, where the worst water quality of Bolin Creek was reported, is undergoing further urbanization. This increased development will make the issue of declining water quality in the Bolin Creek watershed more relevant and apparent.[20] Biotic and abiotic components in ecosystems are complex and interconnected.[8] The impacts of urbanization (both present and future increased levels) on Bolin Creek could be threats to more complex networks of ecosystems.

The declining water quality of Bolin Creek falls under the broader development of urbanization. The process of urbanization has grown rapidly over a short amount of time. Urbanization mostly occurred over the past 200 years.[9] According to data from the Census Bureau, 40% of the US population lived in urban areas in 1900.9 In current times, in the US, 80% of the population lives in urban areas.[12] With increased technological power, and exponential improvements in technology and sciences,69 the rapid growth of urbanization does not appear to be slowing. By 2050 it is predicted that more than ⅔ of the world population will live in urban areas, amounting to 7 billion people.[9] The rapid growth of urbanization suggests that in addition to having to deal with the effects that urbanization has already had, the future effects of urbanization must be managed even more effectively.

Future Mitigation Strategies:

A major factor damaging the water quality of Bolin Creek was identified, both in previous studies and this study, as urban runoff linked to impervious surfaces. In areas with high urban development, it is important to develop conservation strategies to mitigate the impacts of urbanization.[10] Replanting native vegetation to restore the riparian buffer along Bolin Creek would retard runoff and erosion.[70]

Due to the ability of street contaminants to pollute streams in the form of runoff, Sartor *et al.* (1974) sought to explore the general efficacy of conventional street cleaning operations on the reduction of street contaminants.[21] The typical mechanical street cleaning operations conducted by U.S. cities were found to be unable to remove a majority of street contaminants. It was found that when the "effort" of mechanical street cleaning practices was increased, such as through conducting multiple "sweeps" of an area or operating at a slower speed, up to 90% of concentrations of dust and dirt could be removed from street surfaces. Ongoing research is exploring the efficacy of street cleaning as a best management tool.[71] However, the Town of Chapel Hill may still benefit from exploring street cleaning as an option to decrease the impact of urban runoff on aquatic ecosystems.

Green infrastructure (GI), such as green roofs, is also an option that the Town of Chapel Hill could explore. GI is defined by the Conservation Fund to describe the interconnected network of features, natural areas, semi-natural areas, and green spaces that maintain ecological processes in rural and urban areas.[72] GI has been identified as a sustainable method of managing stormwater.[73-75] Green roofs in partsicular contain vegetative layers that can slow and reduce stormwater runoff as well as filter pollution from rainfall.[76] Costs may discourage investment in green roofs; however, those costs may be offset by the environmental benefits green roofs can offer.76 Similarly, various types of permeable surfaces, surfaces that allow the infiltration of water, are effective at reducing runoff and the peak flow of floods.[77,78] Although the reduced durability of permeable surfaces serves as a challenge deterring their widespread adoption, the ability of permeable pavements to mitigate the aforementioned negative effects attributed to urbanization may still validate its consideration by the Town of Chapel Hill as a form of stormwater management.[77, 78] Additionally, future research should be conducted on the efficacy of other GI, such as the bioretention pools constructed as part of the BCRP, to prove if they are an effective solution to improve water quality.

A supplemental resource for the Town of Chapel Hill to consider is the Clean Water State Revolving Fund (CWSRF).[79] This government-sponsored program allows eligible recipients to receive low-interest loans for water infrastructure projects.[79] Chapel Hill could explore this program as a financing resource for water infrastructure projects aimed at improving the water quality of its aquatic ecosystems.

Lastly, it is important to raise the awareness of the community of Chapel Hill about the health of its aquatic ecosystems. Many adults and children live in urban areas; therefore, ecologists and education systems have a unique opportunity to educate the general public on ecological processes.[5] As specific outreach to reach many children, Bolin Creek could be used as an example in classrooms to demonstrate the negative effects of urbanization. Citizens with an increased awareness of the issues affecting their town may feel more inclined to support the mitigation of such issues. The implementation of some or all of the proposed solutions may lead to the improvement of the water quality of Bolin Creek as well as of other creeks affected by urbanization.

Conclusion

This study found meaningful correlations between metrics of developed land use and declining water quality. The sites at Bolin Creek declined further downstream as its immediate watershed became increasingly urbanized. The site at East Franklin Street consistently showed worse water quality than the other tested sites in terms of its conductivity, nitrates, phosphates, NCBI score, biodiversity, and DO levels. Biodiversity alone, however, was not found to meaningfully predict NCBI scores, and the UHI was not reflected by this study's data on temperature. Nonetheless, sensitive BMI such as EPT declined as ISC increased, and nutrient pollution due to developed land cover was reflected by the data of this study. Bolin Creek's site at East Franklin Street has not improved since 2001, and impervious surfaces in Chapel Hill are at high levels. Prior research as well as the data of this study prompted the researchers to determine runoff from impervious land cover to be the major probable cause of urbanization affecting Bolin Creek.

Due to the interconnected nature and sensitivity of ecosystems, and the ecosystem services provided by them, Bolin Creek's case cannot be viewed in isolation. The biological concerns of Bolin Creek are relevant both to the residents living near it, as well as to urban ecosystems in general. The findings of this study on the effects of urbanization are relevant and important because of the rapid growth of urbanization tak

ing place in the US and globally. The authors hope that Bolin Creek's water quality will be restored to healthy levels and that further mitigation of the effects of urbanization will be a priority in the future.

Acknowledgements

The authors of this study wish to thank Mr. Scott Taylor, Mr. Kelly Ruff, and Mr. William McMahan for their instruction, help, and mentorship. Also, thanks are extended to Mr. Eric Fleek from the NCDEQ for providing previous data on benthic macroinvertebrates at the sites tested in this study. The authors would also like to thank Ms. Nina Johnson, Ms. Andromeda Crowell, and Ms. Megan Aeschleman for their comments and suggestions made during the process of writing and editing this paper. Furthermore, the authors extend their thanks to the peer reviewers for their time and effort in giving essential feedback that helped the authors publish this paper. Finally, the researchers wish to thank all of the Appalachian State faculty and especially the program director, Ms. Lori Tyler, who provided important logistical support, guidance, and mentorship through the Summer Ventures in Science and Mathematics program. Summer Ventures presented the researchers with incredible opportunities to develop themselves in science.

References

1. Carpenter, S. R., Stanley, E. H., and Vander Zanden, M. J. (2011) State of the World's Freshwater Ecosystems: Physical, Chemical, and Biological Changes. *Annual Review of Environment and Resources* 36, 75–99.
2. UN-Water. (2021). *Summary Progress Update 2021: SDG 6 — Water and Sanitation for All*, pp 10–15. Rep. PDF Download Link on Website: https://www.unwater.org/publications/summary-progress-update-2021-sdg-6-water-and-sanitation-for-all/
3. MPCA. (2020, November 10) Why You Should Care About Water Quality. *Minnesota Pollution Control Agency*.
4. (2018, September 17). United States Geological Survey. Stream Ecology. *USGS, Water Resources*.
5. Paul, M. J., and Meyer, J. L. (2001) Streams in the Urban Landscape. *Annual Review of Ecology and Systematics 32*, 333–365.
6. Clark, J. R. (1969) Thermal Pollution and Aquatic Life. *Scientific American 220*, 18–27.
7. Daily, G. C., and Mooney, H. (1997) Introduction: What Are Ecosystem Services?, *in Nature's Services: Societal Dependence on Natural Ecosystems*, pp 1–6. essayABBE Pub. Assoc.of WashingtonAnnandale.
8. Folke, C., Holling, C. S., and Perrings, C. (1996) Biological Diversity, Ecosystems, and the Human Scale. *Ecological Applications 6*, 1018–1024.
9. Ritchie, H., and Roser, M. (2018, June 13) Urbanization. *Our World in Data*.
10. Seto, K. C., Guneralp, B., and Hutyra, L. R. (2012) Global forecasts of urban expansion to 2030 and direct impacts on biodiversity and carbon pools. *Proceedings of the National Academy of Sciences 109*, 16083–16088.
11. McGrane, S. J. (2016) Impacts of urbanization on hydrological and water quality dynamics, and Urban Water Management: A Review. *Hydrological Sciences Journal 61*, 2295–2311.
12. Sun, G., and Caldwell, P. (2015) Impacts of Urbanization on Stream Water Quantity and Quality in the United States. *Water Resources IMPACT 17,* 17–20.
13. Carter, R. W., and U.S. Geological Survey. (1961) Magnitude and Frequency of Floods in Suburban Areas, in Short Papers in the Geologic and Hydrologic Sciences: *Scientific Notes and Summaries of Investigations*, pp 9–12. essayU.S. Government Washington, D.C.
14. Chormanski, J., Van de Voorde, T., De Roeck, T., Batelaan, O., and Canters, F. (2008) Improving Distributed Runoff Prediction in Urbanized Catchments with Remote Sensing Based Estimates of Impervious Surface Cover. *Sensors* 8, 910–932.
15. Chithra, S. V., Harindranathan Nair, M. V., Amarnath, A., and Anjana, N. S. (2015) Impacts of Impervious Surfaces on the Environment. *International Journal of Engineering Science Invention ISSN (Online) 4*, 27–31.
16. Zhang, B., Xie, G., Zhang, C., and Zhang, J. (2012) The economic benefits of rainwater-runoff reduction by urban green spaces: A case study in Beijing, China. J*ournal of Environmental Management 100*, 65–71.
17. Barnes, K. B., Morgan, J., and Roberge, M. (2000) Impervious Surfaces and the Quality of Natural and Built Environments. *Researchgate*.
18. United States Environmental Protection Agency. (2020) Protecting Water Quality from Urban Runoff. (PDF File).
19. Xu, Z., Xiong, L., Li, H., Liao, Z., Yin, H., Wu, J., Xu, J., and Chen, H. (2017) Influences of rainfall variables and antecedent discharge on urban effluent concentrations and loads in Wet Weather. *Water Science and Technology 75*, 1584–1598.
20. Ballasiotes, A., Farley, H., Rose, L., and Whitehead, A. (2015) Bolin Creek Watershed
21. Sartor, J. D. (1974) Water Pollution Aspects of Street Surface Contaminants. *Water Pollution Control Federation 46*, 458–467.
22. GW Solution Inc., and Vadgama, J. (2008) *Coalbed Methane and Salmon:* Assessing the Risks. rep. Pembina Institute.
23. Gresens, S. E., Belt, K. T., Tang, J. A., Gwinn, D. C., and Banks, P. A. (2006) Temporal and spatial responses of Chironomidae (Diptera) and other benthic invertebrates to urban stormwater runoff. *Hydrobiologia* 575, 173–190.
24. Rusydi, A. F. (2018) Correlation between Conductivity and Total Dissolved Solid in Various Type of Water: A Review. *IOP Conference Series:* Earth and Environmental Science 118, 012019.
25. (2021) Indicators: Conductivity. *EPA*. United States Environmental Protection Agency.
26. Meride, Y., and Ayenew, B. (2016) Drinking Water Quality Assessment and its Effects on Residents Health in Wondo Genet Campus, Ethiopia. *Environmental Systems Research 5*.
27. Ankcorn, P. D. (2003) Clarifying Turbidity—The Potential and Limitations of Turbidity as a Surrogate for Water-Quality Monitoring. *Proceedings of the 2003 Georgia Water Resources Conferences* .
28. Burton, G. A., and Pitt, R. (2002) Stormwater effects handbook: A Toolbox for Watershed Managers, Scientists, and Engineers. Lewis Boca Raton.
29. Lenat, D. R., and Eagleson, K. W. (1981, January) Ecological Effects of Urban Runoff on North Carolina Streams. *Researchgate*.
30. Nathanson, J. A. (2022, May 9) Pollution. Encyclopædia Britannica. Encyclopædia Britannica, inc.
31. Sallenave, R. (2015, November) Stream Biomonitoring using Benthic Macroinvertebrates. *New Mexico State University.*
32. North Carolina Department of Environmental Quality Division of Water Resources Water Sciences Section Biological Assessment Branch. (2016, February) Standard Operating Procedures for the Collection and Analysis of Benthic Macroinvertebrates.
33. Bornstein, R. D. (1968) Observations of the Urban Heat Island Effect in New York City. *Journal of Applied Meteorology and Cli*

DOI: 10.36838/v4i5.22

Sponge City Construction. *Water, 10*, 172.
78. Zhu, H.; Yu, M.; Zhu, J.; Lu, H.; Cao, R. (2019) Simulation Study on Effect of Permeable Pavement on Reducing Flood Risk of Ur ban Runoff. *International Journal of Transportation Science and Technology, 8,* 373–382.
79. EPA. (2021, July) Learn about the Clean Water State Revolving Fund (CWSRF). *EPA*. United States Environmental Protection Agency.

Authors

Yasmine Ackall, of Brazilian and Palestinian descent, is a junior at East Chapel Hill High School. She is interested in fields of biology such as genetics/genomics, molecular biology, and biochemistry. She wishes to attend a 4-year research university. She enjoys music and can play the violin, piano, and guitar.

Katherine Lopez, an immigrant from El Salvador, is a junior at City of Medicine Academy. She has a passion for learning about the human body and healthcare accessibility within communities. In her spare time, she enjoys painting, reading, and writing. She aims to pursue a career in the medical field.

Pristine Onuoha is a junior at East Chapel Hill High School. She is a Nigerian immigrant and has a love for STEM. She also aspires to become a physician. One of her biggest goals as a physician is to work in underserved communities with high doctor-to-patient ratios.

Micah van Praag, a Senior at Orange High School and an immigrant from Holland, is passionate and curious about the human body and mind, writing, and expressing himself creatively through filmmaking. He is interested in pursuing a medical career—with a focus on psychiatry, psychology, neurology, and bridges between science and philosophy.

Dr. Shea Tuberty oversees the aquatic ecotoxicology lab at Appalachian State University and mentors high school students for Summer Ventures in Science and Math. He received his B.A. at Vanderbilt University, M.S. & Ph.D. at Tulane University, and Postdoctoral training at the University of West Florida/USEPA Gulf Ecology Division

.

GENIUS OLYMPIAD

"Let's build a better future together"

www.geniusolympiad.org

International Environment Project Fair For Grades 9-12

Rochester, New York

Hosted by Rochester Institute of Technology

RIT Rochester Institute of Technology

@GeniusOlympiad

terra science and education

IJHSR International Journal of High School Research

is a publication of

terra science and education

N.Y. based 501.c.3 non-profit organization
dedicated for improving K-16 education